~~NUREG/CR-2509~~
PNL-4155

11A

Materials Test-2 LOCA Simulation in the NRU Reactor

Prepared by J. O. Barner, G. M. Hesson, L. L. King, R. K. Marshall, L. J. Parchen,
J. P. Pilger, W. N. Rausch, G. E. Russcher, B. J. Webb,
N. J. Wildung, C. L. Wilson, M. D. Wismer, C. L. Mohr

Pacific Northwest Laboratory
Operated by
Battelle Memorial Institute

Prepared for
U.S. Nuclear Regulatory Commission

Available from

GPO Sales Program
Division of Technical Information and Document Control
U. S. Nuclear Regulatory Commission
Washington, D. C. 20555

Printed copy price: $6.50

and

National Technical Information Service
Springfield, Virginia 22161

NUREG/CR-2509
PNL-4155
R3

Materials Test-2 LOCA Simulation in the NRU Reactor

Manuscript Completed: January 1982
Date Published: March 1982

Prepared by
J. O. Barner, G. M. Hesson, L. L. King, R. K. Marshall, L. J. Parchen,
J. P. Pilger, W. N. Rausch, G. E. Russcher, B. J. Webb,
N. J. Wildung, C. L. Wilson, M. D. Wismer, C. L. Mohr

Pacific Northwest Laboratory
Richland, WA 99352

Prepared for
Division of Accident Technology
Office of Nuclear Regulatory Research
U.S. Nuclear Regulatory Commission
Washington, D.C. 20555
NRC FIN B2277

Availability of Reference Materials Cited in NRC Publications

Most documents cited in NRC publications will be available from one of the following sources:

1. The NRC Public Document Room, 1717 H Street, N.W.
   Washington, DC 20555
2. The NRC/GPO Sales Program, U.S. Nuclear Regulatory Commission,
   Washington, DC 20555
3. The National Technical Information Service, Springfield, VA 22161

Although the listing that follows represents the majority of documents cited in NRC publications, it is not intended to be exhaustive.

Referenced documents available for inspection and copying for a fee from the NRC Public Document Room include NRC correspondence and internal NRC memoranda; NRC Office of Inspection and Enforcement bulletins, circulars, information notices, inspection and investigation notices; Licensee Event Reports; vendor reports and correspondence; Commission papers; and applicant and licensee documents and correspondence.

The following documents in the NUREG series are available for purchase from the NRC/GPO Sales Program: formal NRC staff and contractor reports, NRC-sponsored conference proceedings, and NRC booklets and brochures. Also available are Regulatory Guides, NRC regulations in the *Code of Federal Regulations,* and *Nuclear Regulatory Commission Issuances.*

Documents available from the National Technical Information Service include NUREG series reports and technical reports prepared by other federal agencies and reports prepared by the Atomic Energy Commission, forerunner agency to the Nuclear Regulatory Commission.

Documents available from public and special technical libraries include all open literature items, such as books, journal and periodical articles, and transactions. *Federal Register* notices, federal and state legislation, and congressional reports can usually be obtained from these libraries.

Documents such as theses, dissertations, foreign reports and translations, and non-NRC conference proceedings are available for purchase from the organization sponsoring the publication cited.

Single copies of NRC draft reports are available free upon written request to the Division of Technical Information and Document Control, U.S. Nuclear Regulatory Commission, Washington, DC 20555.

Copies of industry codes and standards used in a substantive manner in the NRC regulatory process are maintained at the NRC Library, 7920 Norfolk Avenue, Bethesda, Maryland, and are available there for reference use by the public. Codes and standards are usually copyrighted and may be purchased from the originating organization or, if they are American National Standards, from the American National Standards Institute, 1430 Broadway, New York, NY 10018.

ACKNOWLEDGMENTS

The authors would like to thank the Chalk River Nuclear Laboratories (CRNL) for their assistance in performing this test. A special acknowledgment is due to CRNL staff members--B. DeAbreu, S. Z. Hart, C. A. Herriot, P. E. Kelly, J. W. Logie, D. T. Nishimura, and I. D. Ross, who made major contributions in keeping this test on schedule.

The test staff would like to thank CRNL staff members D. J. Axford, I. C. Martin, and S. J. McAuley for ensuring a safe test.

The assistance of R. Van Houten, NRC/RSR/FBR, Program Manager is also acknowledged for providing helpful directives to the program.

The authors would also like to thank B. Breizy, R. A. Keefe, and S. L. Cluck for preparation of this manuscript.

ABSTRACT

A simulated loss-of-coolant accident was performed with a full-length test bundle of pressurized water reactor fuel rods. This third experiment of the program produced fuel cladding temperatures exceeding 1033 K (1400^{o}F) for 155 s and resulted in eight ruptured fuel rods. Experiment data and initial results are presented in the form of photographs and graphical summaries.

SUMMARY

The loss-of-coolant accident (LOCA) simulation program in the National Research Universal (NRU) reactor is being conducted to evaluate the thermal hydraulic and mechanical deformation behavior of a full-length pressurized water reactor fuel bundle under LOCA conditions. The test conditions are designed to simulate the heatup, reflood, and quench phases of a large-break LOCA and are performed in situ using nuclear power fission heat to simulate low-level decay power typical of these conditions.

This document reports the data and initial results from the third experiment in the program, Materials Test Two (MT-2). This test series had four major objectives:

- to maintain Zircaloy high alpha phase temperatures for greater than 100 s to obtain maximum fuel cladding ballooning and rupture conditions
- demonstrate the Disassembly Reassembly Machine (DERM) in reconstituting a test bundle underwater
- demonstrate and develop bundle gauging and profilometry
- evaluate variable reflood rate characteristics and control to maximize the time in the Zircaloy high alpha-phase temperature ballooning and rupture window.

The results of the tests showed that, by using variable reflood conditions, it is possible to alter the peak cladding temperature during the reflood phase. Temperatures in excess of 1033 K (1400^{o}F) were maintained for 155 s. The thermal-hydraulic results were based on using manual selection of three levels of reflood rates of 1.27 cm/s (0.5 in/s), 2.5 cm/s (1.0 in/s), and 4.06 cm/s (1.6 in/s). Ballooning and rupture of the test fuel rod cladding occurred during the adiabatic heatup phase of the experiment. The DERM operation was successful in both performing bundle examination and profilometry and in reconstituting the test assembly under water.

Postirradiation examination using the DERM revealed coplaner blockage and rod-to-rod contact at the maximum blockage areas. Significant decreases

in cladding strain at self-powered neutron detectors (SPNDs) were also noted, which indicates the sensitivity of the deformation of Zircaloy to small changes in cladding temperature.

This report presents the preliminary graphical data and photographs of fuel rod temperatures, test conditions, and cladding mechanical deformation axial profiles obtained during this experiment.

CONTENTS

FIGURES

TABLES

1.0 INTRODUCTION

A loss-of-coolant accident (LOCA) simulation test program is being conducted in the National Research Universal (NRU) reactor at Chalk River Nuclear Laboratories,[a] Chalk River, Ontario, Canada, by Pacific Northwest Laboratory (PNL).[b] The program is sponsored by the Fuel Behavior Research Branch of the U.S. Nuclear Regulatory Commission (NRC) to evaluate the thermal-hydraulic and mechanical deformation behavior of a full-length, 3% enriched pressurized water reactor (PWR) fuel rod bundle during the heatup, reflood, and quench phases of a LOCA. Low-level nuclear fission heat was used to simulate the decay heat in fuel and cladding that are typical of a LOCA.[1]

The test program is composed of a series of thermal-hydraulic tests (PTH) using a single test assembly, and cladding material tests (MT) using different test assemblies. The results of the initial thermal-hydraulic experiment have been reported.[2] That test series provided a data base for predicting the quenching characteristics of Zircaloy-clad fuel rods under various reflood conditions. The MT-1 experiment has also been completed, and its results have been reported.[3]

The MT-2 experiment described in this report used 11 pressurized test fuel rods, 20 unpressurized guard fuel rods, and one nonfueled cladding tube to evaluate the ballooning and fuel cladding rupture due to a LOCA in the high-alpha Zircaloy temperature range. Eight of the fuel rods ruptured during the adiabatic temperature ramp. The test was terminated with a peak cladding temperature of 1205 K (1710^{o}F).

The remainder of this report consists of:

- a description of the MT-2 experiment
- a discussion of the test conditions and results
- a brief analysis of the test results

(a) Operated by Atomic Energy of Canada, Ltd. (AECL).
(b) Operated for the U.S. Department of Energy (DOE) by Battelle Memorial Institute.

- a discussion of the visual and photographic examination
- Appendix A through G presents computer-generated plots of neutronic thermal and hydraulic data
- Appendix H presents mechanical deformation data obtained with the Disassembly, Examination, and Reassembly Machine (DERM).

1.1 EXPERIMENT OBJECTIVES AND SCOPE

The primary objective of the MT-2 experiment was to evaluate the deformation behavior of fuel cladding in a simulated LOCA that produced fuel cladding temperatures above 1033 K (1400^{o}F) for an extended time.

A secondary objective of the experiment was to evaluate the reflood and quench characteristics of fuel rods under variable reflood conditions. Another secondary objective was to use manual control for reflood rates of 1.27 cm/s (0.5 in/s), 2.5 cm/s (1 in/s), and 4.06 cm/s (1.6 in/s) in order to maintain the Zircaloy cladding in the high-alpha temperature range for an extended period of time.

Other objectives included evaluation of the DERM in performing bundle profilometry and in using the DERM to reconstitute a test bundle underwater in the spent fuel storage basin at NRU.

1.2 APPLICABILITY OF RESULTS

The test results from MT-2 provide full-length nuclear-heated cladding rupture data and thermal-hydraulic response data in the high-alpha temperature range for variable reflood conditions. Fuel rupture occurred during the adiabatic heatup in the upper range of the alpha phase temperature region. The variable reflood conditions extend the existing data base on thermal-hydraulic response into LOCA operating conditions not previously investigated by FLECHT or other out-of-pile test programs. These tests provide valuable information on the control of quench fronts and two-phase cooling that will be used to guide subsequent thermal-hydraulics and materials tests. They also provide information on the quench characteristics of deformed rods compared with nondeformed rods. This information was not available from the previous experiment, MT-1, due to the locations of operable instrumentation.

The data from MT-2 will be used in conjunction with MT-1 test results[3] to assess various calculational models for reactor safety analyses and conclusions derived from the large series of electrically heated tests and smaller scale in-pile tests being conducted elsewhere. The experimental results of the program address 17 specific items outlined in the Code of Federal Regulations 10 CFR 50.46 and 10 CFR 50, Appendix K. These results will be used to provide additional data for model calibration and to help define the primary heat transfer mechanisms for new analytical models. The major contribution of these tests to light water reactor (LWR) technology is to reduce the uncertainty on licensing criteria and offer the potential for raising the operating limits on some commercial LWRs.

2.0 TEST DESCRIPTION

This section describes the components of the test train assembly and details the instrumentation that was provided. The test operation consisted of a preconditioning phase, three low-temperature transients, and one high-temperature test.

2.1 TEST TRAIN ASSEMBLY

A schematic of the overall test train is depicted in Figure 1. The total length of the test train (including the head closure, hanger tube, and the test assembly) was 9.18 m (30 ft 1.5 in). The closure region provided the primary pressure boundary and included penetrations for 183 instrumentation leads. The hanger tube was used to suspend the test bundle and shroud from the head closure plug, and instrument leads were attached to the hanger to protect them during transport and testing. The shroud, which supported the fuel bundle and served as a protective liner during the experiment and transfer operations, also provided proper coolant flow distribution during various stages of the experiment. The stainless steel (SS) shroud consisted of two halves clamped together at 17.78-cm (7-in) intervals and attached at the end fittings. The split shroud design makes it possible to disassemble, examine, and reassemble the test train underwater after its irradiation. The shroud and test assembly were approximately 4.27 m (14.17 ft) long and were highly instrumented. The Experiment Operations Plan[4] contains a detailed instrumentation listing.

The test assembly consisted of a 6 x 6 segment of a 17 x 17 PWR fuel assembly with the four corner rods removed (Figure 1) and provided a basic test array of 32 rods. The 20 rods in the outer row were not pressurized and served as guard fuel rods during the test. The materials test section consisted of 11 pressurized fuel rods (Table 1) and one liquid level detector tube, arranged in a cruciform pattern. The 11 test fuel rods were pressurized with helium to 3.1 MPa (450 psig) to provide the internal cladding stress condition that is typical of a PWR rod at beginning of life (BOL).

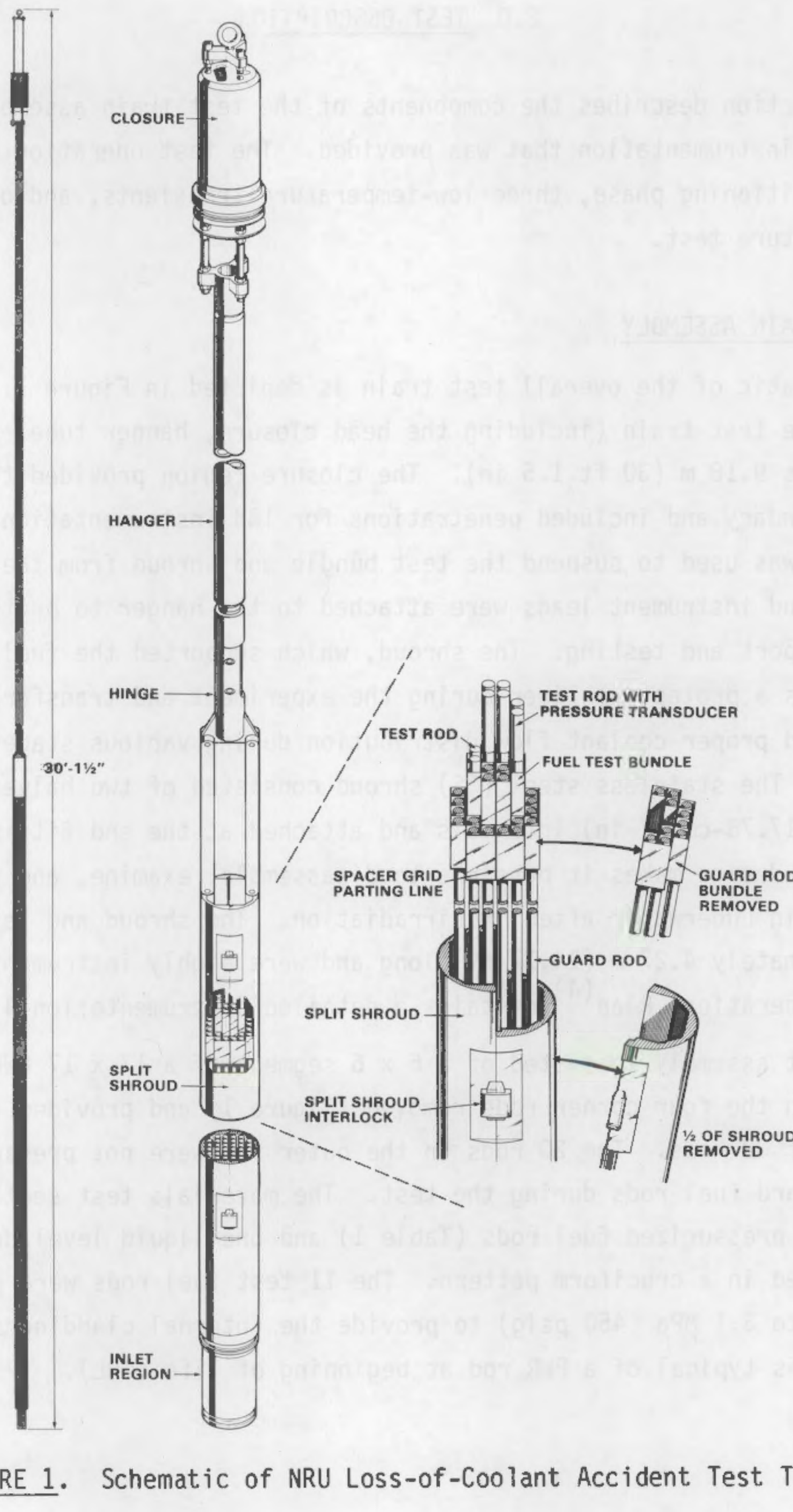

FIGURE 1. Schematic of NRU Loss-of-Coolant Accident Test Train

TABLE 1. Test Fuel Design Variables

Cladding Material	Zircaloy-4
Cladding Outside Diameter (OD)	0.963 cm (0.379 in)
Cladding Inside Diameter (ID)	0.841 cm (0.331 in)
Pitch (rod to rod)	1.275 cm (0.502 in)
Fuel Pellet OD	0.826 cm (0.325 in)
Fuel Pellet Length	0.953 cm (0.375 in)
Active Fueled Length	365.76 cm (144 in)
Total Shroud Length	423.1 cm (170.125 in)
Helium Pressurization	3.1 MPa (450 psig)
Fuel Enrichment	2.93% U-235

The test train instrumentation included: 24 self-powered neutron detectors (SPNDs), 115 fuel rod thermocouples (TCs), 18 steam probe TCs, 4 closure head TCs, 2 pressure tranducers, 9 pressure switches, and a liquid level detector (LLD) float with a linear variable differential transformer (LVDT) sensor in instrument tube location 4D. The LLD design was based on the buoyant principle with a float supported by a spring; the LVDT at level 19 measured the relative displacement.

The instrumentation was located at 21 elevations (levels) along the test train assembly. Each of these levels is defined in Figure 2, and Figures 3 through 6 detail the instrumentation at these levels. Four TCs are located at level 22 in order to measure the closure temperature. Additional detail and nomenclature can be found on the blue prints referenced in Figure 3.

Turbine flowmeters and TCs provided the main source of thermal-hydraulic data. Local coolant temperatures were measured with steam probe TCs that protruded into the coolant channel and with TCs attached to the shroud. TCs were also located at the fuel centerline and attached to the inside of the cladding surface to measure azimuthal temperature variations. These cladding TCs were spot welded to the interior cladding surface and monitored the cladding temperature without interference from fuel pellet chips or unintentional TC relocation.

SPNDs provided neutron flux measurements within the fuel bundle. They can also detect coolant density variations (through flux changes) associated

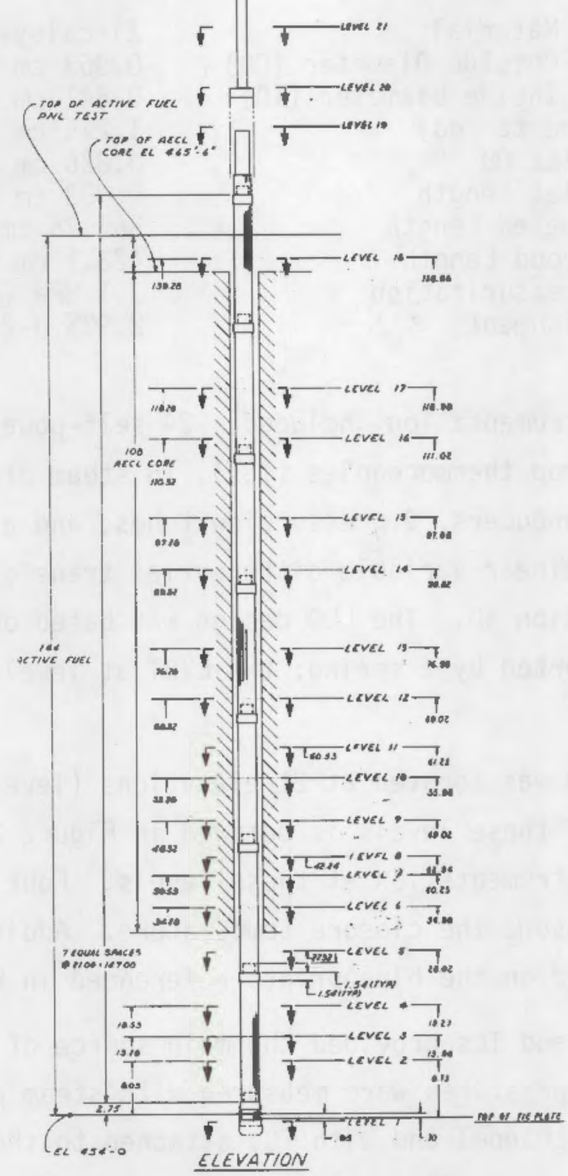

FIGURE 2. Instrumentation Levels in the MT-2 Test Assembly

with the quench front that passed each SPND during the reflood phase of the transient. SPND data is being evaluated with regard to coolant density.

Each cruciform test fuel rod had either a pressure transducer or a pressure switch attached to the upper end cap. Pressure transducers monitored the internal pressures of test fuel rods 3C and 5C, while pressure switches identified the drop in plenum pressure below 250 psi for other test fuel rods.

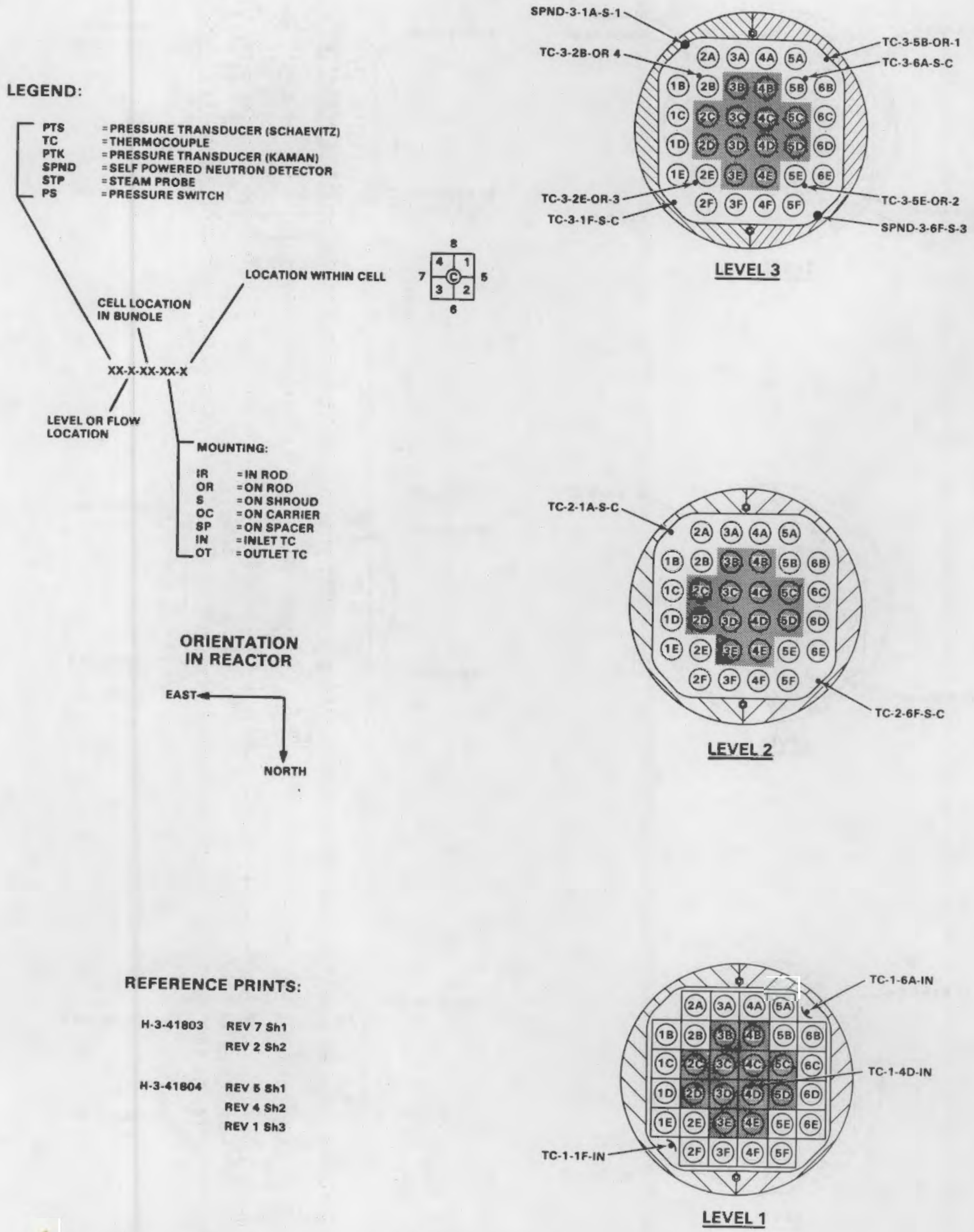

FIGURE 3. Nomenclature and Instrumentation at Levels 1 Through 3 in the MT-2 Test Assembly

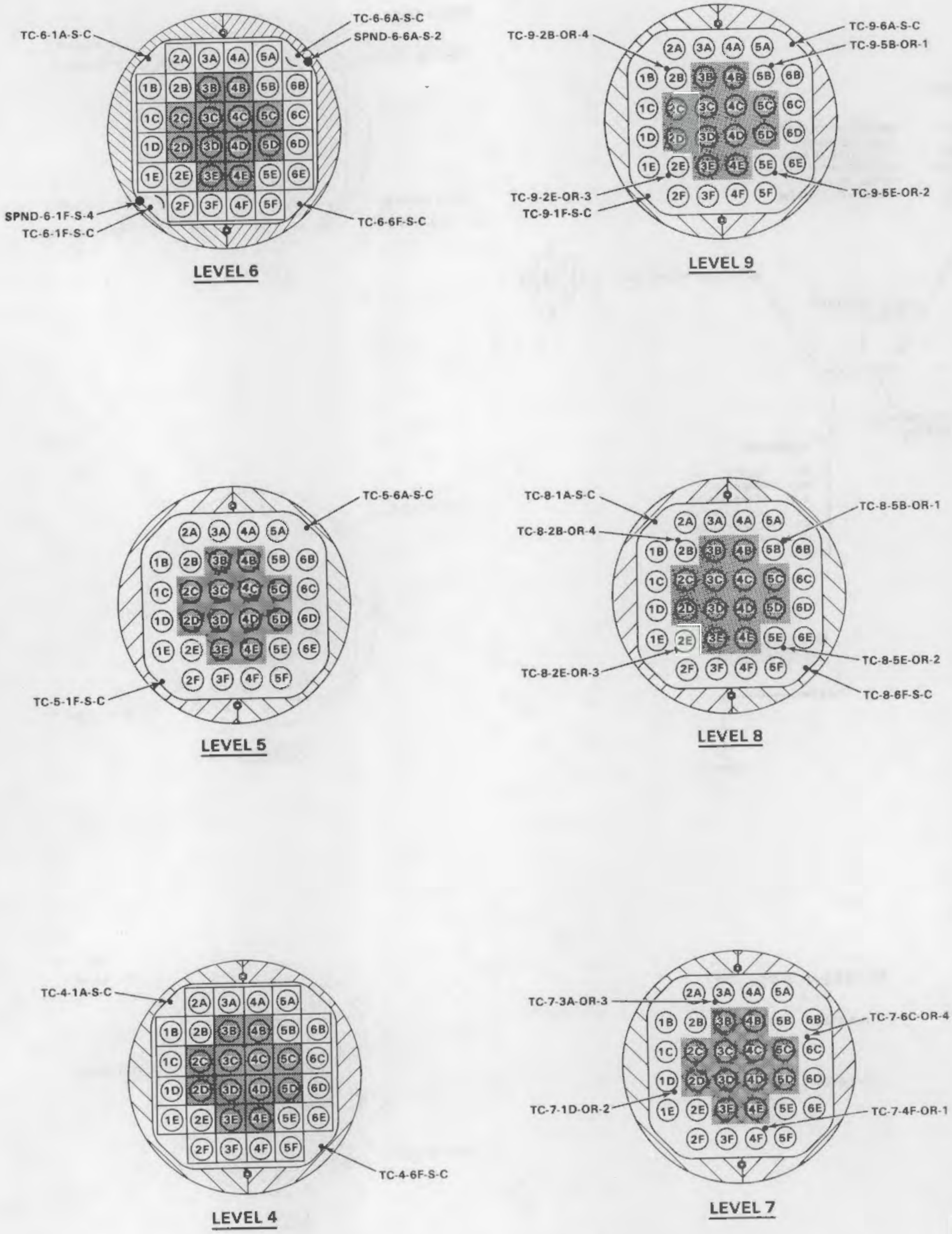

FIGURE 4. Instrumentation at Levels 4 Through 9 in the MT-2 Test Assembly

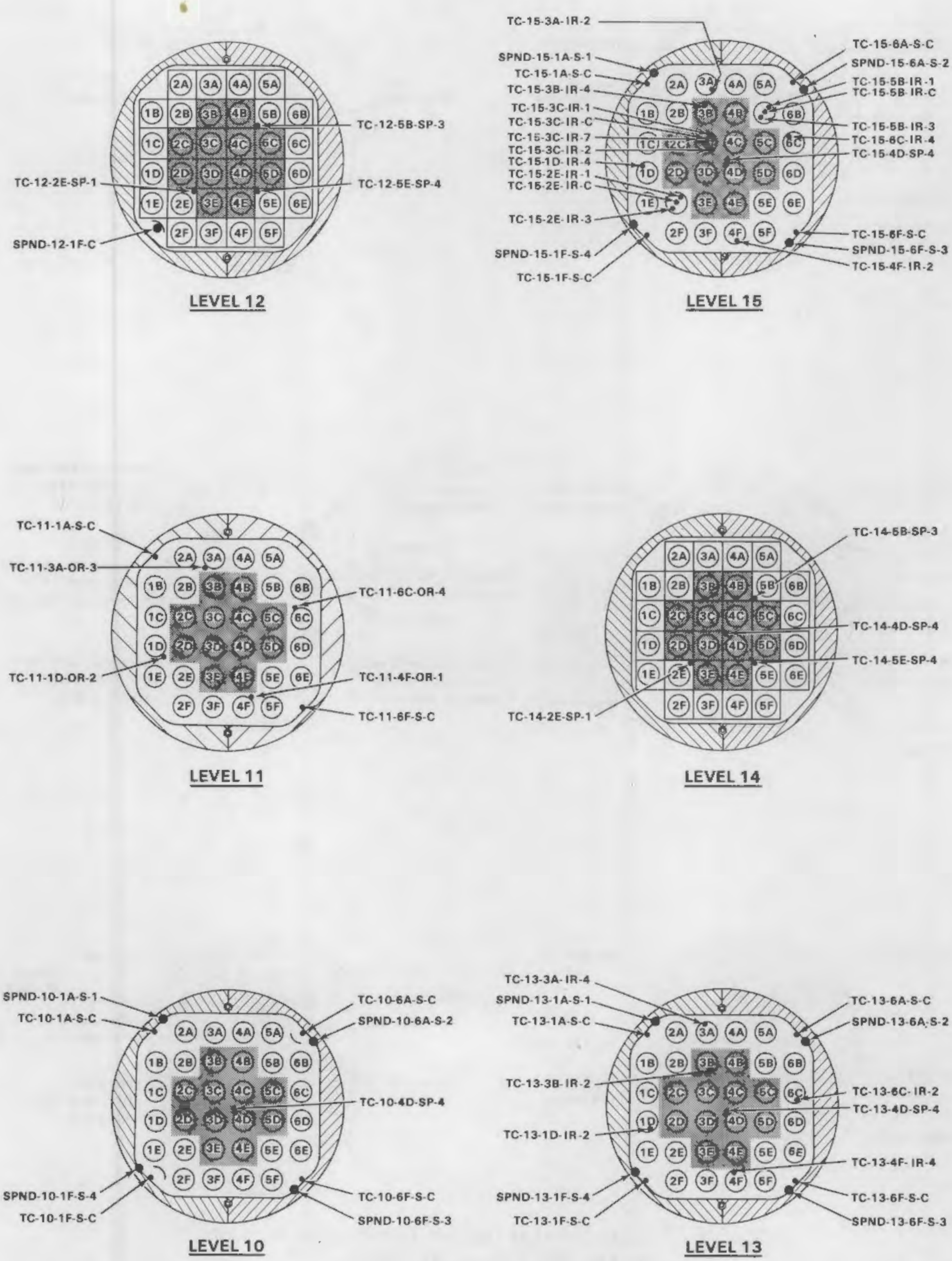

FIGURE 5. Instrumentation at Levels 10 Through 15 in the MT-2 Test Assembly

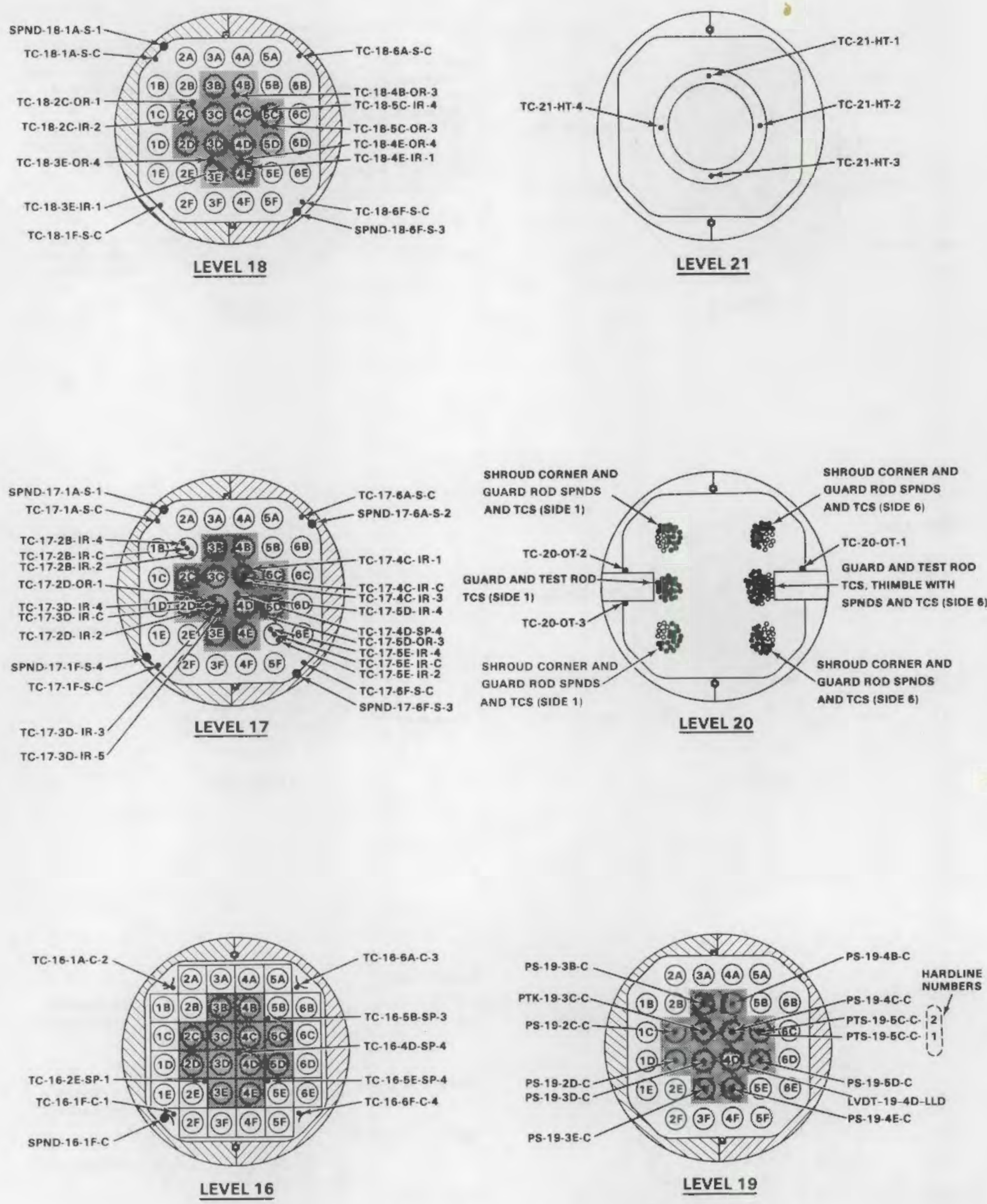

FIGURE 6. Instrumentation at Levels 16 Through 21 in the MT-2 Test Assembly

The instrument signals were monitored on a real-time basis with the data acquisition and control system (DACS). The recorded data characterized the coolant flow rates, temperature, neutron flux, operating history, and provided a record of cladding rupture time.

2.2 EXPERIMENT OPERATION

The MT-2 experiment included preconditioning operation and four successive tests, each having a pretransient and transient phase. These tests all used position L-24 in the NRU reactor (see Figure 7). The assembly is oriented in the reactor with side F facing north (fuel rods 2F, 3F, 4F and 5F face north).

The preconditioning operation was conducted at an average test assembly fuel rod power of about 18.7 kW/m (5.7 kW/ft) with the U-2 loop providing water cooling. Three short runs to full power permitted the fuel to crack and relocate within the cladding in a prototypic manner. System loop pressure was held at 8.62 MPa (1250 psia).

The pretransient conditions for the first three transient tests (MT-2.1.1, MT-2.1.2, and MT-2.1.3) were conducted with steam cooling (provided by the U-1 loop) at a mass flow rate of about 0.189 kg/s (1500 lbm/h) and a reactor power of about 4.0 MW. Test assembly fuel rod power was about 0.6 kW/m (0.2 kW/ft). Steam flow during the pretransient maintained the peak cladding temperature below 727K (850^{o}F). System back pressure was controlled at 0.276 MPa (40 psia) throughout each pretransient and the entire transient test series.

The first three transient tests provided multiple-stage reflood calibration data for the fourth variable reflood test, MT-2.2. The first three transient tests used lower reactor powers and lower steam flow rates than MT-2.2 to provide greater reflood coolant control over peak cladding temperatures. By using a lower reactor power, the adiabatic heatup rate was reduced giving a longer response time than would be encountered in the fourth test.

The transient phase for each of the first three tests began when the steam coolant flow was reduced from 0.189 kg/s (1500 lbm/h) to zero and reactor power was maintained at about 3.7 MW. As soon as the steam was shut

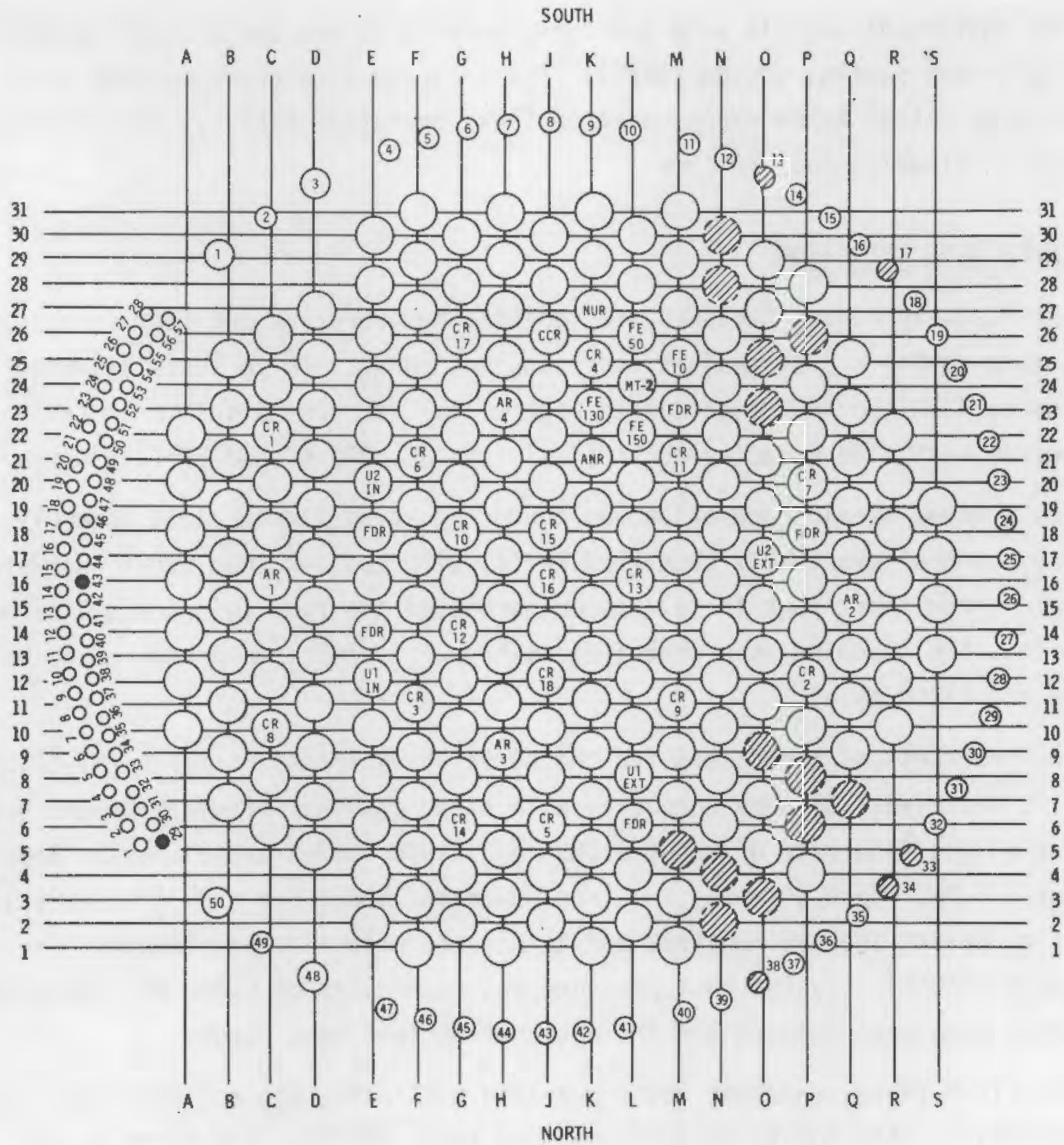

CR CONTROL ROD
AR ADJUSTER ROD
FDR FLUX DETECTOR ROD
U-1 IN / U-2 IN DOWN FLOW CHANNEL-DUMMY FUEL
U-1 EXT / U-2 EXT UP FLOW CHANNEL-DUMMY FUEL
○ STANDARD LATTICE POSITION
⊘ BLOCKED CHANNEL-NOT FUELED

CCR COBALT CARRIER ROD
NUR NATURAL URANIUM ROD
ANR ALUMINUM NITRIDE ROD
FE 50 FUEL ELEMENT - 50 MWD BURNUP
FE 10 FUEL ELEMENT - 10 MWD BURNUP
FE 130 FUEL ELEMENT - 130 MWD BURNUP
FE 150 FUEL ELEMENT - 150 MWD BURNUP

FIGURE 7. NRU Reactor Core Configuration

off, reflood water was injected into the test assembly at an average rate of 0.157 m/s (6.2 in/s) for a period of 13 seconds. At this time in MT-2.1.1, the reflood rate was reduced to 0.030 m/s (1.2 in/s) and varied as required to stabilize the peak cladding temperature. For MT-2.1.2, the average initial reflood rate was 0.131 m/s (5.15 in/s) for 13 seconds and was then reduced to 0.026 m/s (1.0 in/s). The initial average reflood rate for MT-2.1.3 was 0.170 m/s (6.7 in/s) for 13 seconds and was then decreased to 0.026 m/s (1.0 in/s). For each test, reflood rates were subsequently varied as required to maintain the peak cladding temperature below 839K (1050^{0}F).

The fourth test--MT-2.2--used a reactor power of approximately 7.4 MW and a corresponding steam flow rate of 0.378 kg/s (3000 lbm/hr) for the pretransient to provide more prototypic fuel rod radial temperature and axial power profiles. Reactor power was again held constant throughout the transient to simulate fuel decay energy. The average linear power designed to be 1.23 kW/m (0.375 kW/ft) however was subsequently found to be approximately 1.04 kW/m (0.320 kW/ft).

The objectives of MT-2.2 were to evaluate the deformation and rupture and quenching characteristics of nuclear fuel cladding under variable reflood rate conditions and to maintain the peak cladding temperature in the temperature range from 1033 to 1089 K (1400 to 1500^{0}F) for an extended period of time. However, the peak cladding temperature ranged from 1033 to 1205 K (1400 to 1710^{0}F) for 180 s. Although operating conditions to provide the desired cladding temperature had been determined based upon results from the first three experiments, operating problems resulted in an increase in the effective delay time of 36 seconds for the initiation of reflood water flow to the bundle (see Figure 8). A schematic experiment description is presented in Figure 9 and Table 2.

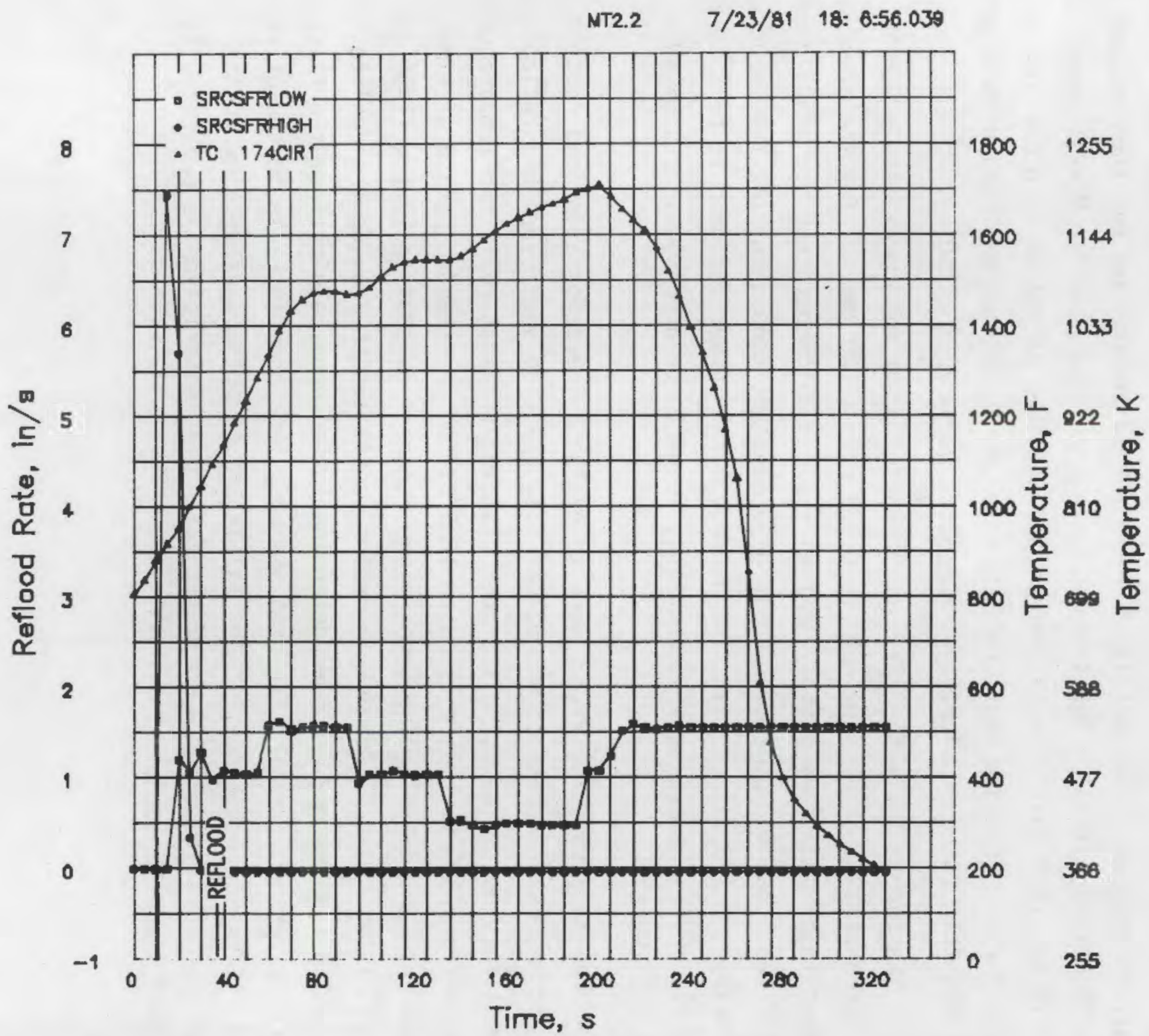

FIGURE 8. MT-2.2 Reflood Flow Rates and Peak Cladding Temperature at Level 17

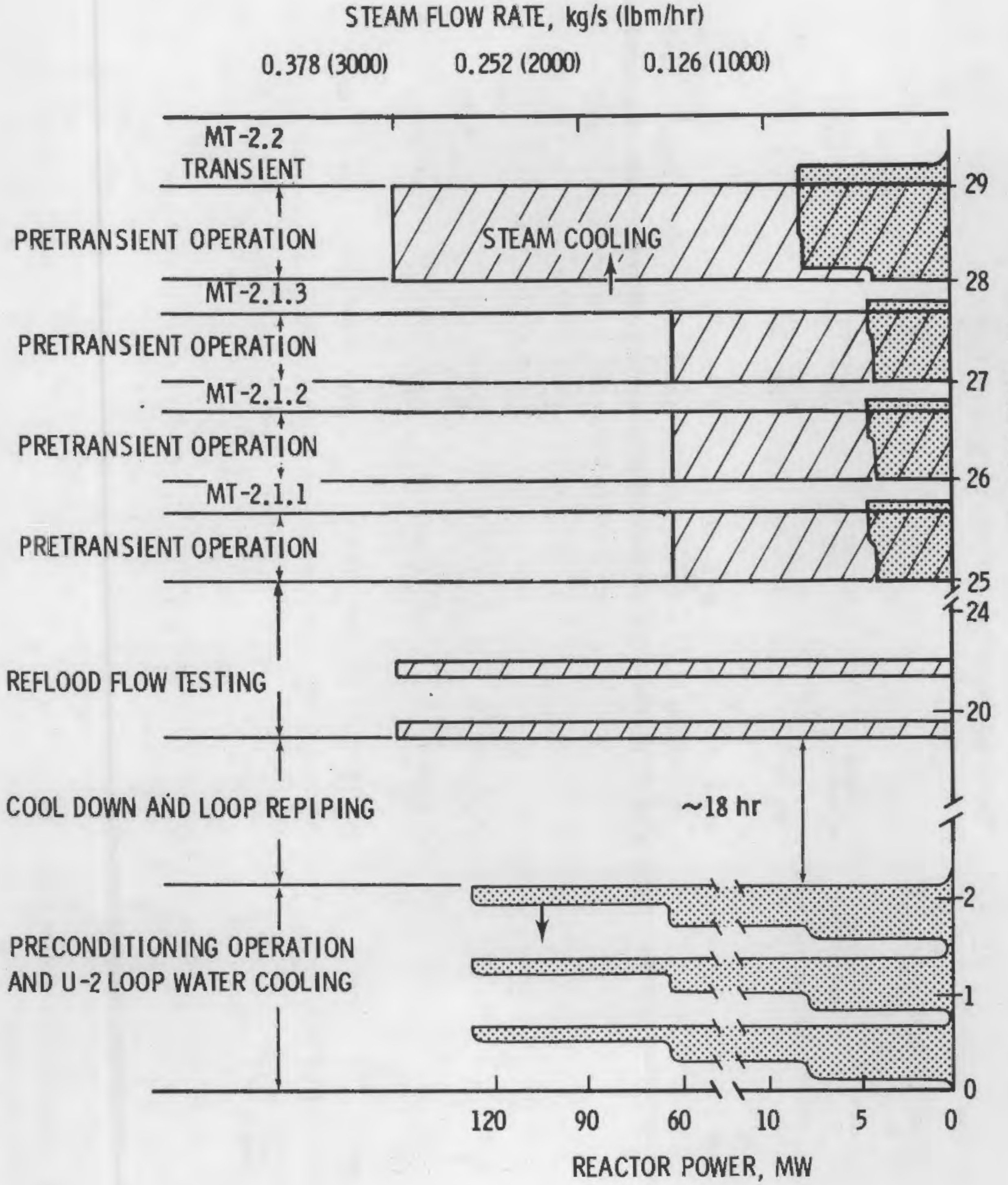

FIGURE 9. Experiment and NRU Operations Schematic

TABLE 2. Measured Experiment Operating Conditions

Parameter	Preconditioning	Reflood Calibration	Transient MT-2.1.1	Transient MT-2.1.2	Transient MT-2.1.3	Transient MT-2.2
Reactor Power	127 MW	0	3.7 MW	3.7 MW	3.7 MW	7.4 MW
Coolant	U-2 water	U-1 steam/ reflooding	U-1 steam/ reflooding	U-1 steam/ reflooding	U-1 steam/ reflooding	U-1 steam/ reflooding
Coolant Flow	0 to 129,400 lbm/h	0 to 3000 lbm/h	0.189 kg/s (1500 lbm/h)	0.189 kg/s (1500 lbm/h)	0.189 kg/s (1500 lbm/h)	0.378 kg/s (3000 lbm/h)
Reflood Delay	NA[b]	0	35 s	11 s	11 s	36 s
Reflood Rates	NA	0.5, 1.0 in/s	0.157 m/s (6.20 in/s) for 13 s 0.0307 m/s (1.21 in/s) for 16 s 0.150 m/s (0.59 in/s) for 148 s	0.131 m/s (5.15 in/s) for 13 s 0.0259 m/s (1.02 in/s) for 20 s 0.0363 m/s (1.43 in/s) for 12 s 0.0124 m/s (0.49 in/s) for 81 s	0.170 m/s (6.71 in/s) for 13 s 0.0257 m/s (1.01 in/s) for 14 s 0.0135 m/s (0.53 in/s) for 12 s 0.0401 m/s (1.58 in/s) for 14 s 0.0244 m/s (0.96 in/s) for 14 s 0.0135 m/s (0.53 in/s) for 109 s	0.267 m/s (1.05 in/s) for 21 s 0.396 m/s (1.56 in/s) for 42 s 0.0267 m/s (1.05 in/s) for 42 s 0.124 m/s (0.49 in/s) for 57 s 0.0274 m/s (1.08 in/s) for 14 s 0.0396 m/s (1.56 in/s) for duration
Transient[a] Initiation Time			July 23, 1981 12:41:18	July 23, 1981 14:53:27	July 23, 1981 16:49:18	July 23, 1981 18:06:56
Pretransient Cladding Temperatures	NA	NA	675 K (755°F)	683 K (770°F)	678 K (760°F)	702K (805°F)
Peak Cladding Temperature (PCT)	800°F	320°F	786 K (955°F)	908 K (1175°F)	803 K (985°F)	1205 K (1710°F)
Reactor Conditional Trip Criteria (peak cladding temperature)	peak cladding temperature	NA	1200 K (1700°F)	1200 K (1700°F)	1200 K (1700°F)	1200 K (1700°F)
PCT Turnaround Time[c]			100 s	85 s	55 s	205 s
Bundle Quench Time[c]			145 s	155 s	150 s	260 s

a) Transient initiated by termination of steam flow.
b) Not applicable.
c) Time after initiation of transient.

3.0 TEST CONDITIONS AND RESULTS

A summary of the test conditions measured during the experiment is described in Table 2. Reflood rates, reflood delay time, and peak cladding temperatures are included. The cladding temperatures reported are those at pretransient (at the start of the adiabatic heatup) and the maximum temperatures measured during the transient. Both temperatures were measured by TCs on the inside surface of the fuel rods. Times for both the peak fuel cladding temperature turnaround and the bundle quench are summarized in Table 2.

This section consists primarily of summaries of the data resulting from MT-2.2. Computer-generated plots for MT-2.2 and selected data for the qualification tests (MT-2.1.1 through 2.1.3) are presented in Appendices A through G. Results of DERM measurements of the individual fuel rods and bundle are reported in Appendix H.

3.1 TEST ASSEMBLY TEMPERATURES

Test assembly temperatures were measured in and on test fuel rods, inner and outer guard fuel rods, the test assembly shroud, and the instrument lead carrier. The temperature of the coolant in five subchannels was also measured from grid spacers. Temperature data for each of these locations can be found in Appendices A through D. Temperature data for the preconditioning operation are presented in Appendix A, temperature data for the pretransient in Appendix B, and data for the transient in Appendices C and D.

Preconditioning Test Assembly Temperatures

MT-2 data were recorded during the power ascension and during the full-power, steady-state preconditioning phase of NRU reactor operation. The average axial temperature profile for the test assembly shroud is shown in Figure A-1 of Appendix A, and the individual corner channel axial temperature profiles are presented in Figure A-2. Modest (<12K) coolant temperature gradients (in water) across the test assembly are evident from this comparison of individual corner channel temperatures. Inlet piping temperature at -27.43 m (-1080 in) upstream from the test assembly, the outlet region coolant temperature (level 20), the coolant temperature at the hanger tube (level 21), and the outlet piping temperature 8.23 m (324 in) downstream from the test assembly are provided in Figure A-3. Intervening data (levels 1 through 18) represent average shroud temperatures in the test assembly. These temperatures are very comparable to temperatures measured in MT-1.[3] Axial and radial coolant channel temperatures are provided by steam probe TCs (in water during preconditioning) and are shown in Figures A-4 and A-5, respectively.

Average cladding temperatures of the guard fuel rods during preconditioning are shown in Figure A-6. TCs located on both the interior and exterior of the guard fuel rod cladding provided axial temperature distributions. Coolant temperatures determined by steam probes at two elevations are also included on Figure A-6 for comparison. Temperatures for exterior TCs for four different fuel rods at three levels are shown in Figure A-7 to illustrate the negligible effect of radial power gradients.

Test fuel rod (cruciform region) temperatures during preconditioning were measured by sixteen interior TCs, four fuel centerline TCs at level 17, and seven exterior TCs at levels 17 and 18. The average of the interior cladding temperatures is shown in Figure A-8 along with plots of average exterior cladding temperatures and the average fuel centerline temperature for level 17.

Pretransient and Transient Test Assembly Temperatures

Pretransient and transient temperature data summaries are presented in Appendices B and C, respectively. Data for four major test assembly components are summarized: the shroud, guard fuel rods, test fuel rods, and instrument lead carriers. The temperatures of subchannel coolant are primarily shown in Appendix D. During early operations and previous transient operation, some sensors failed; data from these sensors are noted "failed" and subsequently deleted from the graphs.

The test assembly coolant temperature profiles across the (corner-to-corner) diagonals for MT-2.2 pretransient operation at level 16 and levels 13, 15, and 17 are shown in Figures B-1 and B-2, respectively. Similar gradients are found in the transient test. These plots are a combination of data from coolant subchannel steam probes and instrument lead carrier TCs.

A set of axial temperature profiles obtained from steam probe, carrier TC, and shroud TC Data for each corner of the shroud during pretransient operation (see Figures B-3 through B-6) shows typical radial temperature gradients of <38 K (70^{o}F) in steam. The steam probes also provide an average axial profile of the coolant during pretransient operation. Figure B-7 shows it for test MT-2.2.

Average fuel rod temperatures recorded during all four transient tests (MT-2.1.1, -2.1.2, -2.1.3 and -2.2) are presented in Figures C-1 through C-8 as averaged values at each of the sensor levels (13, 15, and 17). These data are from TCs located on the guard fuel rod and test fuel cladding interiors. Typical temperature differences between individual guard fuel rods can be seen in the preconditioning data summary, Appendix A.

A set of elapsed time/temperature profiles is also provided in Figure C-9 that shows the axial temperature gradients and average temperatures of the shroud at ten time intervals during the transient, MT-2.2, between the time when steam was shutoff, reflooding was started, and when the shroud was quenched. TC data at the test assembly inlet (level 1), the test assembly outlet (level 20), and the hanger tube (level 21) provide temperature data continuity over the test train.

Figures C-10 through C-19 contain the base temperature histories for each test fuel rod at the sensor levels 13, 15, and 17. These data are from interior TCs, fuel centerline TCs, shroud corner TCs, steam probe TCs, and one exterior cladding TC.

3.2 TEST COOLANT TEMPERATURES

A special section of coolant and shroud transient temperature data for the test assembly and test train are provided in Appendix D. Coolant temperatures for each of the four transient tests are described in this section.

Steam probe temperatures during each transient test (MT-2.1.1, 2.1.2, 2.1.3, and 2.2) are shown in Figures D-1 through D-8. The first graph in each set compares data from levels 1 through 14, and the second, levels 15 through 21. Steam probe TCs measure the temperature of the steam/water environment in the test assembly. Their response is quite similar to that of TCs at the inlet and outlet, levels 1 and 20, respectively. Steam probe and shroud temperatures are also compared for the transient MT-2.2. Results are shown in Figures D-9 through D-12 for levels 10, 13, 15, and 17, respectively.

3.3 POWER COUPLING

The NRU reactor power was recorded by the REDACE computer as a percentage of full reactor power and as megawatts. The reactor powers presented here are based on the percentage of full-power, 127 MW.

Preconditioning Power Coupling

The test assembly power during preconditioning was determined by calorimetric methods at several power levels during the first of the three rises to full reactor power. Test assembly power was determined by the flow rates provided by U-2 loop instrumentation and inlet and outlet temperatures obtained by averaging two of the three test assembly inlet region (level 1) temperatures and three outlet region (level 20) temperatures (see Figures A-3 and A-4 in Appendix A). Using the test assembly temperatures rather than the loop temperatures eliminated the effect of heat losses in the loop piping. The power coupling calculated in this manner is shown in Table 3. The zero value of calculated test assembly power at zero reactor power is a measure of the accuracy of the inlet and outlet temperature difference.

The average coupling value of 25.9 is larger than the value (21.1) determined during preconditioning for the PTH test series and probably represents a difference in the reactor loading between the two tests. It is also larger than the 22.7 coupling found in the MT-1 experiment.

Pretransient Power Coupling

The test assembly power was also determined during the steady-state pretransient operation of MT-2.2 in the same manner used during preconditioning operation. The test assembly power was 139.5 kW and the reactor power was 5.8%, which gives a coupling value of 24.1. This value is also slightly higher than the value (22.8) determined during the PTH test series but is very close to that of the MT-1 experiment (24.3). Section 4.1 outlines another way of computing power which does not rely on flow rate measurements but looks only at transient heating rates for the fuel. This method indicates that the actual test assembly power was 16% less or 117.2 kW.

TABLE 3. Preconditioning Power Coupling

Reactor Power, %	Test Assembly Power, kW	Coupling[a]
0.0	0	--
44.0	1152	26.2
100.0[b]	2562	25.6
	Average	25.9

(a) Coupling is defined as test assembly power divided by percent of full reactor power.
(b) Average of two rises to power.

3.4 NEUTRON FLUX

Neutronics data are presented in Appendix E. SPNDs were mounted in the corners of the test assembly shroud at several levels.

Preconditioning Neutron Flux

Figure E-1 shows the axial distribution of neutron flux in each of the four corners during preconditioning operation. Several of the original SPNDs failed in previous tests, and one (SPND 13 1FSC) responds consistently and suspiciously low. However the operating instruments show that the worst (level 10) radial power skew [(max-min)/nominal] is less than 20%. This power skew is illustrated in Figure E-2, where neutron flux in diagonal corners is compared at levels 10, 17, and 18 during preconditioning.

Pretransient and Transient Neutron Flux

Pretransient neutron flux data are quite similar to preconditioning data, except that power levels are at about 5.8% of full-power levels. The greatest power skew is evident from shroud corner 6A to corner 6F (aproximately 33%) at level 10 (see Figure E-3). No explanation is offered for the ~13% increase from preconditioning to pretransient operations.

Differential neutron flux is being reviewed to investigate the relation between changing coolant density during the reflood period and changing neutron flux in the vicinity of the liquid/vapor interface. Average values of the neutron flux at several levels are illustrated in Figures E-4 through E-6.

3.5 LIQUID LEVEL MEASUREMENTS

A liquid level measuring device was used in the MT-2 test assembly similar to the one used in MT-1 to measure the reflood liquid level during the transient. The device was positioned inside an open-ended cladding tube at rod location 4D (see Figure 3), and it replaced the TCs and SPNDs positioned in the instrument tube (location 4D) during the PTH test series.

The upper end of the liquid displacement float was connected to the core of an LVDT to measure the axial movement of the float. The LLD was designed so that a 3.65-m (12-ft) change in fluid elevation inside the tube would produce a 2.54-cm (1-in) change in movement of the float and LVDT core. The response of the LLD during the MT-2.2 transient is shown in Figure 10. The output from the LLD/LVDT, as shown in Figure 10, could not be correlated with the TC data or hydraulic conditions measured during the transient. Consequently, it is assumed that for some undetermined reason the device was not functioning properly.

3.6 INSTRUMENTATION FAILURE

Since the test train assembly used in this experiment was previously used in MT-1,[3] some of the sensors or instruments that failed during that experiment were not available for this one due to radiation fields that made some repairs/replacements impractical. However, instruments and sensors associated with the test fuel rods were replaced as part of the cruciform test fuel bundle.

Final Pretest Configuration

Checkout of the instrumentation during pretest operations showed that the final instrument status was as recorded in Table 4. Sensors that were not operational are noted as "failed."

MT-2 Instrument Failures

During the course of this experiment some instrument failures were evident. Other failures were not obvious, but the instruments showed a tendency to drift or respond suspiciously high or low compared to neighboring sensors (see Table 5).

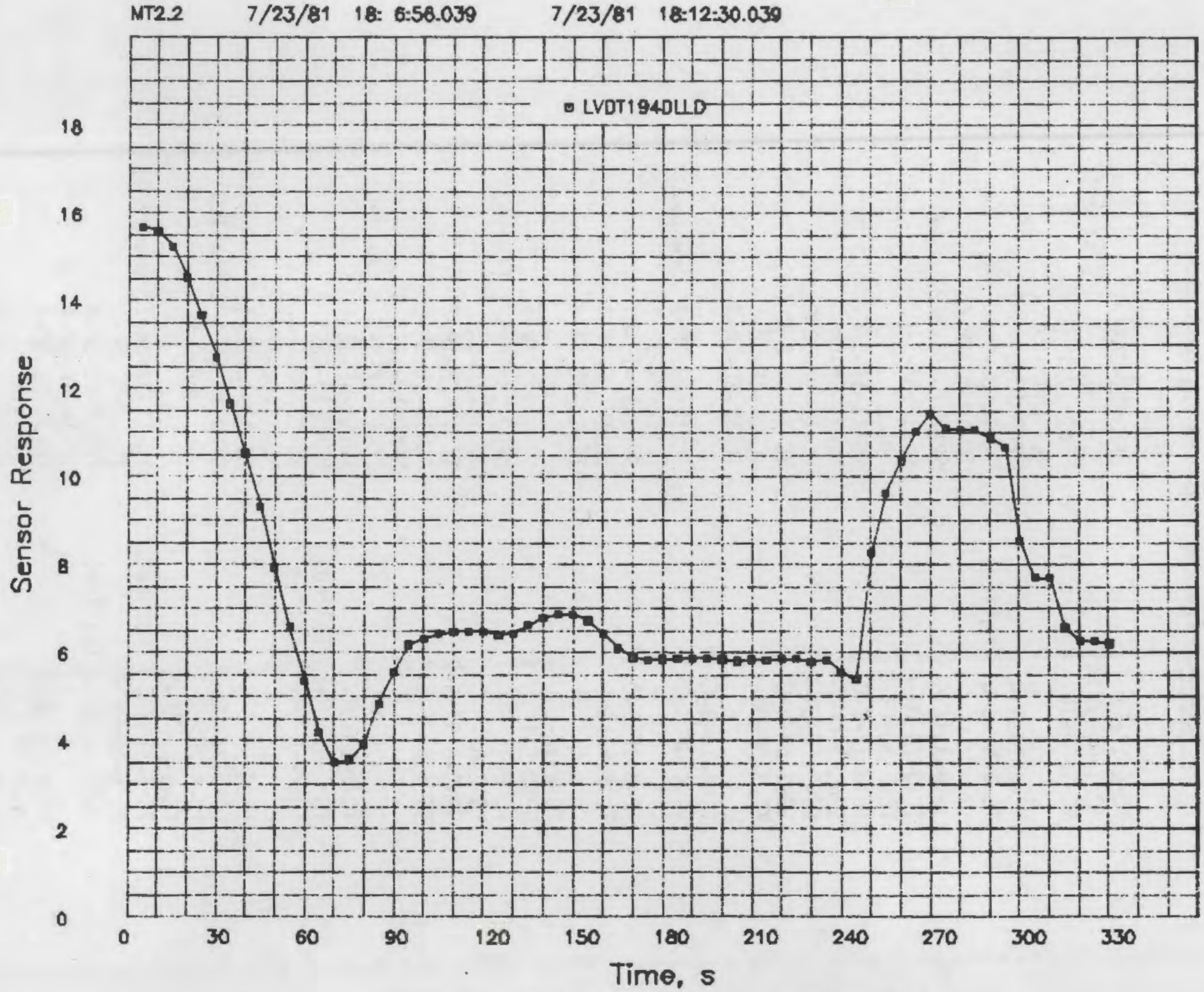

FIGURE 10. LVDT LLD Response Versus Time

TABLE 4. Pretest Instrumentation Status

Instrument	Status
TC-1-1F-IN	
TC-1-4D-IN	
TC-1-6A-IN	
TC-2-1A-S-C	
TC-2-6F-S-C	(failed)
SPND-3-1A-S-1	
TC-3-2B-OR-4	
TC-3-2E-OR-3	
TC-3-1F-S-C	
SPND-3-6F-S-3	
TC-3-5E-OR-2	
TC-3-6A-S-C	
TC-3-5B-OR-1	
TC-4-1A-S-C	
TC-4-6F-S-C	
TC-5-1F-S-C	
TC-5-6A-S-C	
TC-6-1A-S-C	
SPND-6-1F-S-4	
TC-6-1F-S-C	
TC-6-6F-S-C	
SPND-6-6A-S-2	
TC-6-6A-S-C	
TC-7-3A-OR-3	
TC-7-1D-OR-2	
TC-7-4F-OR-1	(failed)
TC-7-6C-OR-4	
TC-8-1A-S-C	
TC-8-2B-OR-4	
TC-8-2E-OR-3	
TC-8-2E-OR-3	
TC-8-6F-S-C	(failed)
TC-8-5E-OR-2	
TC-8-5B-OR-1	(failed)
TC-9-2B-OR-4	
TC-9-1F-S-C	
TC-9-2E-OR-3	
TC-9-5E-OR-2	
TC-9-6A-S-C	
TC-9-5B-OR-1	
SPND-10-1A-S-1	
TC-10-1A-S-C	(failed)
SPND-10-1F-S-4	
TC-10-1F-S-C	
SPND-10-6F-S-3	
TC-10-6F-S-C	
TC-10-4D-SP-4	
SPND-10-6A-S-2	
TC-10-6A-S-C	
TC-11-1A-S-C	
TC-11-3A-OR-3	
TC-11-1D-OR-2	
TC-11-6F-S-C	
TC-11-4F-OR-1	
TC-11-6C-OR-4	
TC-12-2B-SP-2	(removed)
TC-12-2E-SP-1	
SPND-12-1F-C	
TC-12-5E-SP-4	
TC-12-5B-SP-3	
TC-13-3A-IR-4	
SPND-13-1A-S-1	(failed)
TC-13-1A-S-C	
TC-13-3B-IR-2	
TC-13-1D-IR-2	
SPND-13-1F-S-4	
TC-13-1F-S-C	(failed)
TC-13-4F-IR-4	
SPND-13-6F-S-3	
TC-13-6F-S-C	
TC-13-6C-IR-2	
TC-13-4D-SP-4	
SPND-13-6A-S-2	(failed)
TC-13-6A-S-C	
TC-14-2B-SP-2	(removed)
TC-14-2E-SP-1	
TC-14-5E-SP-4	
TC-14-4D-SP-4	
TC-14-5B-SP-3	
TC-15-3A-IR-2	
SPND-15-1A-S-1	
TC-15-1A-S-C	
TC-15-3B-IR-4	

TABLE 4. contd

TC-15-3C-IR-1	TC-17-5E-IR-C
TC-15-3C-IR-C	TC-17-5E-IR-4
TC-15-3C-IR-7	TC-17-5D-OR-3
TC-15-3C-IR-2	TC-17-5D-IR-4
TC-15-1D-IR-4	TC-17-4D-SP-4
SPND-15-1F-S-4	SPND-17-6A-S-2 (failed)
TC-15-1F-S-C (failed)	TC-17-6A-S-C
TC-15-2E-IR-3	TC-17-4C-IR-1
TC-15-2E-IR-C	TC-17-4C-IR-C
TC-15-2E-IR-1	TC-17-4C-IR-3
TC-15-4F-IR-2	
SPND-15-6F-S-3	SPND-18-1A-S-1
TC-15-6F-S-C	TC-18-1A-S-C
TC-15-4D-SP-4	TC-18-2C-OR-1
TC-15-6C-IR-4	TC-18-2C-IR-2
SPND-15-6A-S-2	TC-18-3E-OR-4
TC-15-6A-S-C	TC-18-3E-IR-1 (failed)
TC-15-5B-IR-1	TC-18-1F-S-C (failed)
TC-15-5B-IR-C	TC-18-4E-OR-4
TC-15-5B-IR-3	TC-18-4E-IR-1
	SPND-18-6F-S-3
TC-16-1A-C-2	TC-18-6F-S-C
TC-16-2B-SP-2 (removed)	TC-18-5C-OR-3
TC-16-2E-SP-1	TC-18-5C-IR-4
SPND-16-1F-C	TC-18-6A-S-C
TC-16-1F-C-1	TC-18-4B-OR-3
TC-16-6F-C-4	
TC-16-5E-SP-4 (failed)	PS-19-3B-C
TC-16-4D-SP-4	PTK-19-3C-C
TC-16-5B-SP-3	PS-19-2C-C
TC-16-6A-C-3	PS-19-2D-C
	PS-19-3D-C
SPND-17-1A-S-1	PS-19-3E-C
TC-17-1A-S-C	PS-19-4E-C
TC-17-2B-IR-4	PS-19-5D-C
TC-17-2B-IR-C	PTS-19-5C-C-1
TC-17-2B-IR-2	PTS-19-5C-C-2
TC-17-2D-OR-1	PS-19-4C-C
TC-17-2D-IR-2	PS-19-4B-C
SPND-17-1F-S-4 (failed)	
TC-17-1F-S-C	TC-20-OT-2
TC-17-3D-IR-4	TC-20-OT-3
TC-17-3D-IR-3	TC-20-OT-1
TC-17-3D-IR-C	
TC-17-3D-IR-5	TC-21-HT-4
SPND-17-6F-S-3	TC-21-HT-3
TC-17-6F-S-C	TC-21-HT-2
TC-17-5E-IR-2	TC-21-HT-1

TABLE 5. Instruments Failed During MT-2

TC-3-6A-S-C
TC-7-1D-OR-2
TC-7-6C-OR-4
TC-11-6C-OR-4
TC-14-5B-SP-3
TC-16-6A-C-3
TC-16-2E-SP-1
PTK-19-3C-C
PTS-19-5C-C

3.7 REFLOOD FLOW MEASUREMENTS

The reflood flow system included a Fisher-Porter turbine flowmeter in the high flow rate line and series-connected Barton and Fisher-Porter turbine flowmeters in a parallel low flow rate line. A parallel standby reflood line was also provided to supply emergency reflood coolant. However, the standby line was not used during the MT-2 experiment.

The reflood control system was calibrated before the first transient using steam probe data to monitor the water/steam interface during reflood operation. Prior to the pretransient test phase, two reflood flow tests were performed at 0.013 m/s (0.5 in/s) and 0.025 m/s (1.0 in/s) to calibrate the reflood loop (see Figures F-1 and F-2 for the flow rate recordings).

Steam probe temperature histories provided independent measurements of the reflood coolant level (and reflood flow rate) in the test assembly. Figures F-3 and F-4 provided the data for the first pretest reflood rate calibration (measuring the time required between subsequent level quenches).

Transient test starting times and reflood delay times are dependent on the flow conditions at the bottom of the active fuel. These flow conditions are related to the temperature response of TCs located at instrument level 1, which is located 0.013 m (0.5 in) below the active fuel. The transients start when steam coolant is shut off, as determined from a quick drop in temperature at level 1. The reflood initiation times occur when the reflood water quenches TCs at level 1, as indicated by a second quick drop in temperature at level 1.

At the start of each reflood transient test, a fast reflood rate was used to bring the reflood coolant level up to the bottom of the fuel rods (instrument level 1). The demand control valve in the high flow rate reflood line was preset fully open for 2 s. After 2 s, solenoid valves switched flow to the low flow line where the flow control valve was preset to 0.05 m/s (2.0 in/s) and subsequently controlled to as low as 0.013 m/s (0.5 in/s).

The first three reflood transients (MT-2.1.1, -2.1.2, and -2.1.3) used different combinations of reflood rates (see Figures F-5 through F-12, which illustrate the hydraulic inertia and "overshoot" as flow rates are changed). The reflood initiation time for MT-2.1.1 was July 23, 1981, at 12:41:21. The reflood initiation time for MT-2.1.2 was July 23, 1981, at 14:53:38, and for MT-2.1.3 was July 23, 1981, at 16:49:29. Liquid/steam entrainment (or splashing) during reflood cooling is also evident in the steam probe data collected during the transients (see Figures F-7, F-10, and F-13).

The principal transient test (MT-2.2) used four reflood rates that varied from 0.254 to 0.013 m/s (10 to 0.5 in/s) over a period of about 300 s (see Figures F-14 and F-15). The reflood initiation time for MT-2.2 was July 23 at 18:07:32. Steam probe temperatures oscillate markedly as the probes are repeatedly quenched by entrained water droplets and dried out by steam. An indication of this mechanism is shown in Figure F-16, where steam probe data are shown for four instrumentation levels. Inlet reflood water temperature varied from 303 to about 328 K (85 to 130^{O}F) during the principal transient (see Figure F-17).

3.8 FUEL ROD PLENUM PRESSURE MEASUREMENTS

Gas pressure changes in the plenums of the test rods were determined using pressure switches attached to the upper ends of nine of the test fuel rods and pressure transducers attached to two (3C and 5C) of the test fuel rods. Eleven test fuel rods were pressurized with helium to 3.1 MPa (450 psig) at room temperature and are located in the bundle as shown in Figure 6 (level 19).

Pressure Switches

Pressure switches are electrical devices[5] that indicate a change in output when the pressure in the fuel rod plenum drops below a cutoff pressure level. In the MT-2 experiment, the switch consisted of a bare TC junction that was grounded when the plenum pressure exceeded the cutoff pressure level and switched to an ungrounded mode (open position) when the pressure dropped below the cutoff level. The temperature of the bare TC junction and the electrical output of the grounded circuit are plotted in Figures G-1, G-2, and G-3. The upper group of curves on each figure shows the temperature of the bare TC junction as a function of time; the lower group, the output of the TC junction to a grounded circuit plotted as relative output. The latter curves show a stable output as long as the plenum pressure is above the cutoff pressure, which for the operating temperature of MT-2 is about 2.07 MPa (300 psia). When the pressure dropped below the cutoff pressure, the grounded circuit TC response either disappeared or its behavior changed radically.

If rupture of the cladding occurs, the change in the switch output does not necessarily indicate the time of fuel rod rupture. The helium communication delay due to the tortuous path through the pellet stack between the location of the fuel rod rupture site and the fuel rod plenum must be considered.

Pressure switches on five fuel rods--3B, 4B, 2D, 3D, and 5D--indicated that plenum pressures dropped below the cutoff pressure of ~2.07 MPa (300 psia) between 55 and 65 s into the transient. The pressure switches on rods 4E and 3E indicated (Figure G-2) that their plenum pressures dropped below 2.07 MPa (300 psia) at 225 and 120 s, respectively. The output from pressure switches on rods 2C and 4C showed pressures below 2.07 MPa (300 psia) prior to the transient; however, the output from their TC circuits were recorded (see Figures G-3 and G-1, respectively, and Table 6).

Pressure Transducers

Two test fuel rods (3C and 5C) were fitted with pressure transducers to measure the changing fuel rod plenum pressure during the transient. One transducer operated on the eddy current principle (identified in Figure 6 as PTK) and the other used an LVDT [identifed in Figure 6 (level 19) as PTS-19-5C-C].

TABLE 6. Summary of Pressure Switch and Pressure Transducer Data

Fuel Rod	Rupture Time(s)[a]	Type of Instrument
3B	58	PS[b]
4B	66	PS
2C	Switch open before transient	PS
3C	Failed before transient	PTK[c]
4C	Switch open before transient	PS
5C	Failed before transient	PTS[d]
2D	66	PS
3D	67	PS
5D	68	PS
3E	67[e]	PS
4E	65	PS

(a) Time into transient when plenum pressure dropped below ~2.07 MPa (300 psia).
(b) PS = pressure switch.
(c) PTK = pressure transducer, eddy current type.
(d) PTS = pressure transducer, LVDT bellows type.
(e) Questionable rupture time.

Both of these transducers failed before the transient (Figure G-4); however, transducer PTK appeared to operate satisfactorily during preconditioning.

Summary of Pressure Switch and Pressure Transducer Data

Pressure switch and pressure transducer data are summarized in Table 6. Rods 3B, 4B, 2D, 3D, 5D, 3E, and 4E showed plenum pressure reductions below ~2.07 MPa (300 psia), which indicated cladding ballooning and possibly rupture. The switches on rods 2C and 4C were open prior to the transient, indicating a loss of pressure (prior to the transient). The pressure transducer on rod 5C (PTS-19-5C-C) operated satisfactorily during the preconditioning period but either the transducer failed or the rod lost pressure or both prior to the transient. Since the transducer on rod 3C (PTK-19-3C-C) failed before the test assembly was inserted into the reactor, no conclusions can be drawn from the data. However, the results of a posttest (DERM) examination showed that all rods except 3C, 4C, and 5C had ruptured.

4.0 TEST RESULT ANALYSIS

Two computer codes, TRUMP-FLECHT and FRAP-T5, were used to predict fuel cladding temperature behavior of the MT-2.2 LOCA test. Section 4.1 presents the TRUMP-FLECHT analysis, and Section 4.2 presents the FRAP-T5 calculations.

4.1 COMPARISON OF DATA WITH TRUMP-FLECHT CODE ANALYSES

Pretest calculations were made using heat transfer coefficients determined from the FLECHT correlation[6] as input to the TRUMP heat conduction code. The FLECHT correlation used in these calculations was outside the range of conditions for which it is valid. However, the code predicted the time/temperature relationships for constant reflood rate tests of the PTH test series and the MT-1 experiment quite well. The FLECHT correlation input was modified to accommodate the changes in reflood rate used during the course of MT-2.2. The heat transfer coefficients calculated were then used as input to the TRUMP code.

Two values of average fuel rod power were used in the calculations. The fixed value--1.230 kW/m (0.375 kW/ft)--was obtained from calorimetric calculations summarized in Section 3.3.2. The second method used interior cladding temperature ramp rates during the nominally adiabatic heatup period between the times when the steam cooling was turned off and the reflood cooling was turned on. The temperature ramp rate is a function of the rod power at the TC location and of the effective heat capacity of the rod. The local power of each TC elevation was determined with this technique. Integration of the axial power distribution so obtained gave an average fuel rod power of 1.033 kW/m (0.315 kW/ft). A difference of about 16% between the calorimetric and adiabatic power calculation techniques is evident.

The power calculation method using temperature ramp rates was checked against four thermal-hydraulic test calorimetric power results and against MT-1 calorimetric power results. The temperature ramp calculation agreed reasonably well with the calorimetric power result; but, in all cases, the powers deduced from the ramp rates were less than the calorimetric values. Sources of error in both methods of calculation are being investigated.

Subsequent discussions with reactor personnel indicated the probability that sensor pressure lines from the steam flow meter were improperly bled, and consequently, the data may have been biased.

Figures 11 through 13 compare measured cladding temperature data with the predictions from FLECHT-TRUMP calculations for both the temperature ramp and calorimetric values of test fuel rod linear power. These figures illustrate temperature histories at levels 13, 15, and 17, 1.94 m (76.3 in), 2.47 m (97.3 in), and 3.00 m (118.3 in), respectively. The predictions based upon an average fuel rod power (deduced from temperature ramp calculations) of 1.033 kW/m (0.315 kW/ft) are closest to measured temperatures.

4.2 COMPARISON OF DATA WITH FRAP-T5 CALCULATIONS

The MT-2.2 transient test was also simulated with the FRAP-T5[7] computer program. The varying reflood rate was input directly to the code as a function of time (Figure F-14).

Fuel cladding temperature histories predicted by the code are compared with test data for different axial positions, as shown in Figures 14, 15, and 16. At axial level 13 [1.94 m (76.3 in)], the FRAP-T5 predicted temperatures are about 100 K ($180^{o}F$) lower than the data. At level 15 [2.47 m (97.3 in)], however, the code calculation is approximately correct in magnitude but the shape of the temperature-time curve is not. The level 17 [3.00 m (118.3 in)] comparison is reasonable, except that the code predicts the peak temperature to occur almost 40 s before the measured data.

FRAP-T5 also calculated fuel cladding deformation during the simulation. These results are shown in Figure 17 as percent hoop strain versus axial position for Rod MT2-2D. The data, at a cladding rupture location, were collected with the DERM (Disassembly, Examination, and Reassembly Machine) during the posttest examination. The time of fuel cladding rupture predicted by FRAP-T5 was approximately 120 s into the transient. Measurements indicated that the fuel rods actually ruptured at about 65 s (see Figure G-2 and Table 6).

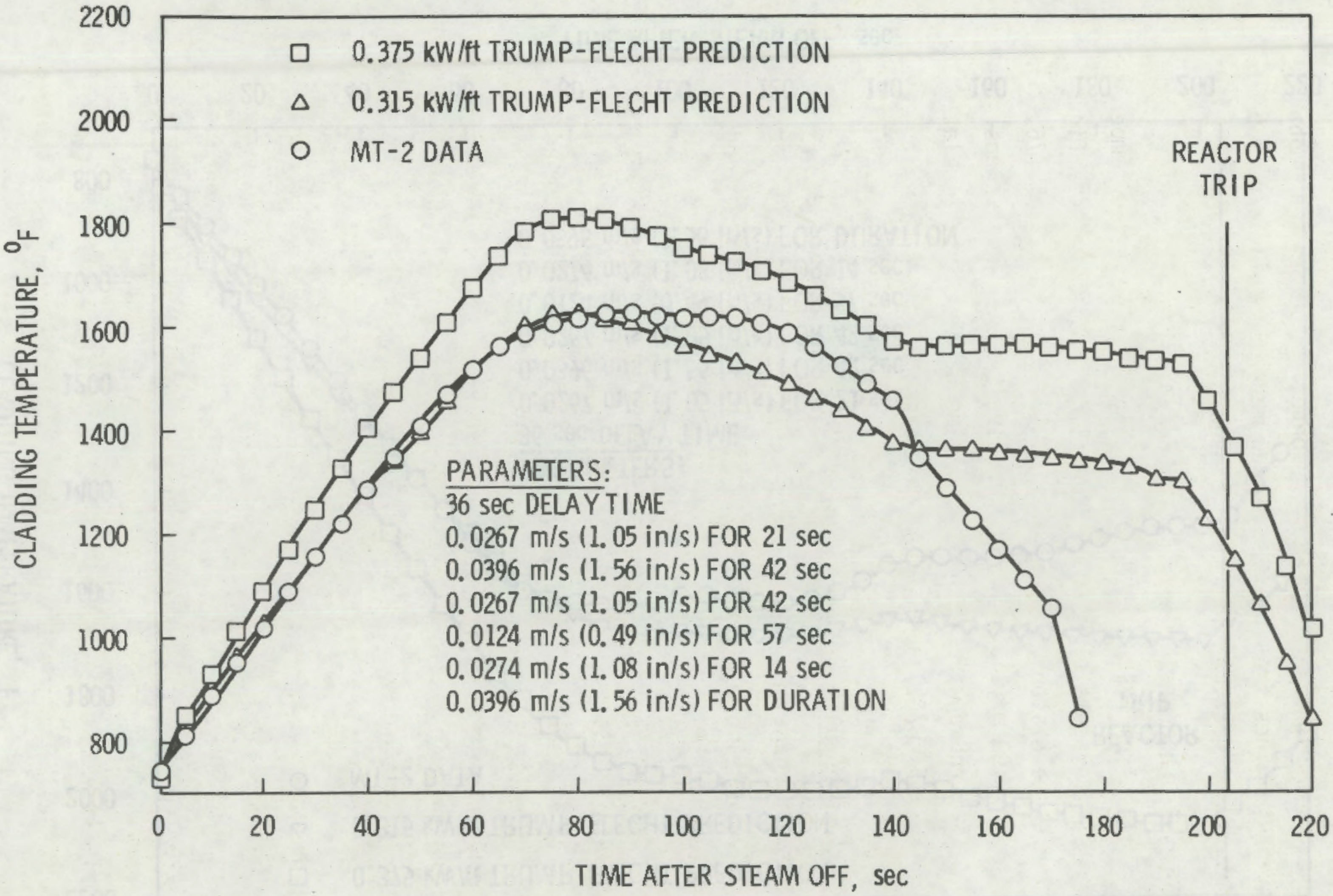

FIGURE 11. Comparison of Cladding Temperature at Level 13 in MT-2.2 with TRUMP-FLECHT Calculations

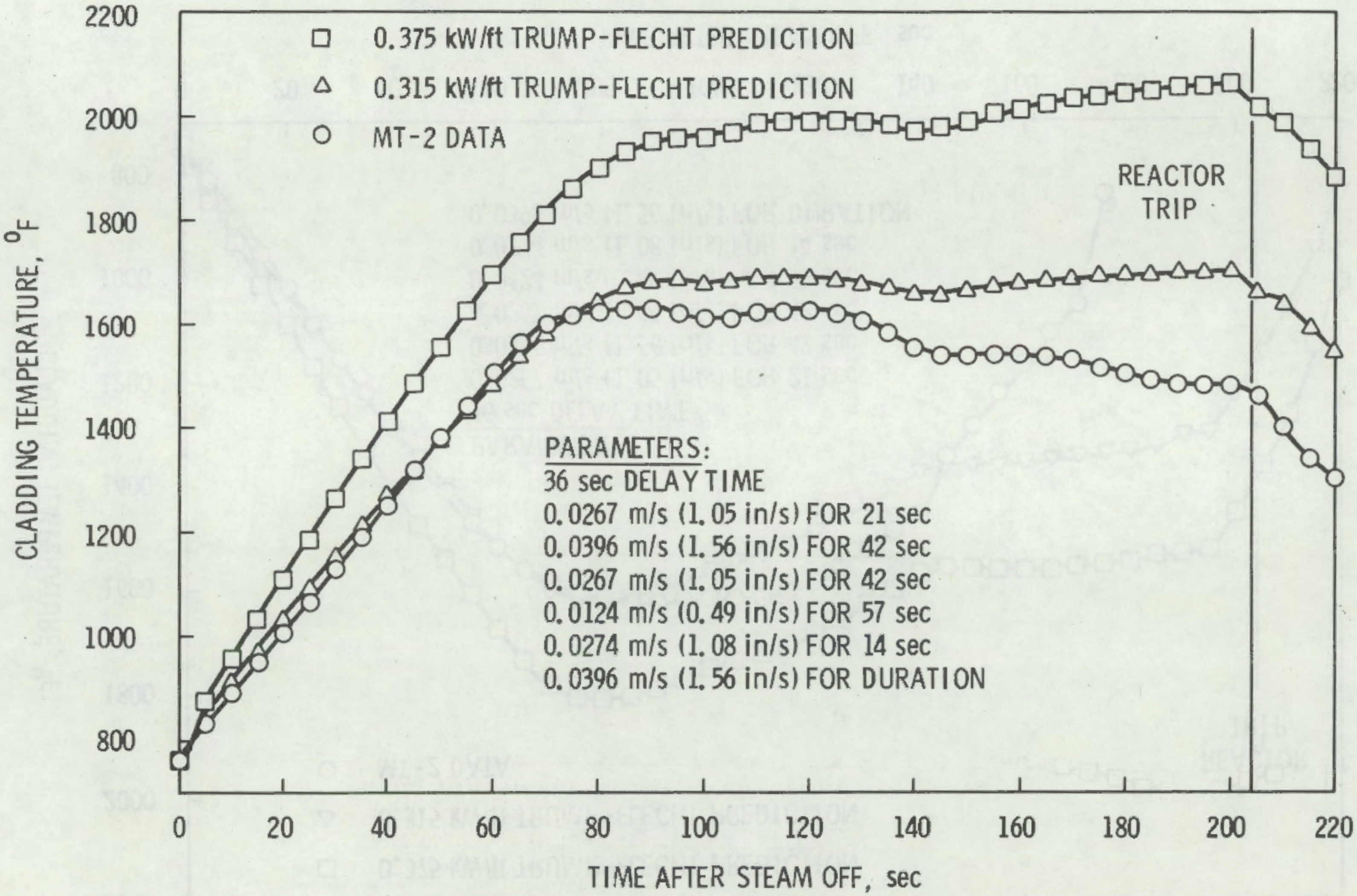

FIGURE 12. Comparison of Cladding Temperatures at Level 15 in MT-2.2 with TRUMP-FLECHT Calculations

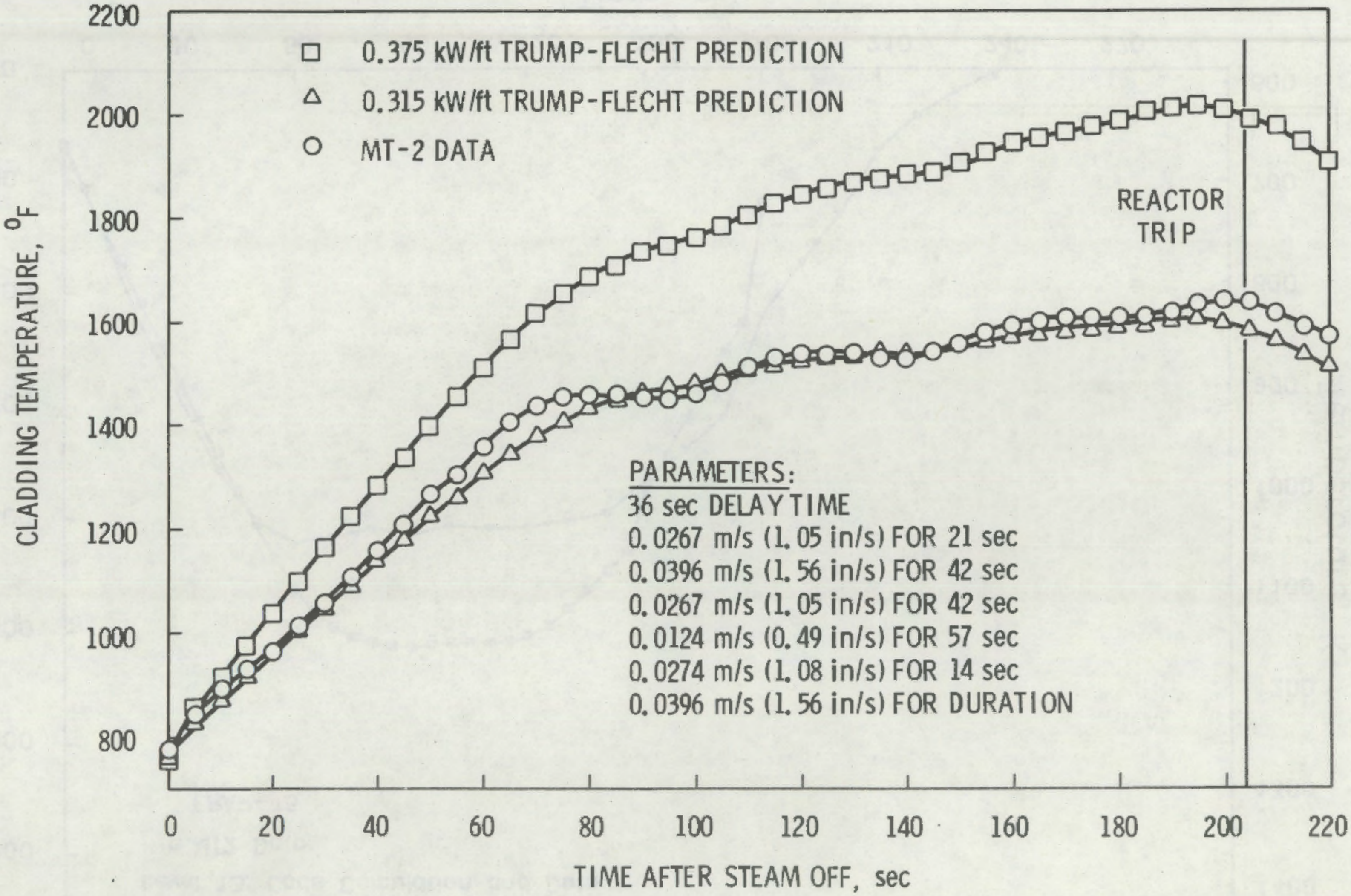

FIGURE 13. Comparison of Cladding Temperatures at Level 17 in MT-2.2 with TRUMP-FLECHT Calculations

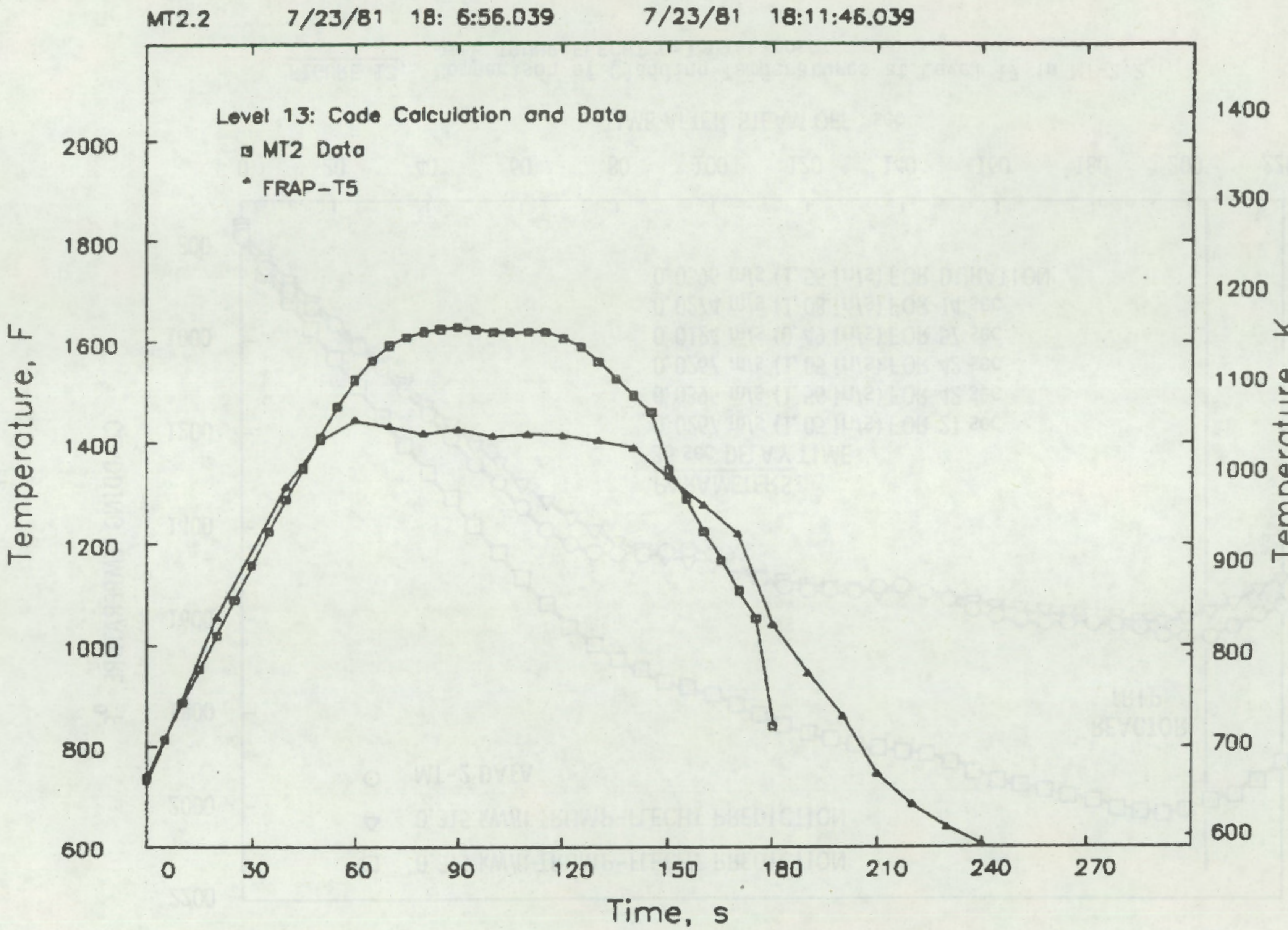

FIGURE 14. Comparison of Cladding Temperatures at Level 13 in MT-2.2

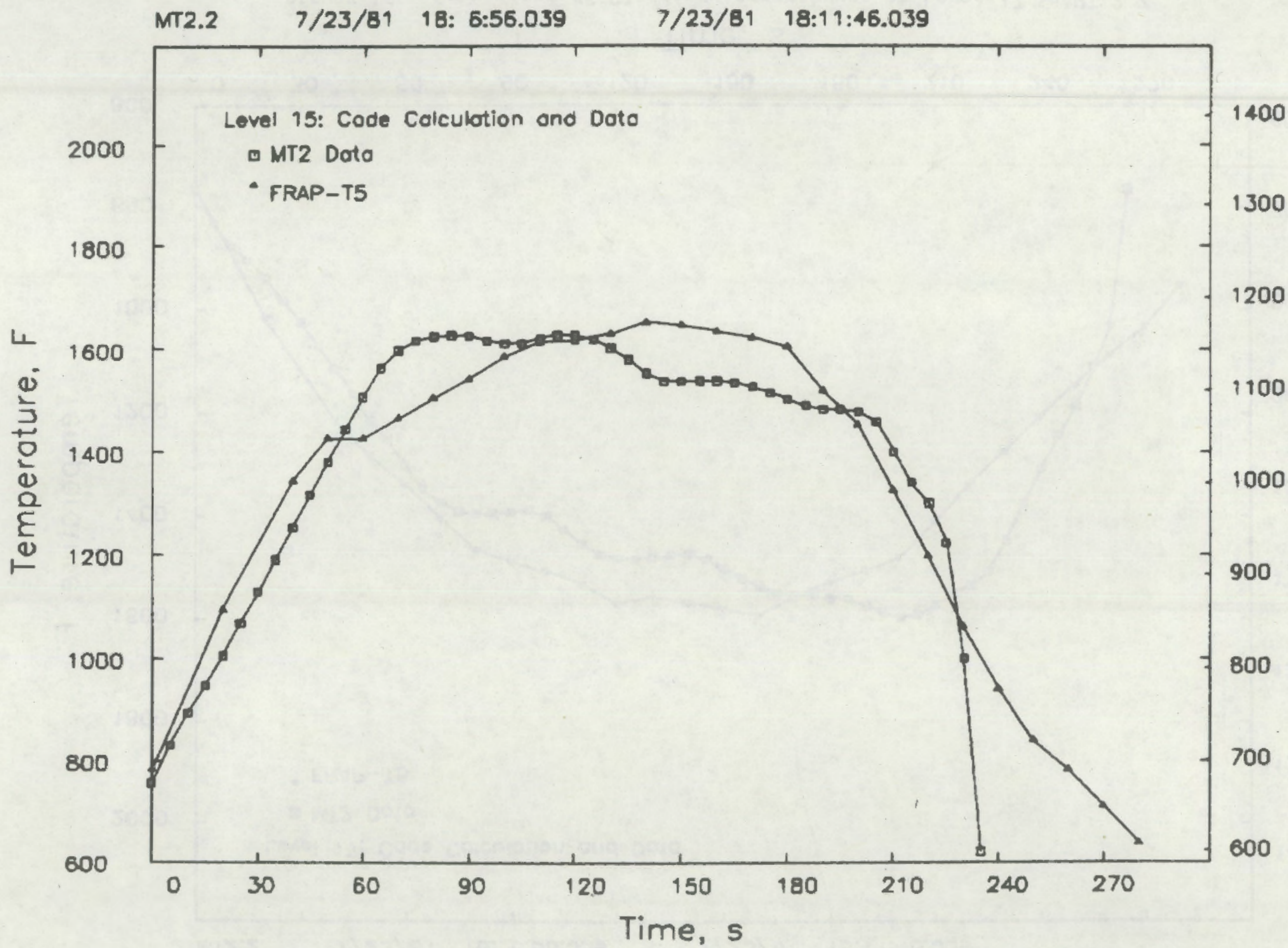

FIGURE 15. Comparison of Cladding Temperatures at Level 15 in MT-2.2

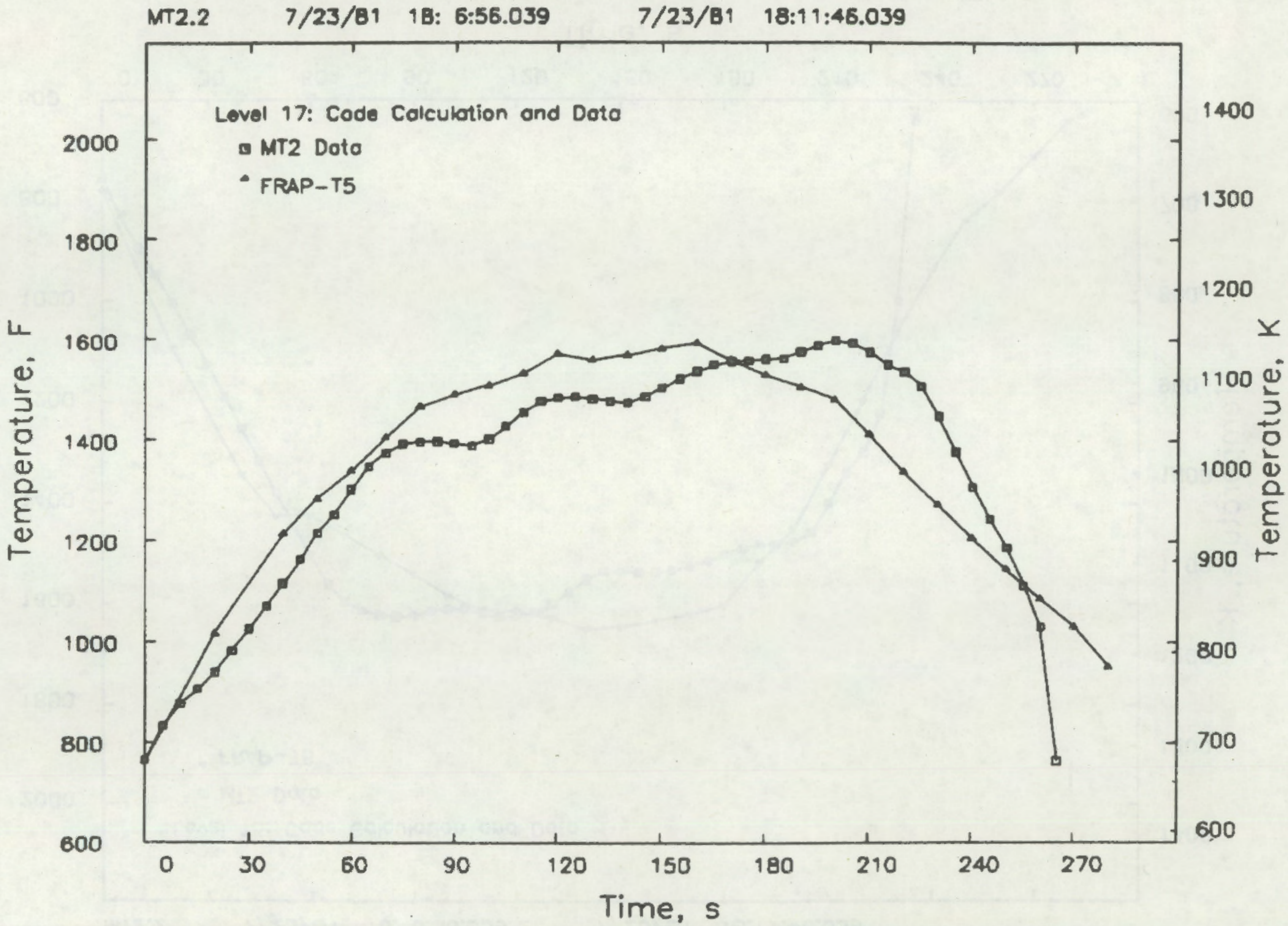

FIGURE 16. Comparison of Cladding Temperatures at Level 17 in MT-2.2

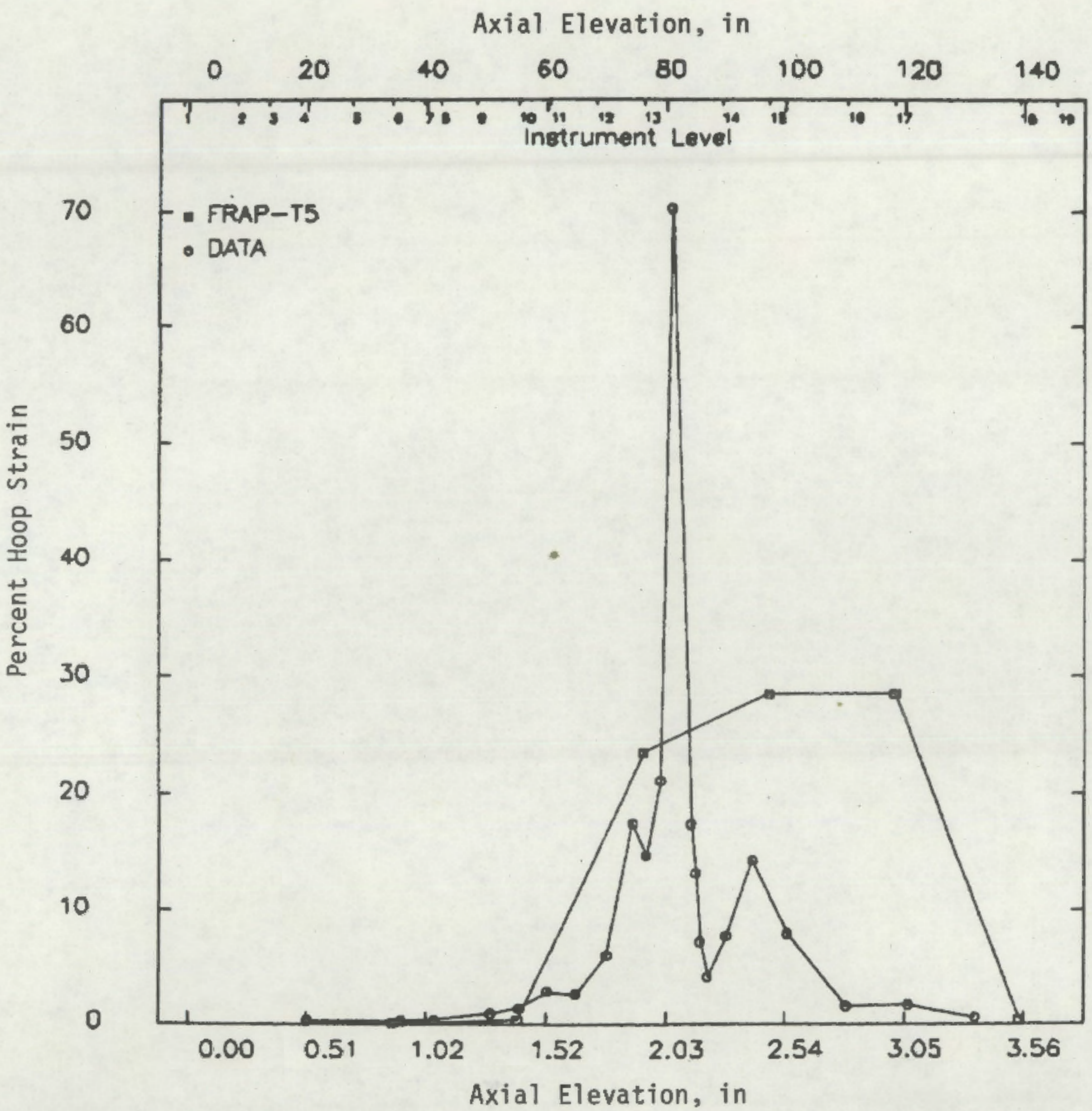

FIGURE 17. Cladding Deformation Measurements and Computer Code Predictions for Rod MT2-2D

5.0 VISUAL AND PHOTOGRAPHIC EXAMINATION

Mensuration data for the MT-2 test assembly and fuel rods were collected and computer-stored using the Disassembly, Examination, and Reassembly Machine (DERM). The DERM was designed to remotely perform these functions on the radioactive test assembly components when they are available for postirradiation examination. Within 48 hr of the MT-2 experiment conclusion, the visual examinations and data collection were well underway.

The test train assembly was placed on the DERM for visual examination under 1.83 in (6.0 ft) of water in the CRNL fuel rod bay. Television scans and visual inspection of the shroud seal surfaces indicated minimum distortion of the shroud. The following Sections 5.1 and 5.2 provide a summary of the guard fuel bundle and test fuel rod bundle examination.

Appendix H provides a summary of the bundle and single rod mensuration data collected with the DERM around the rupture zone. Fuel rod bundle deformation is shown at five elevations near the rupture region (Figures H-1 through H-5). The deformation shown illustrates the relative diametral strain (or rupture) and the unrestrained lateral fuel rod (bowing) movement. Examples of the detailed individual fuel rod data are also shown for a ruptured fuel rod (2C) and an unruptured fuel rod (3C) in Figures H-6 through H-8 and H-9 through H-11, respectively. In summary, the axial profiles of fuel cladding diametral deformation are provided for all of the test fuel rods in the Figures H-12 through H-22. Further reduction and analysis of this data will be provided later in a topical report.

5.1 GUARD FUEL ROD BUNDLE EXAMINATION

One side of the shroud was removed for visual inspection and television scanning of the guard fuel rod bundle. No photographs were made of the guard bundle in place. Although visual examination indicated some distortion of the guard fuel rods in the vicinity of instrument levels 13, 15, and 17, this distortion was less than 0.102 cm (0.04 in).

5.2 TEST FUEL ROD BUNDLE EXAMINATION

Visual examination first indicated that at least six rods were ruptured above instrument level 13 [1.94 m (76.3 in) above the bottom of the test assembly]. After disassembly of the test fuel rod bundle, it was determined that all fuel rods except 3C, 4C, and 5C had ruptured. A visual interpretation of the rod failure pattern is shown in Figure 18 as viewed from the top of the test assembly.

Television scans and photographs were taken with the test fuel rod bundle in place but with half of the guard fuel rod bundle and shroud (side 1) removed (see Figure 19). After the test fuel rod bundle was removed from the shroud and guard fuel rod bundle, three of its exposed sides (Side 6, Side A, and Side F) were photographed (see Figures 20, 21, and 22, respectively). These photographs were taken near instrument level 13. Subsequently, each fuel rod was individualy measured and photographed. Figures 23 through 27 indicate typical cladding ruptures.

The orientation of the Figures H-1 through H-5 are viewed from the bottom of the assembly looking toward the top. It is very important to orient the rods and bundle with reference to the reactor orientation, i.e., North and South. The photographs (Figures 23 through 27) show a side orientation which is referenced from the feducial mark on each rod located (South) and the view angle which is the direction the viewer must face to look at the rod in question. The view angle is indicated in each photograph.

There is an additional orientation for photograph interpretation. All photographs are inverted mirror images.

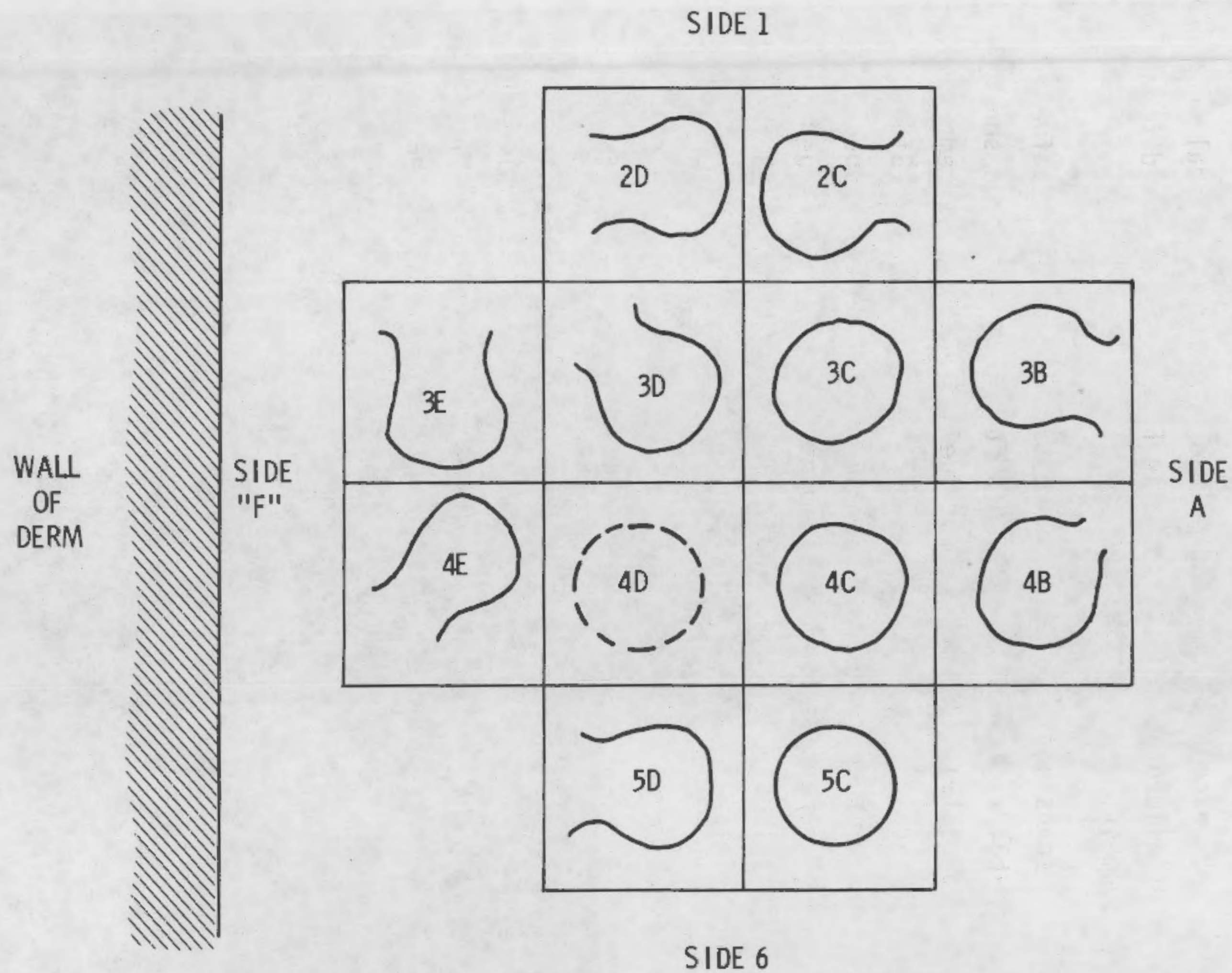

FIGURE 18. Visual Interpretation of Fuel Rod Ruptures Viewed from Top End

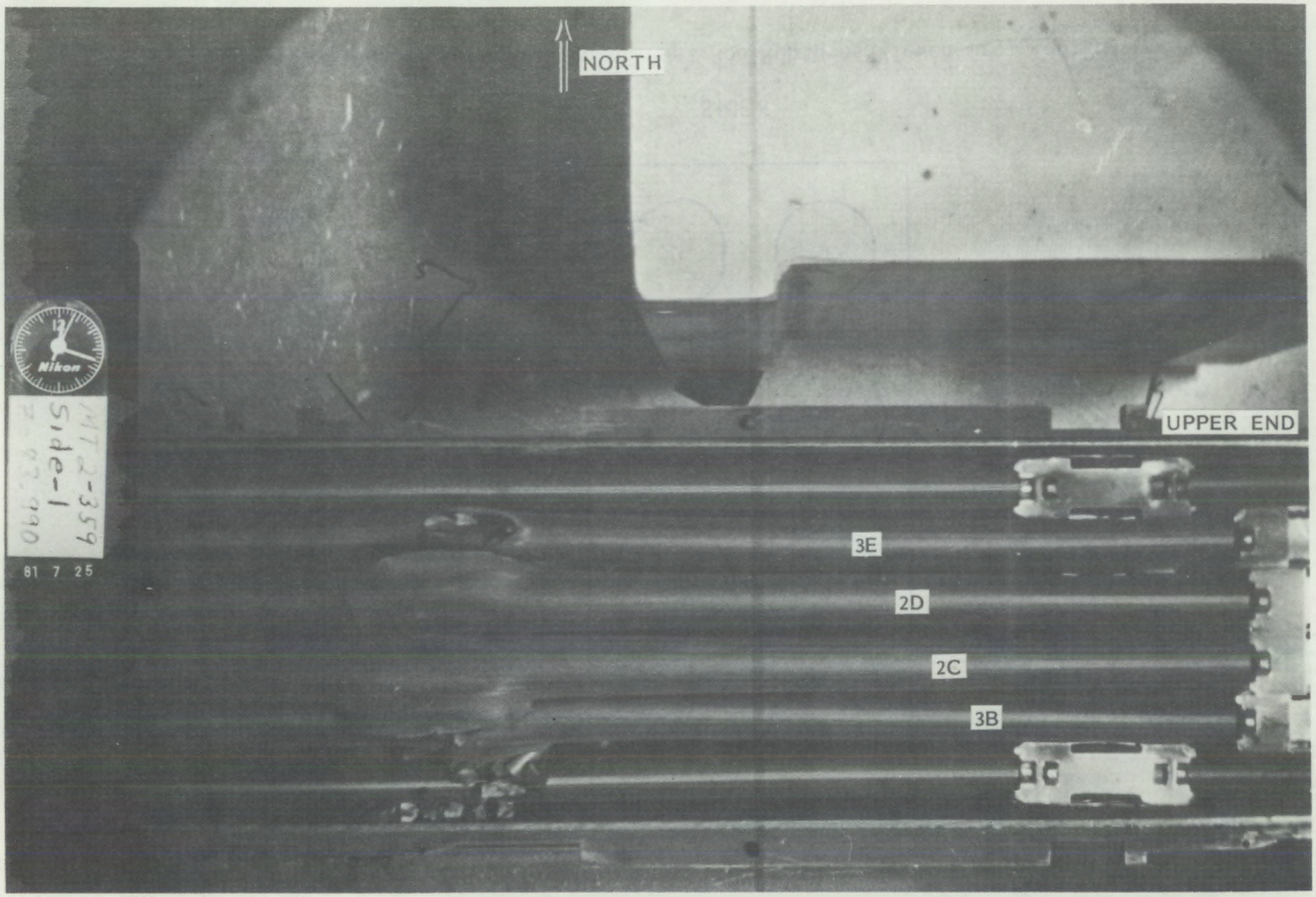

FIGURE 19. Fuel Rod Rupture Zone with One-Half of the Shroud and Guard Rods Removed

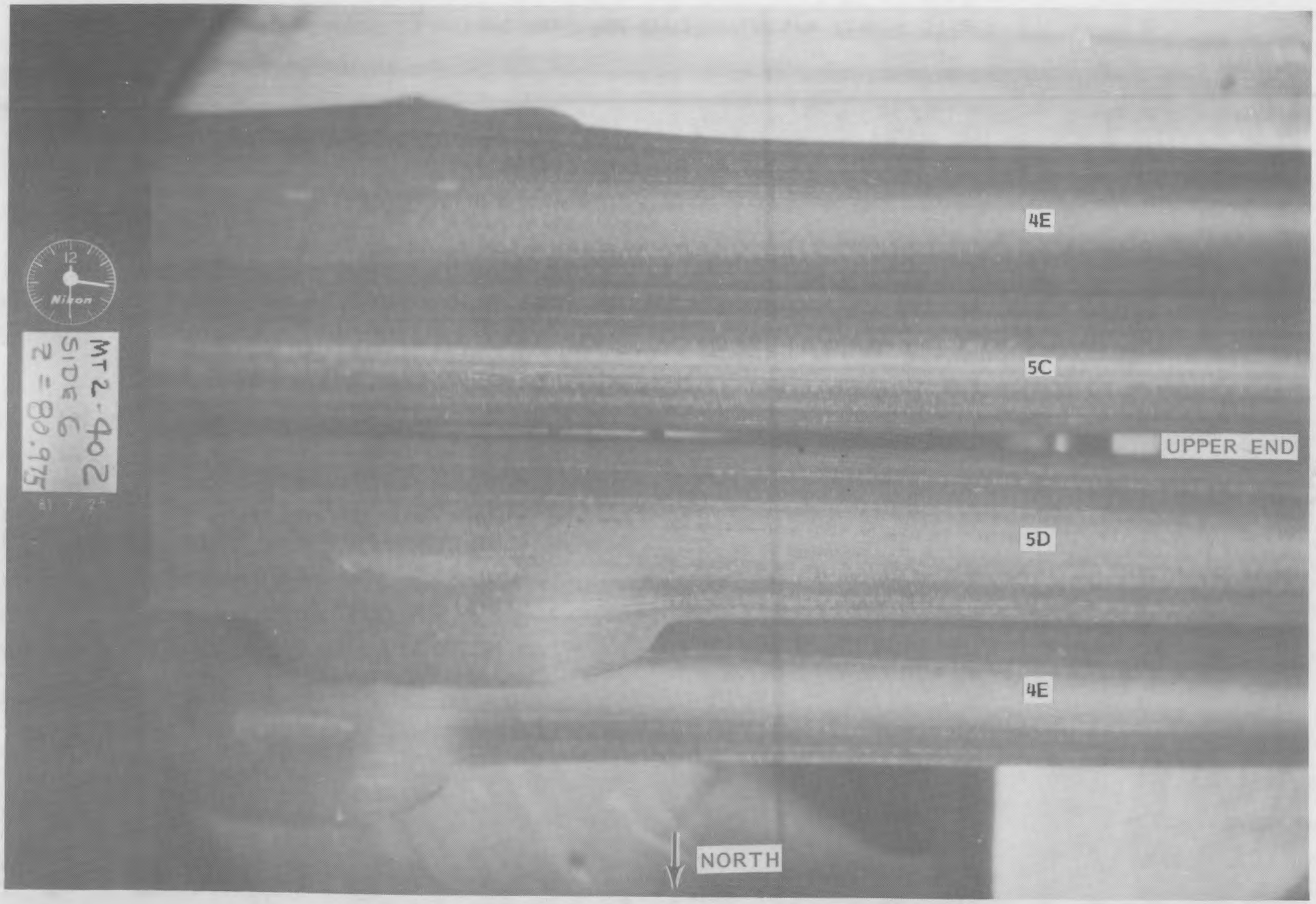

FIGURE 20. Test Fuel Rod Bundle Rupture Zone - Side 6

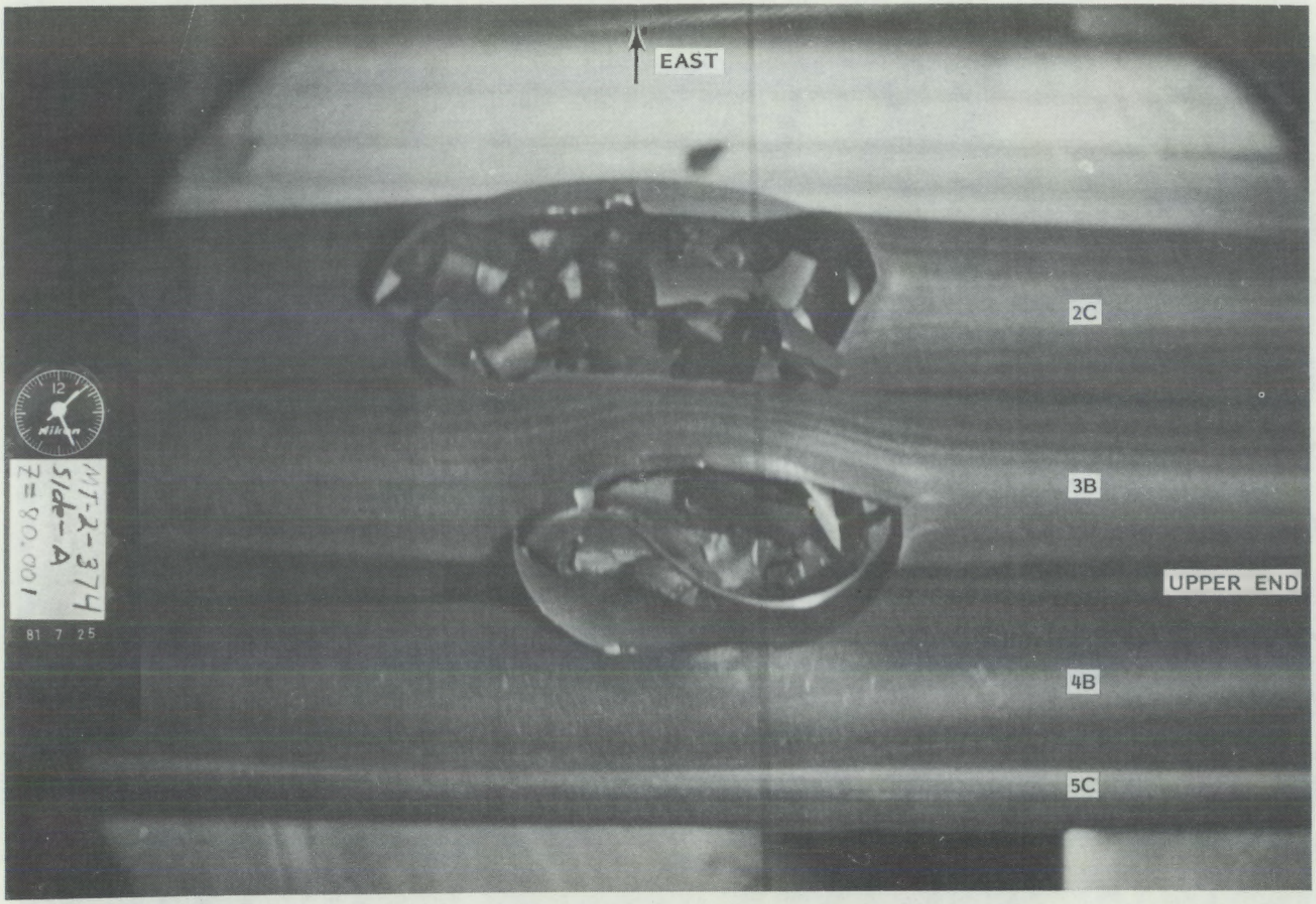

FIGURE 21. Test Fuel Rod Bundle Rupture Zone - Side A

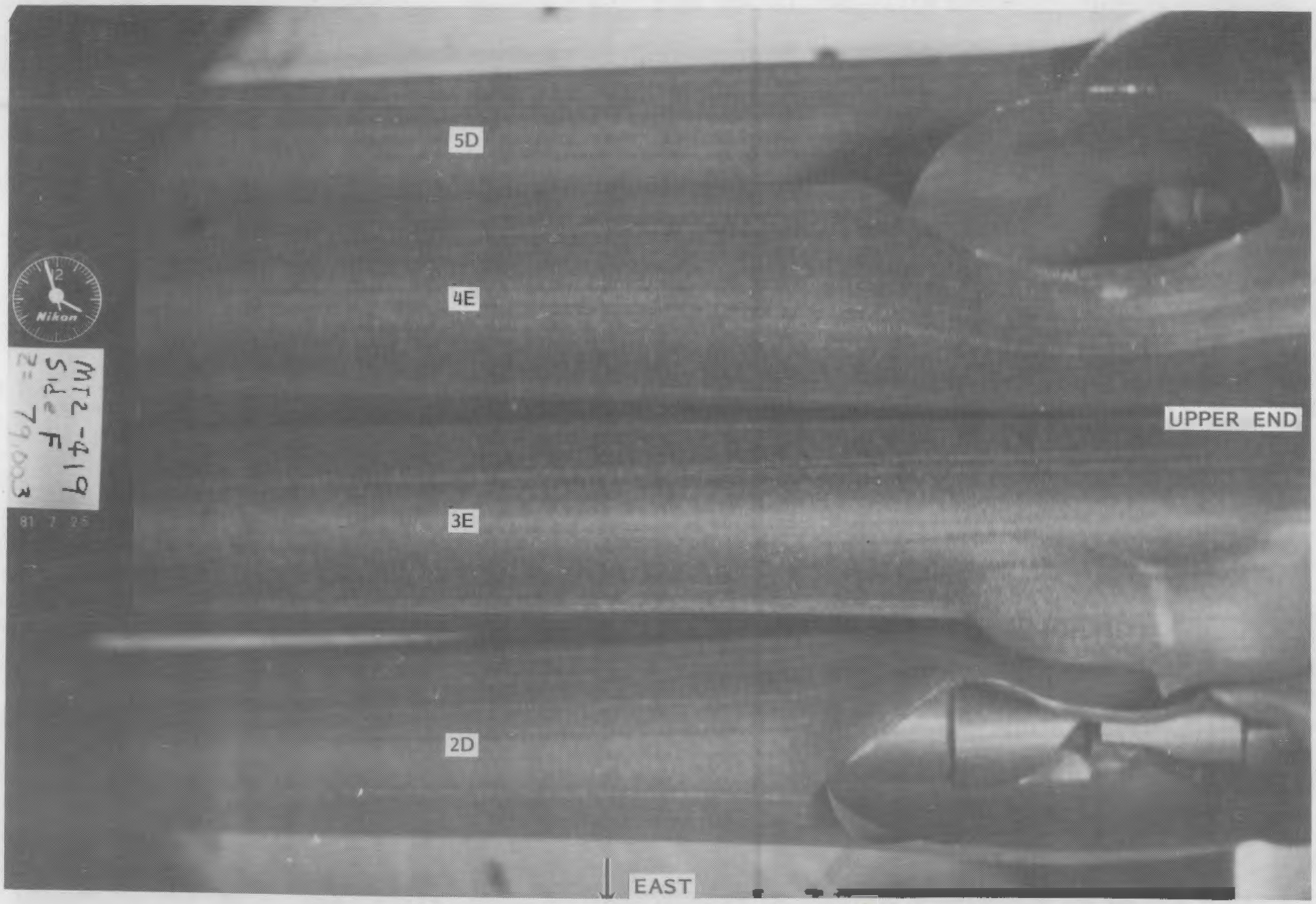

FIGURE 22. Test Fuel Rod Bundle Rupture Zone - Side F

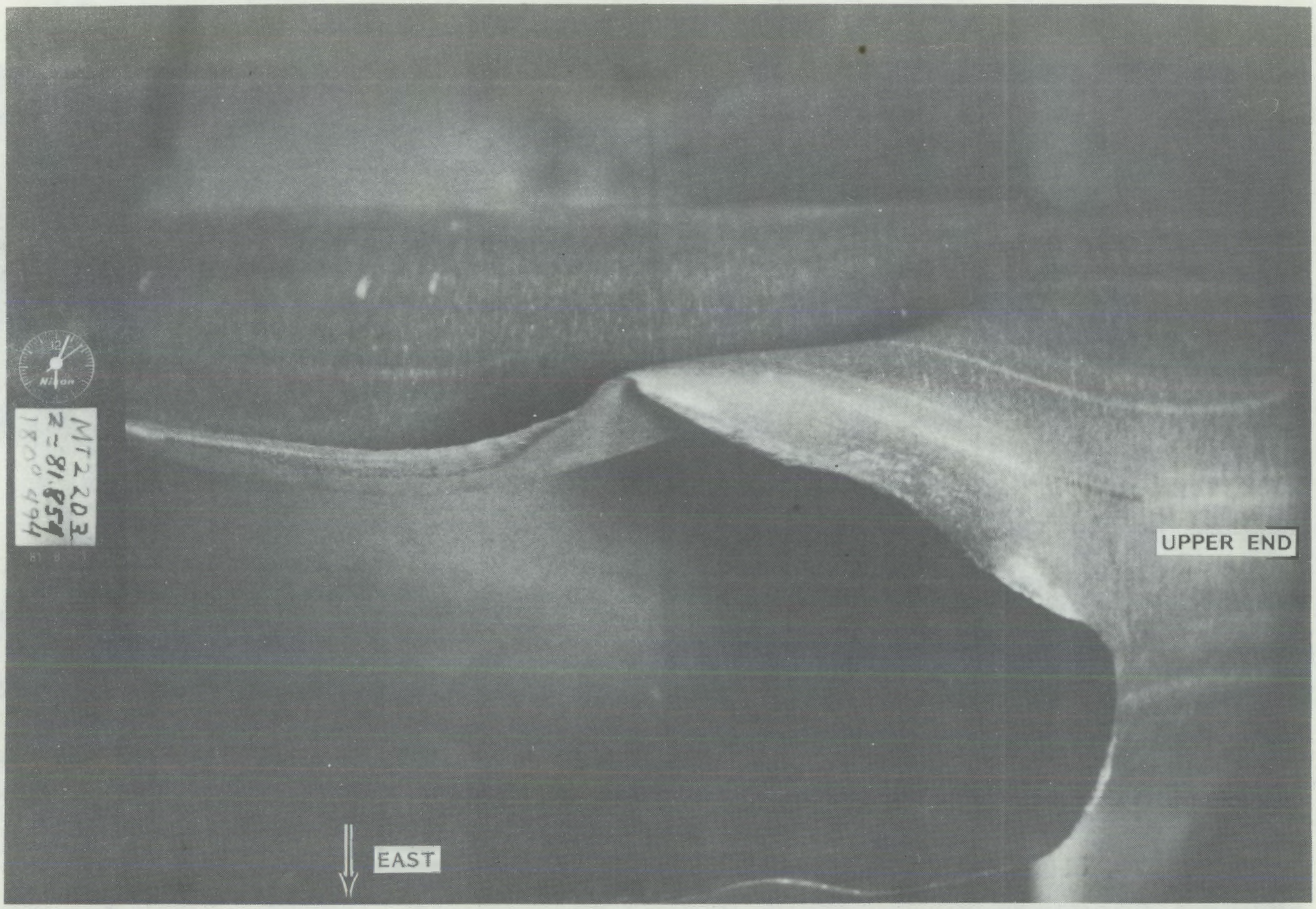

FIGURE 23. Rupture Zone - Fuel Rod 20, 180° View Angle, 0° Side

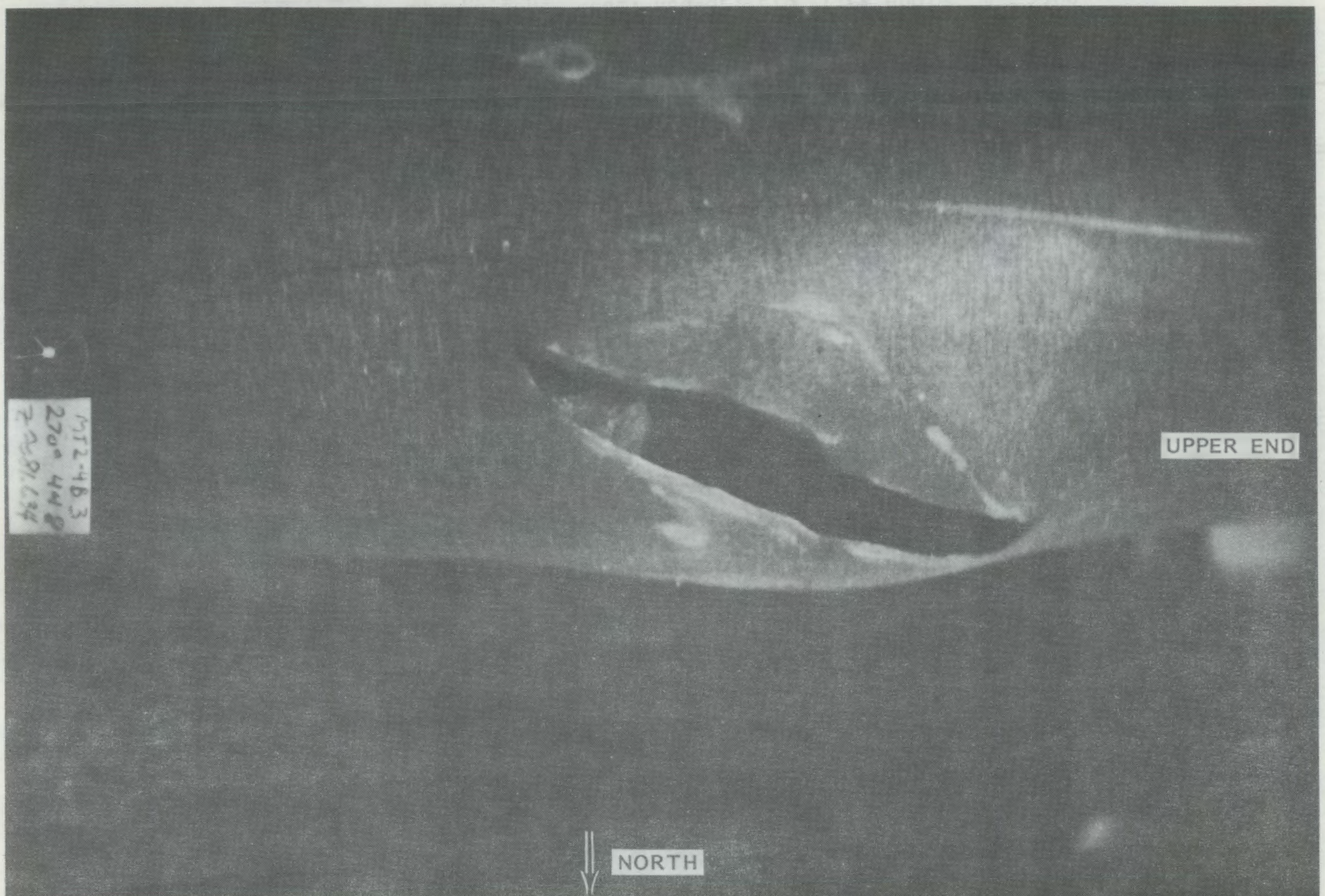

FIGURE 24. Rupture Zone - Fuel Rod 4B, 90^{o} View Angle, 270^{o} Side

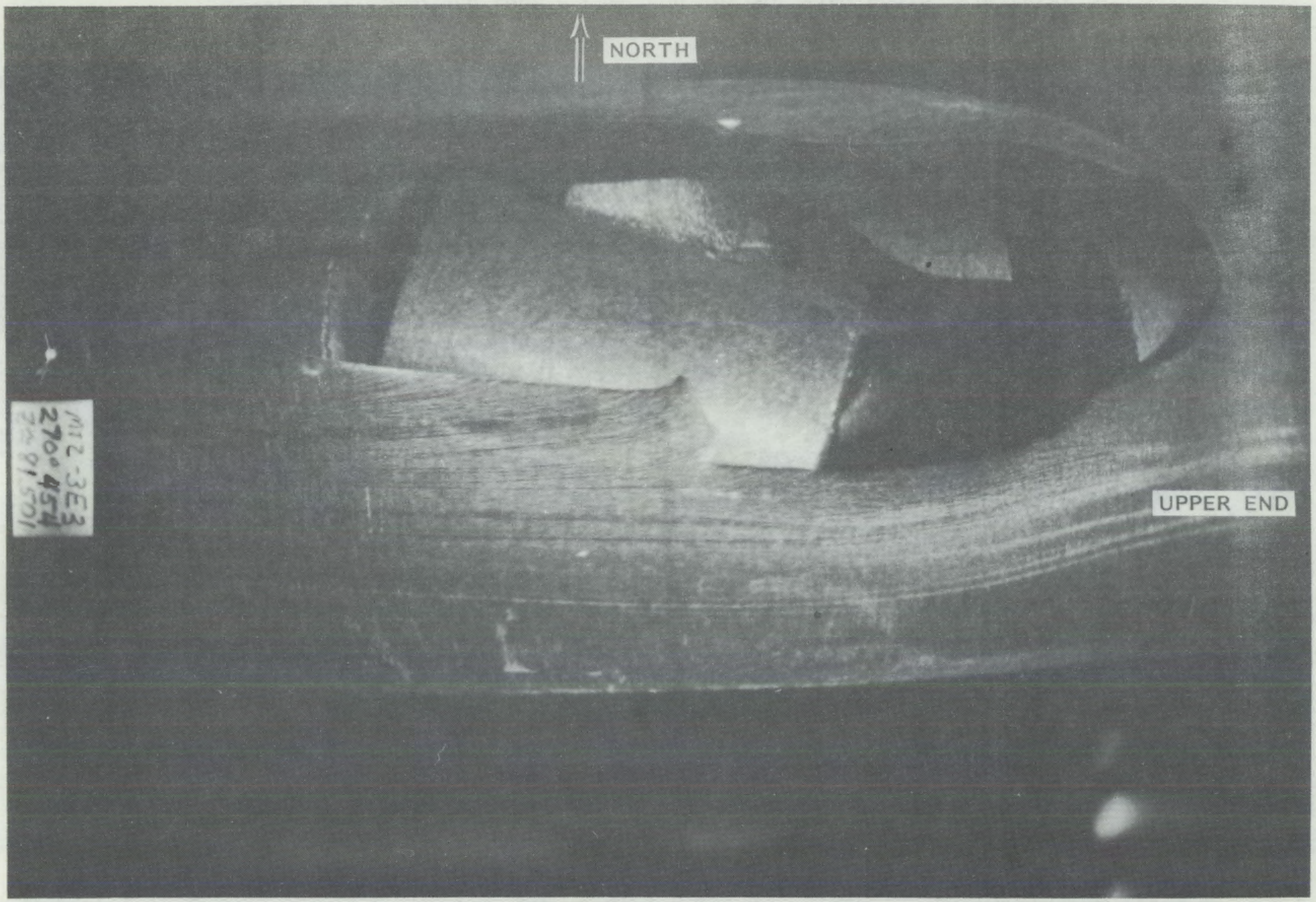

FIGURE 25. Rupture Zone - Fuel Rod 3E, 270^{0} View Angle, 90^{0} Side

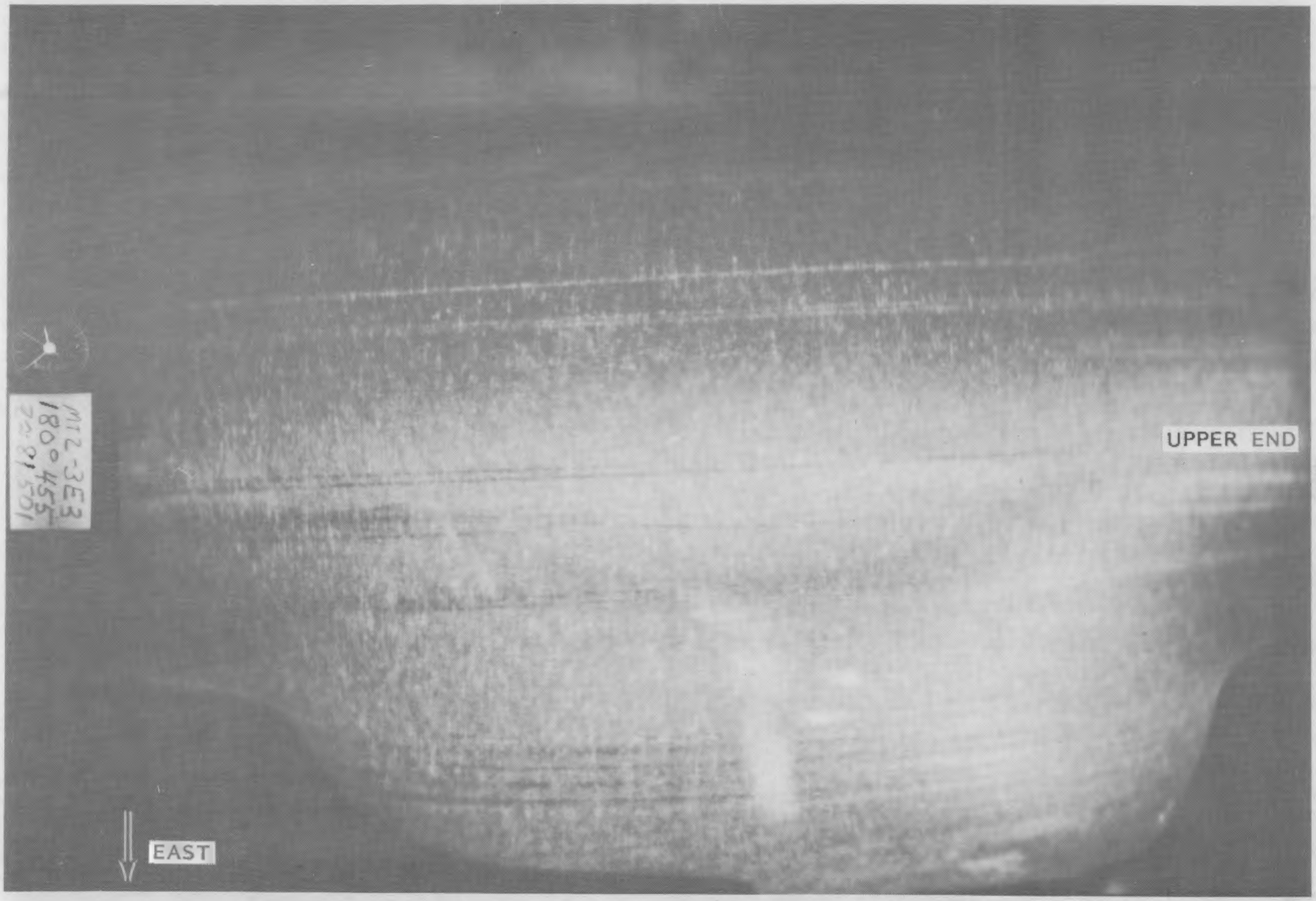

FIGURE 26. Rupture Zone - Fuel Rod 3E, 180° View Angle, 0° Side

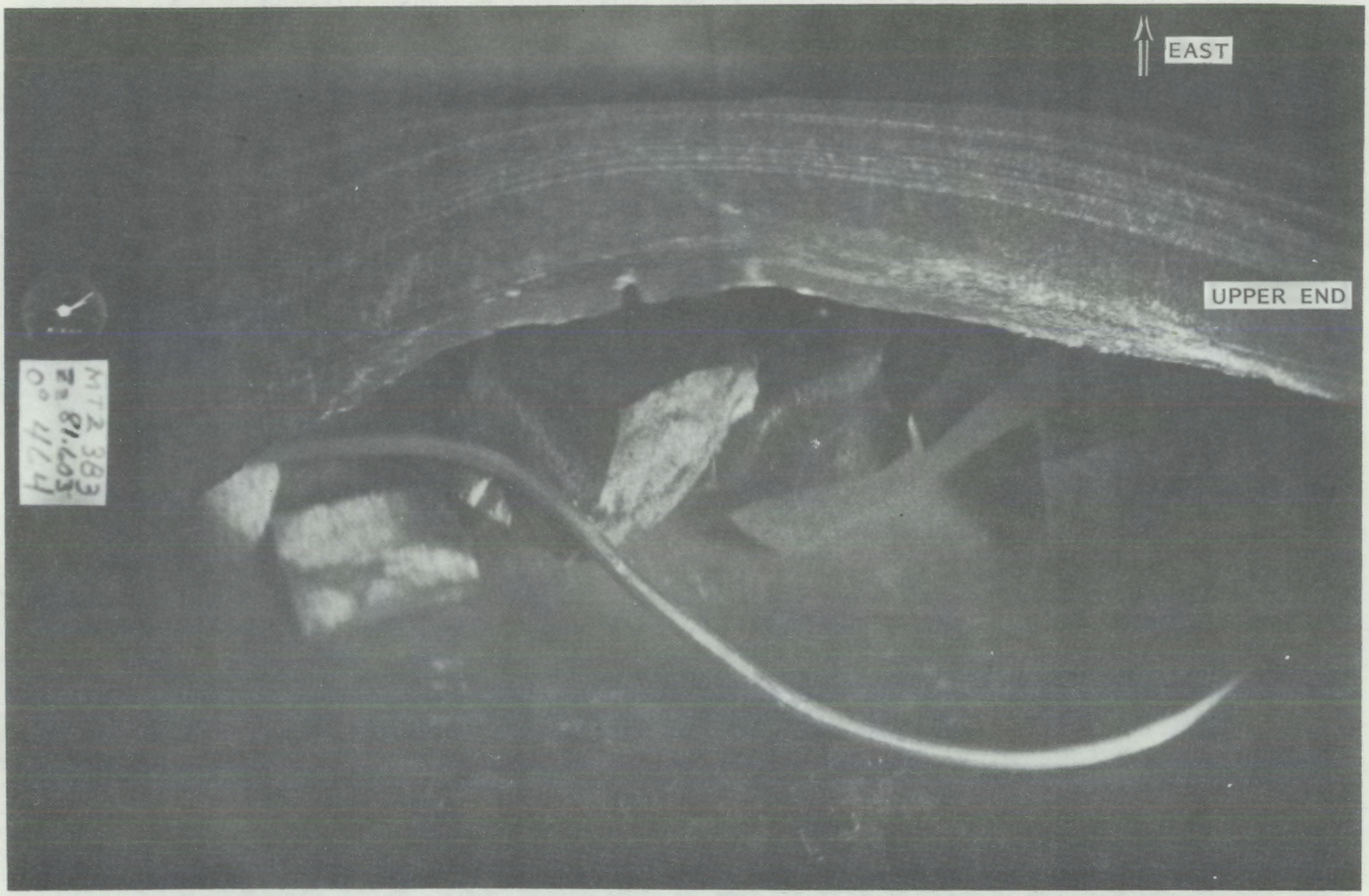

FIGURE 27. Rupture Zone - Fuel Rod 3B, 0^{0} View Angle, 180^{0} Side

6.0 REFERENCES

1. Hann, C. R. 1979. Program Plan for LOCA Simulation in the National Research Universal (NRU) Reactor. PNL-3056, Pacific Northwest Laboratory, Richland, Washington.

2. Mohr, C. L., et al. 1980. Prototypic Thermal-Hydraulic Experiments in NRU to Simulate Loss-of-Coolant Accidents. PNL-3681, NUREG/CR-1882, Pacific Northwest Laboratory, Richland, Washington.

3. Russcher, G. E., et al. 1981. Materials Test-1 LOCA Simulation in the NRU Reactor. NUREG/CR-2152 Vol. 1, PNL-3835, Pacific Northwest Laboratory, Richland, Washington.

4. Russcher, G. E. et al. 1981. Experiment Operations Plan for Loss-of-Coolant Accident Simulation in the National Research Universal Reactor. Addendum 1: Materials Tests 1 and 2. PNL-3765, NUREG/CR-1735, Add. 1, Pacific Northwest Laboratory, Richland, Washington.

5. Marshall, R. K. and C. L. Mohr. 1980. LOCA Simulation in NRU-Heatup Instrumentation Package. PNL-SA-8742, Pacific Northwest Laboratory, Richland, Washington.

6. Lilly, G. P. et al. 1977. PWR FLECHT Cosine Low Flooding Rate Test Series Evaluation Report. WCAP-8838, Westinghouse Electric Corporation, Pittsburgh, Pennsylvania.

7. Siefken, L. J., et al. June 1979. FRAP-T5: A Computer Code for the Transient Analysis of Oxide Fuel Rods. NUREG/CR-0840, TREE-1282, EG&G Idaho, Inc., Idaho Falls, Idaho.

8. Mohr, C. L., et al. May 1979. GAPCON-THERMAL-3: A Technique for Evaluation of Transient Gap Conductance and Stored Energy. PNL-SA-7712, SMIRT-V, D-6/3, Pacific Northwest Laboratory, Richland, Washington.

6.0 REFERENCES

1. Hann, C. R. 1979. Program Plan for LOCA Simulation in the National Research Universal (NRU) Reactor. PNL-3056, Pacific Northwest Laboratory, Richland, Washington.

2. Mohr, C. L., et al. 1980. Prototypic Thermal-Hydraulic Experiments in NRU to Simulate Loss-of-Coolant Accidents. PNL-3681, NUREG/CR-1882, Pacific Northwest Laboratory, Richland, Washington.

3. Russcher, G. E., et al. 1981. Materials Test-1 LOCA Simulation in the NRU Reactor. NUREG/CR-2152 Vol. 1, PNL-3835, Pacific Northwest Laboratory, Richland, Washington.

4. Russcher, G. E. et al. 1981. Experiment Operations Plan for Loss-of-Coolant Accident Simulation in the National Research Universal Reactor, Addendum 1: Materials Tests 1 and 2. PNL-3765, NUREG/CR-1763, Add. 1, Pacific Northwest Laboratory, Richland, Washington.

5. Marshall, R. K. and C. L. Mohr. 1980. LOCA Simulation in NRU-Heatup Instrumentation Package. PNL-SA-8742, Pacific Northwest Laboratory, Richland, Washington.

6. Lilly, G. P. et al. 1977. PWR FLECHT Cosine Low Flooding Rate Test Series Evaluation Report. WCAP-8838, Westinghouse Electric Corporation, Pittsburgh, Pennsylvania.

7. Siefken, L. J., et al. June 1979. FRAP-T5: A Computer Code for the Transient Analysis of Oxide Fuel Rods. NUREG/CR-0840, TREE-1282, EG&G Idaho, Inc., Idaho Falls, Idaho.

8. Mohr, C. L., et al. May 1979. GAPCON-THERMAL-3: A Technique for Evaluation of Transient Gap Conductance and Stored Energy. PNL-SA-7712, SMIRT-5, D 6/3, Pacific Northwest Laboratory, Richland, Washington.

APPENDIX A

PRECONDITIONING TEMPERATURES

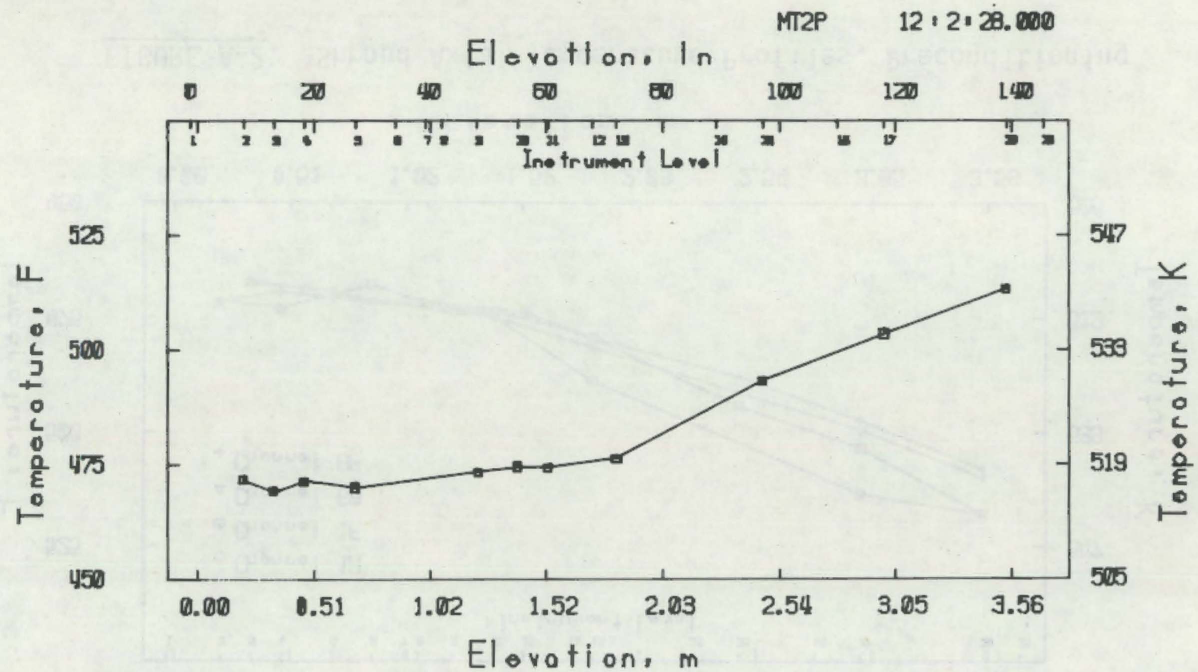

FIGURE A-1. Average Shroud Axial Temperature Profile, Preconditioning

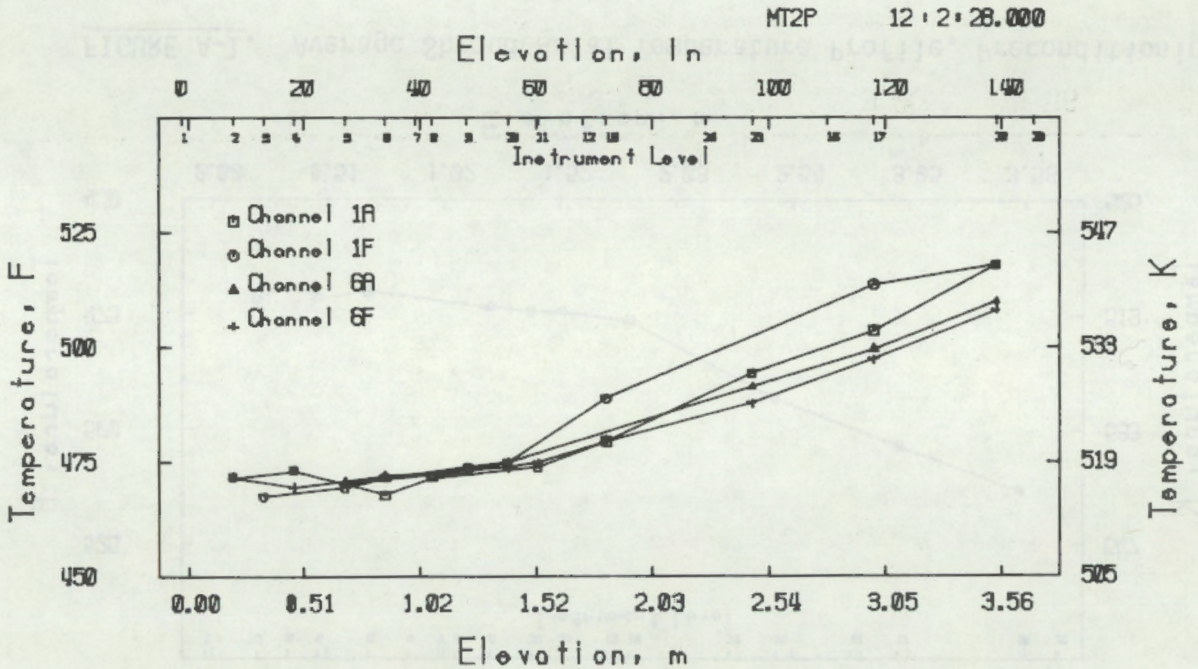

FIGURE A-2. Shroud Axial Temperature Profiles, Preconditioning

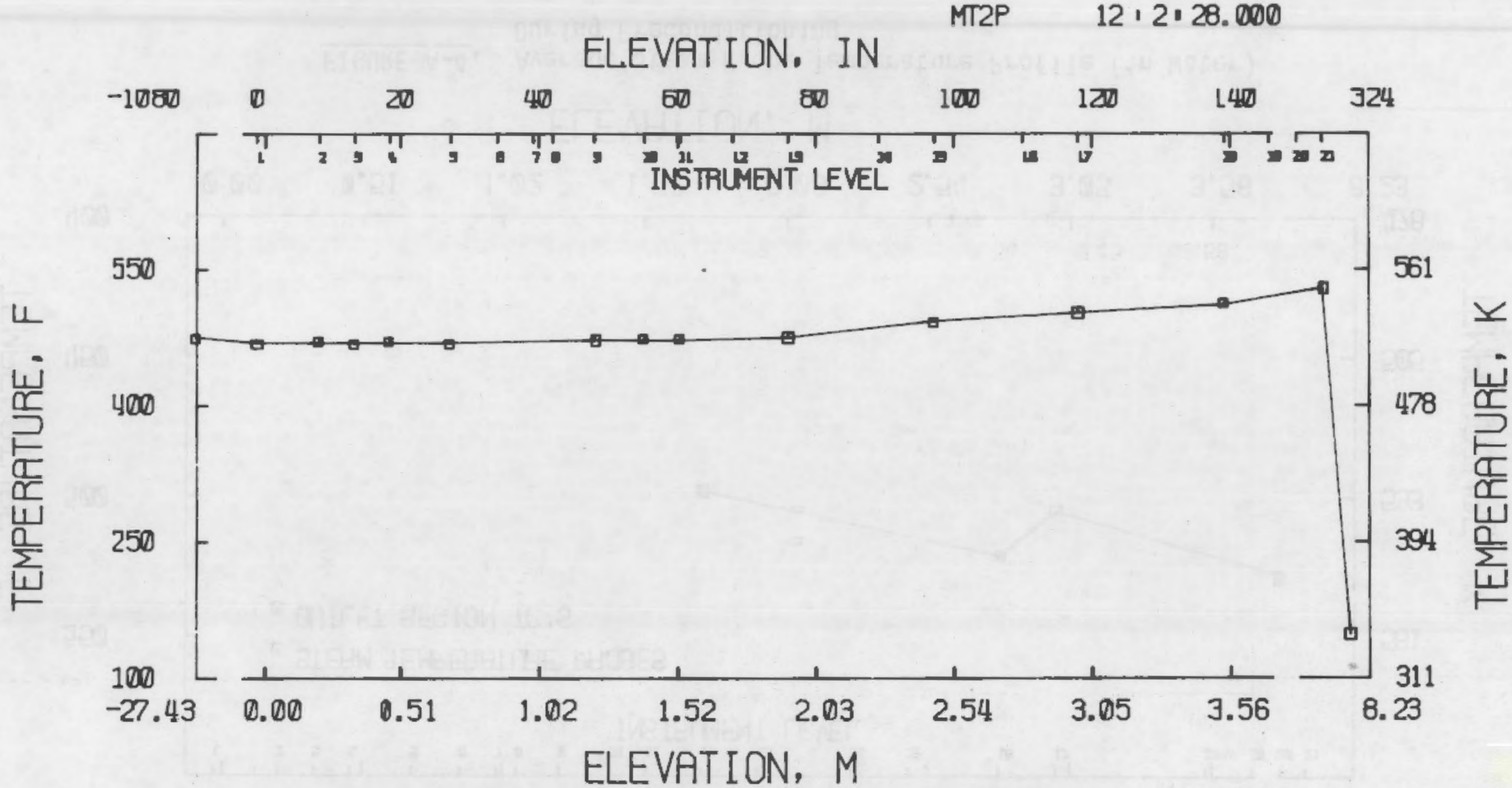

FIGURE A-3. Shroud and Test Train Coolant Temperatures, Preconditioning

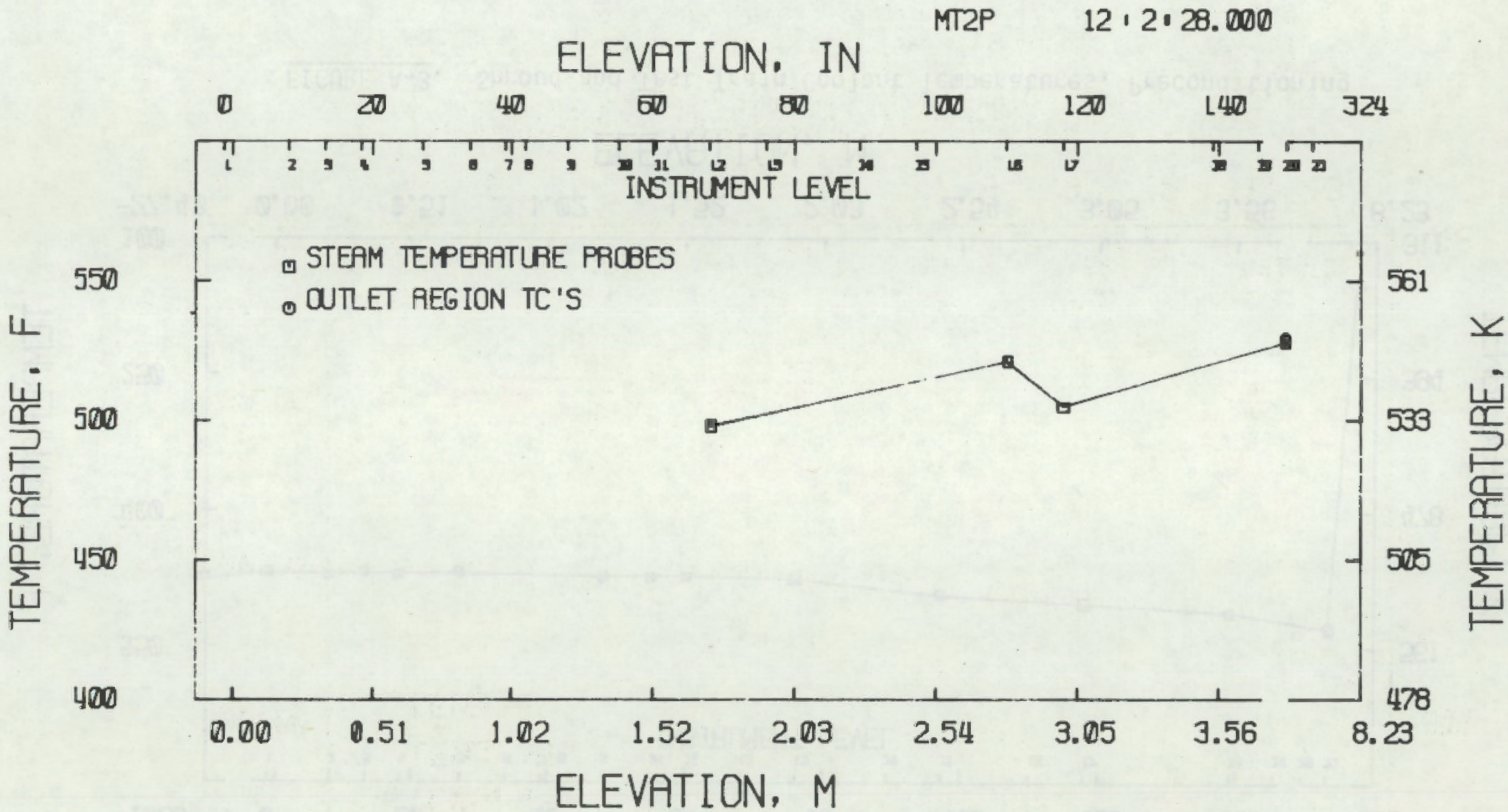

FIGURE A-4. Average Steam Probe Temperature Profile (in Water) During Preconditioning

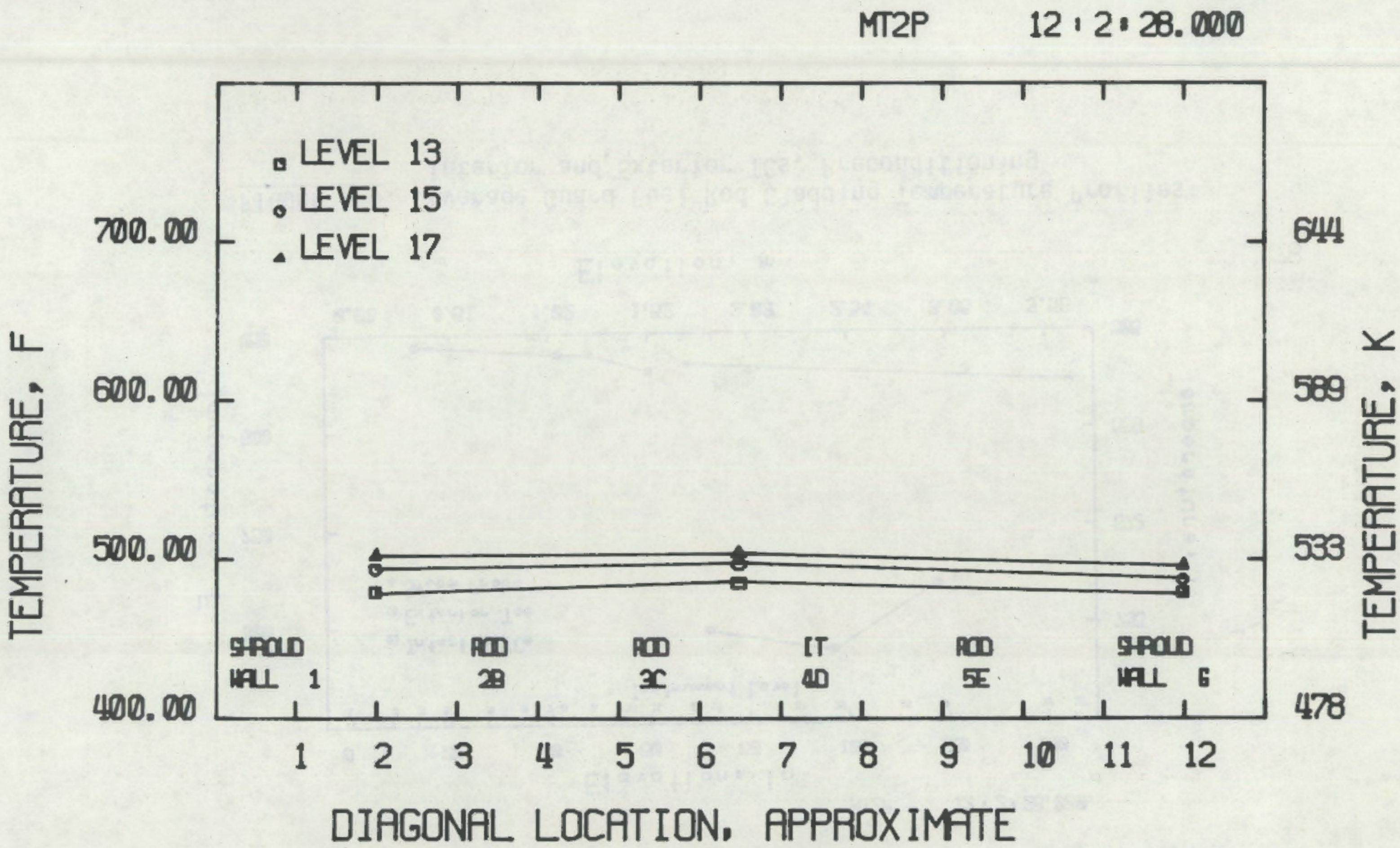

FIGURE A-5. Diagonal Temperature Profiles Across Test Assembly Coolant at Levels 13, 15, and 17, Preconditioning

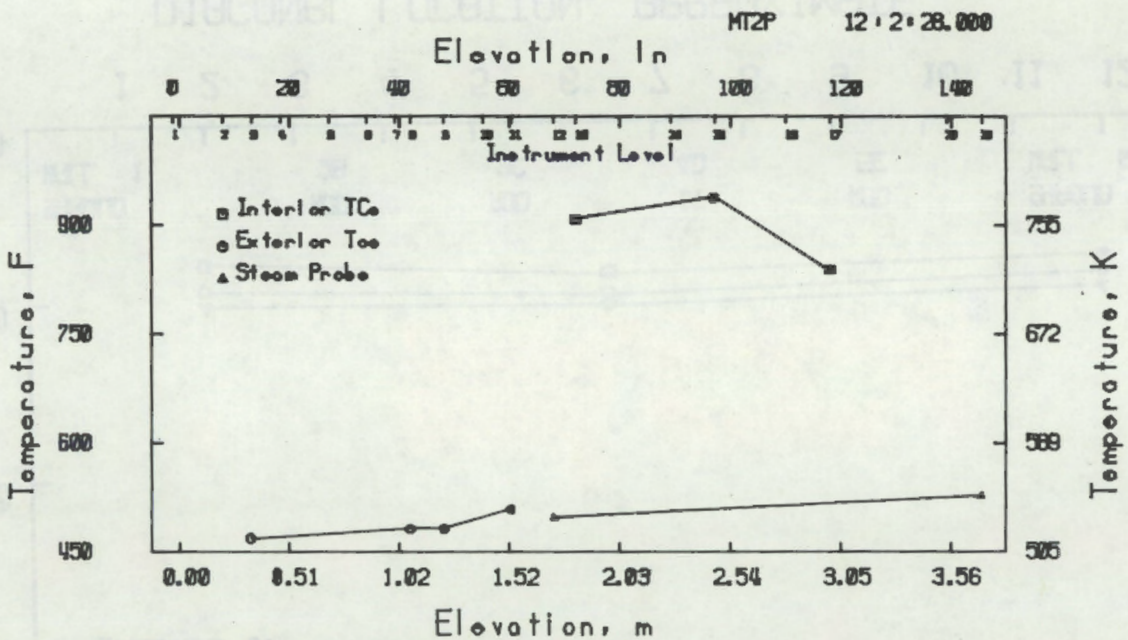

FIGURE A-6. Average Guard Fuel Rod Cladding Temperature Profiles Interior and Exterior TCs, Preconditioning

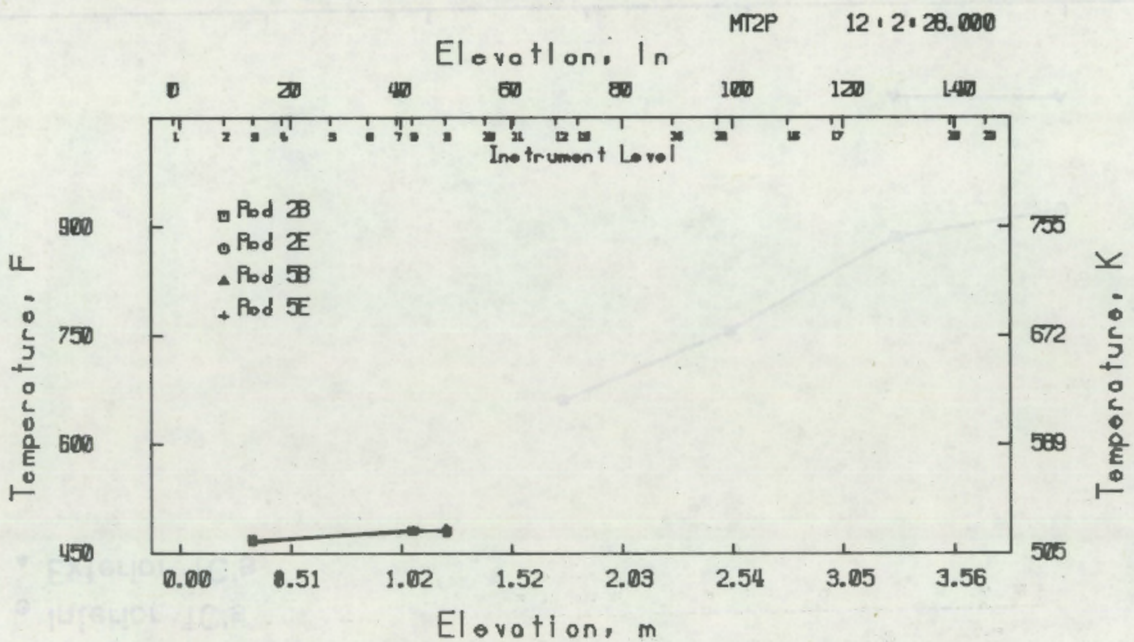

FIGURE A-7. Individual Guard Fuel Rod Cladding Exterior Temperature Profiles, Preconditioning

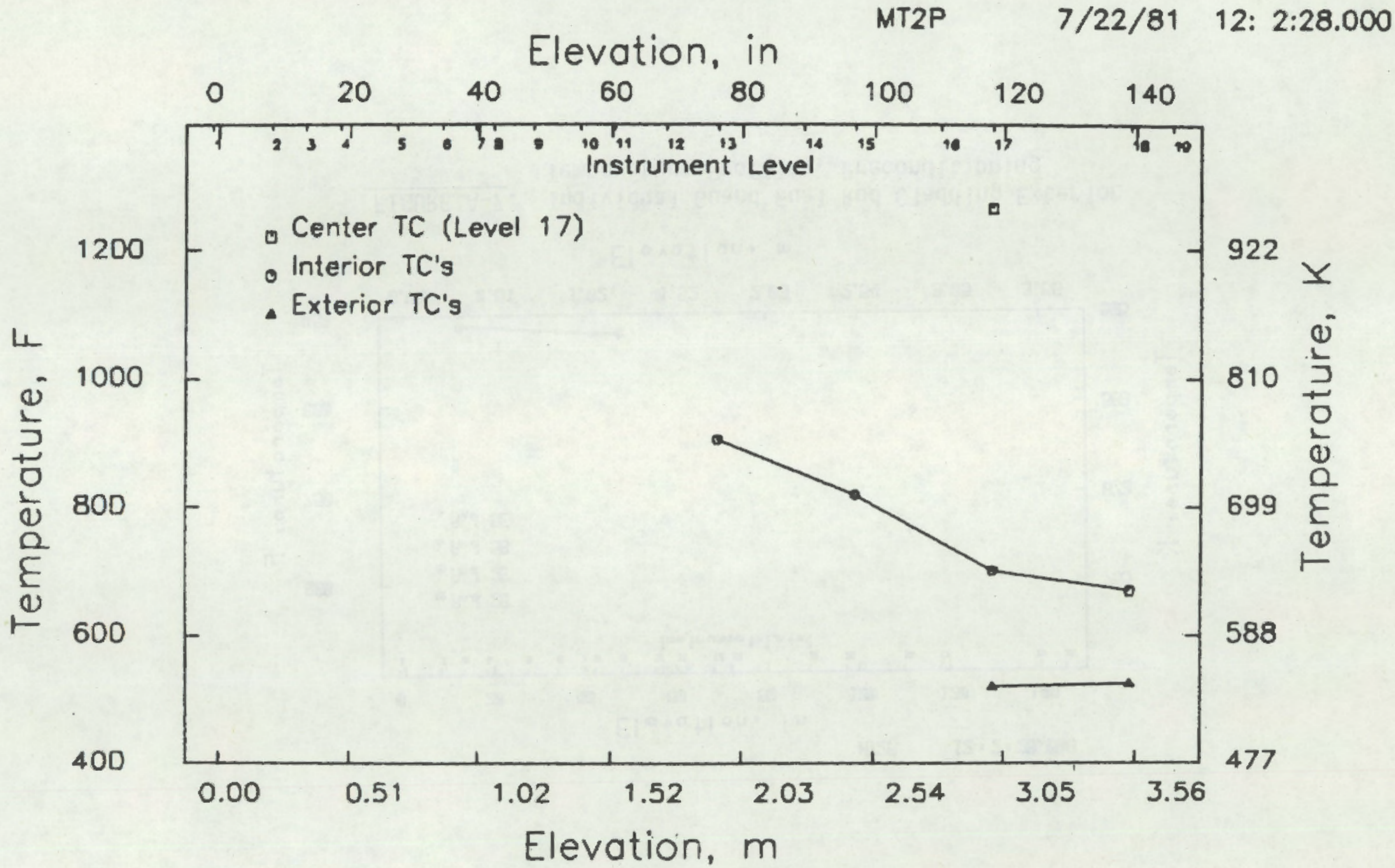

FIGURE A-8. Average Test Fuel Rod Temperature Profiles--Exterior, Interior, and Center TCs, Preconditioning

APPENDIX B

PRETRANSIENT TEMPERATURES

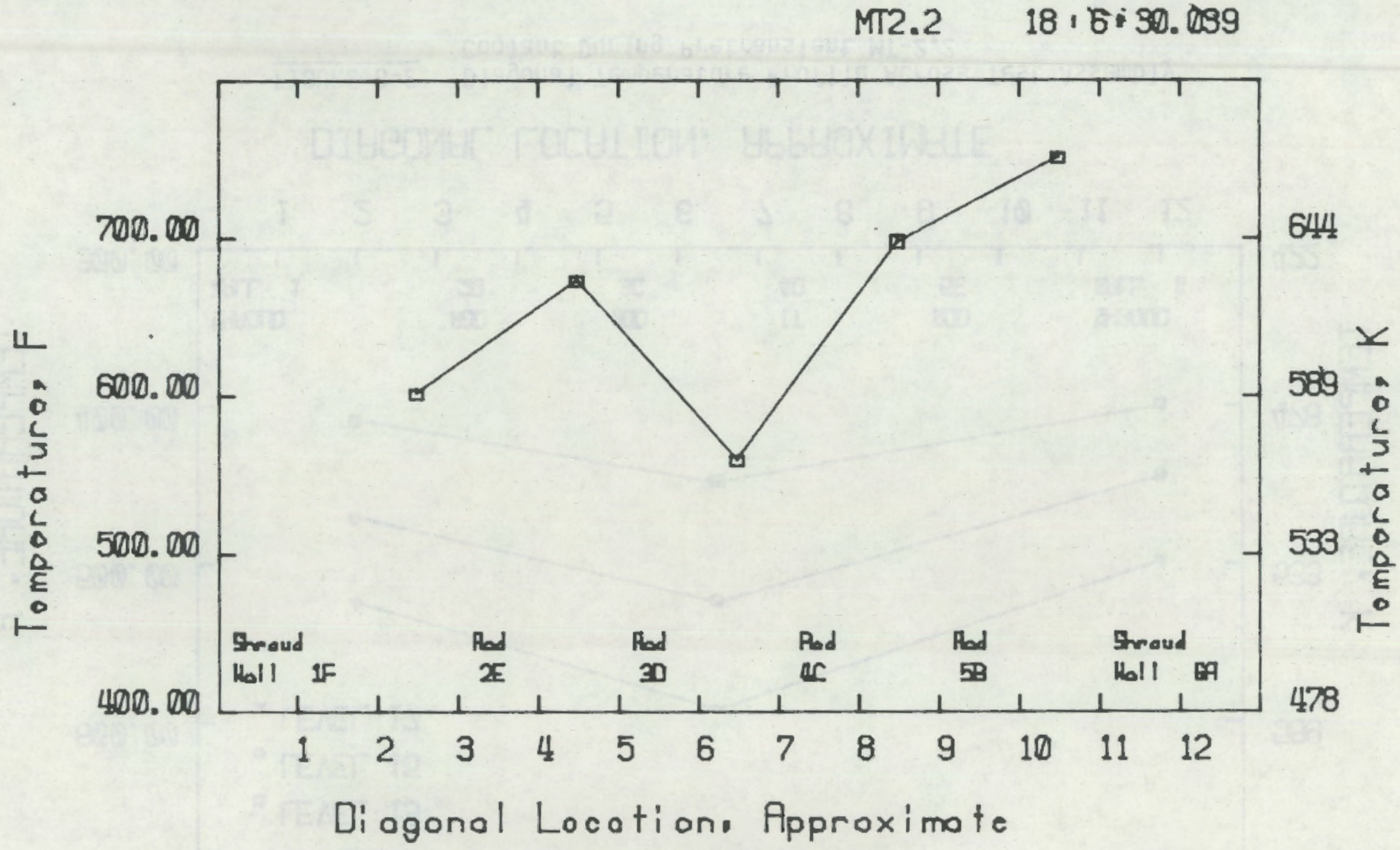

FIGURE B-1. Diagonal Temperature Profile Across Test Assembly Coolant During Pretransient MT-2.2, Level 16

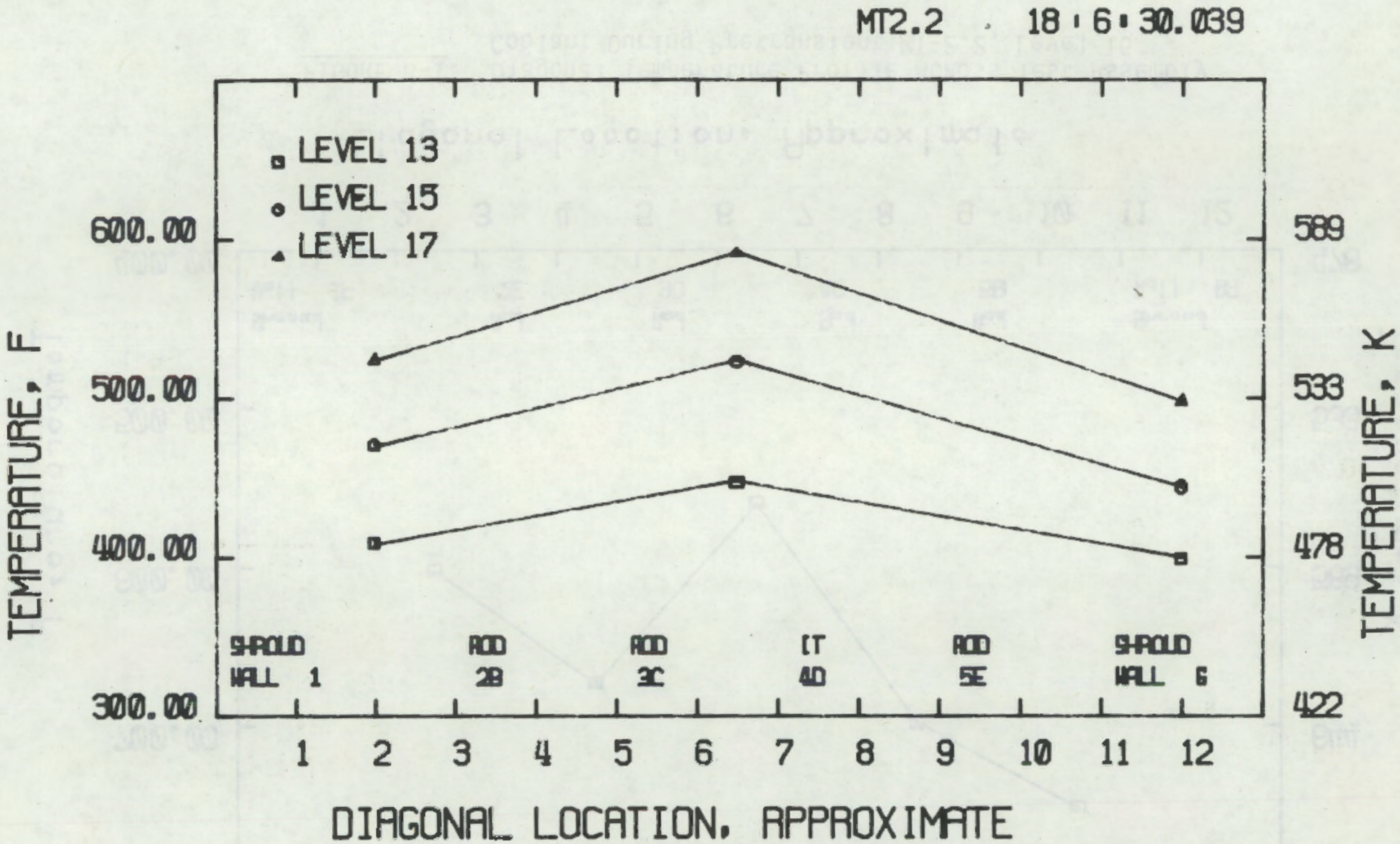

FIGURE B-2. Diagonal Temperature Profile Across Test Assembly Coolant During Pretransient MT-2.2

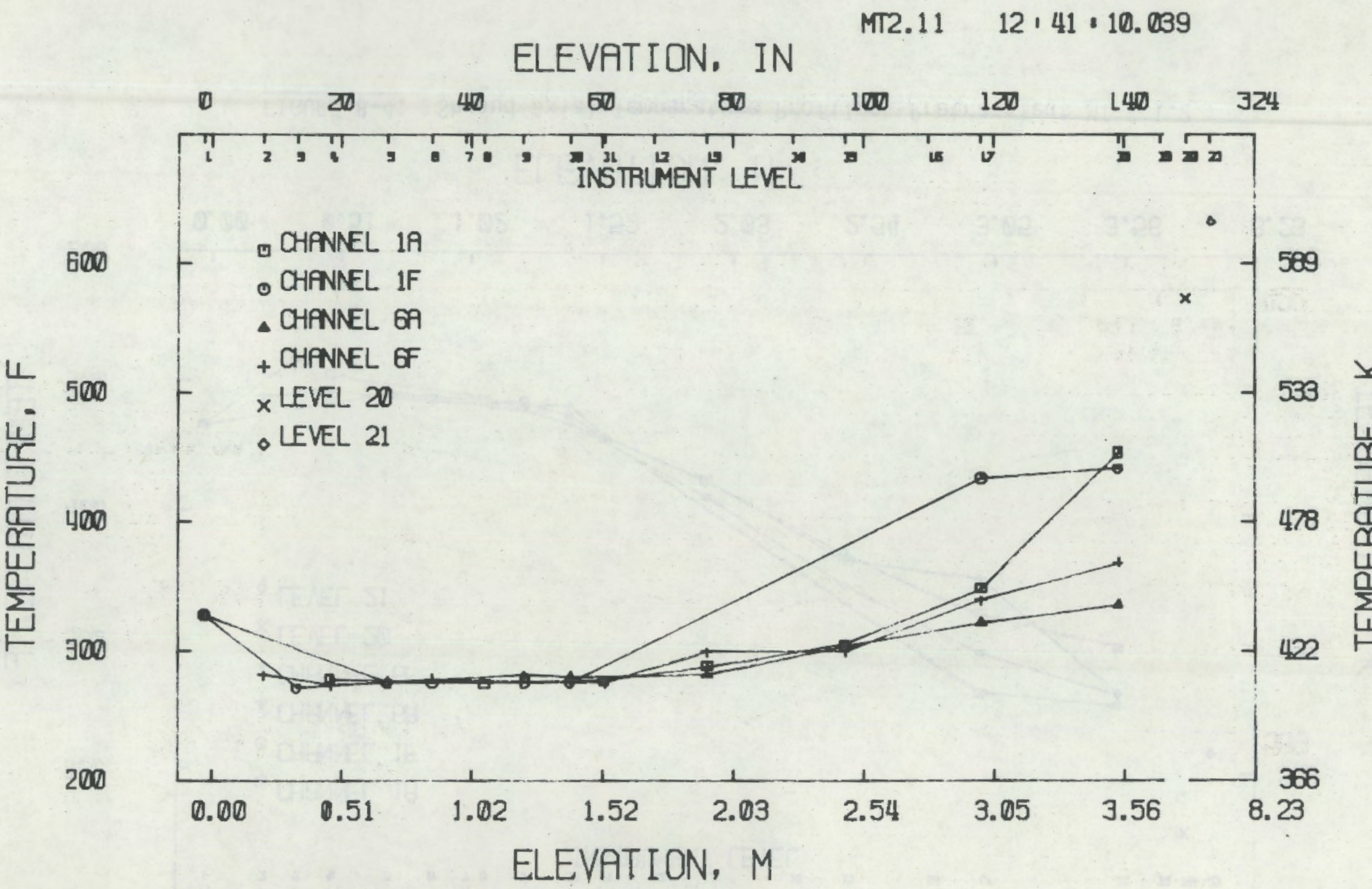

FIGURE B-3. Shroud Axial Temperature Profiles--Pretransient MT-2.1.1

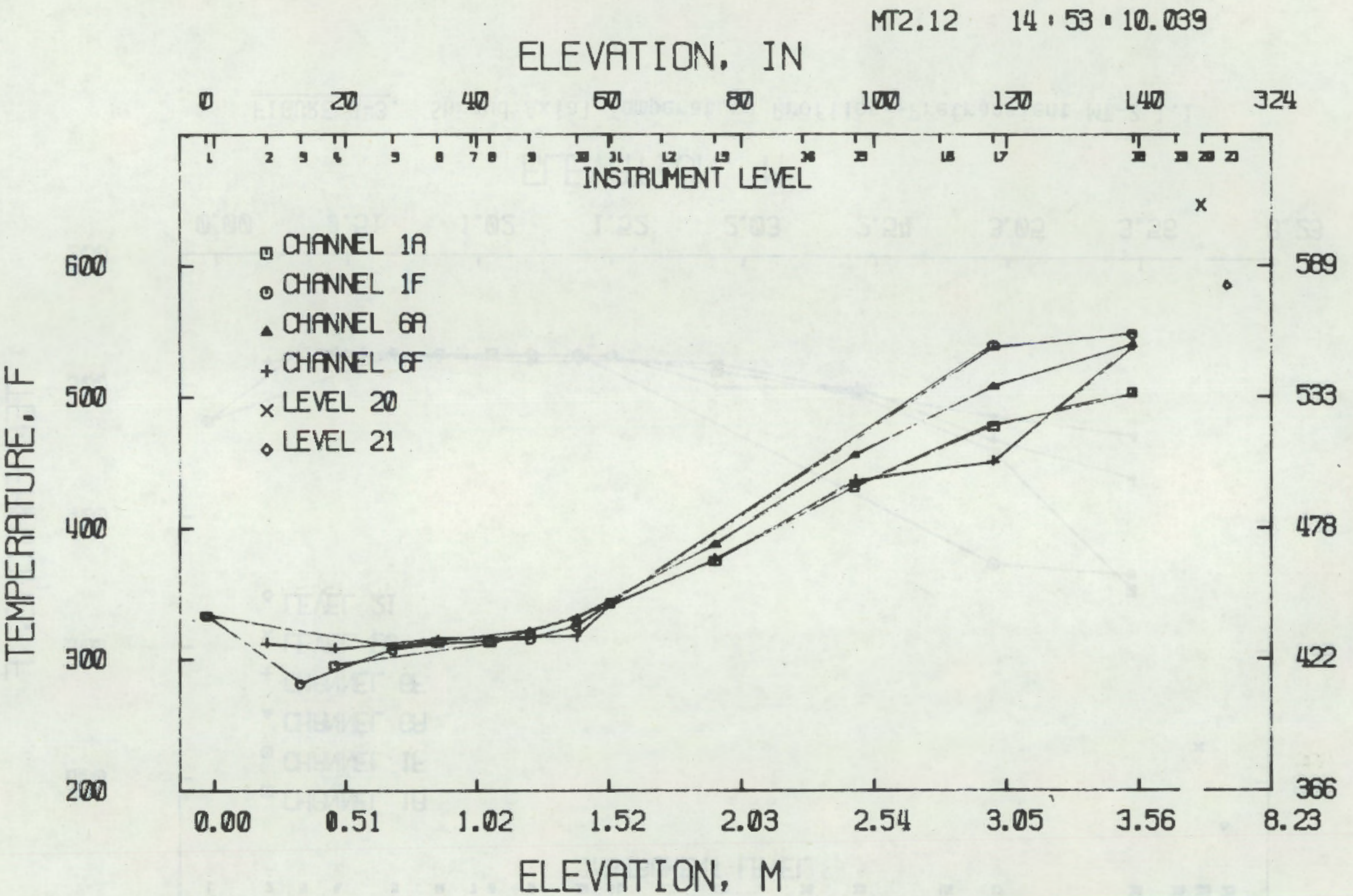

FIGURE B-4. Shroud Axial Temperature Profiles--Pretransient MT-2.1.2

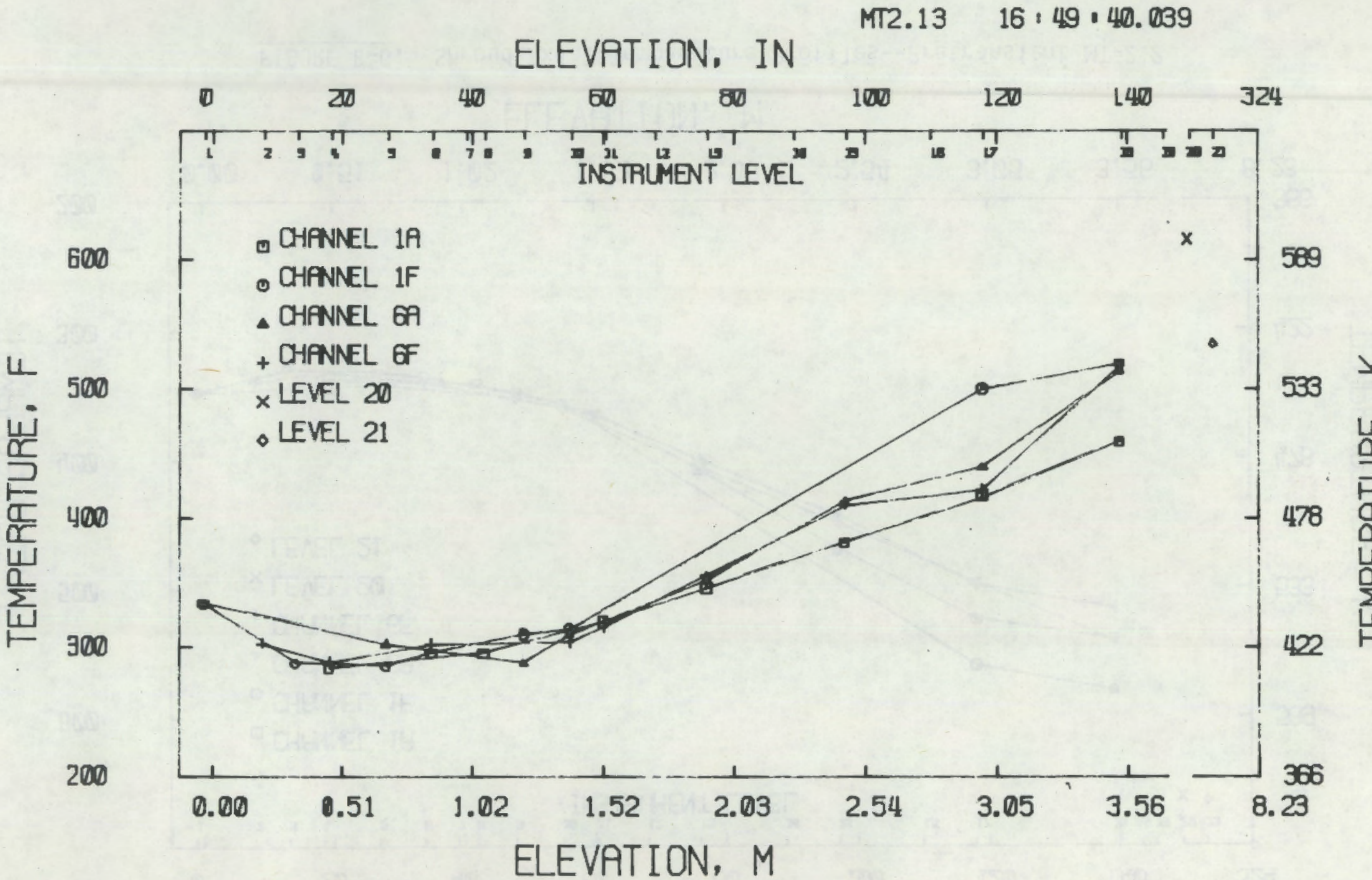

FIGURE B-5. Shroud Axial Temperature Profiles--Pretransient MT-2.1.3

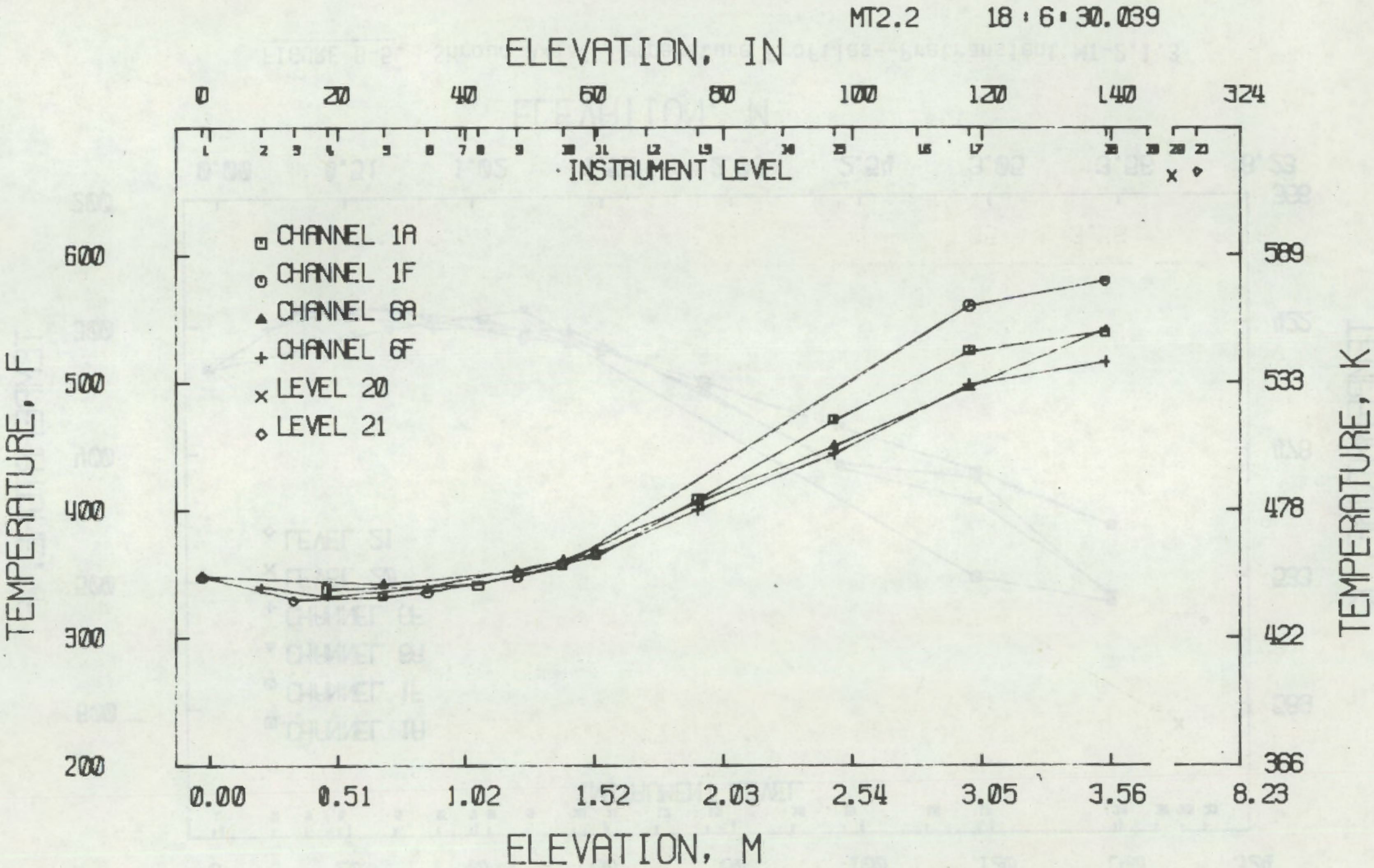

FIGURE B-6. Shroud Axial Temperature Profiles--Pretransient MT-2.2

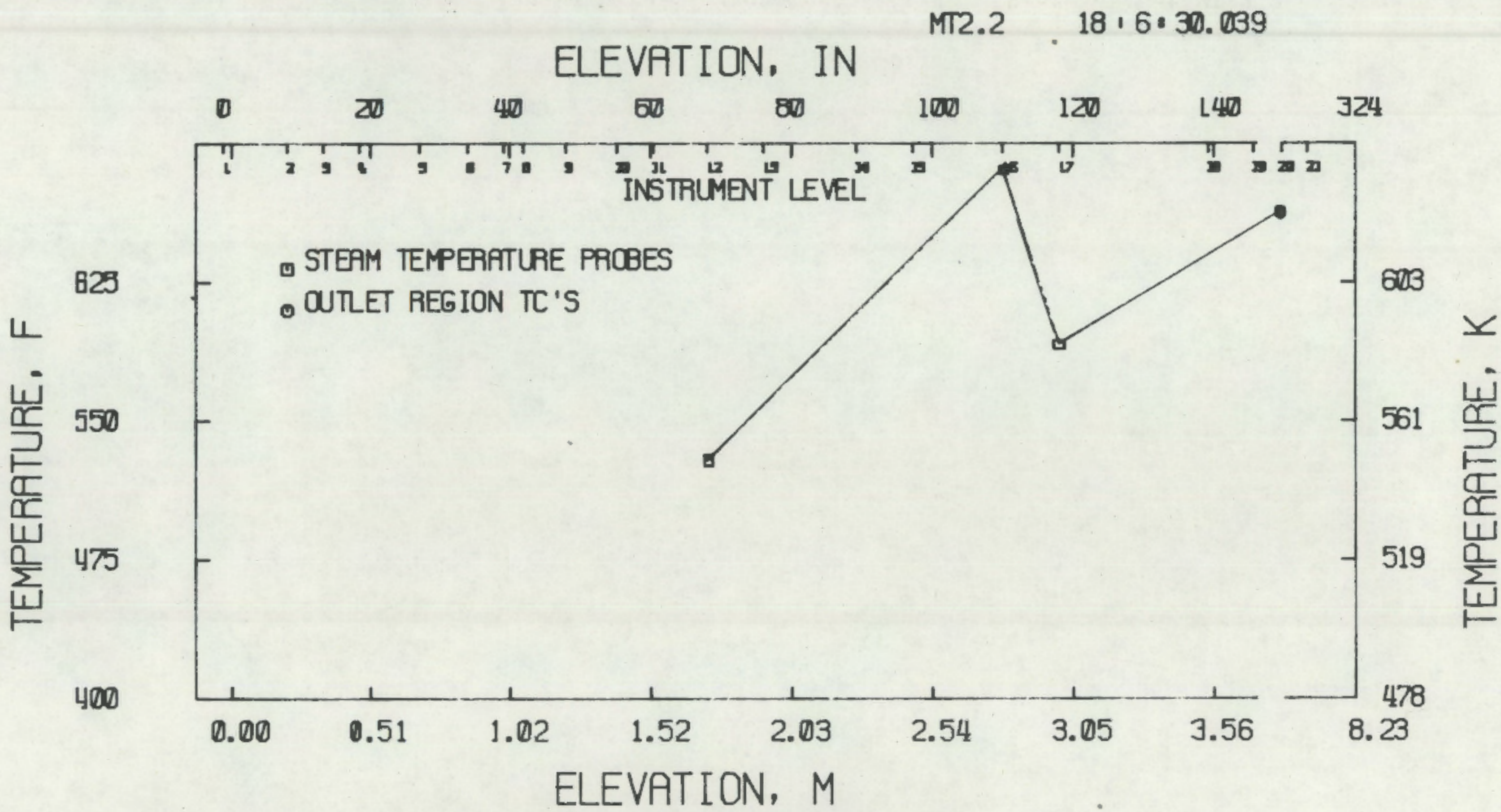

FIGURE B-7. Average Steam Probe Temperature Profile (in Steam) During Pretransient MT-2.2

APPENDIX C

TRANSIENT FUEL AND CLADDING TEMPERATURES

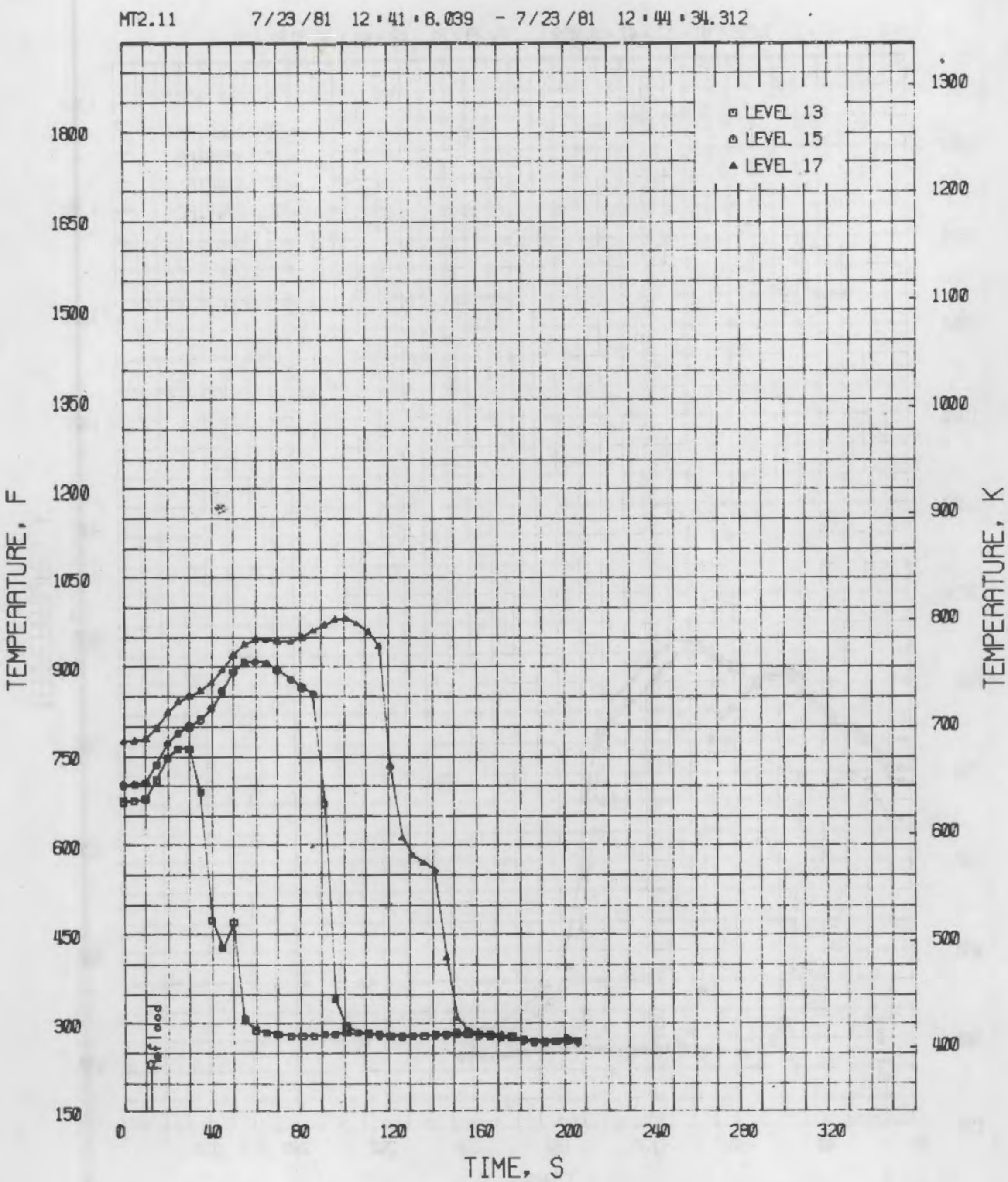

FIGURE C-1. Average Guard Fuel Rod Cladding Temperature Histories (Interior TCs) During Transient MT-2.1.1

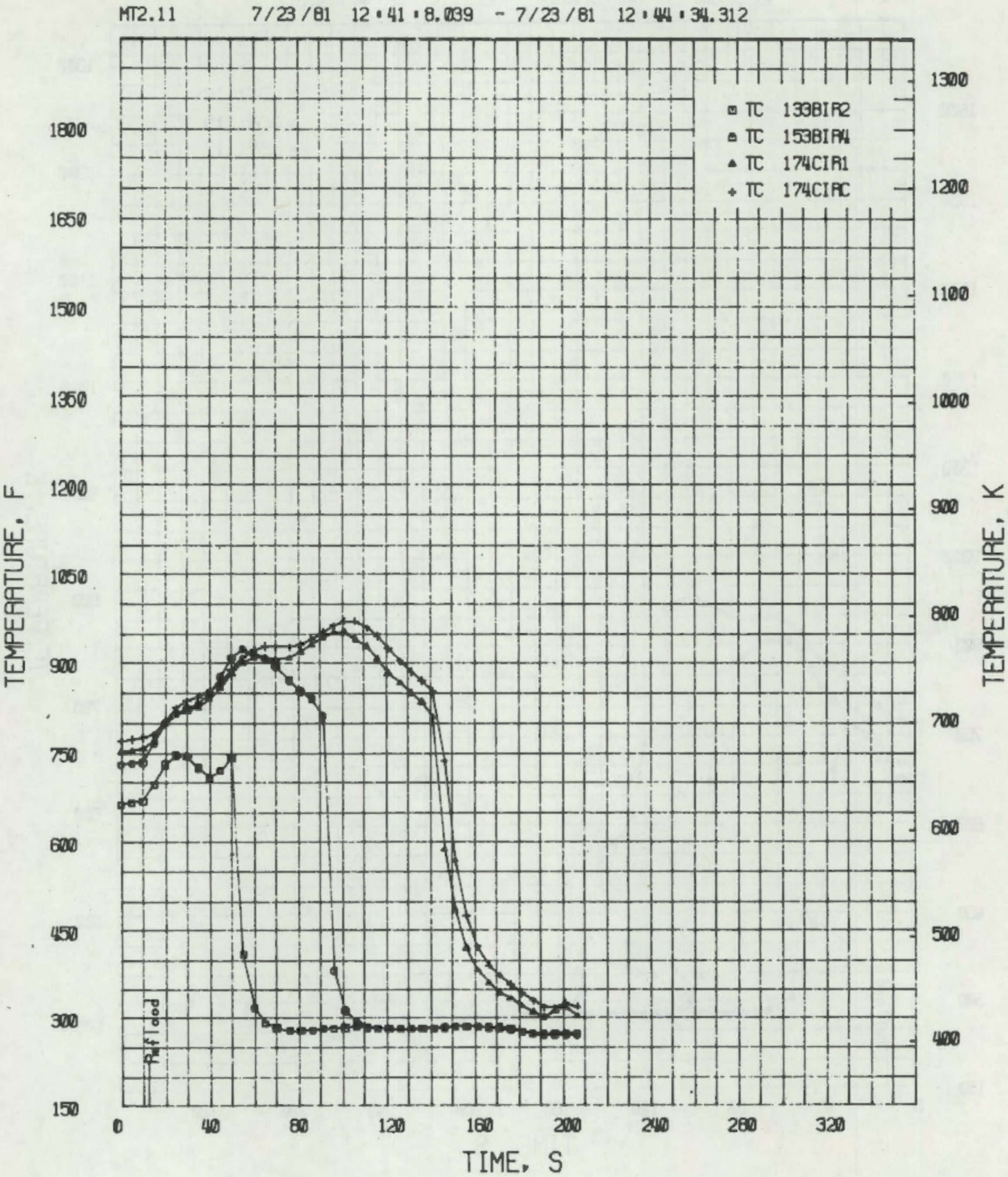

FIGURE C-2. Test Rod Center and Interior Cladding Temperature Histories During Transient MT-2.1.1

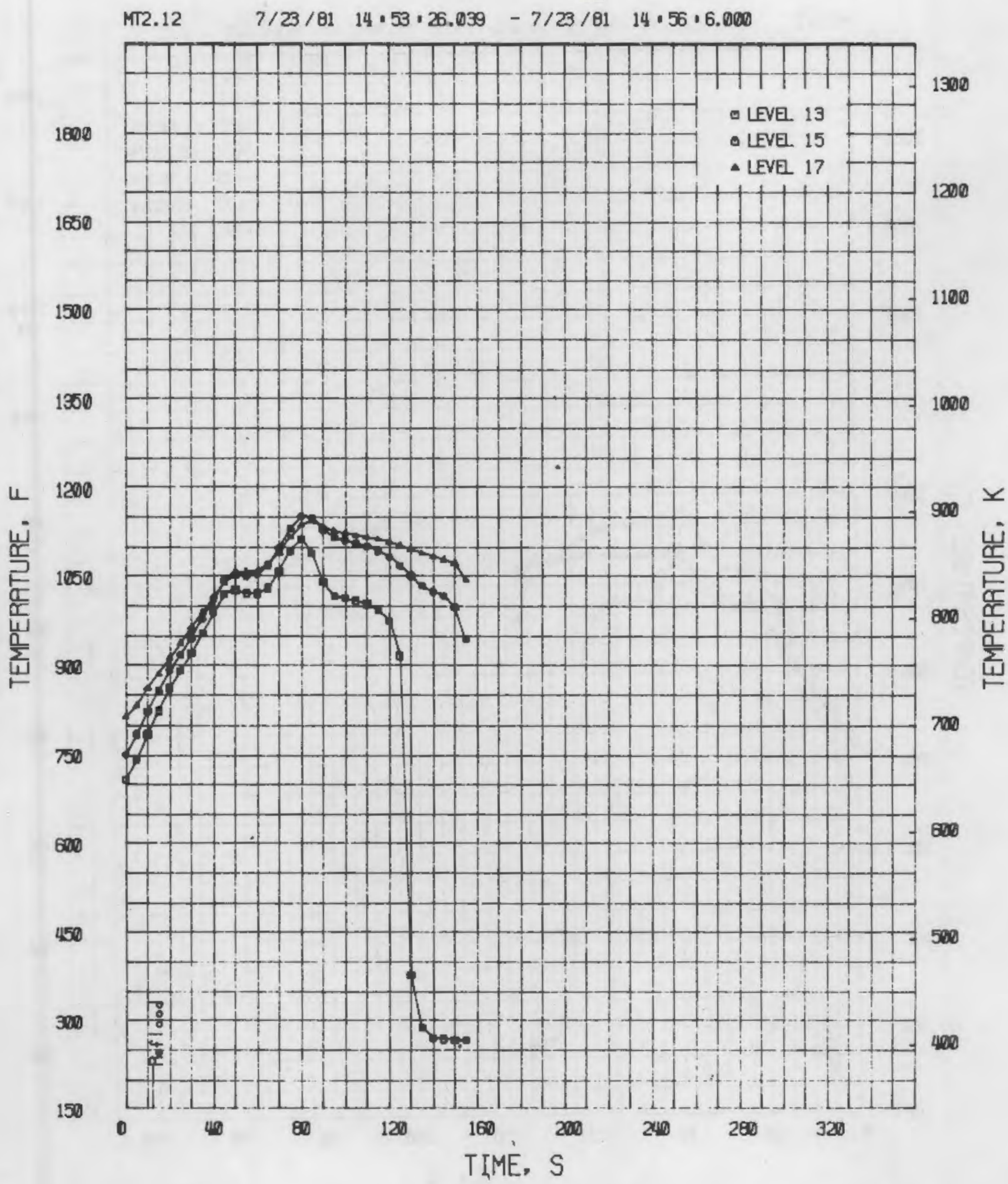

FIGURE C-3. Average Guard Fuel Rod Cladding Temperature Histories (Interior TCs) During Transient MT-2.1.2

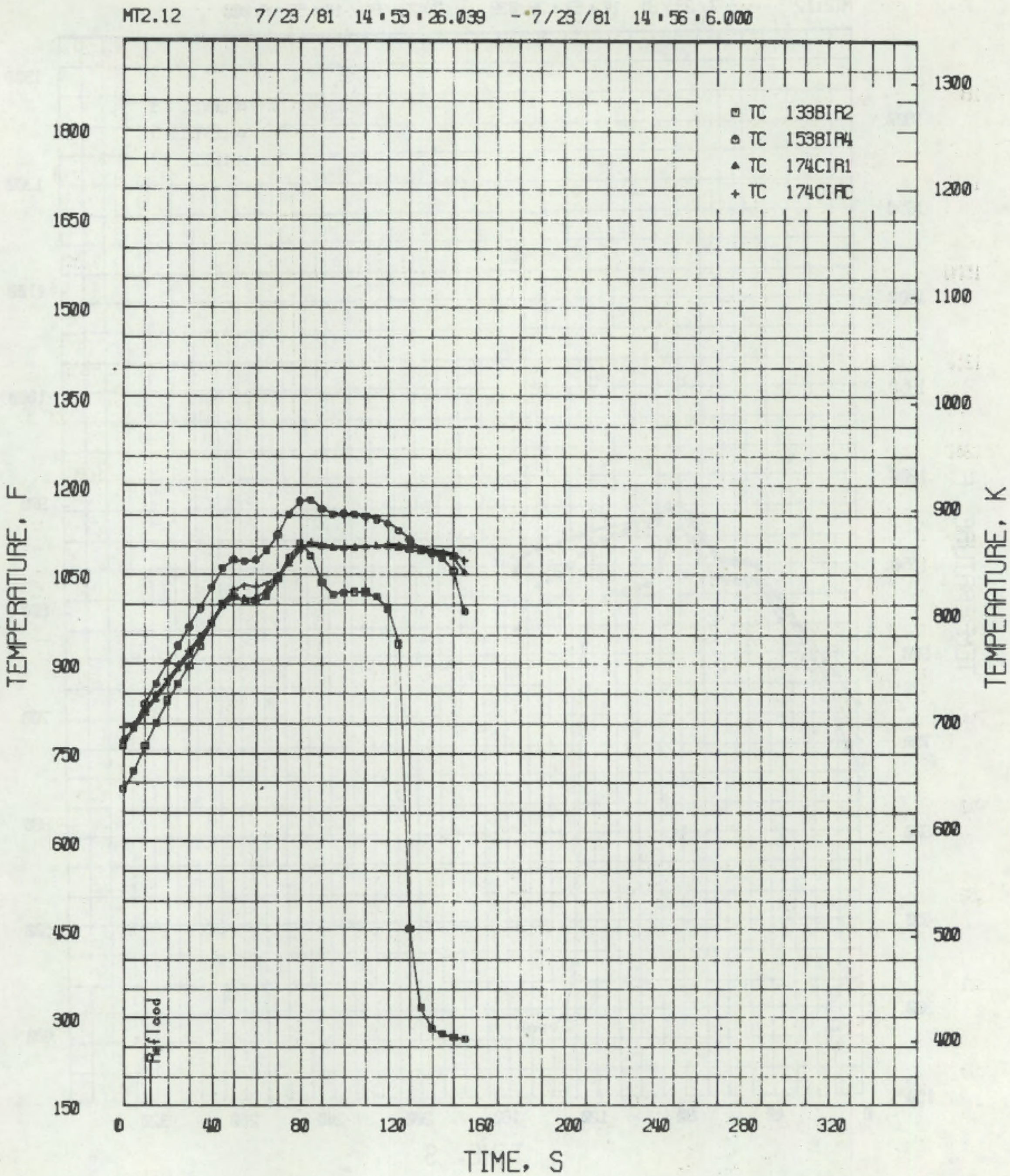

FIGURE C-4. Test Rod Center and Interior Cladding Temperature Histories During Transient MT-2.1.2

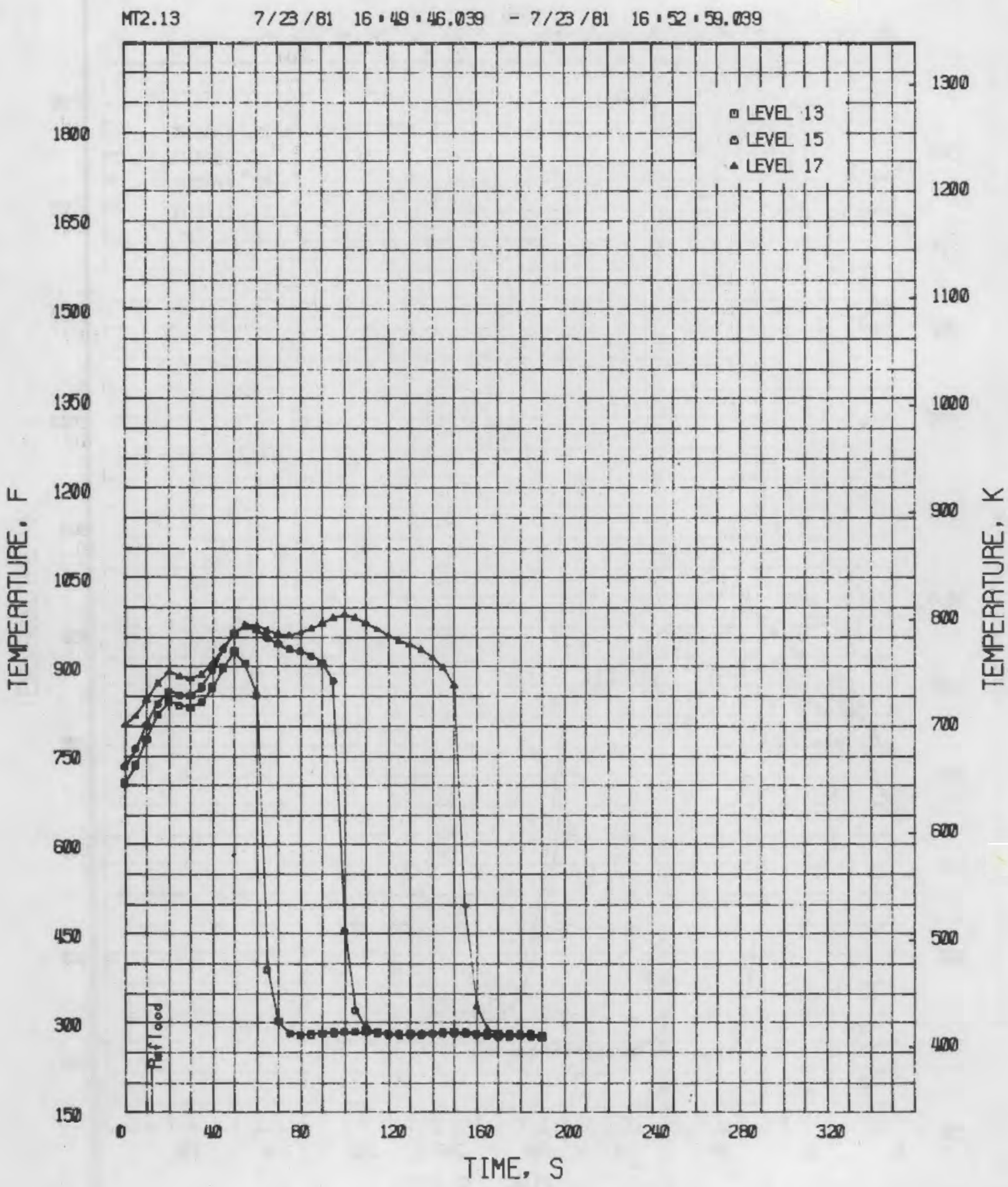

FIGURE C-5. Average Guard Fuel Rod Cladding Temperature Histories (Interior TCs) During Transient MT-2.1.3

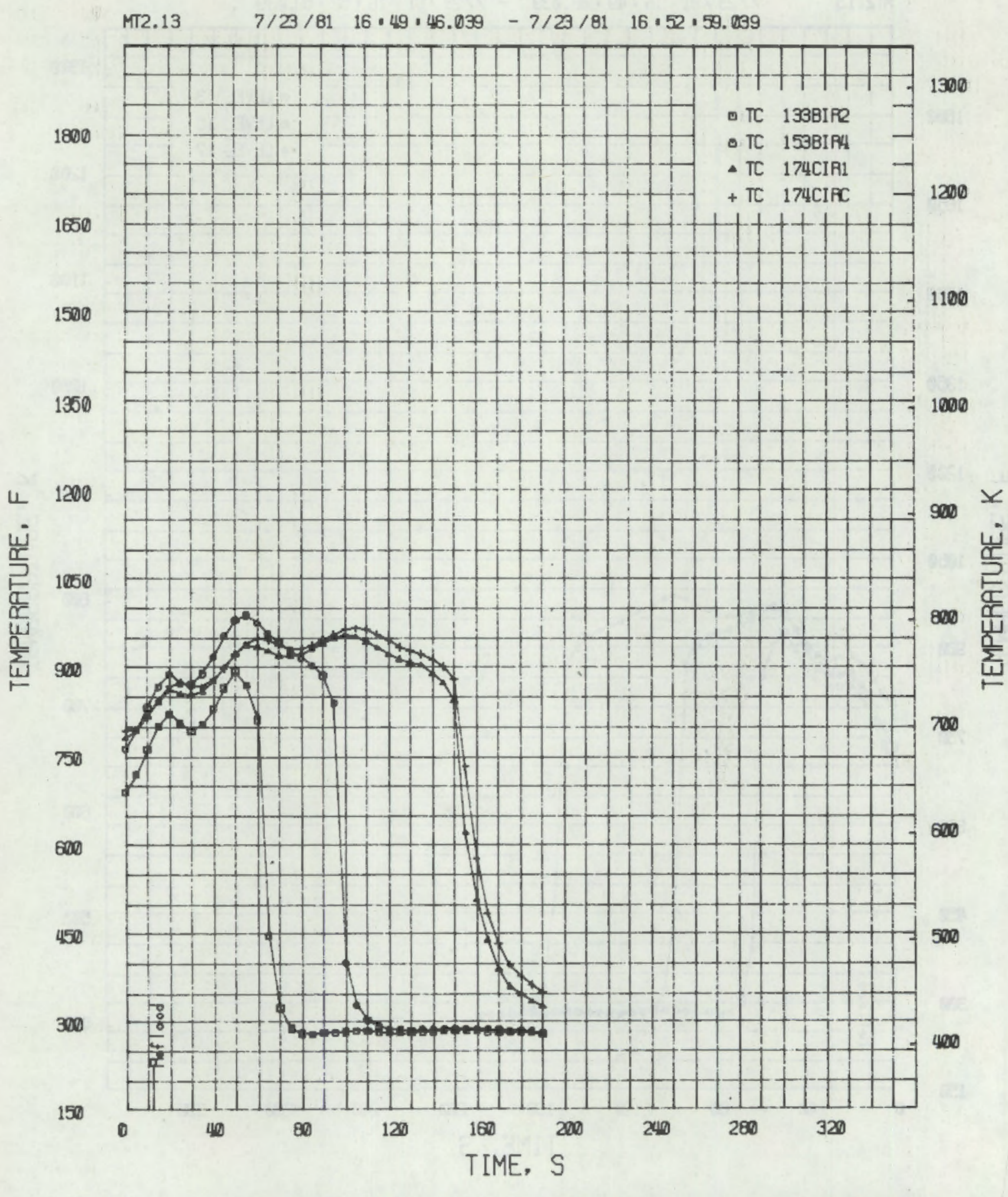

FIGURE C-6. Test Rod Center and Interior Cladding Temperature Histories During Transient MT-2.1.3

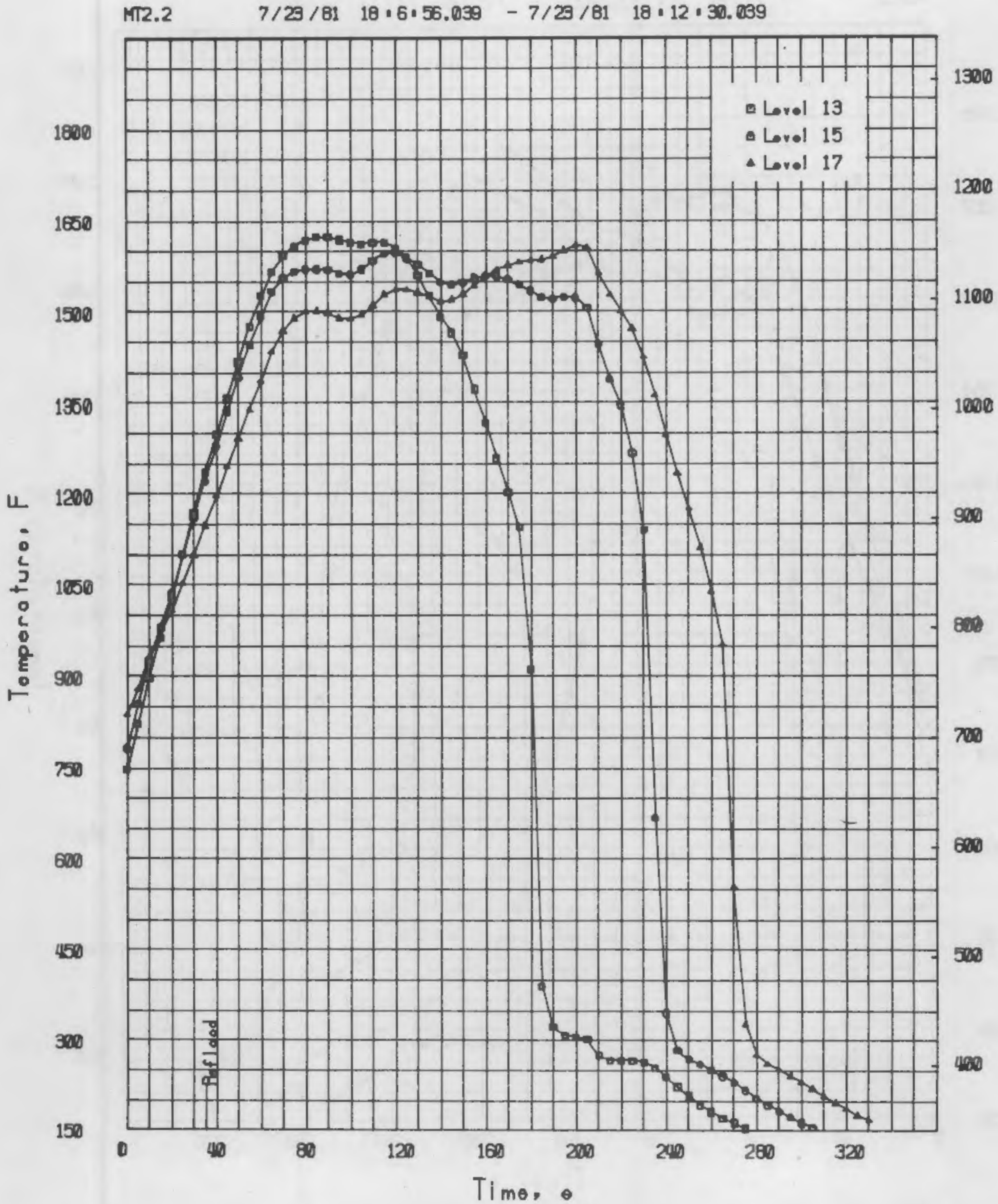

FIGURE C-7. Average Guard Fuel Rod Cladding Temperature Histories (Interior TCs) During Transient MT-2.2

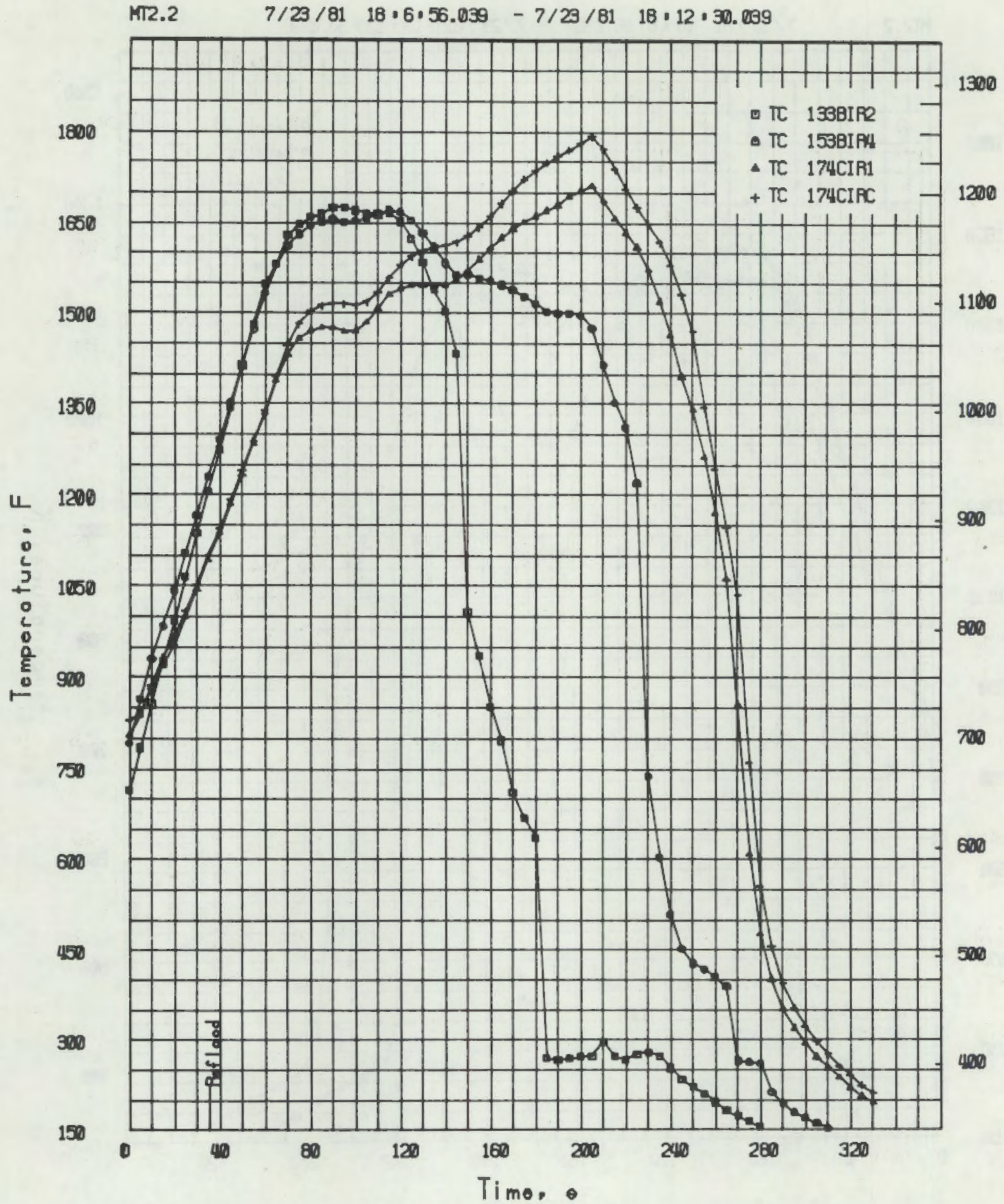

FIGURE C-8. Test Rod Center and Interior Cladding Temperature Histories During Transient MT-2.2

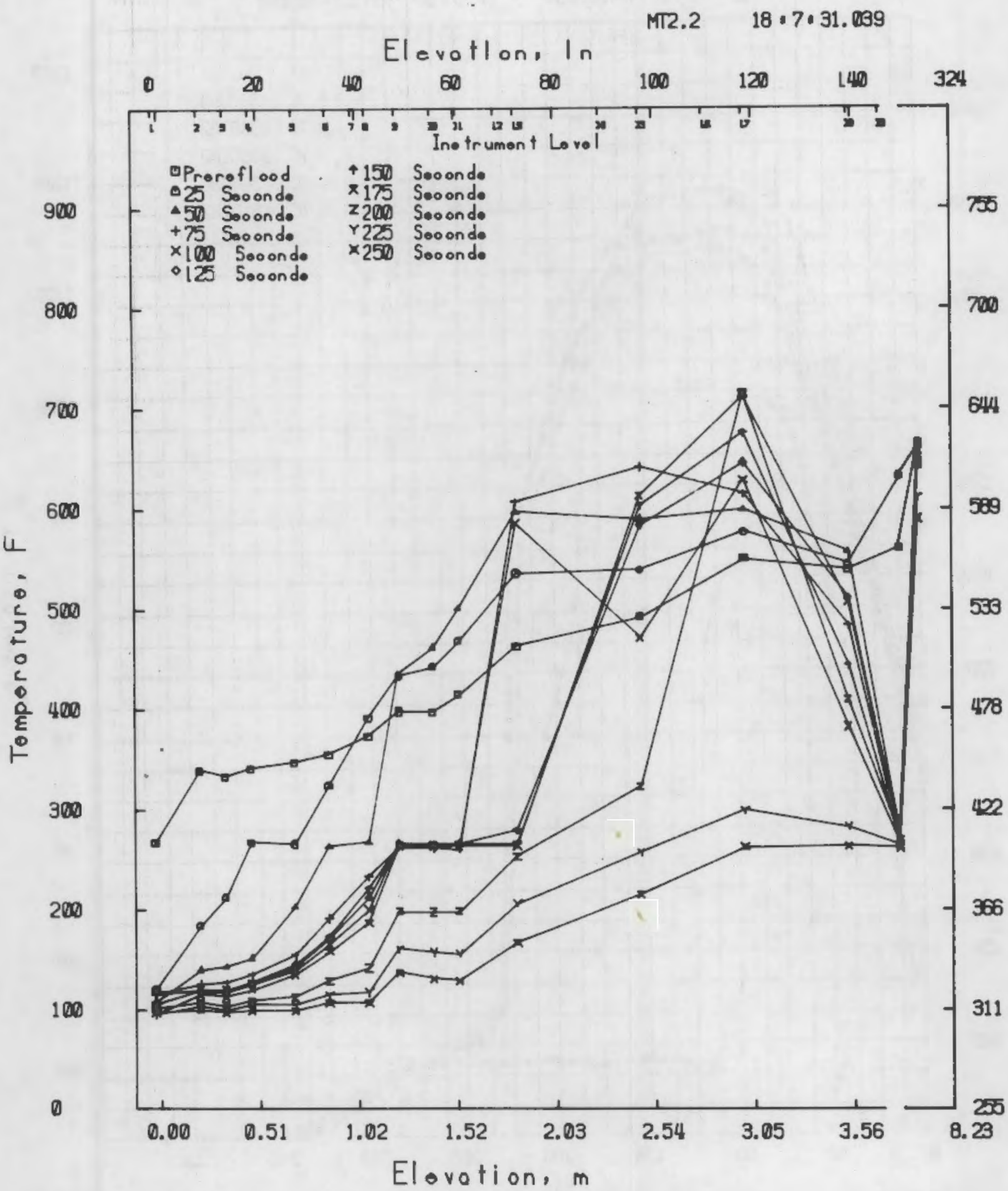

FIGURE C-9. Shroud and Test Train Temperature Profiles During Reflooding at 25 s Intervals, Transient MT-2.2

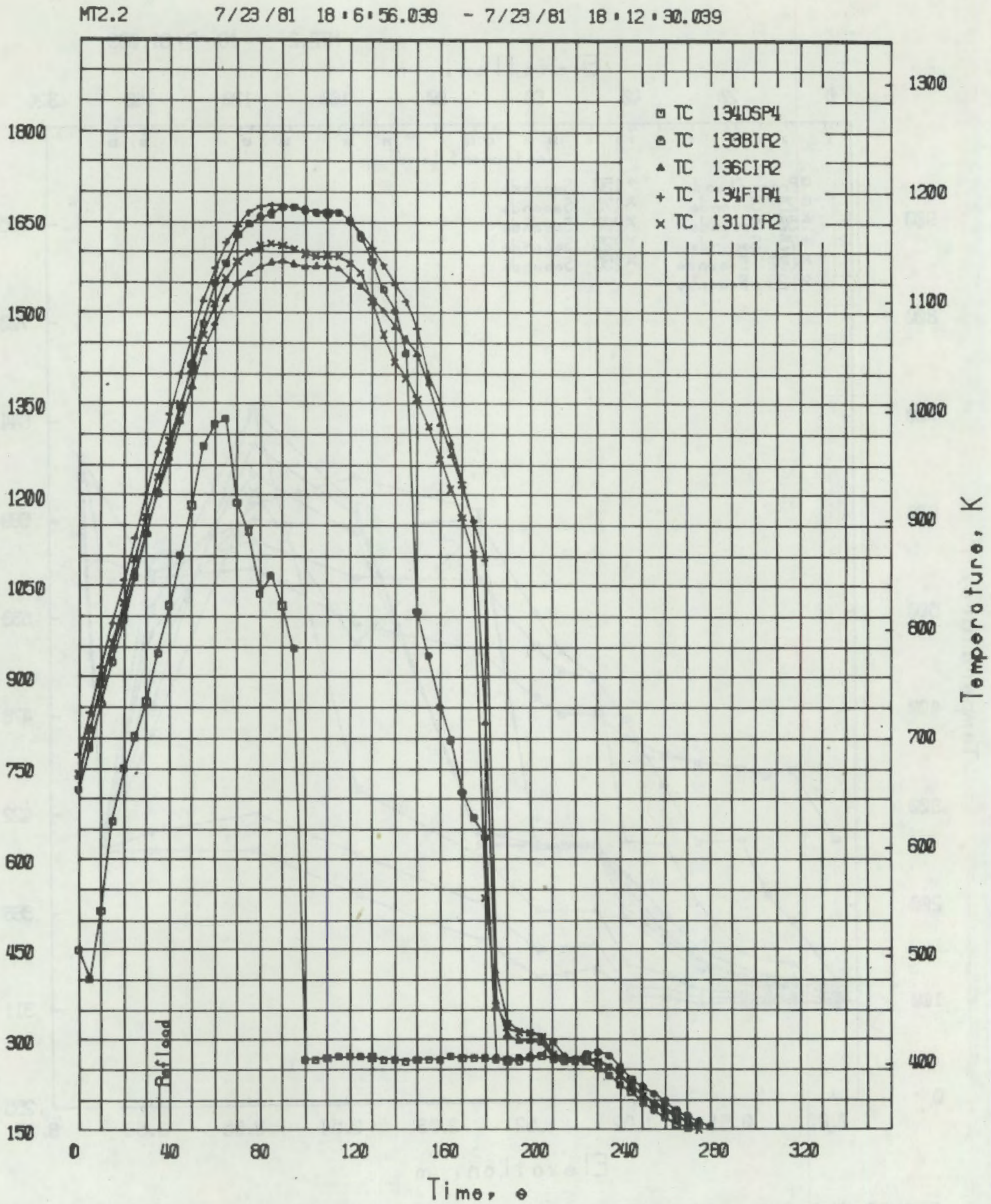

FIGURE C-10. Data for Level 13 - Coolant Channel, Test Fuel Rod, and Guard Fuel Rod Temperatures, MT-2.2

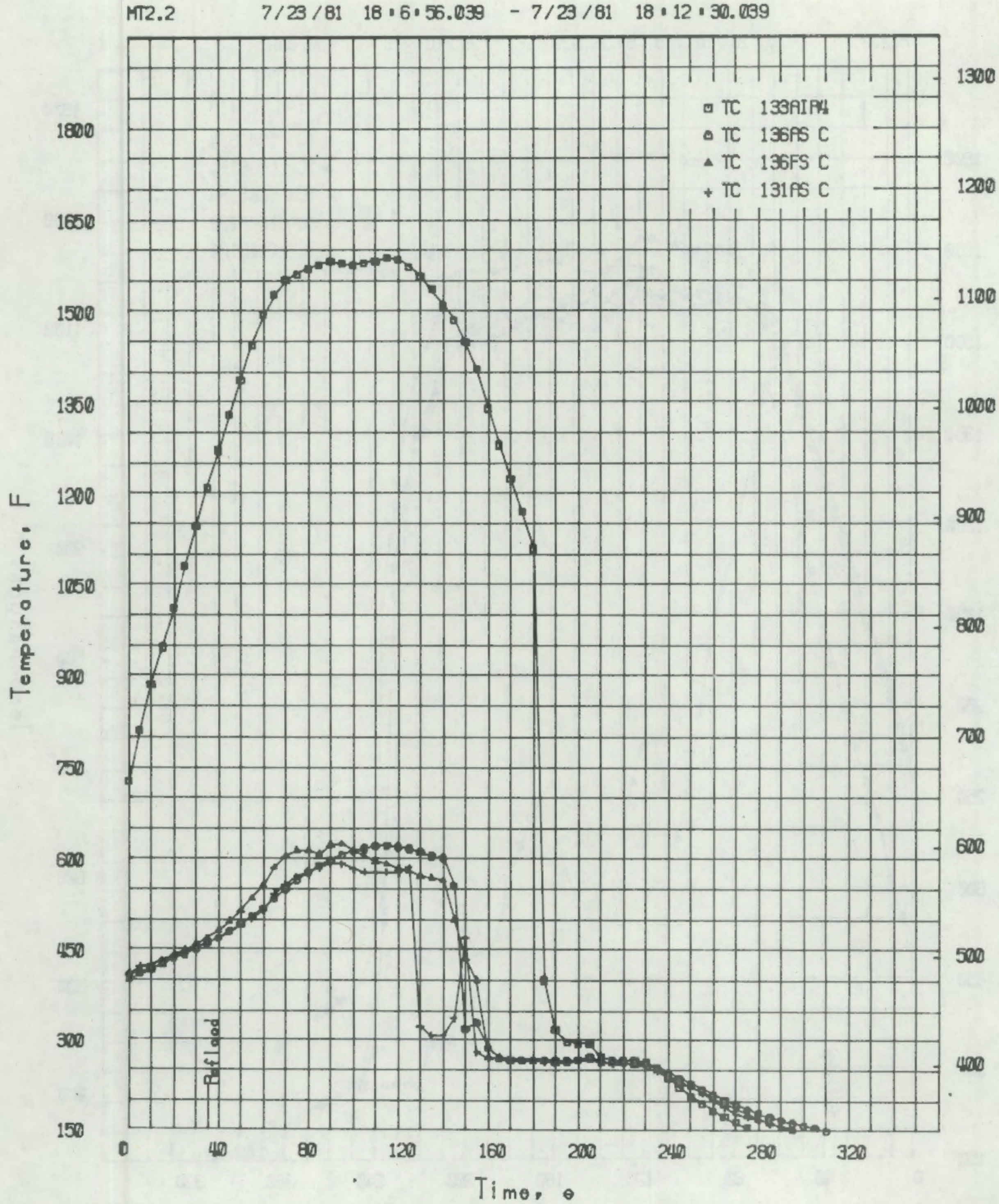

FIGURE C-11. Data for Level 13 - Three Shroud Corners and One Guard Fuel Rod Temperatures, MT-2.2

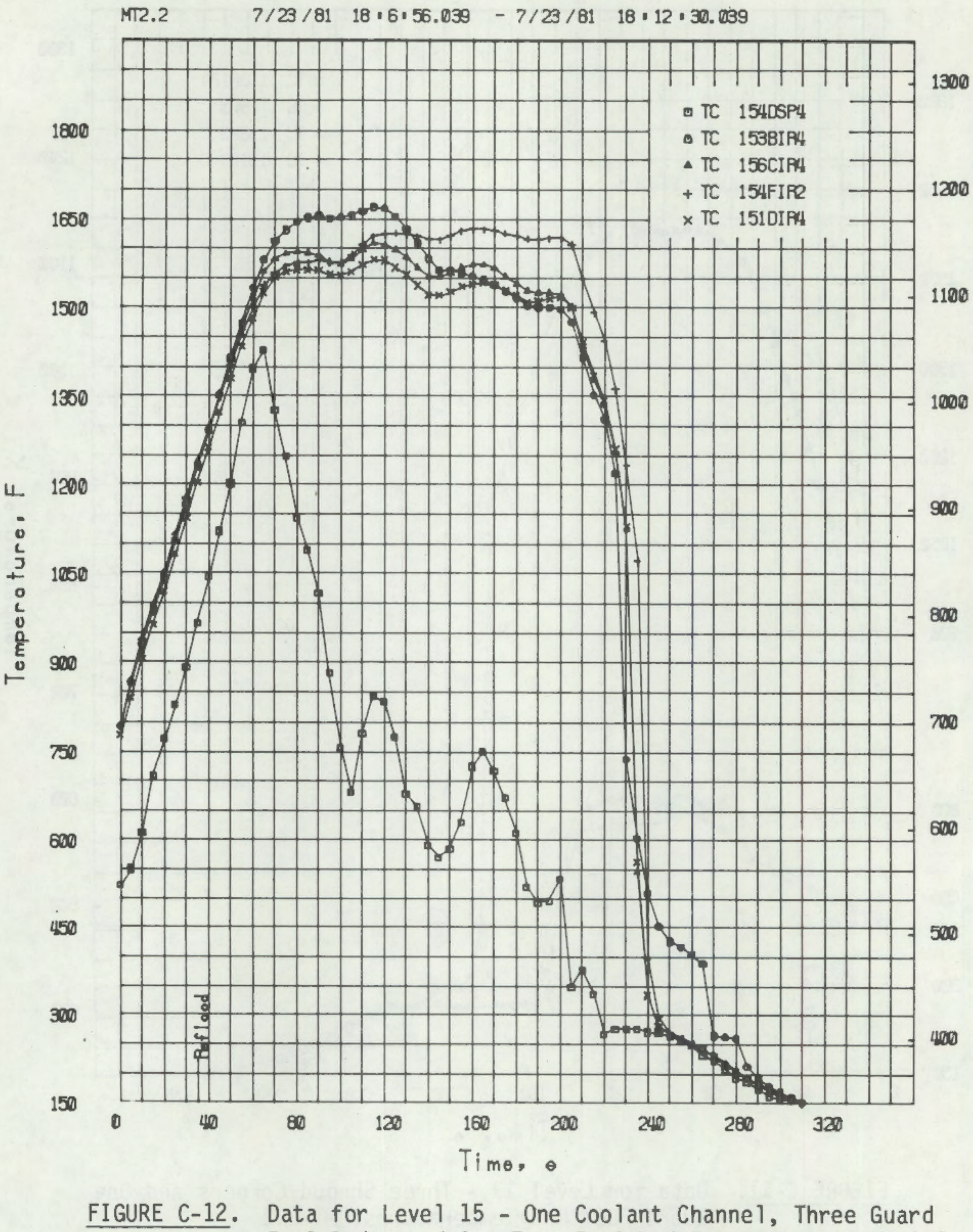

FIGURE C-12. Data for Level 15 - One Coolant Channel, Three Guard Fuel Rods, and One Test Fuel Rod Temperatures, MT-2.2

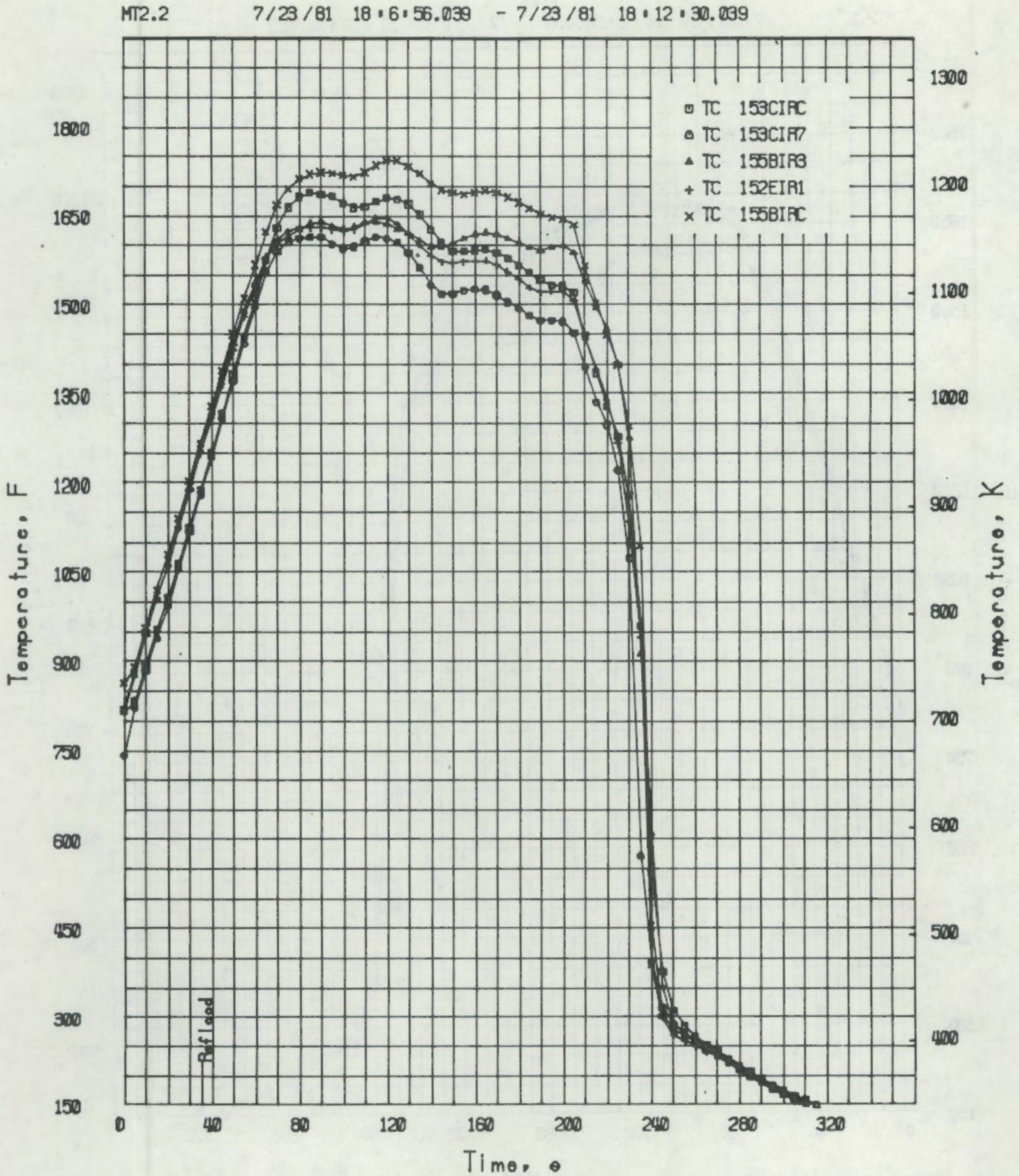

FIGURE C-13. Data for Level 15 - Three Guard Fuel Rods, Inside Cladding and Fuel Centerline Temperatures, MT-2.2

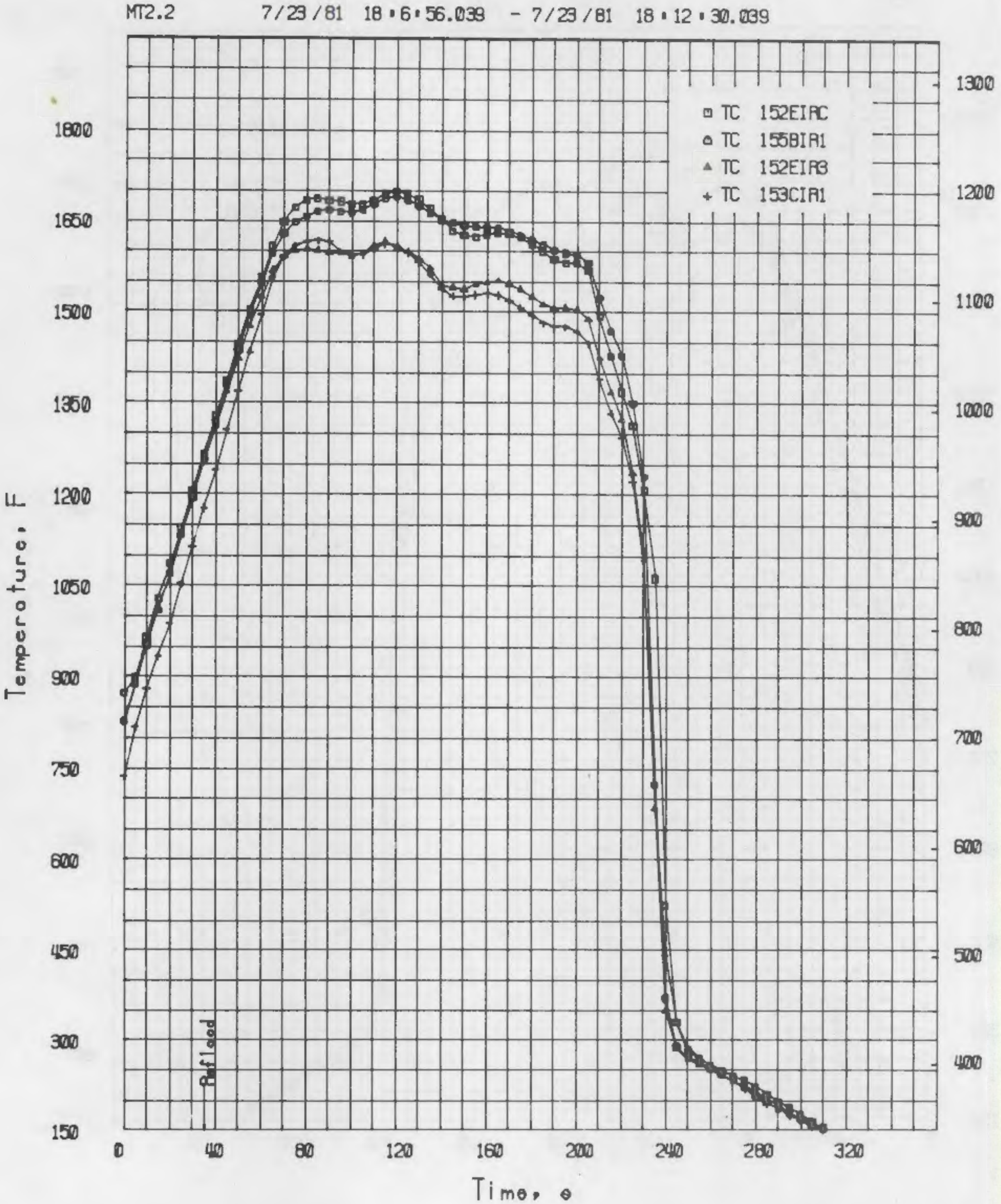

<u>FIGURE C-14</u>. Data for Level 15 - Three Guard Fuel Rods, One Centerline and Two Inside Cladding Temperatures, MT-2.2

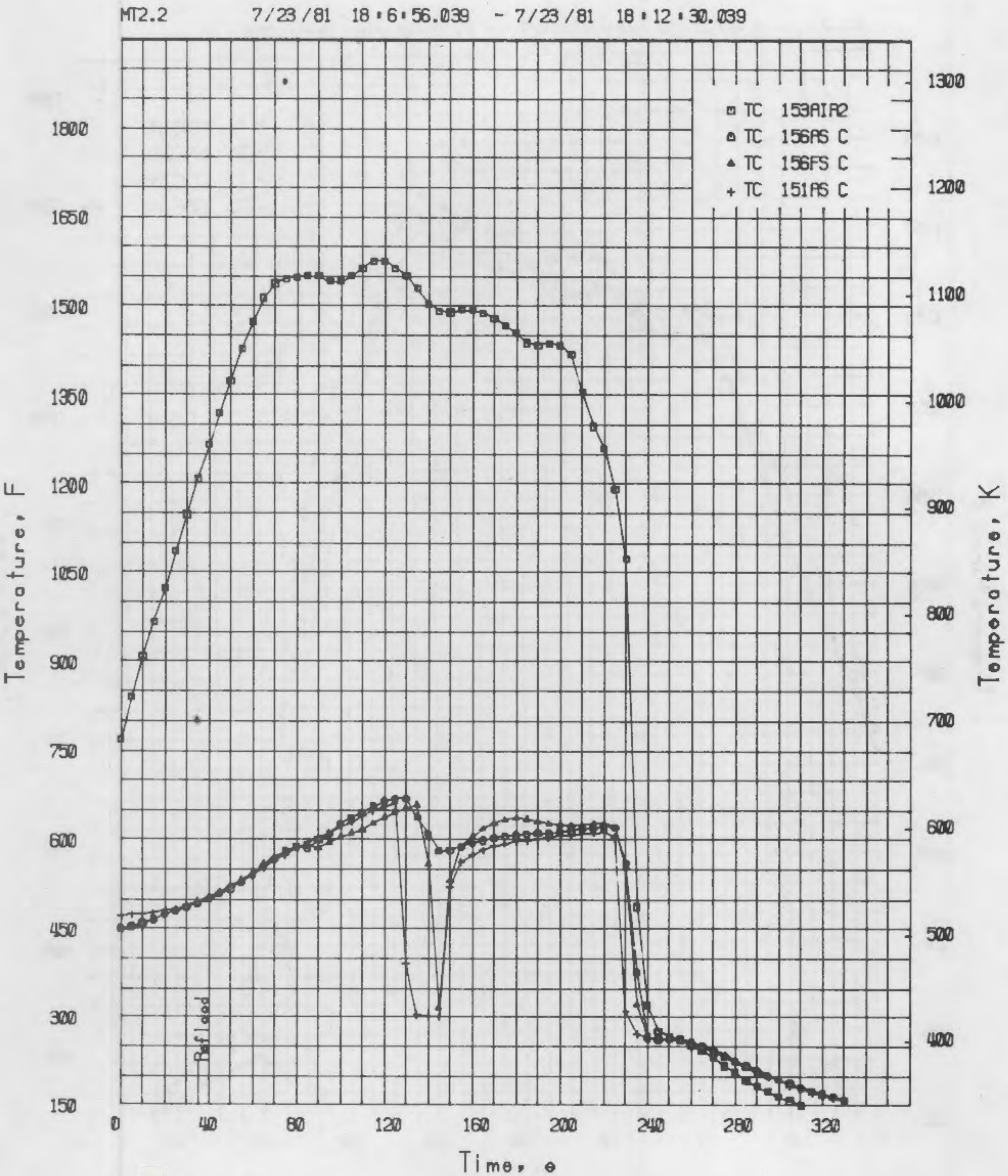

FIGURE C-15. Data for Level 15 - One Guard Fuel Rod and Three Shroud Corner Temperatures, MT-2.2

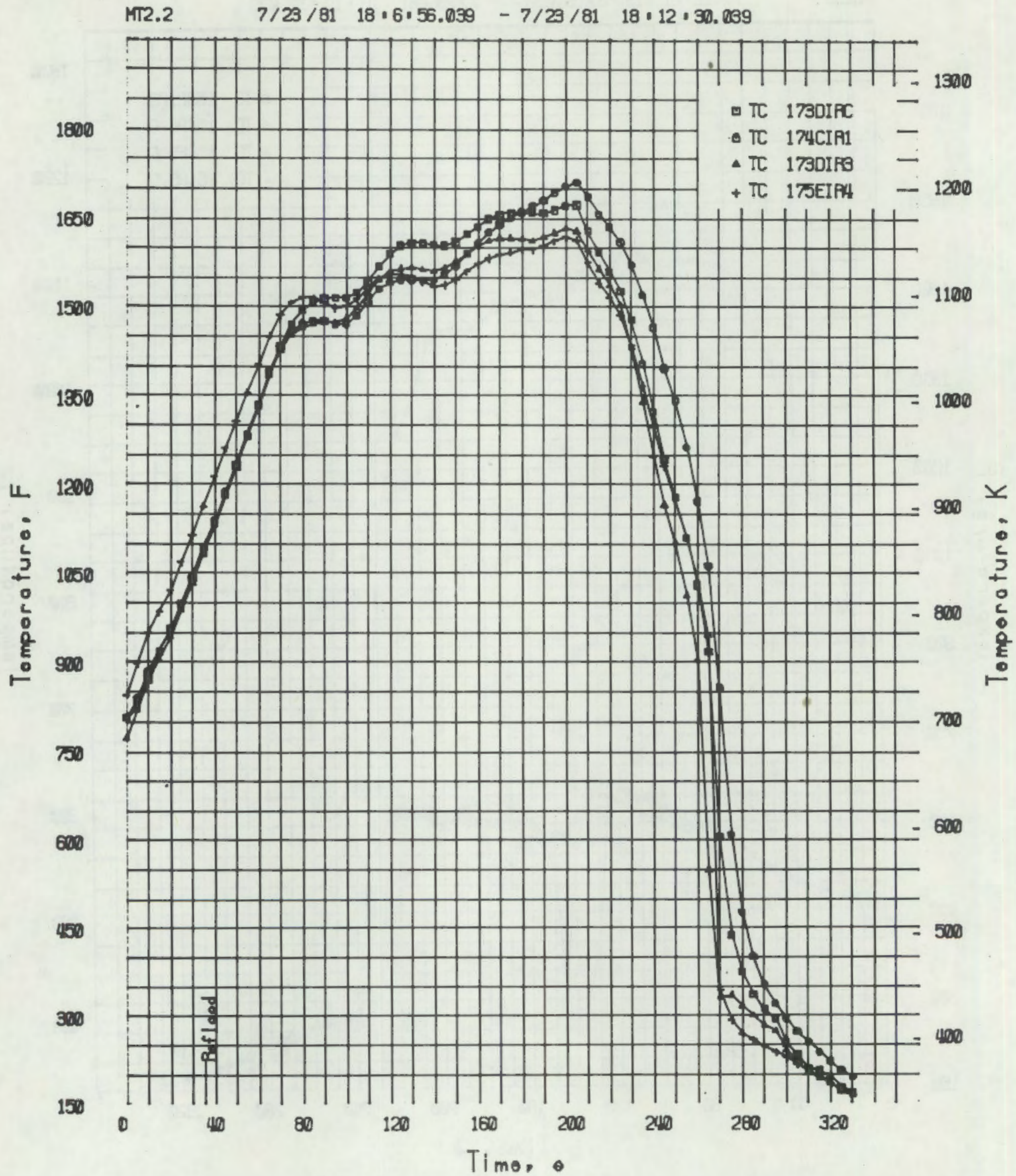

FIGURE C-16. Data for Level 17 - Three Test Fuel Rods and One Guard Fuel Rod Temperatures, MT-2.2

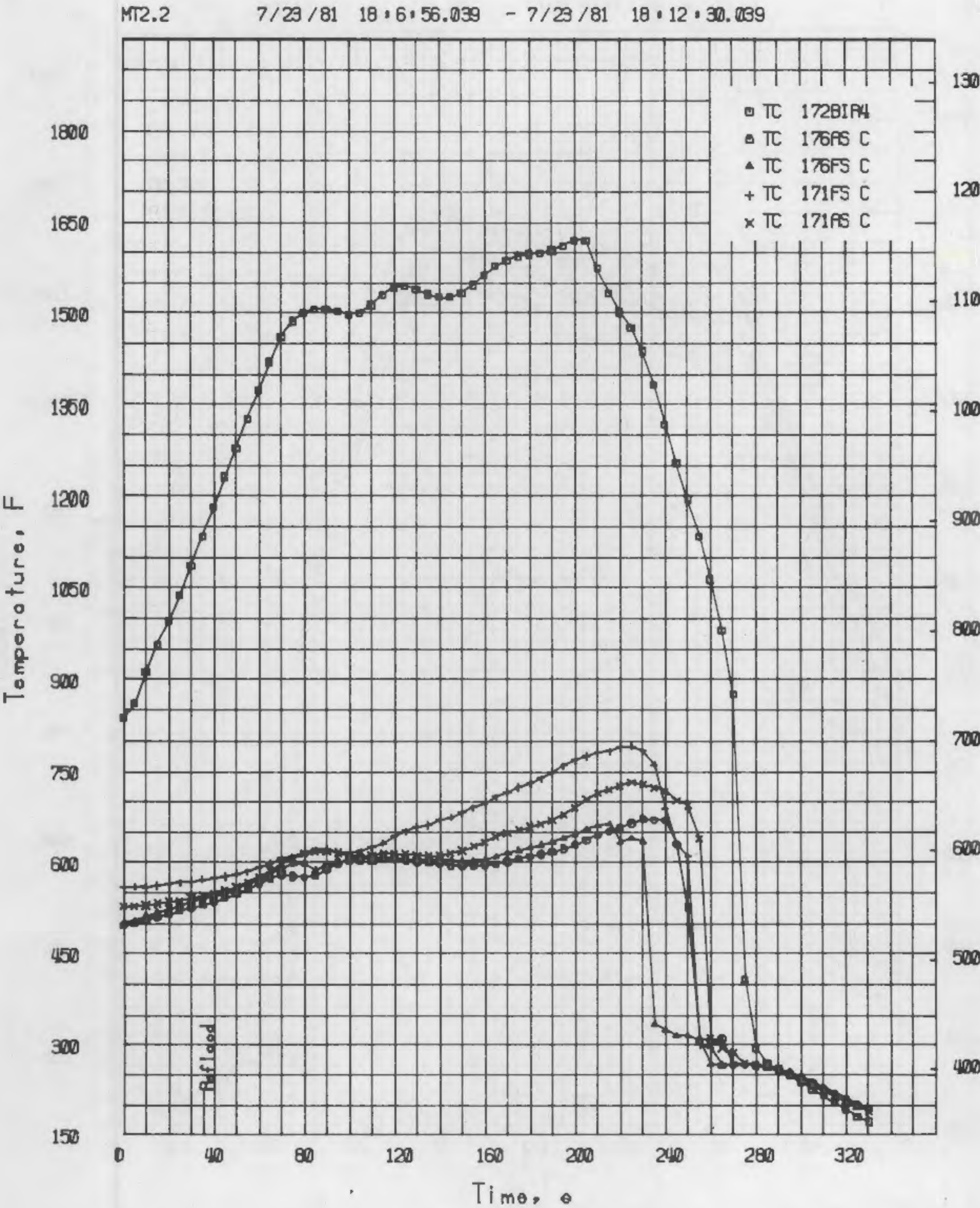

FIGURE C-17. Data for Level 17 - One Guard Fuel Rod and Four Shroud Corner Temperatures, MT-2.2

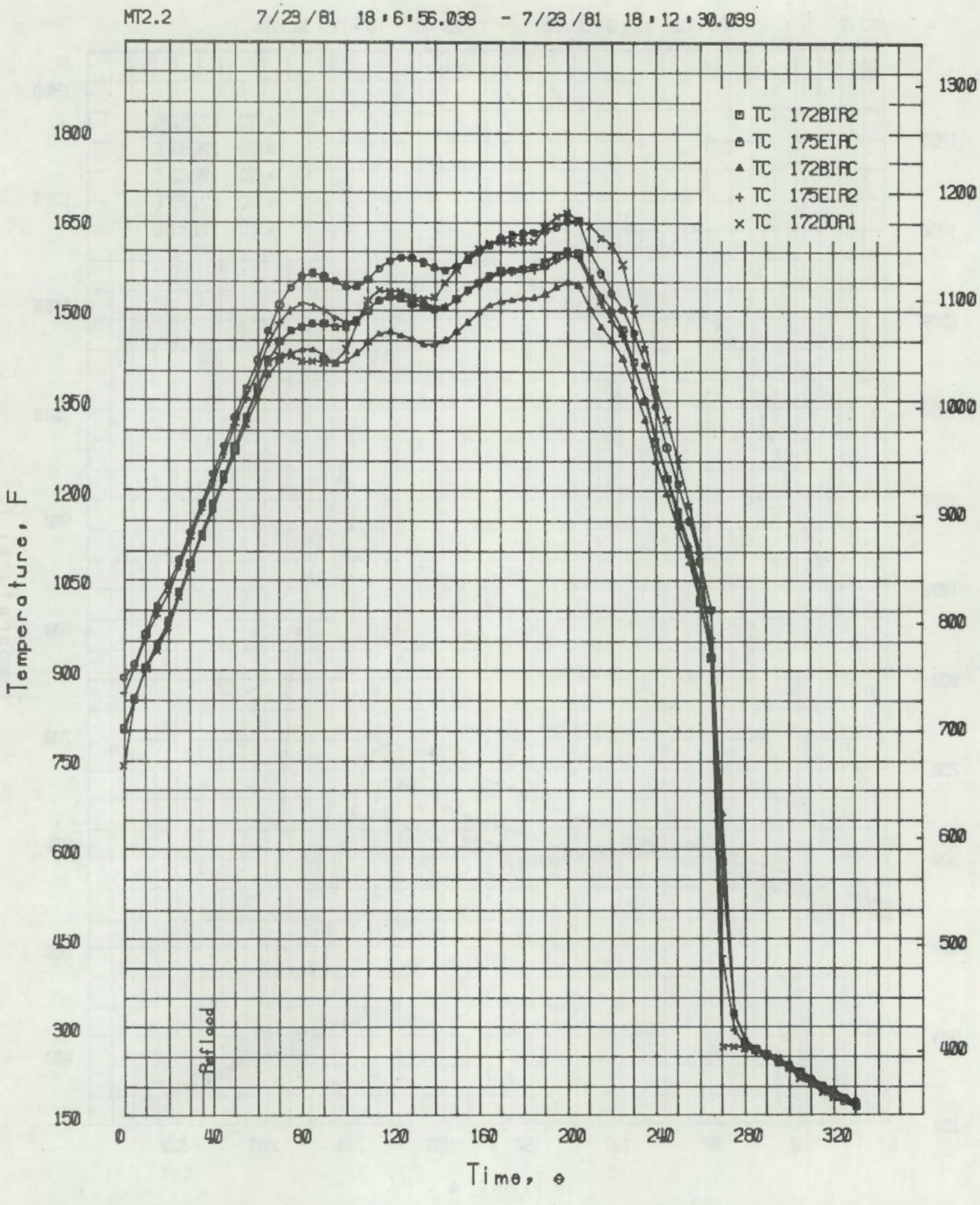

FIGURE C-18. Data for Level 17 - One Test Fuel Rod Outside Cladding, Two Guard Fuel Rod Cladding, and Two Centerline Fuel Temperatures, MT-2.2

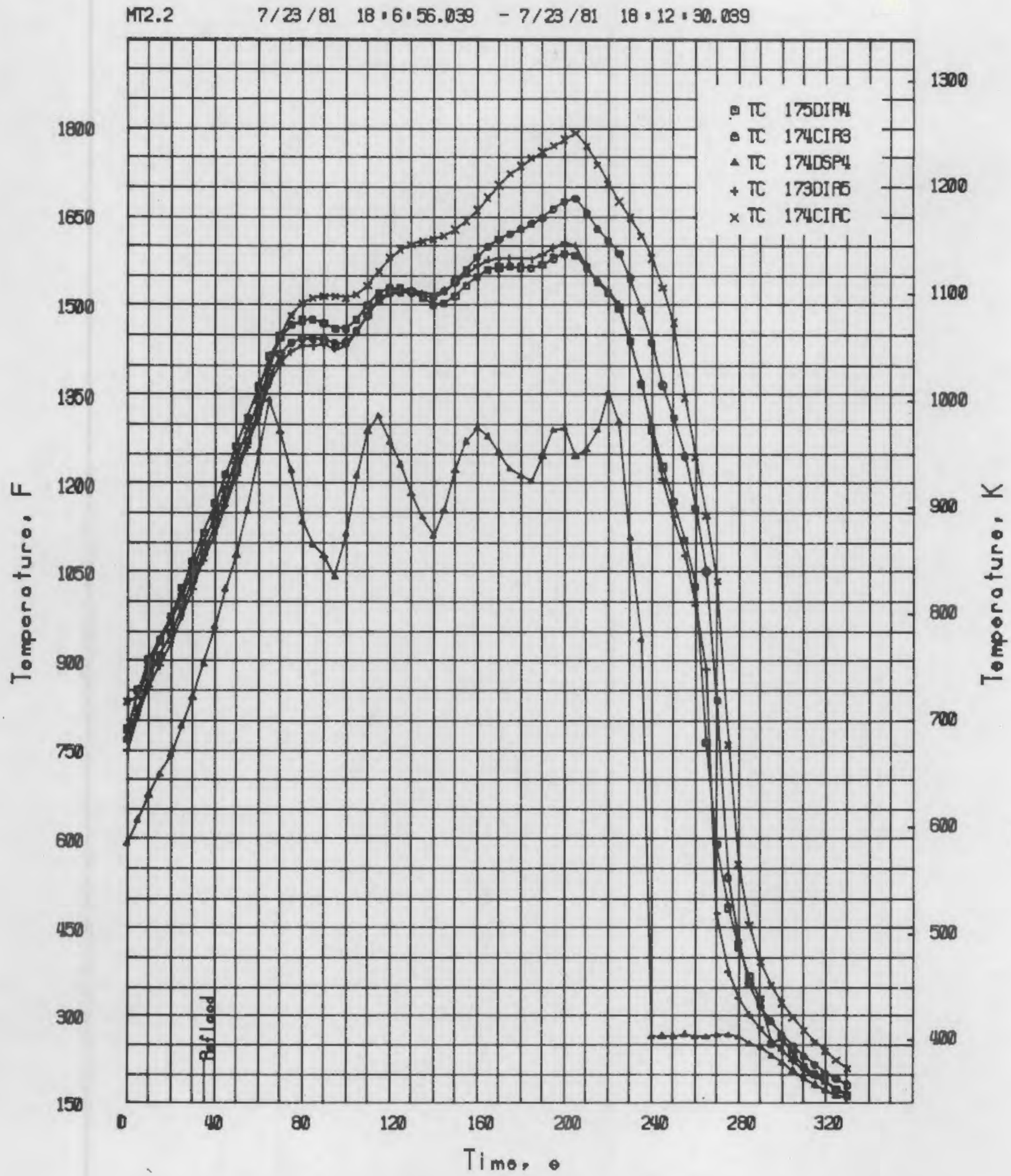

FIGURE C-19. Data for Level 17 - Three Test Fuel Rods, Inside Cladding and Fuel Centerline, and One Coolant Channel Temperatures, MT-2.2

APPENDIX D

TRANSIENT COOLANT AND SHROUD TEMPERATURES

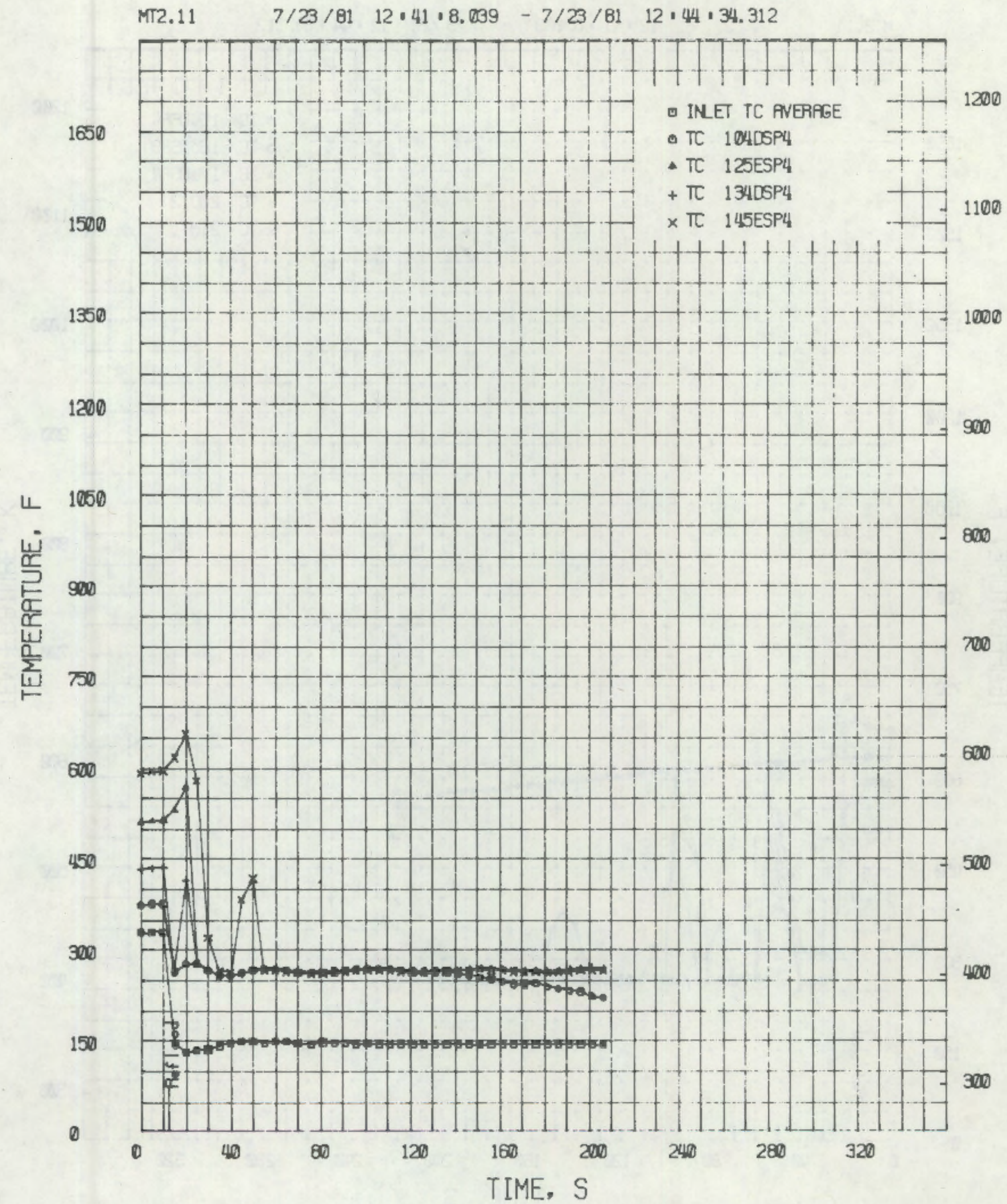

FIGURE D-1. Steam Probe and Inlet TC Temperature Histories for Levels 1 to 14 During Transient MT-2.1.1

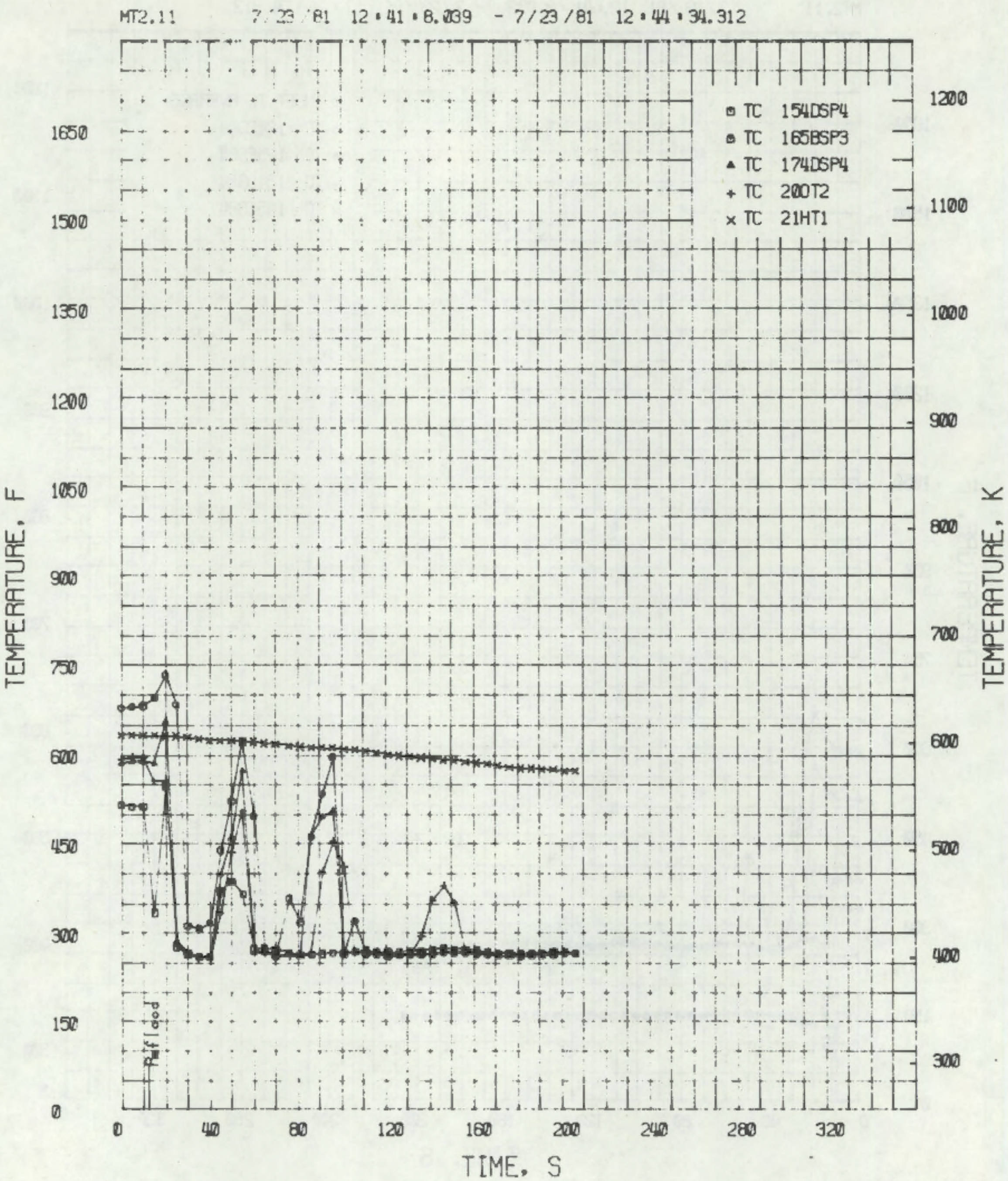

FIGURE D-2. Steam Probe and Outlet Region Temperature Histories for Levels 15 to 21 During Transient MT-2.1.1

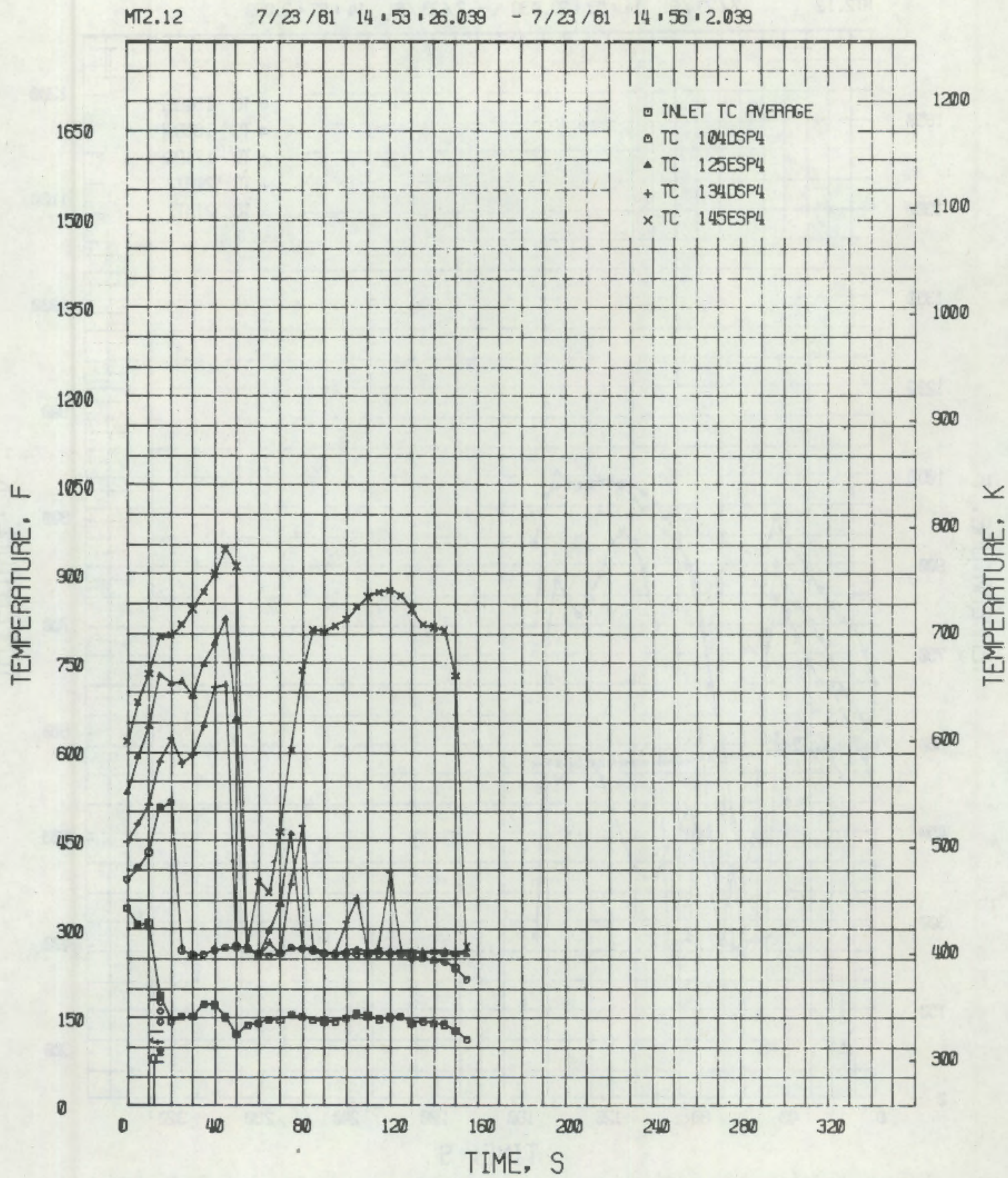

FIGURE D-3. Steam Probe and Inlet TC Temperature Histories for Levels 1 to 14 During Transient MT-2.1.2

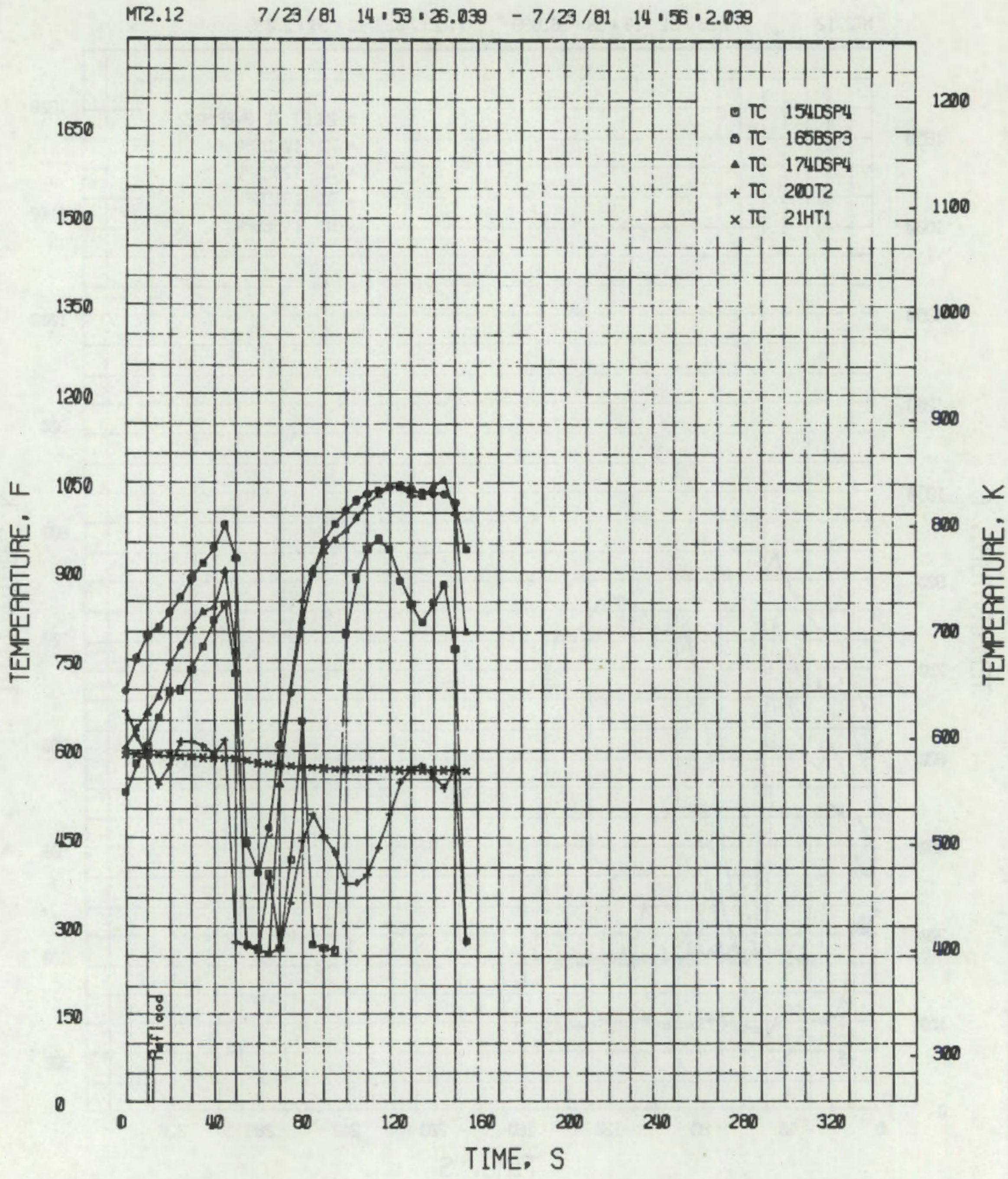

FIGURE D-4. Steam Probe and Outlet Region Temperature Histories for Levels 15 to 21 During Transient MT-2.1.2

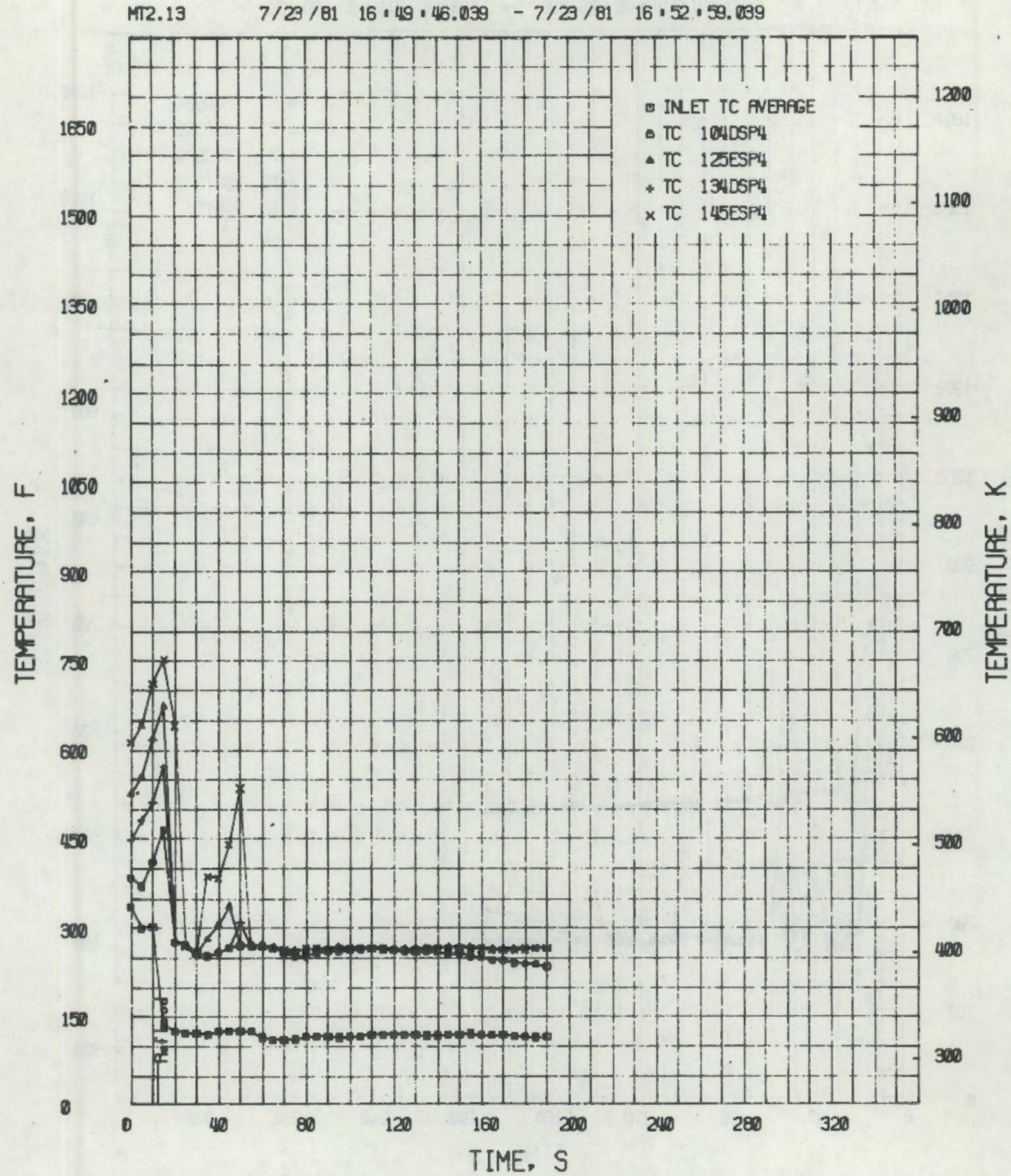

FIGURE D-5. Steam Probe and Inlet TC Temperature Histories for Levels 1 to 14 During Transient MT-2.1.3

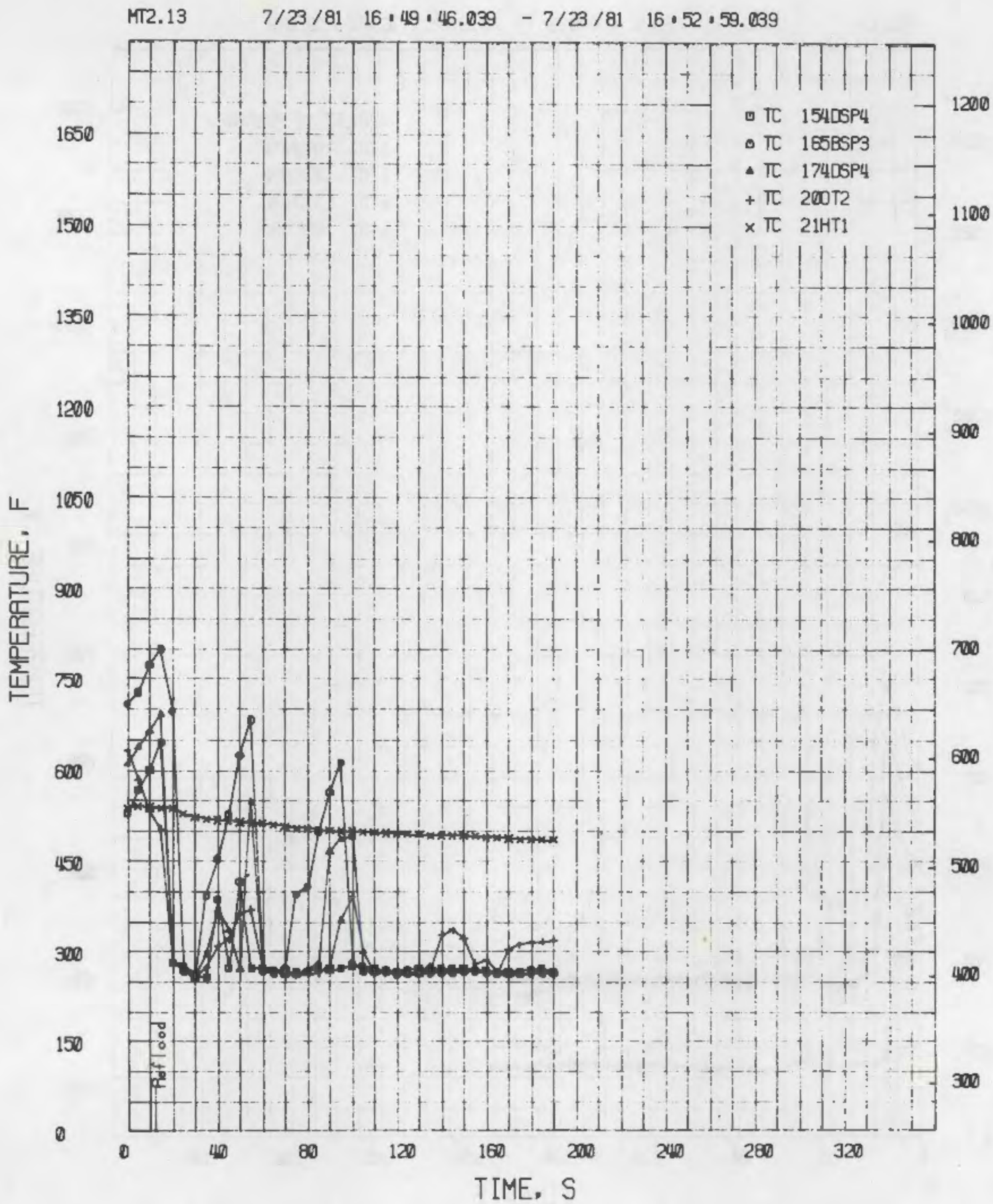

FIGURE D-6. Steam Probe and Outlet Region Temperature Histories for Levels 15 to 21 During Transient MT-2.1.3

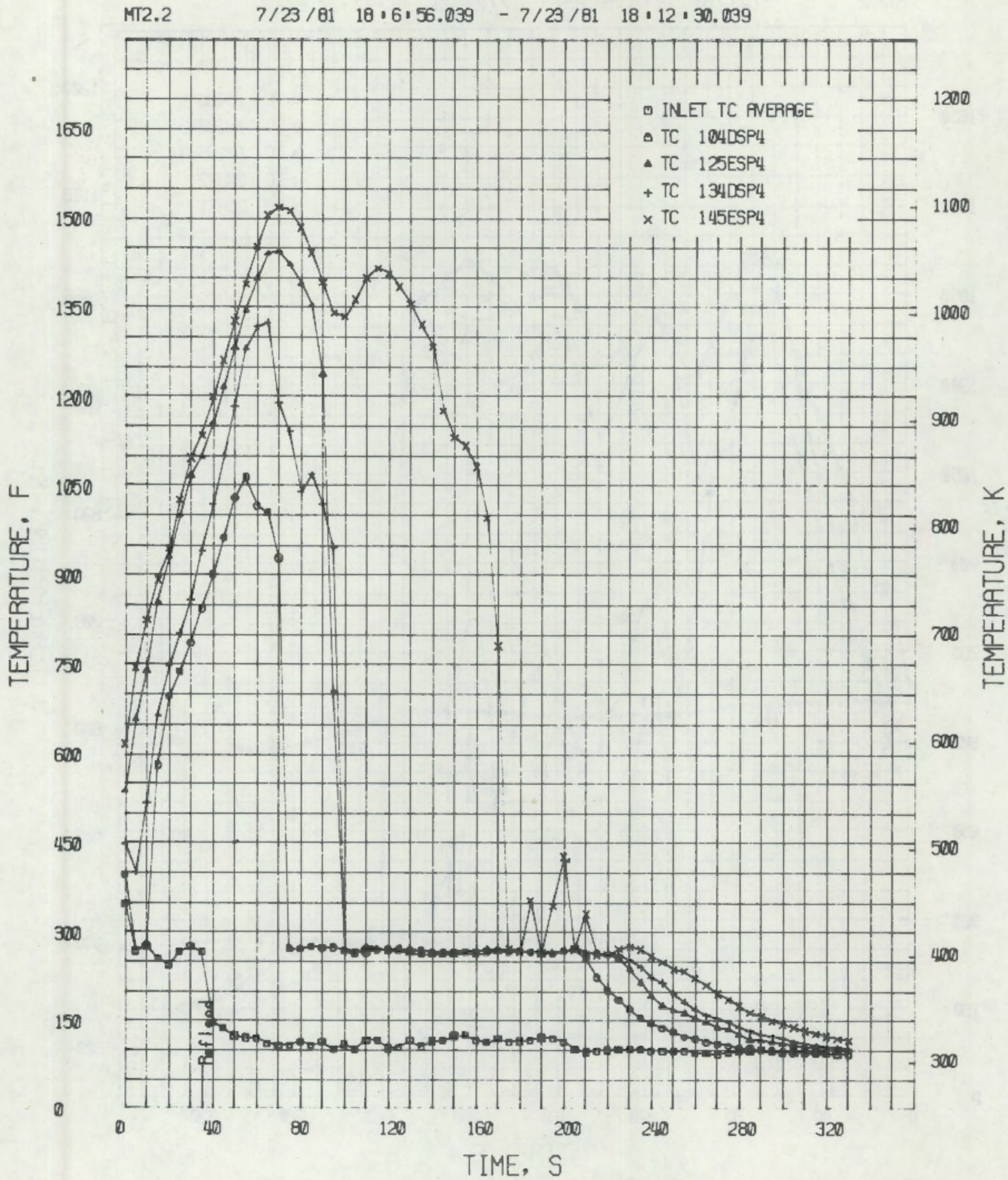

FIGURE D-7. Steam Probe and Inlet TC Temperature Histories for Levels 1 to 14 During Transient MT-2.2

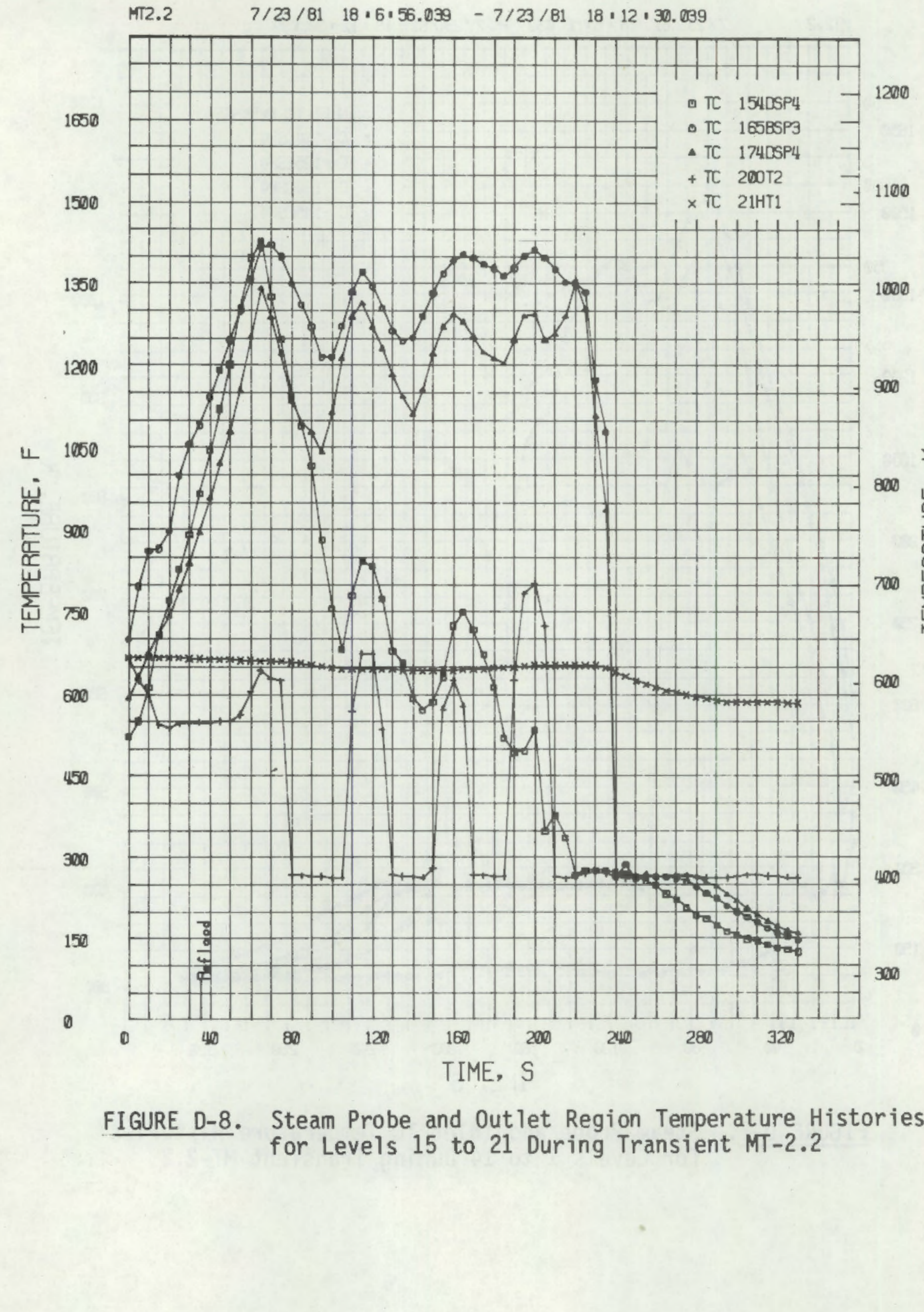

FIGURE D-8. Steam Probe and Outlet Region Temperature Histories for Levels 15 to 21 During Transient MT-2.2

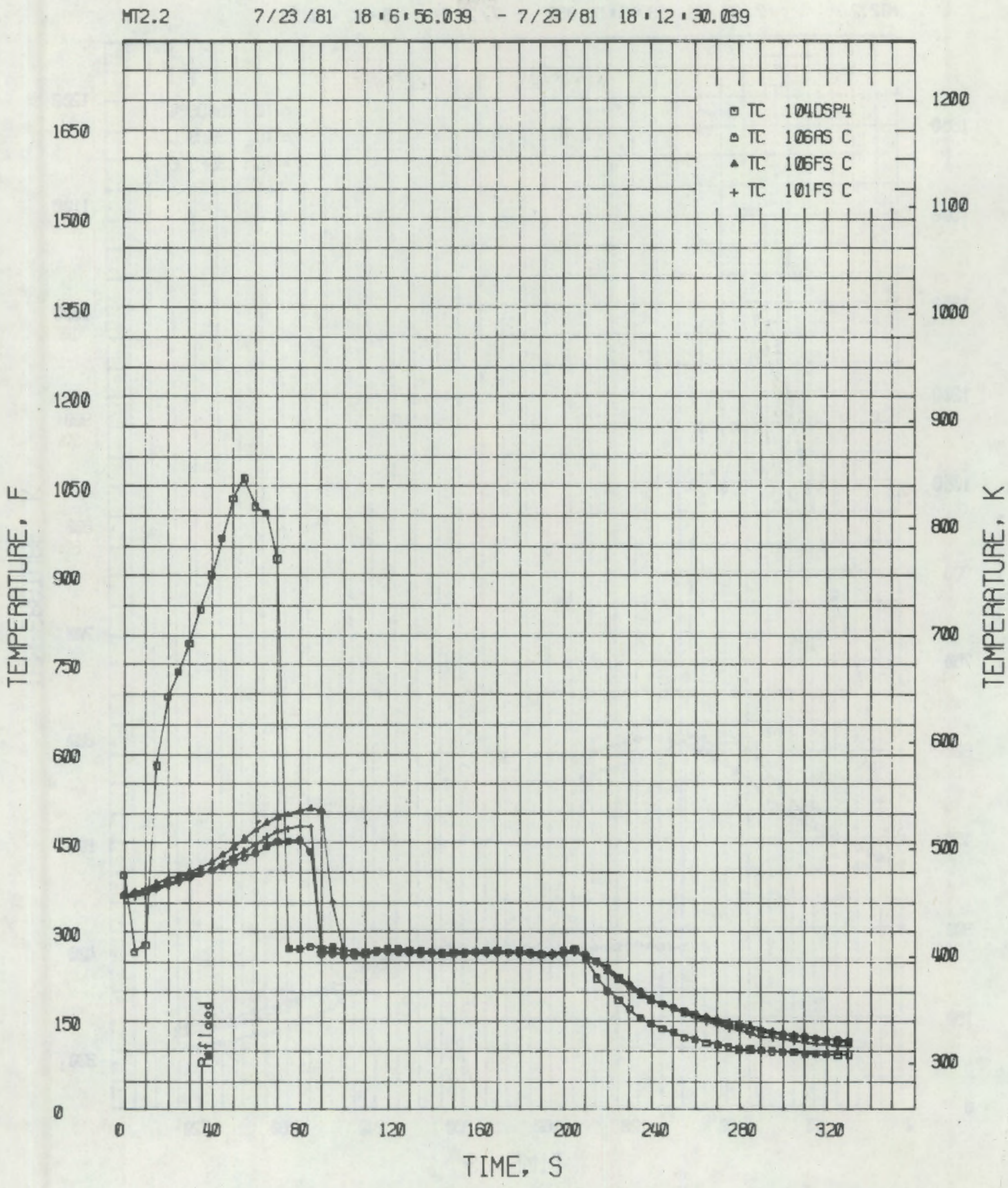

FIGURE D-9. Steam Probe and Shroud Temperature Histories at Level 10 During Transient MT-2.2

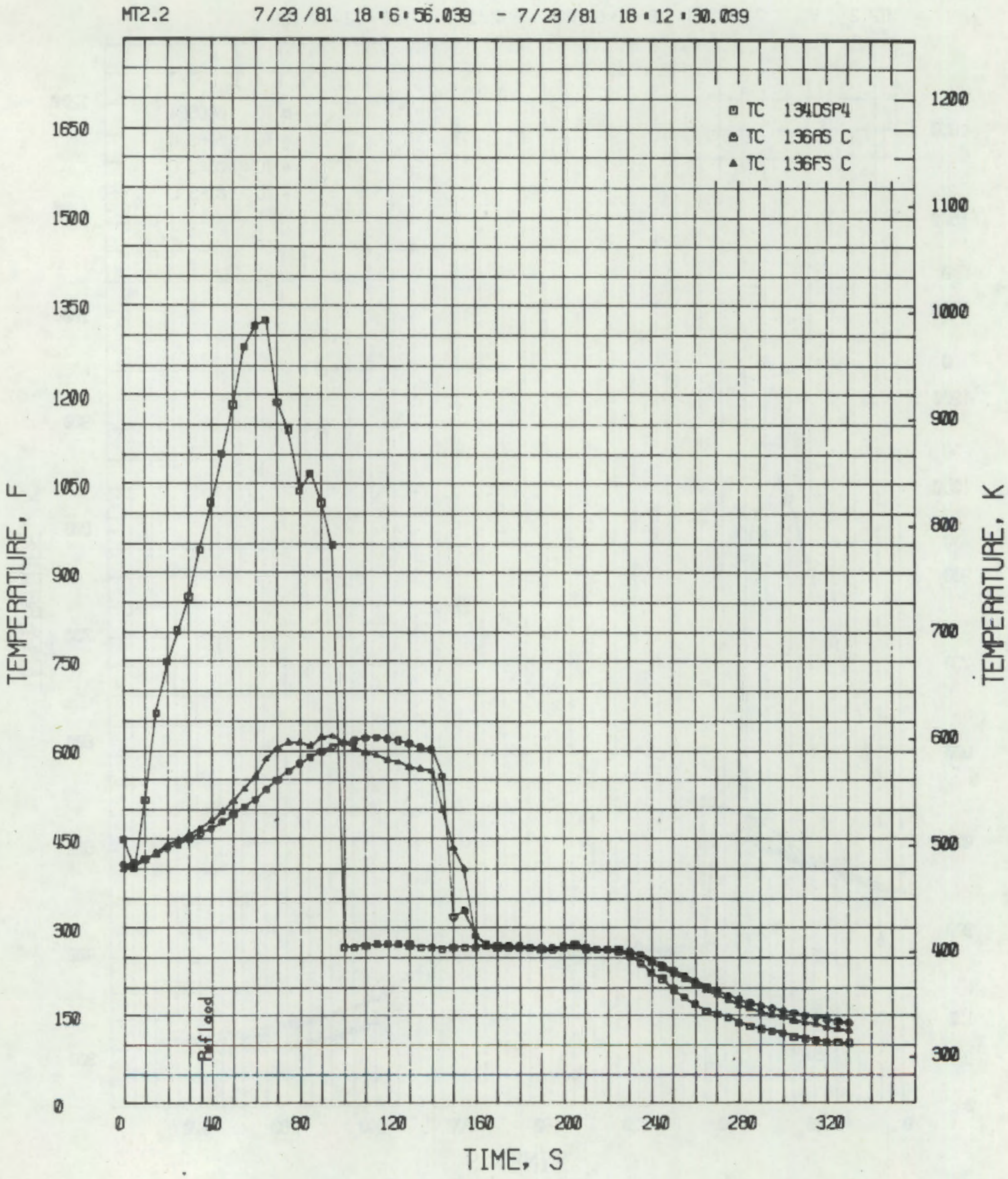

FIGURE D-10. Steam Probe and Shroud Temperature Histories at Level 13 During Transient MT-2.2

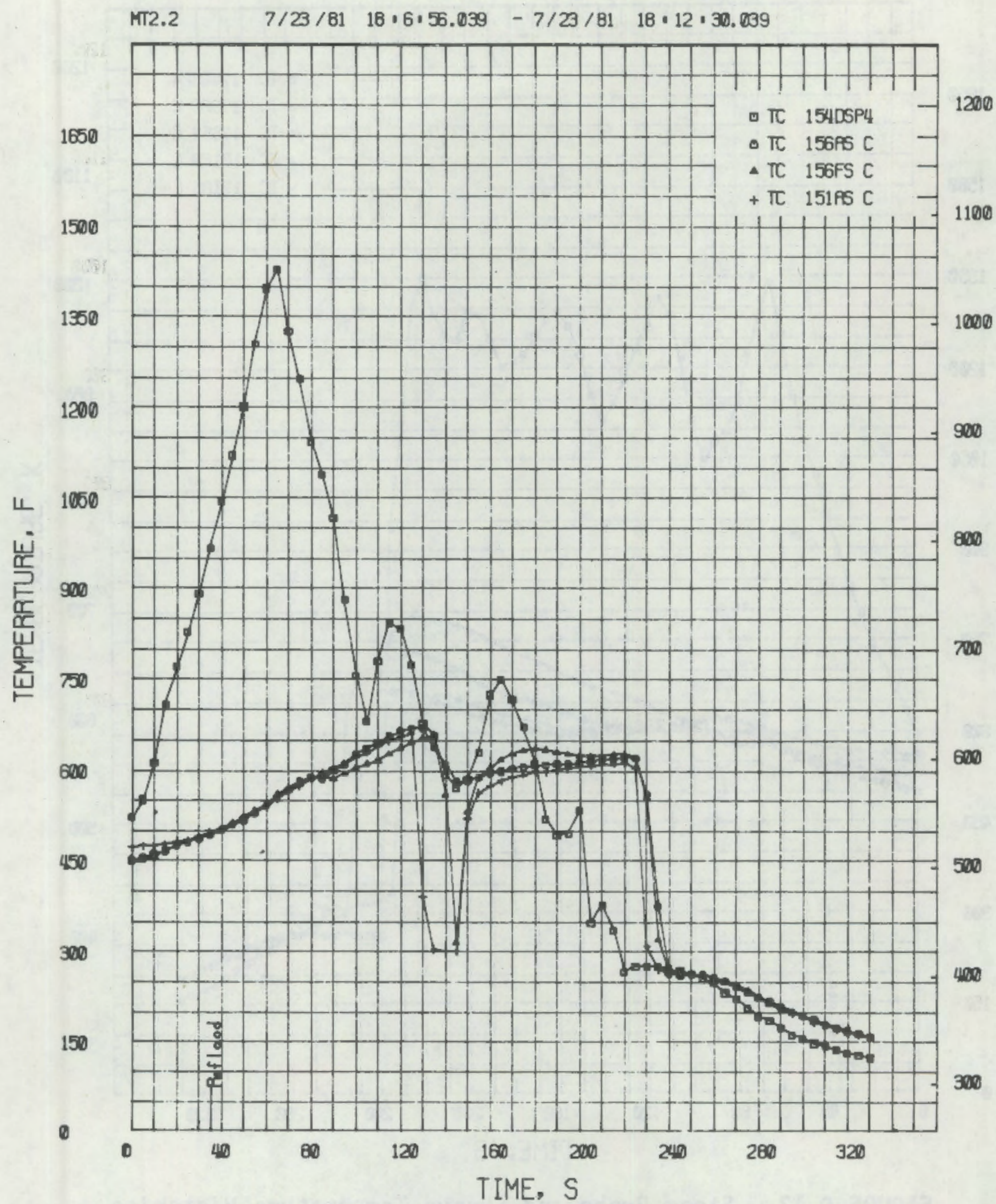

FIGURE D-11. Steam Probe and Shroud Temperature Histories at Level 15 During Transient MT-2.2

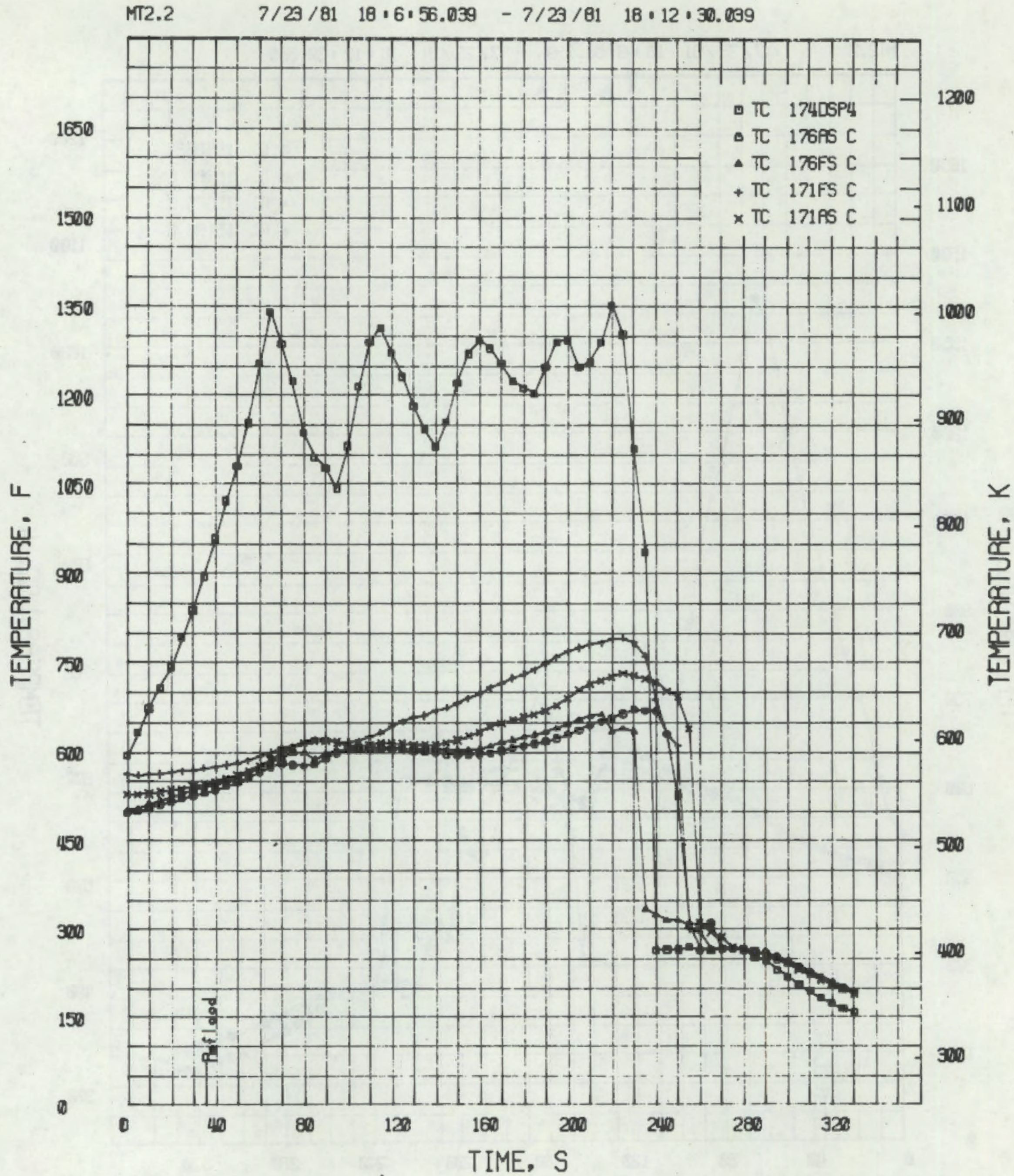

FIGURE D-12. Steam Probe and Shroud Temperature Histories at Level 17 During Transient MT-2.2

APPENDIX E

NEUTRON FLUX

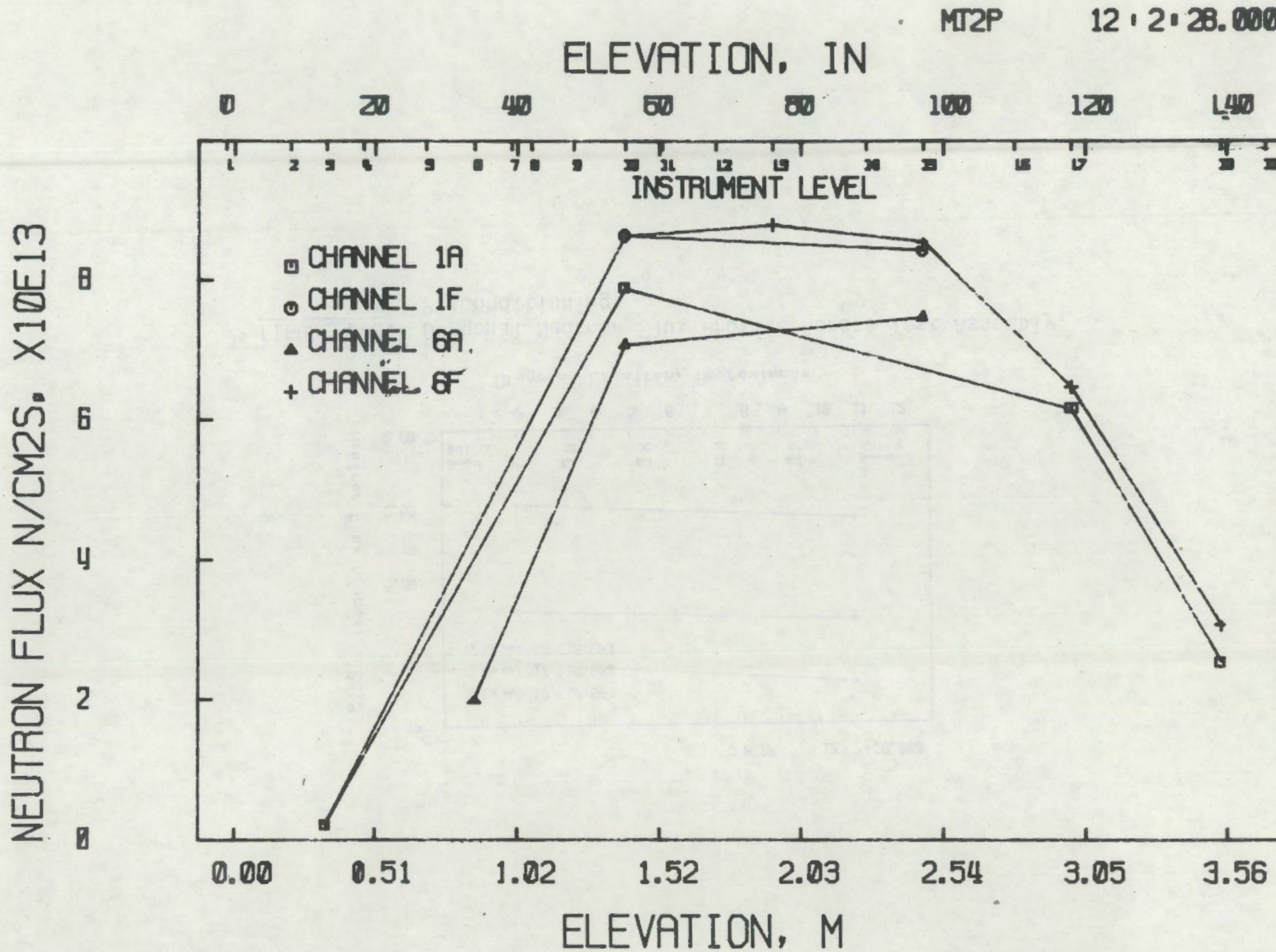

FIGURE E-1. Neutron Flux Axial Profiles, Preconditioning

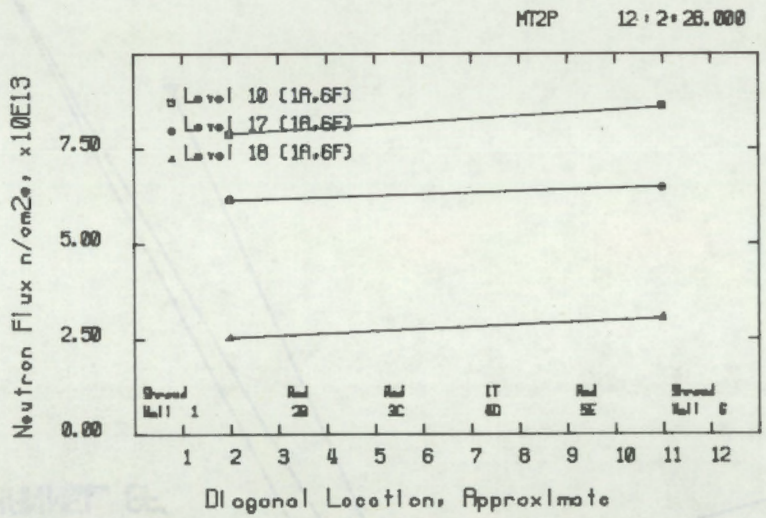

FIGURE E-2. Diagonal Neutron Flux Profile Across Test Assembly, Preconditioning

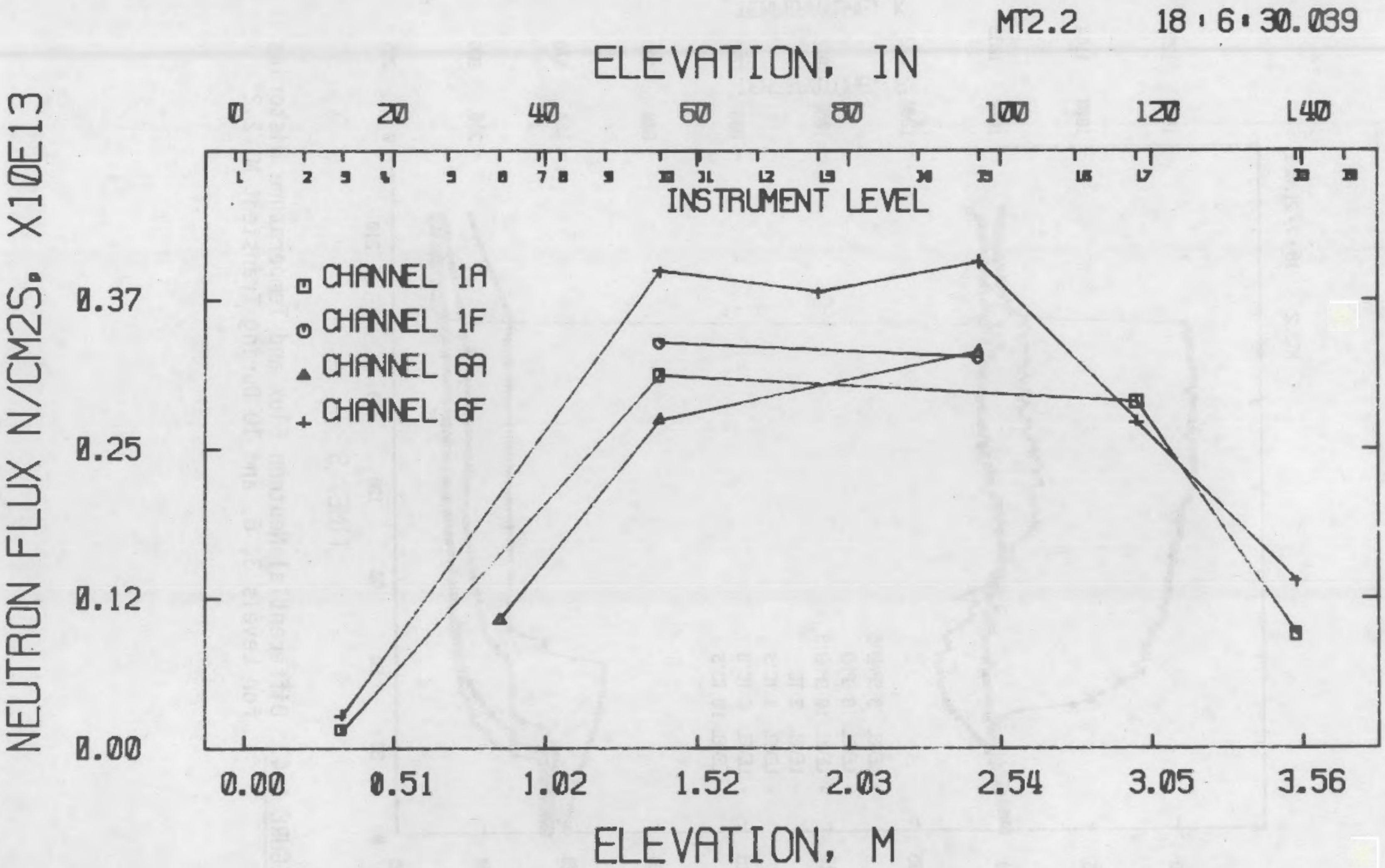

FIGURE E-3. Axial Neutron Flux Profile in the Shroud, Pretransient

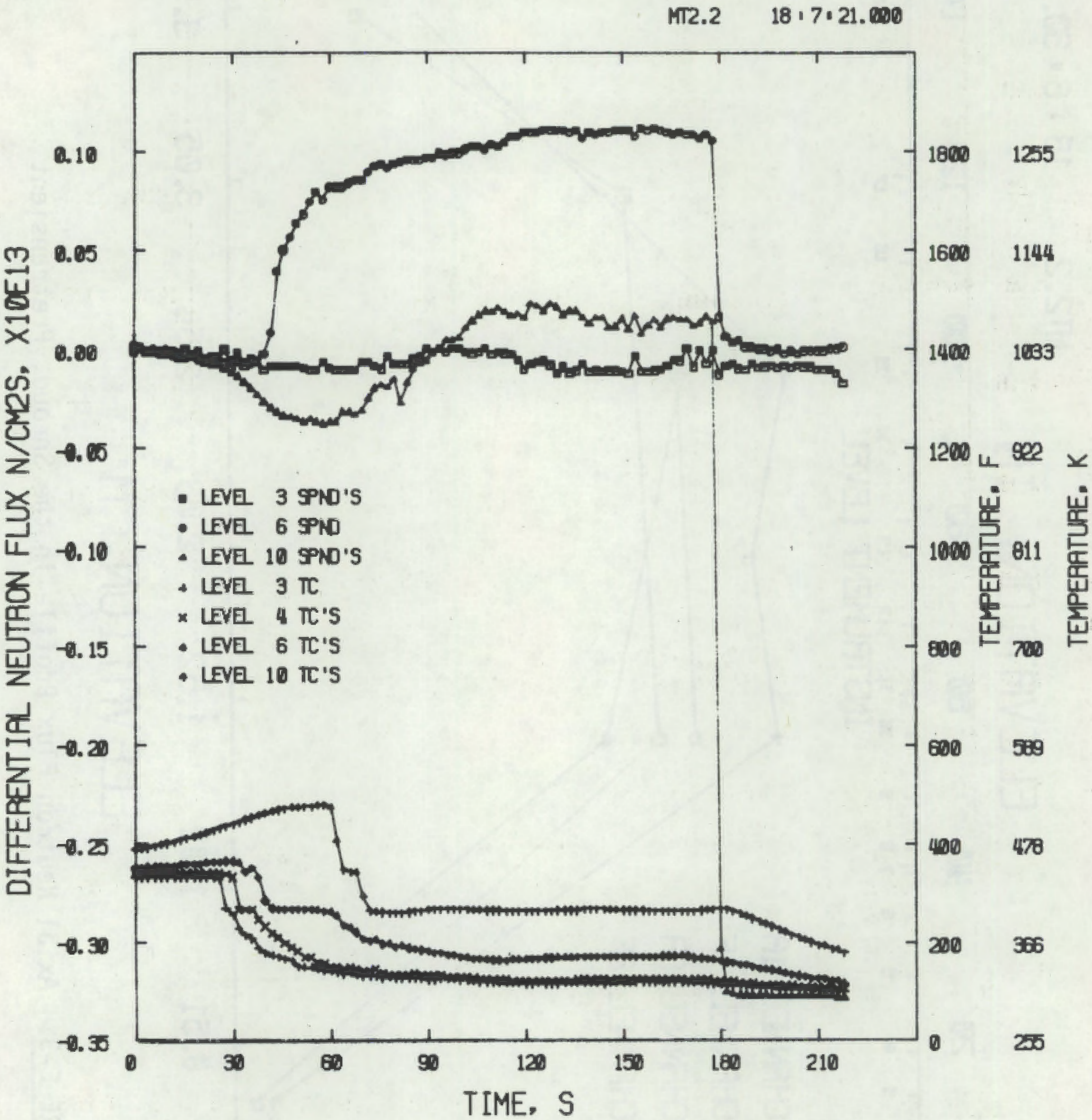

FIGURE E-4. Differential Neutron Flux and Temperature Histories for Levels 3, 6, and 10 During Transient MT-2.2

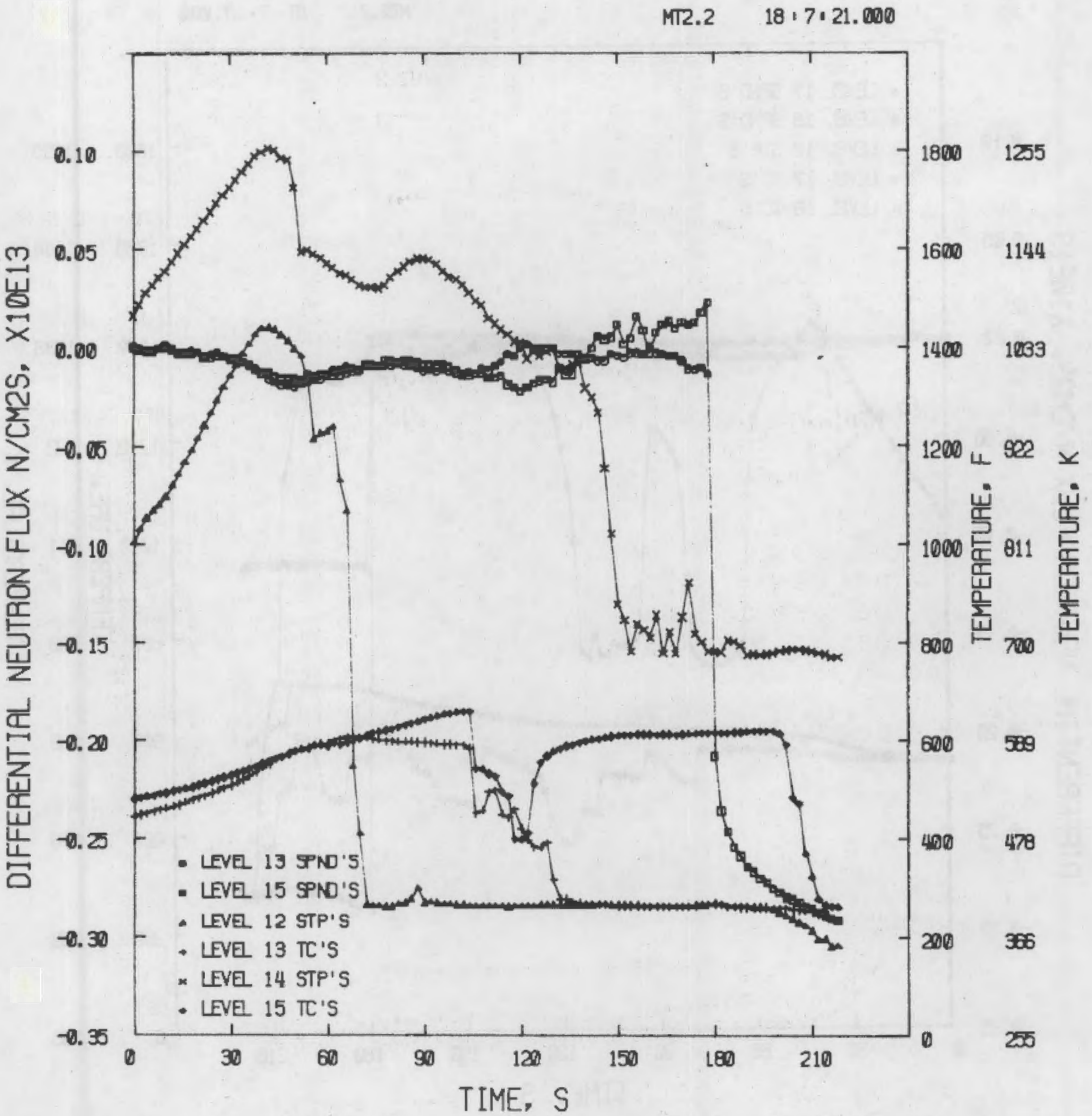

FIGURE E-5. Differential Neutron Flux and Temperature Histories for Levels 13 and 15 During Transient MT-2.2

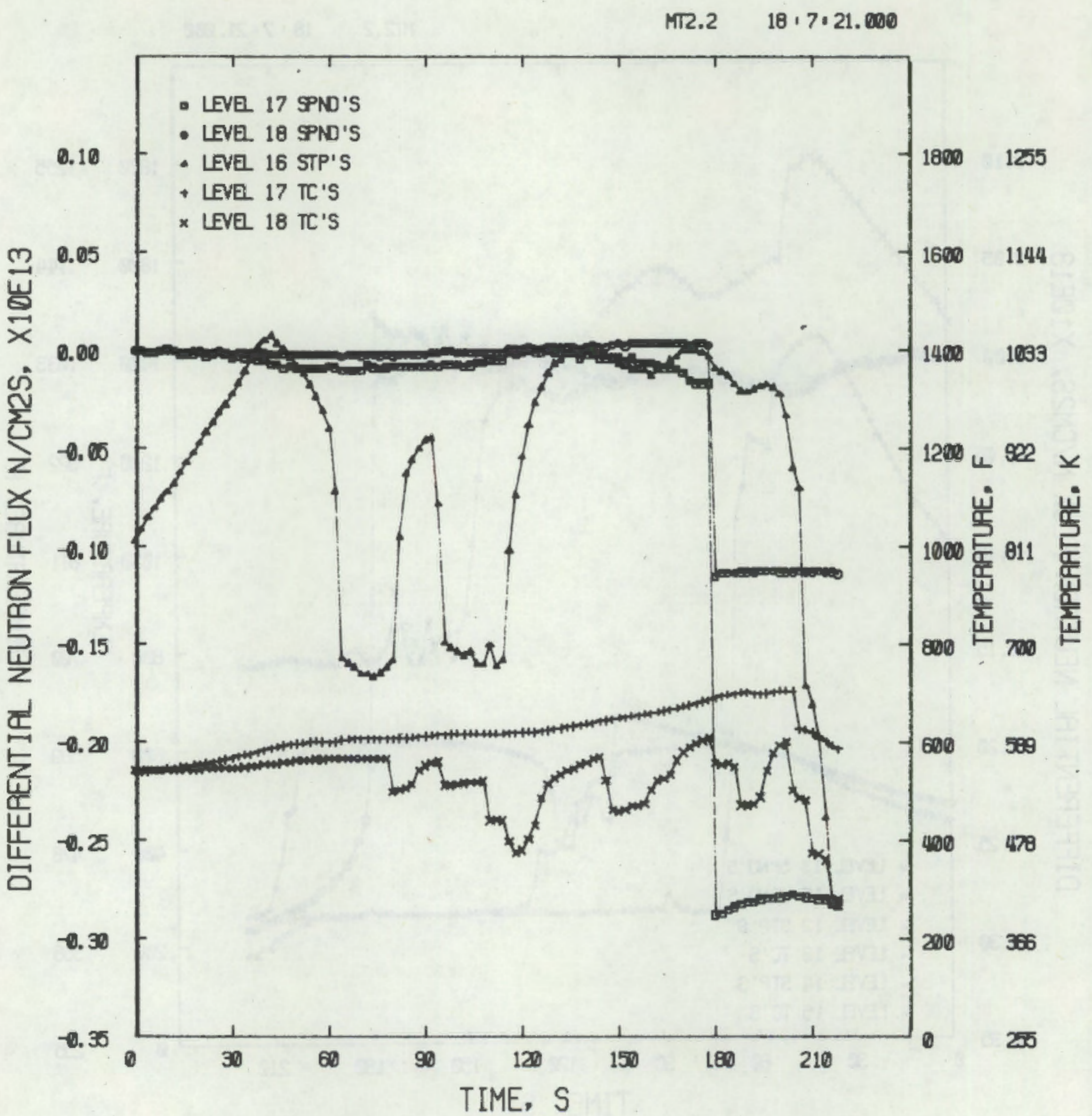

FIGURE E-6. Differential Neutron Flux and Temperature Histories for Levels 17 and 18 During Transient MT-2.2

APPENDIX F

REFLOOD FLOW RATES AND TEMPERATURES

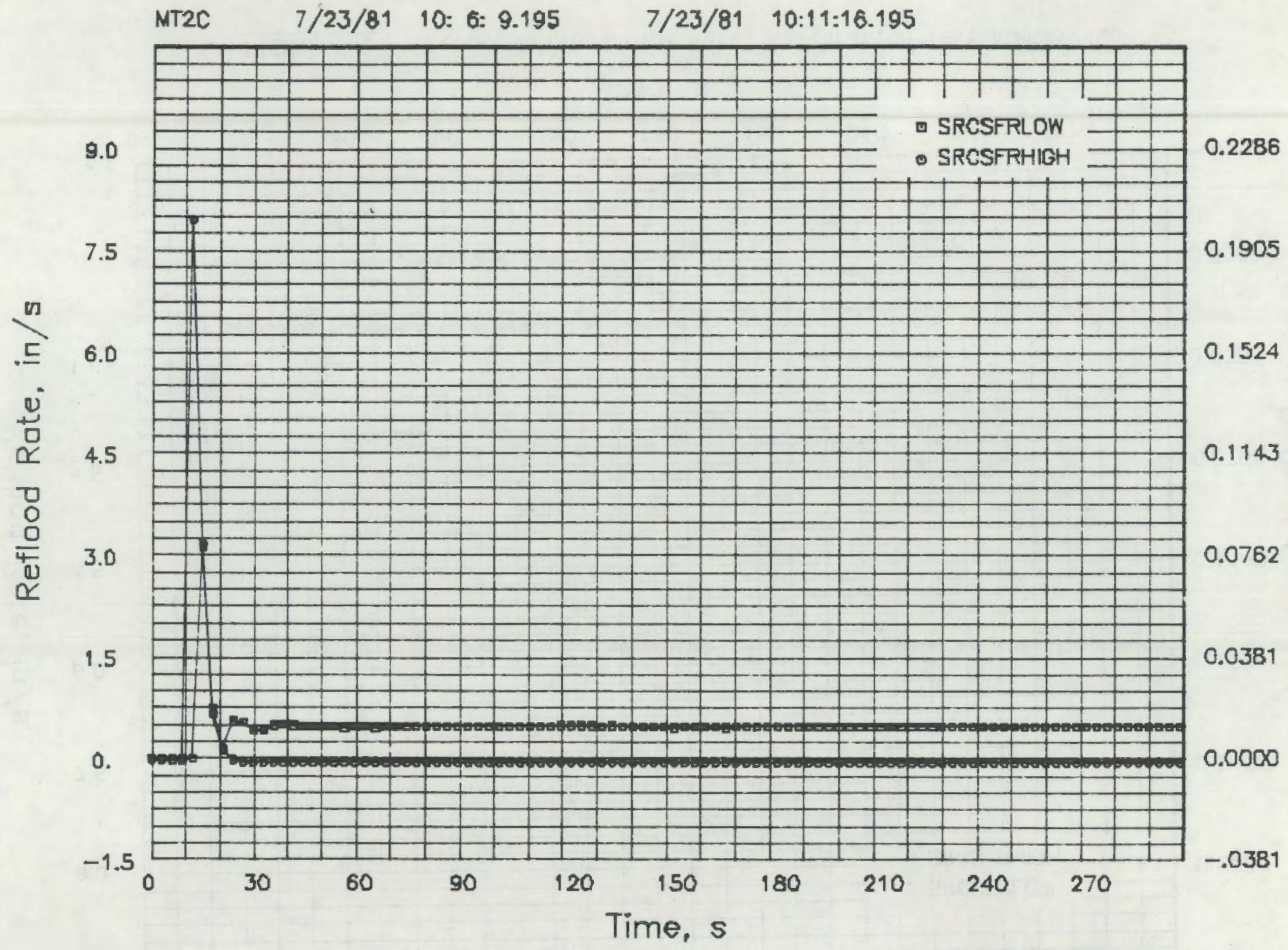

FIGURE F-1. Pretest Reflood Flow Rate, Calibration Test Number One

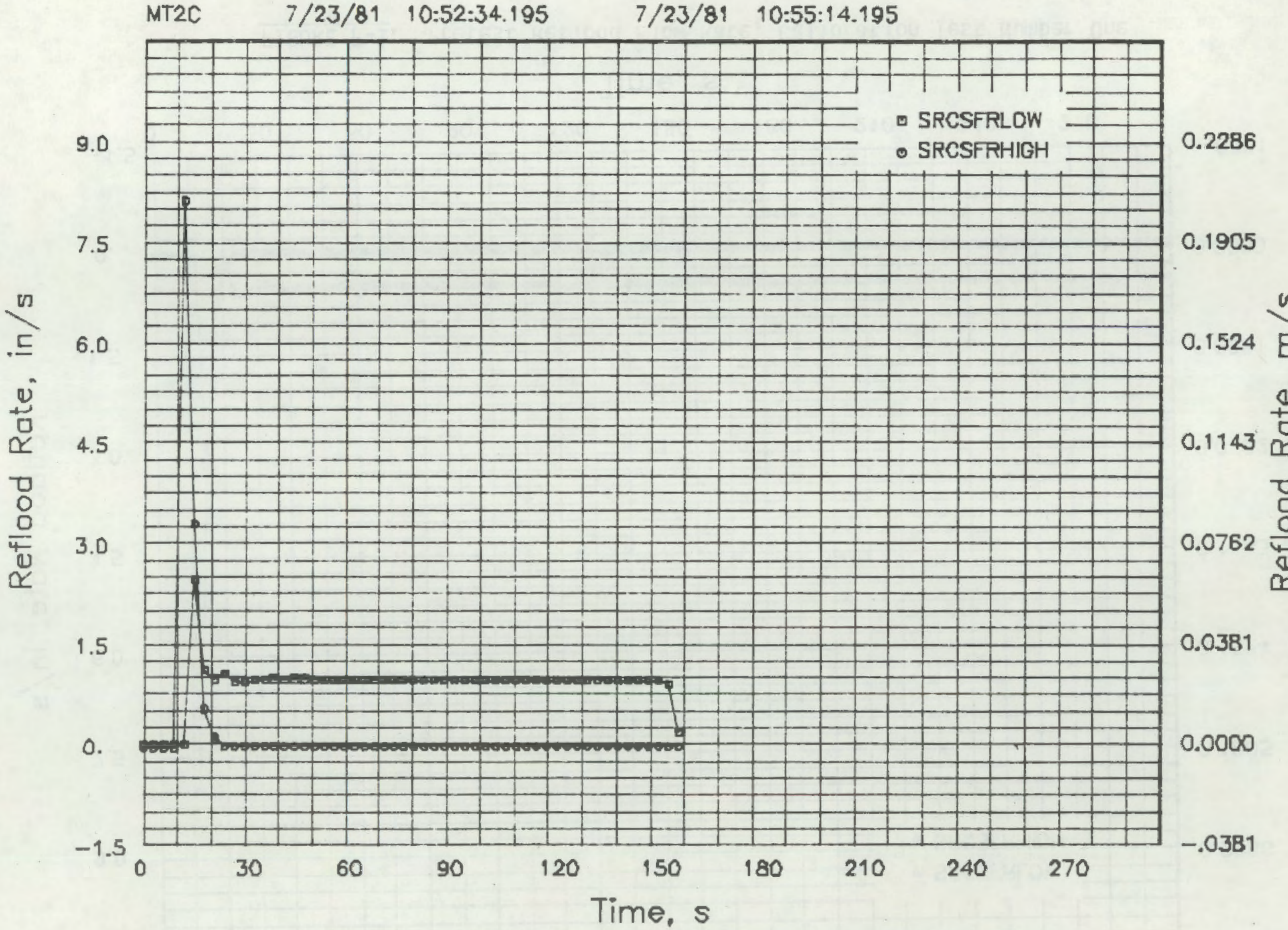

FIGURE F-2. Pretest Reflood Flow Rate, Calibration Test Number Two

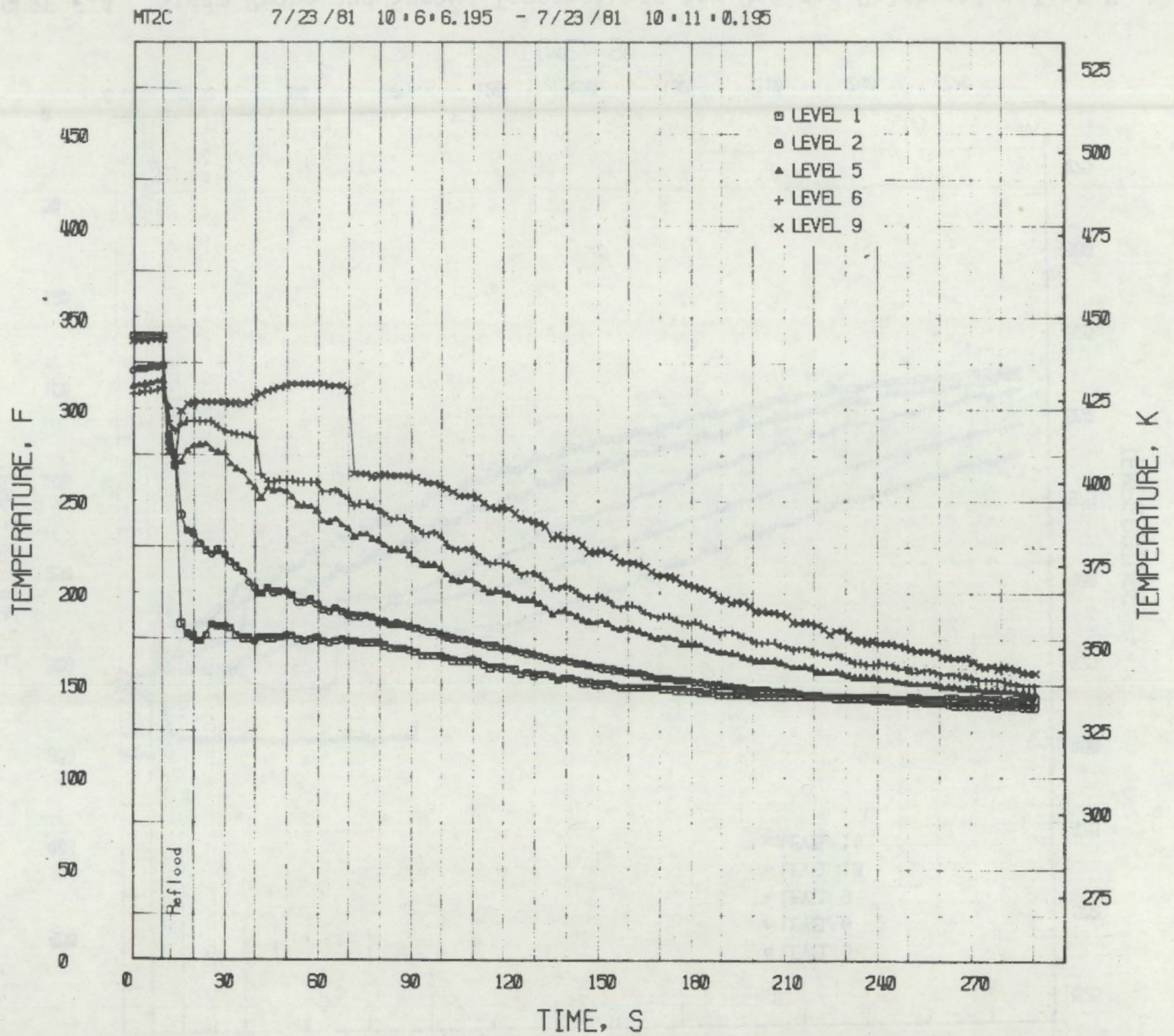

FIGURE F-3. Steam Probe and Shroud Temperatures for Reflood Calibration Test Number One

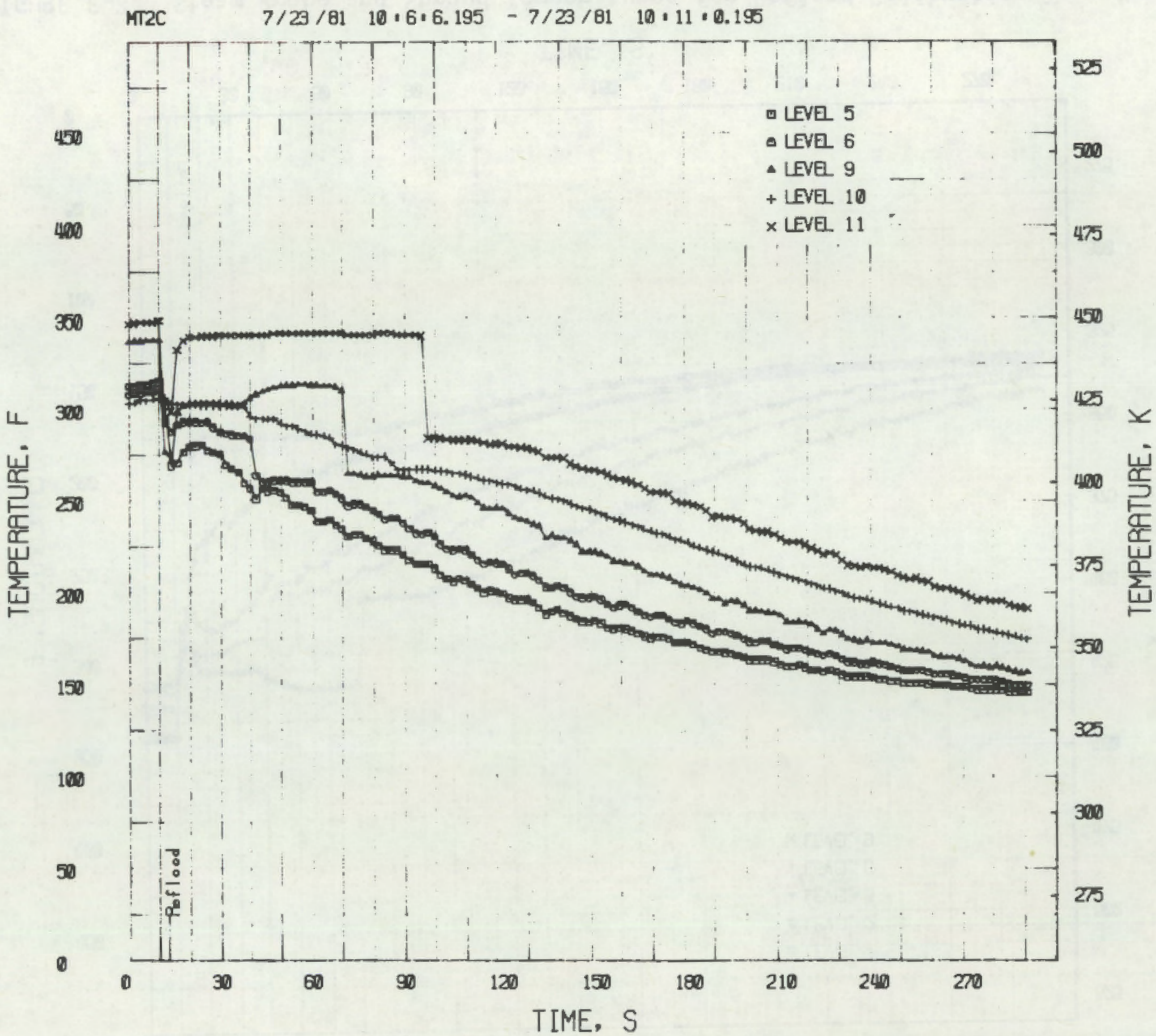

FIGURE F-4. Steam Probe and Shroud Temperatures for Reflood Calibration Test Number One

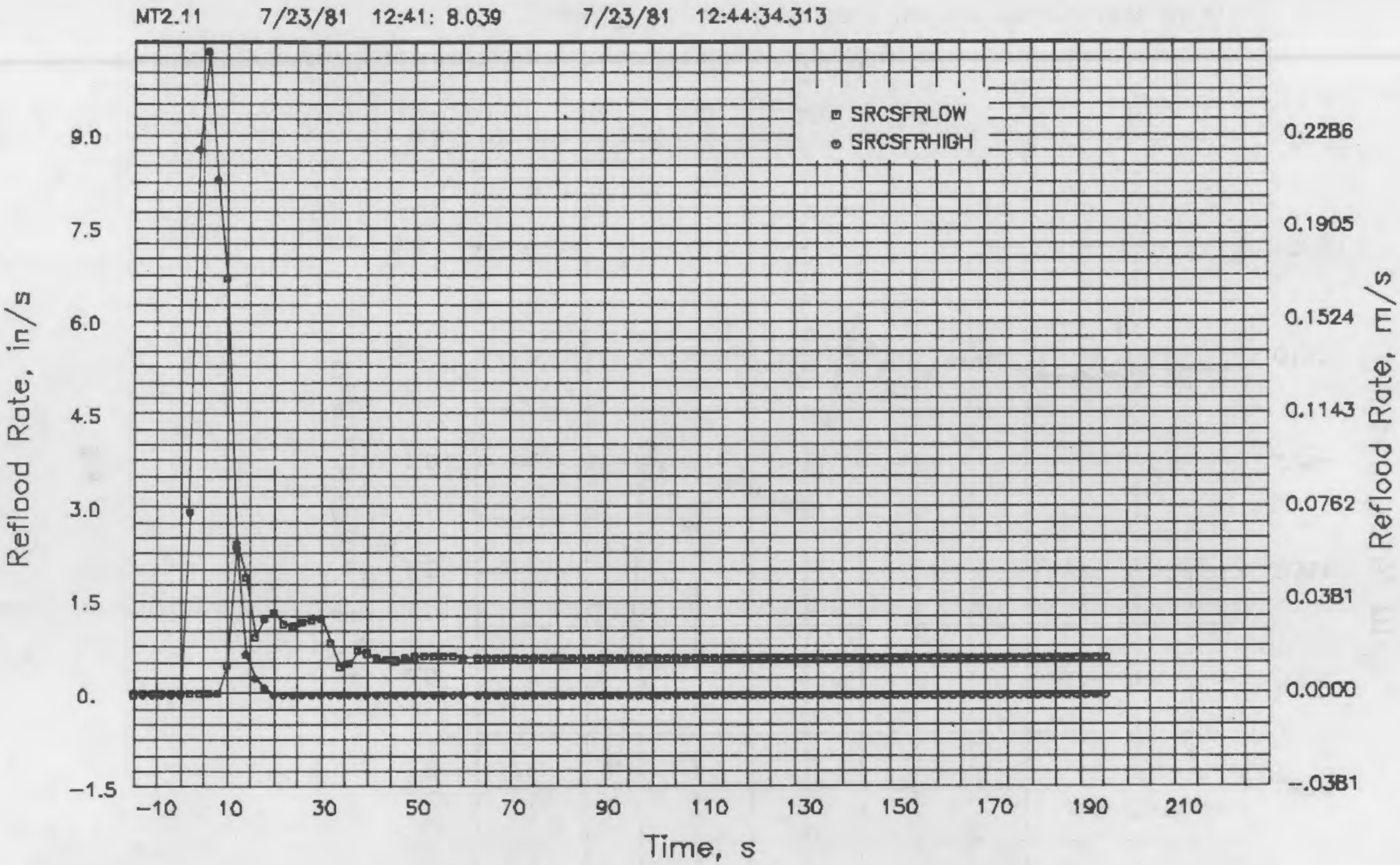

FIGURE F-5. Turbine Flow Meter, Test MT-2.1.1

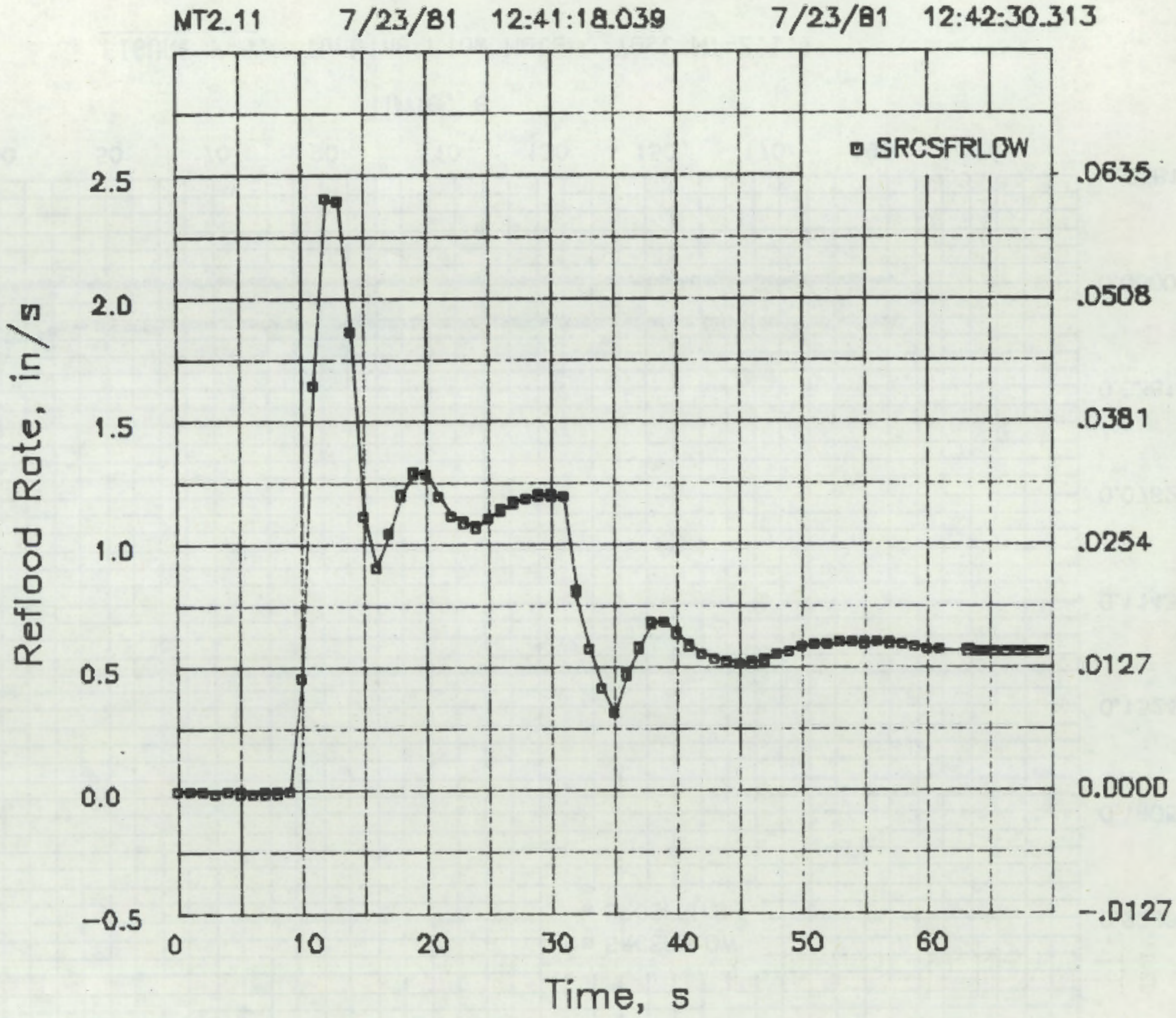

FIGURE F-6. Low Flow Rate Turbine Meter, Test MT-2.1.1

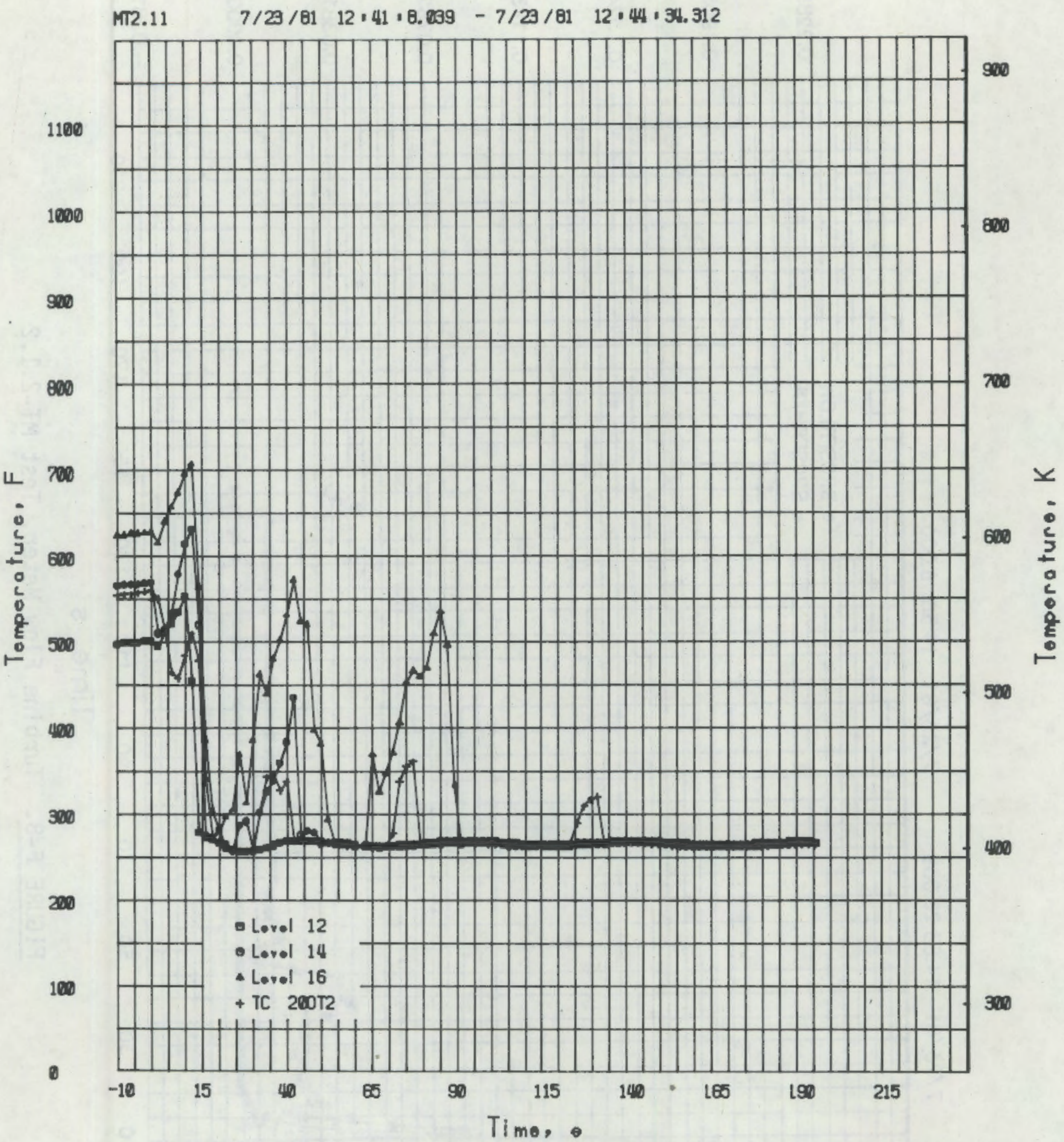

FIGURE F-7. Temperatures from the Grid Spacer Steam Probes, Test MT-2.1.1

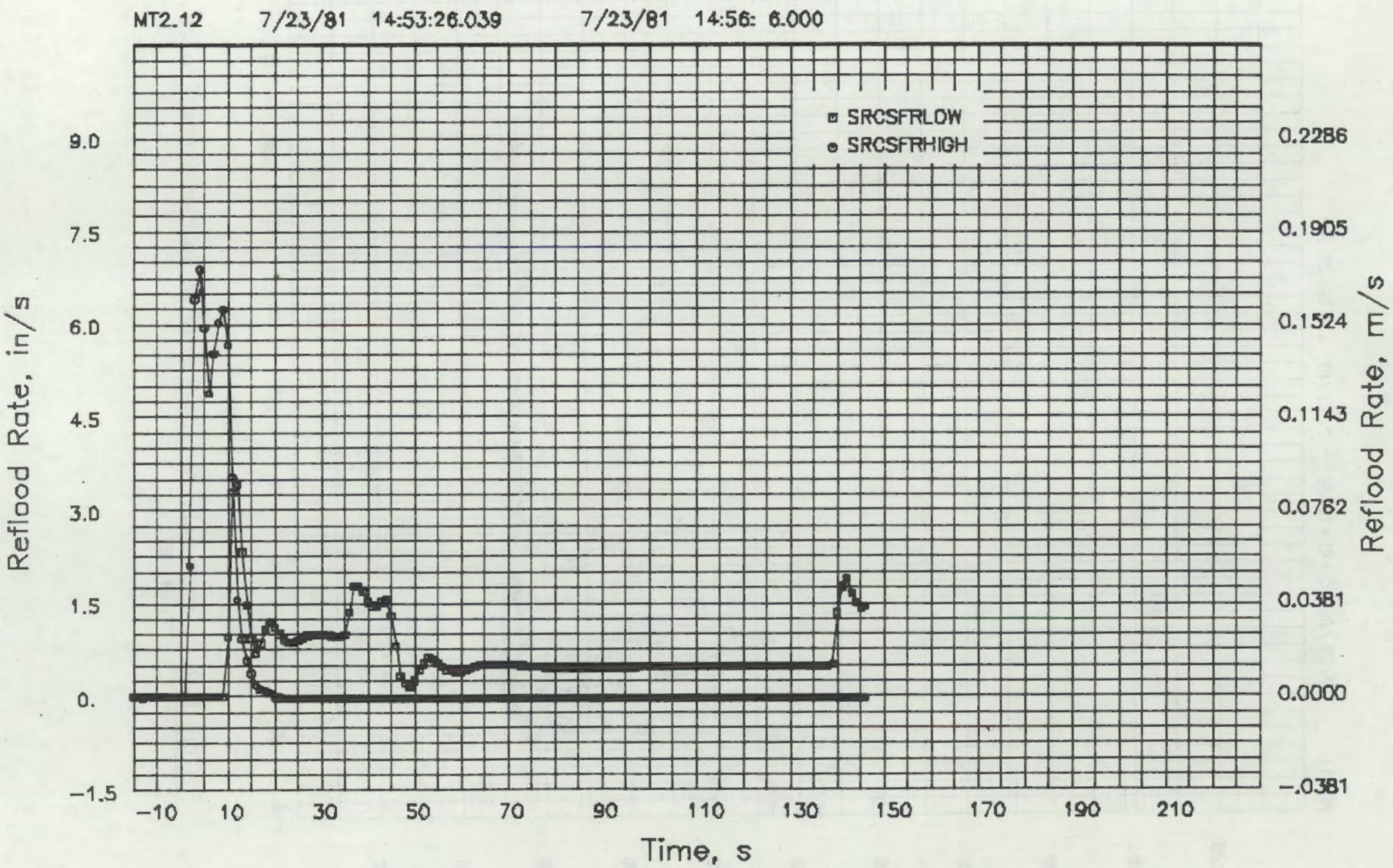

FIGURE F-8. Turbine Flow Meter, Test MT-2.1.2

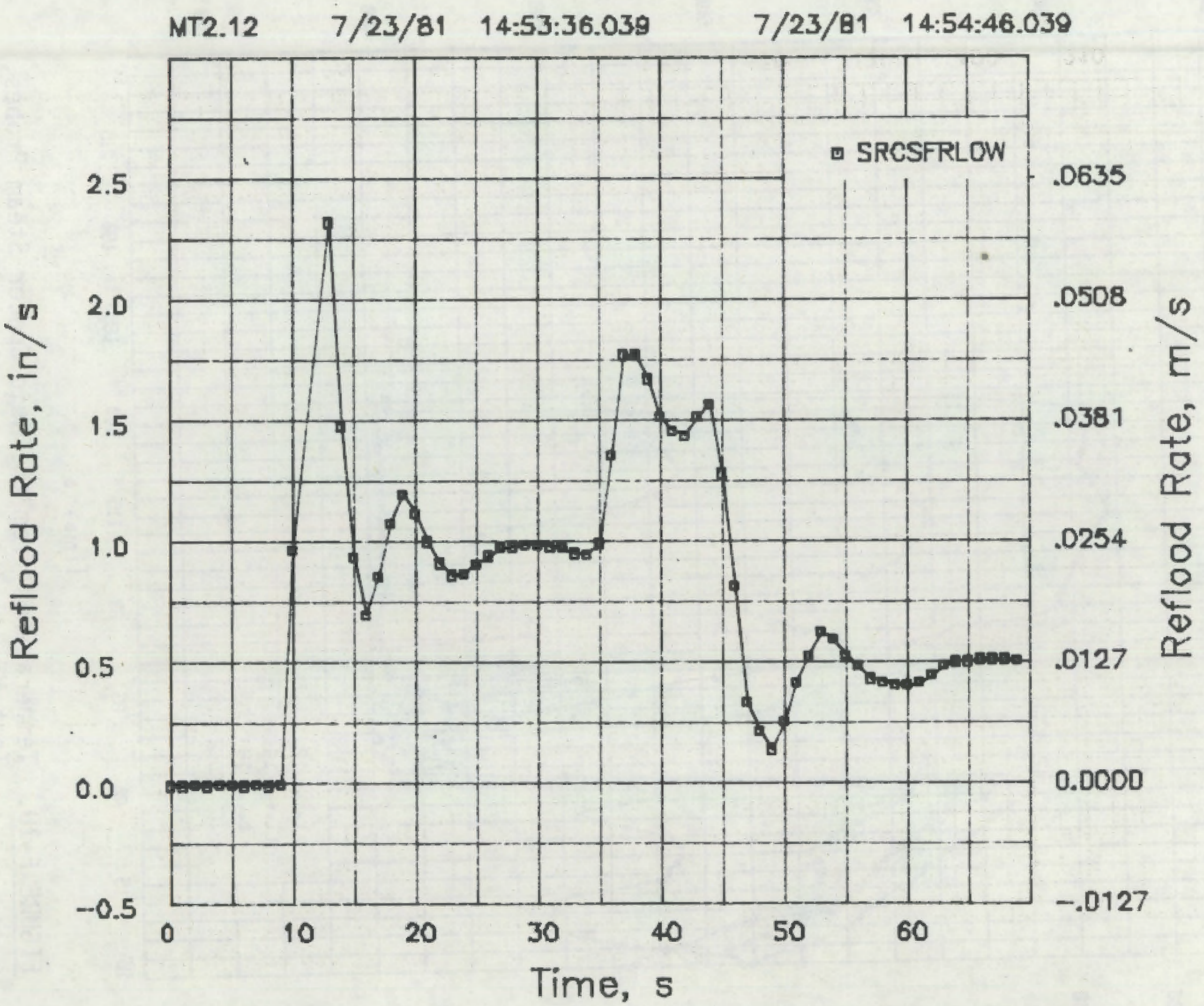

FIGURE F-9. Low Flow Rate Turbine Meter, Test MT-2.1.2

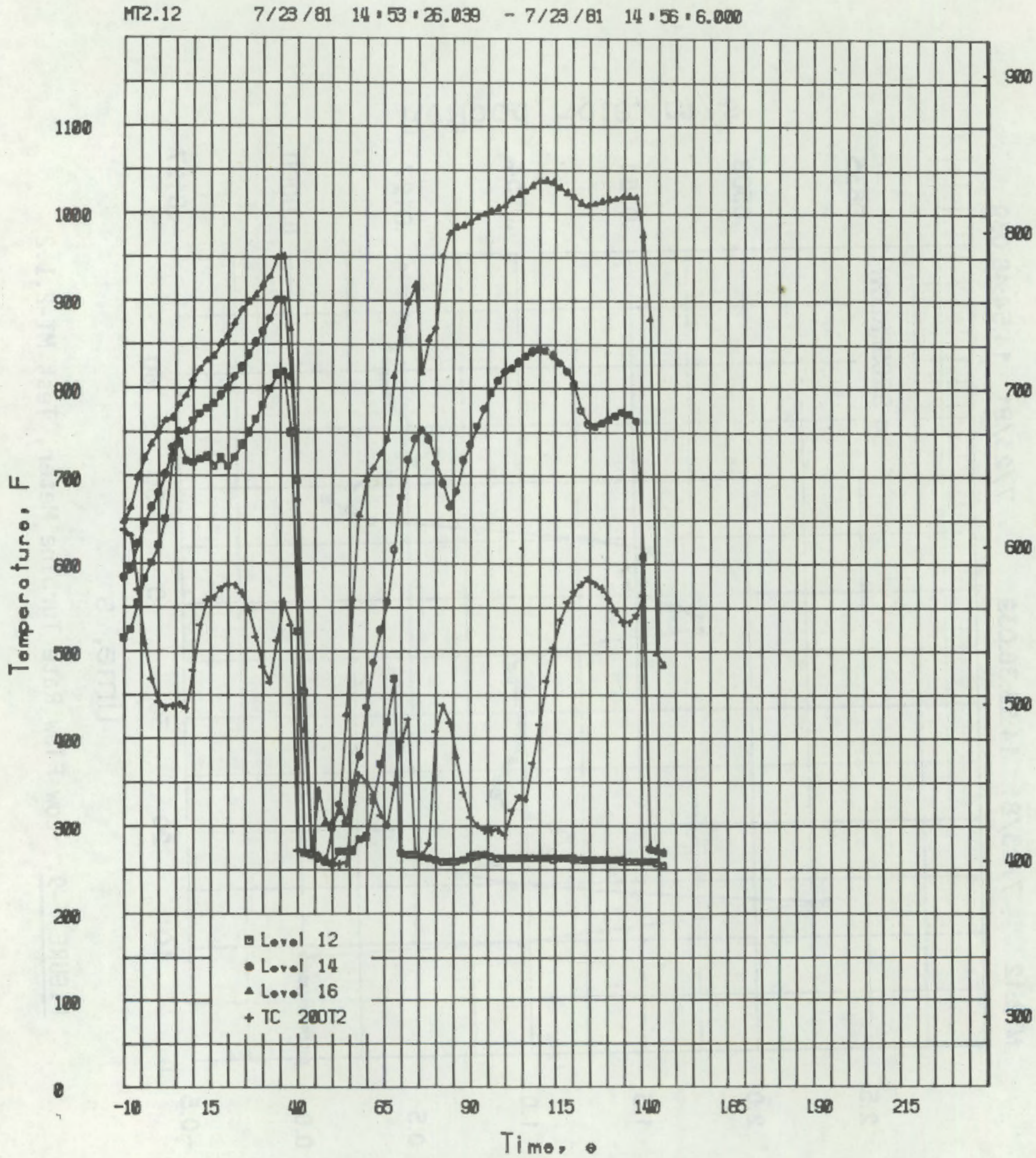

FIGURE F-10. Temperatures from the Grid Spacer Steam Probes, Test MT-2.1.2

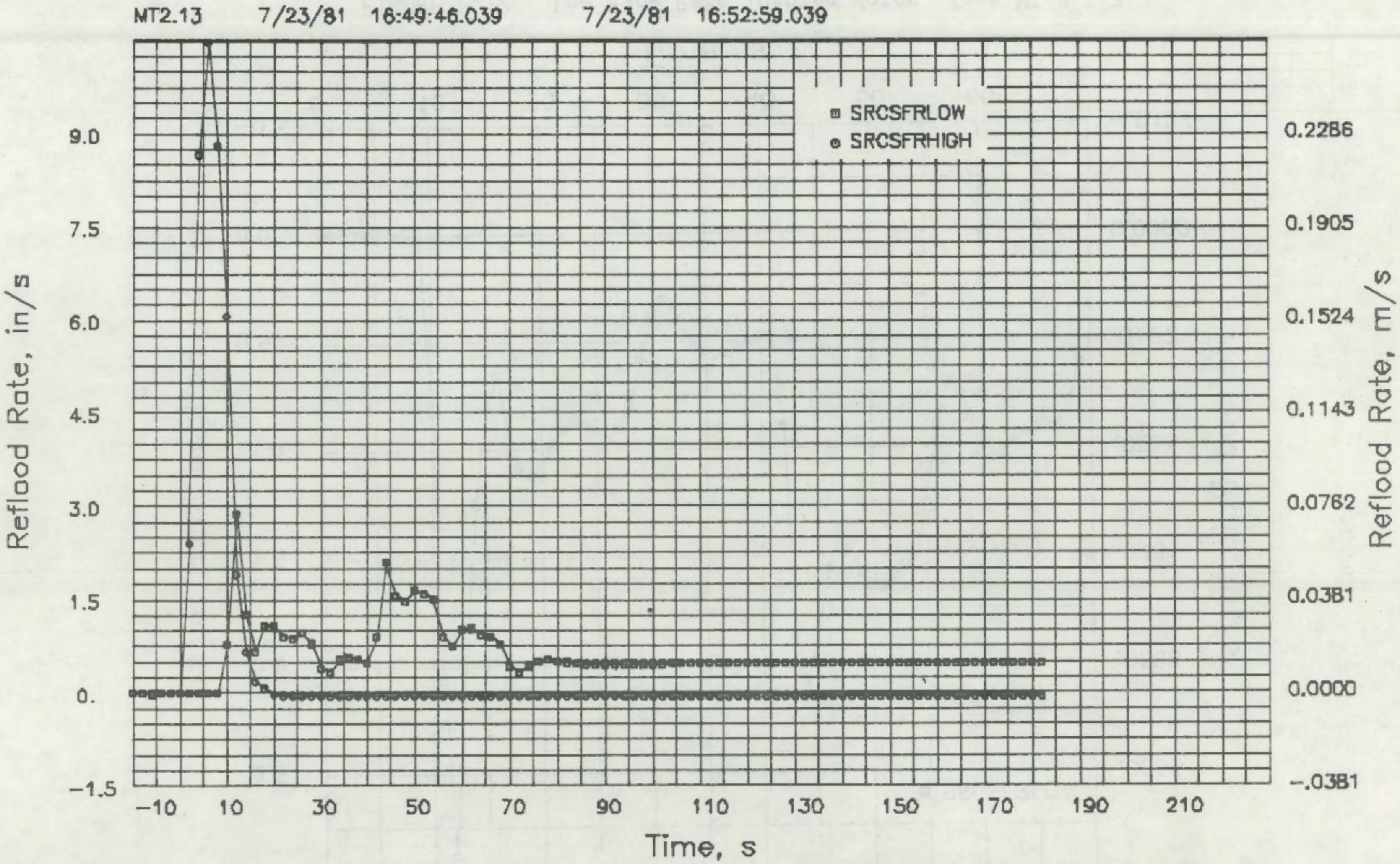

FIGURE F-11. Turbine Flow Meter, Test MT-2.1.3

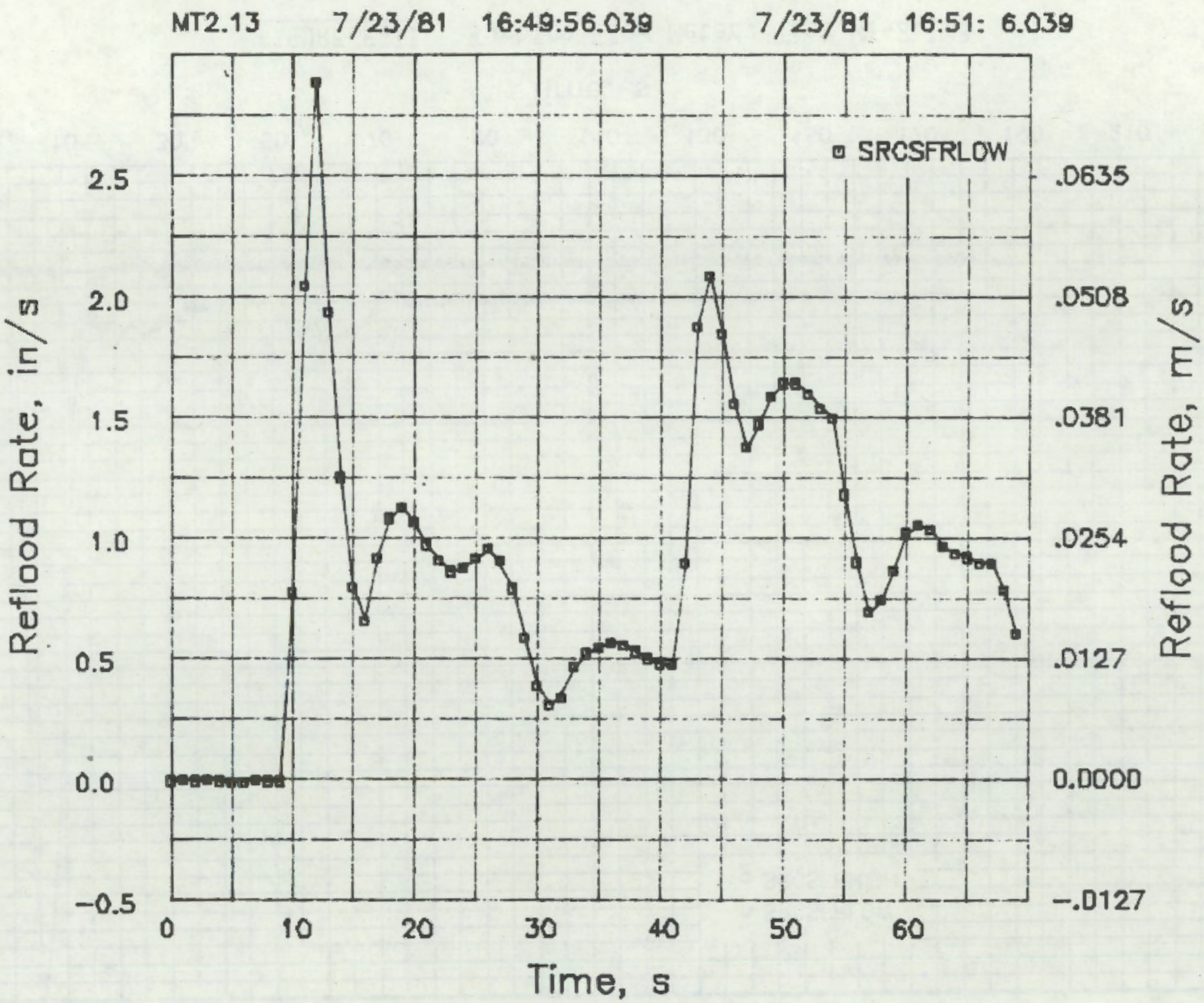

FIGURE F-12. Low Flow Rate Turbine Meter, Test MT-2.1.3

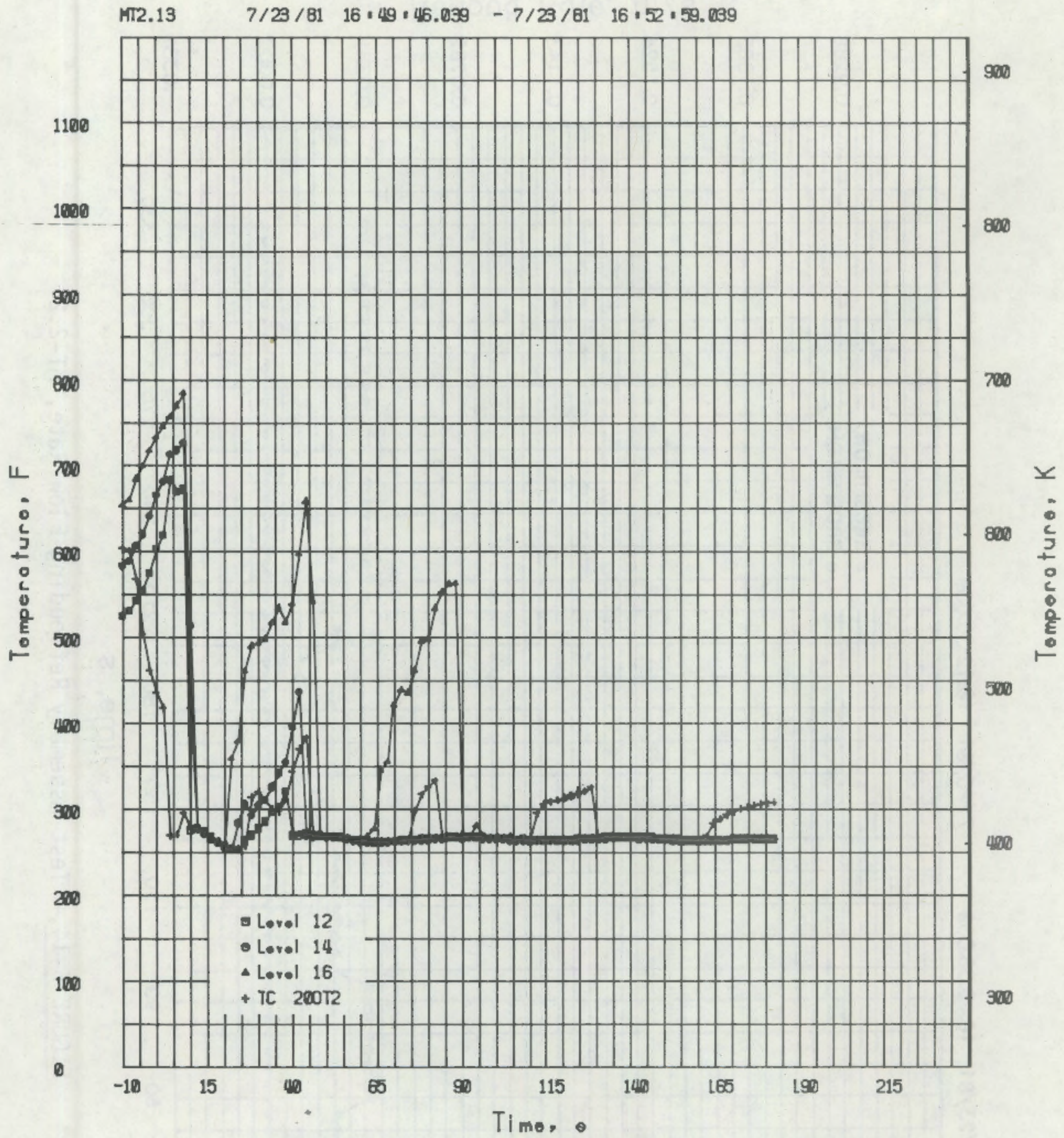

FIGURE F-13. Temperatures from the Grid Spacer Steam Probes, Test MT-2.1.3

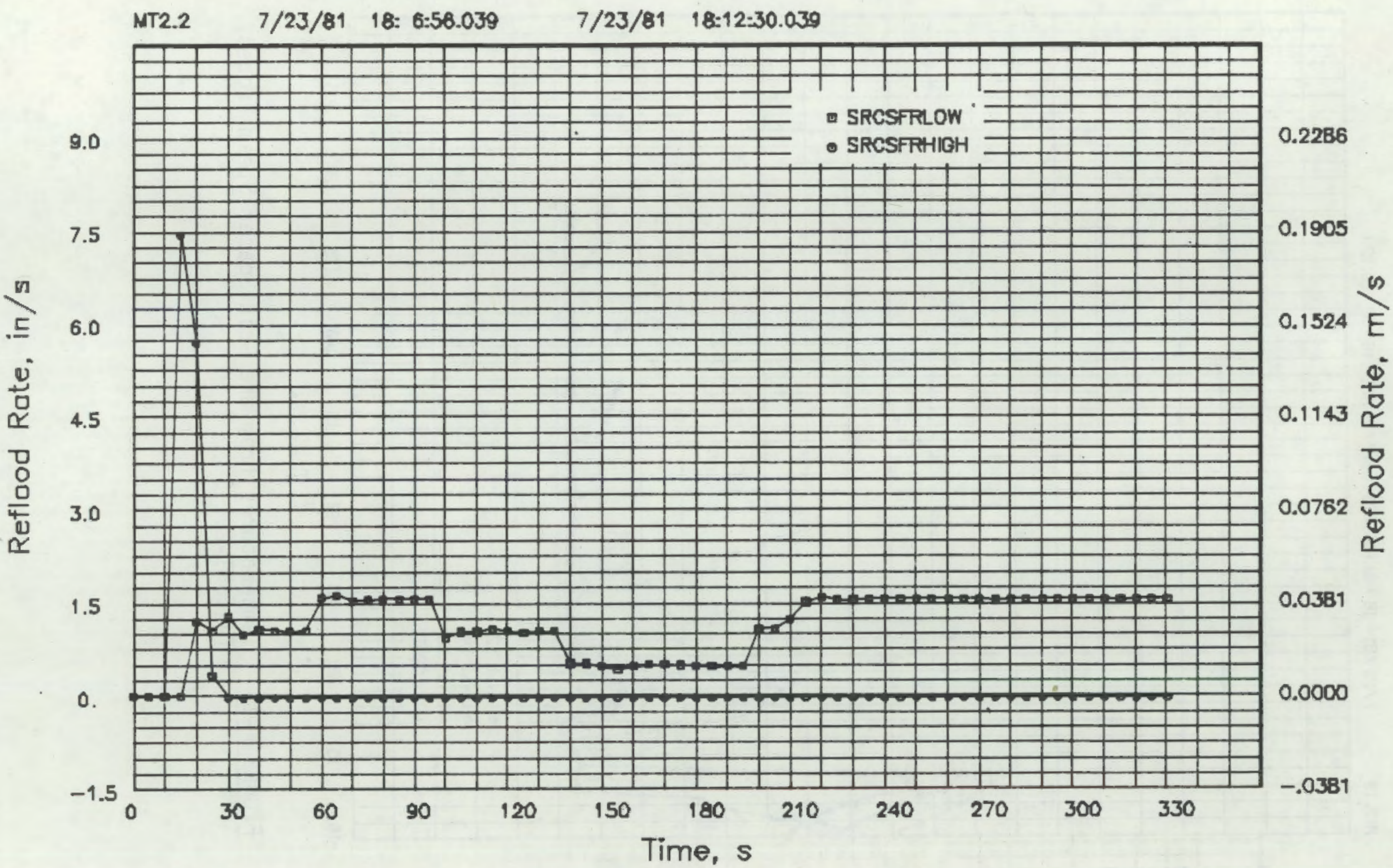

FIGURE F-14. Test Assembly Reflooding Flow Rate, MT-2.2

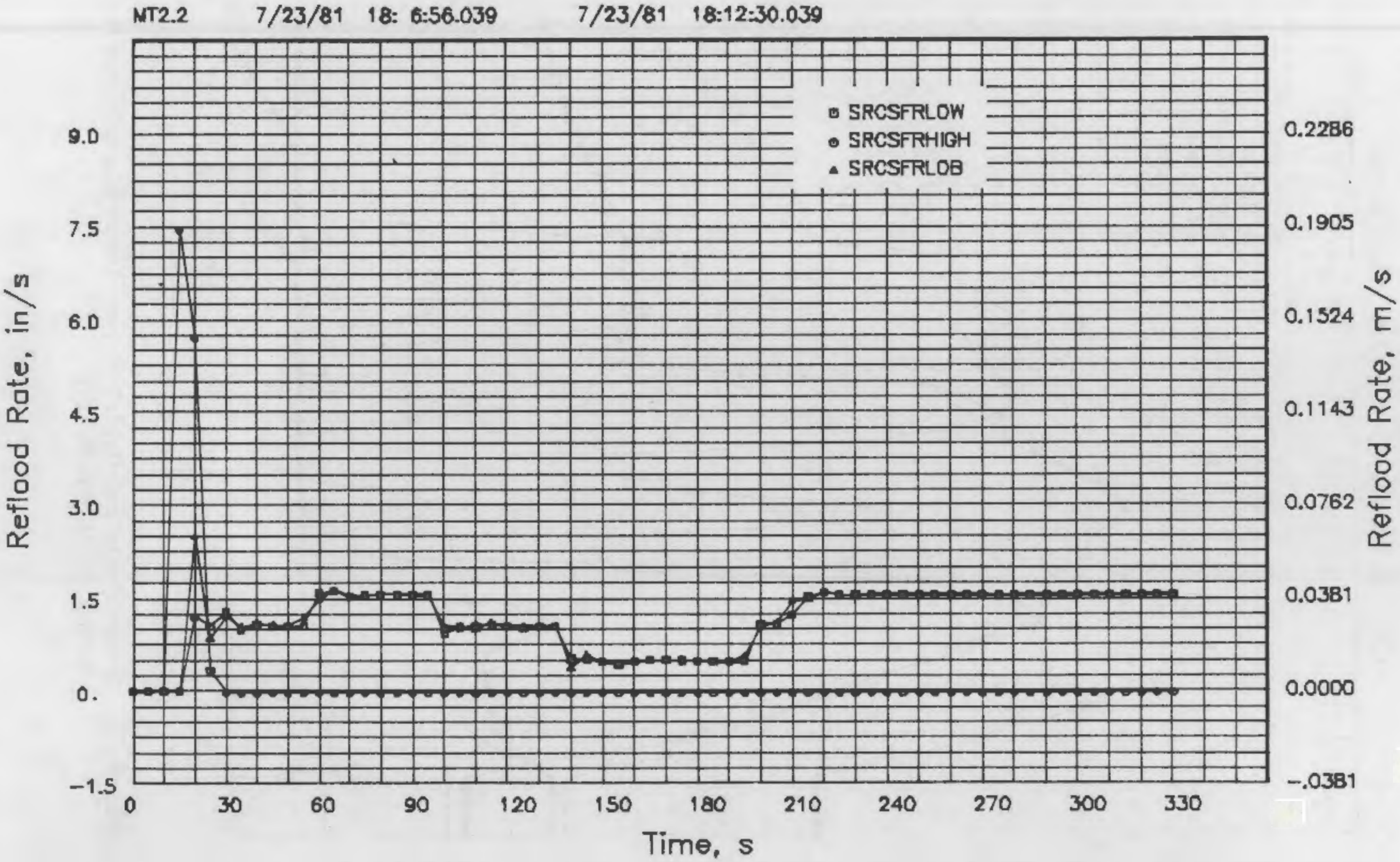

FIGURE F-15. Test Assembly Reflooding Flow Rate, MT-2.2

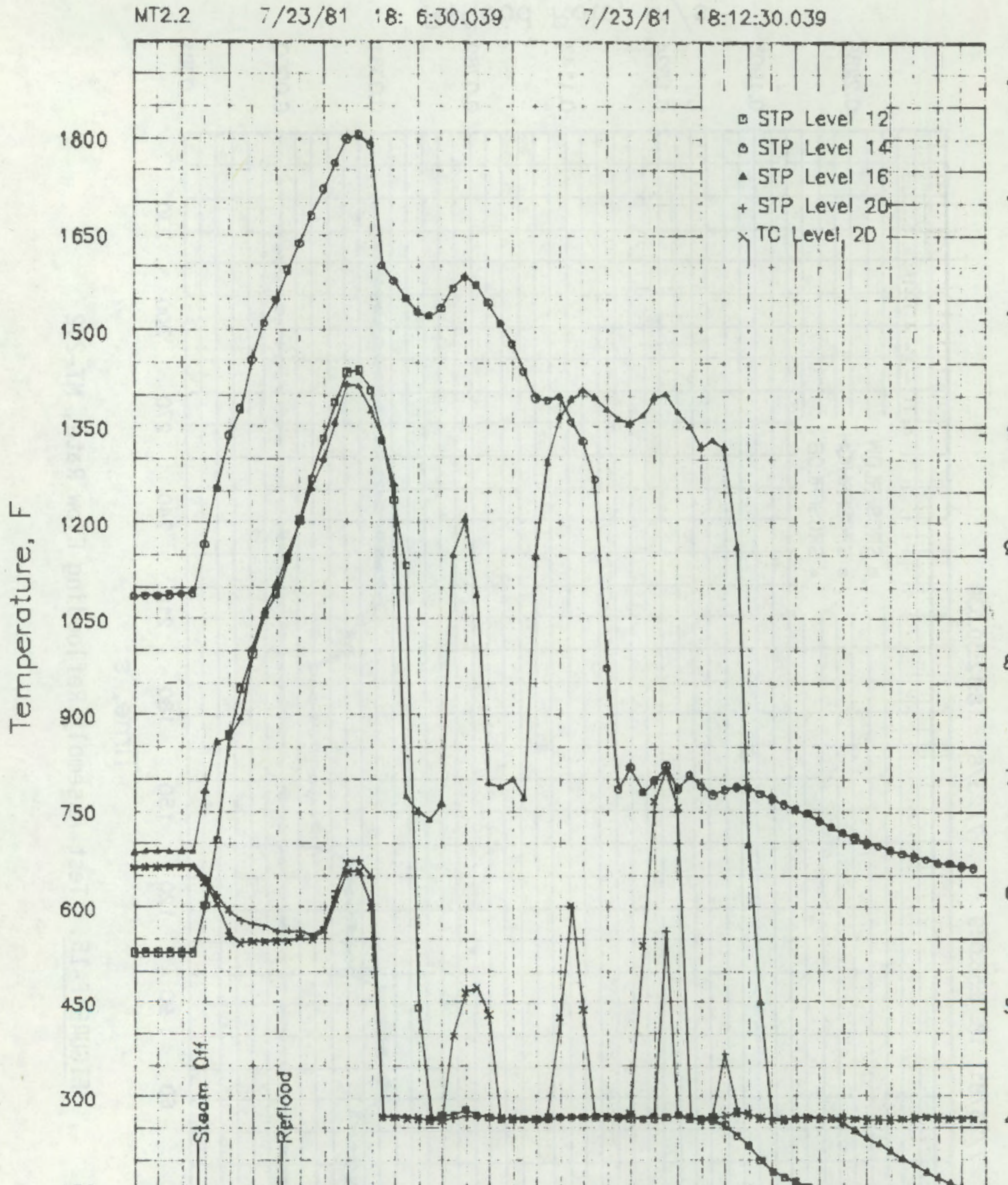

FIGURE F-16. Steam Probe and Outlet Region Temperature Histories During Transient MT-2.2

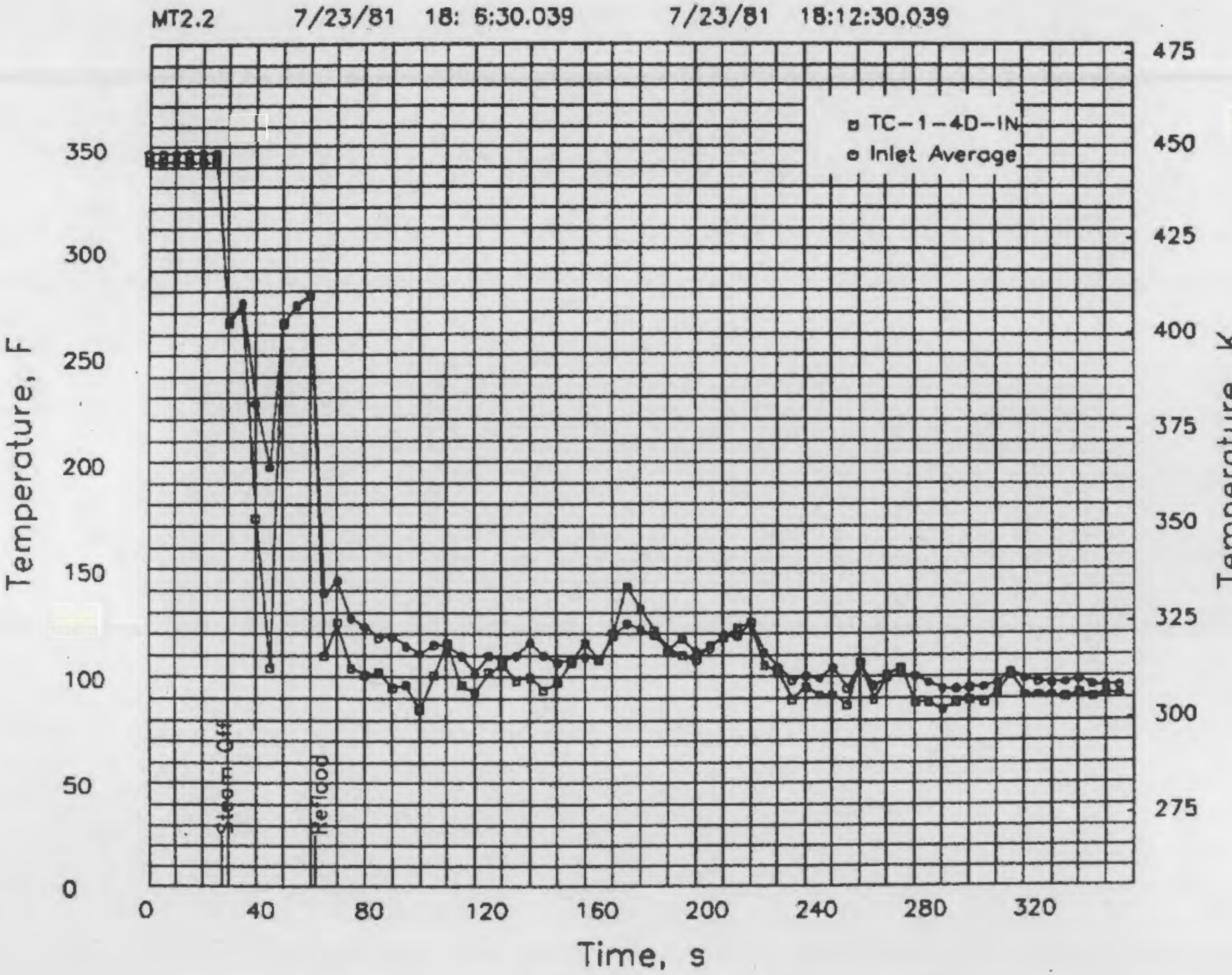

FIGURE F-17. Reflooding Inlet Temperature History

APPENDIX G

FUEL ROD PLENUM PRESSURES

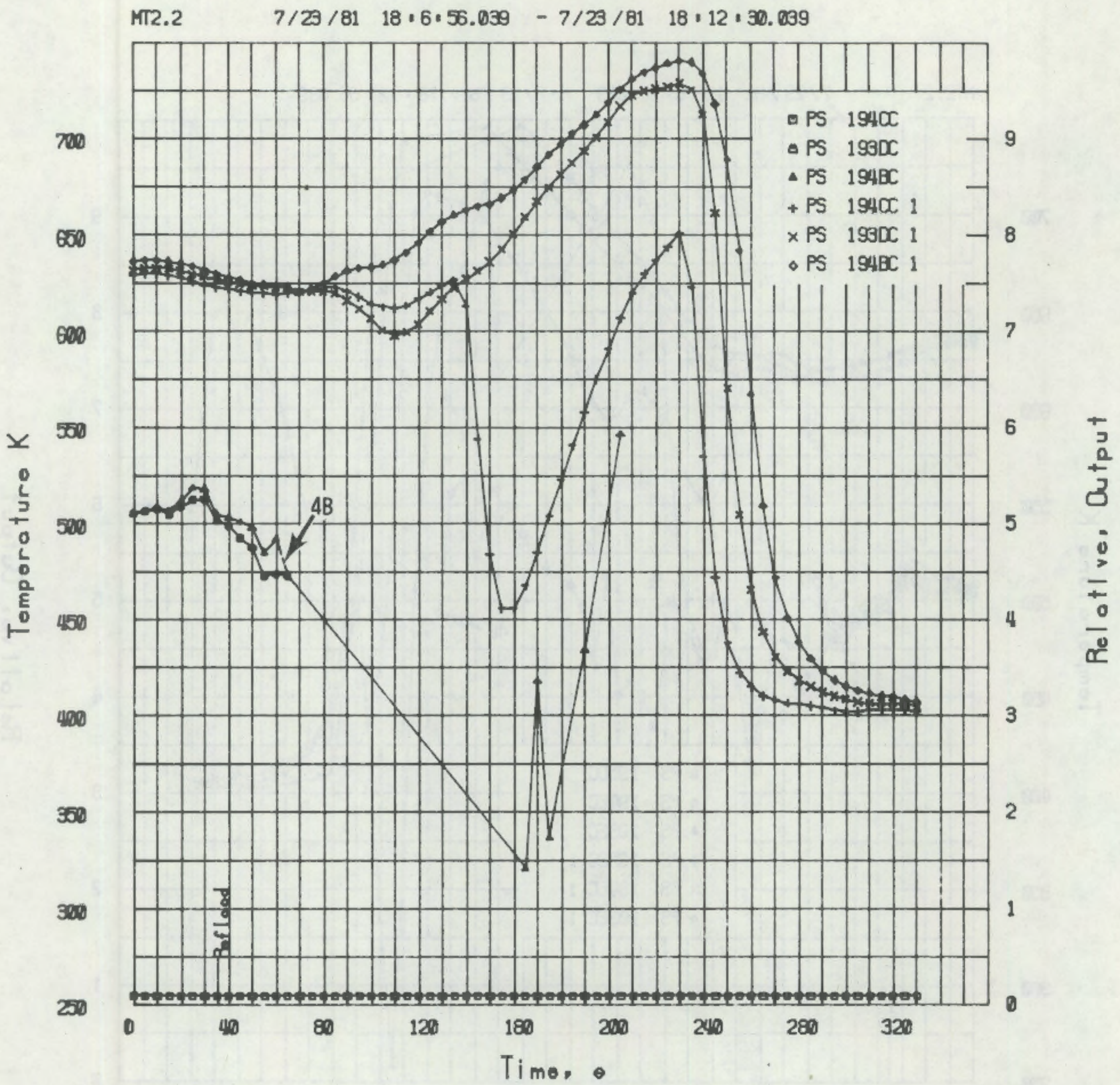

FIGURE G-1. Pressure Switch Response During Transient MT-2.2

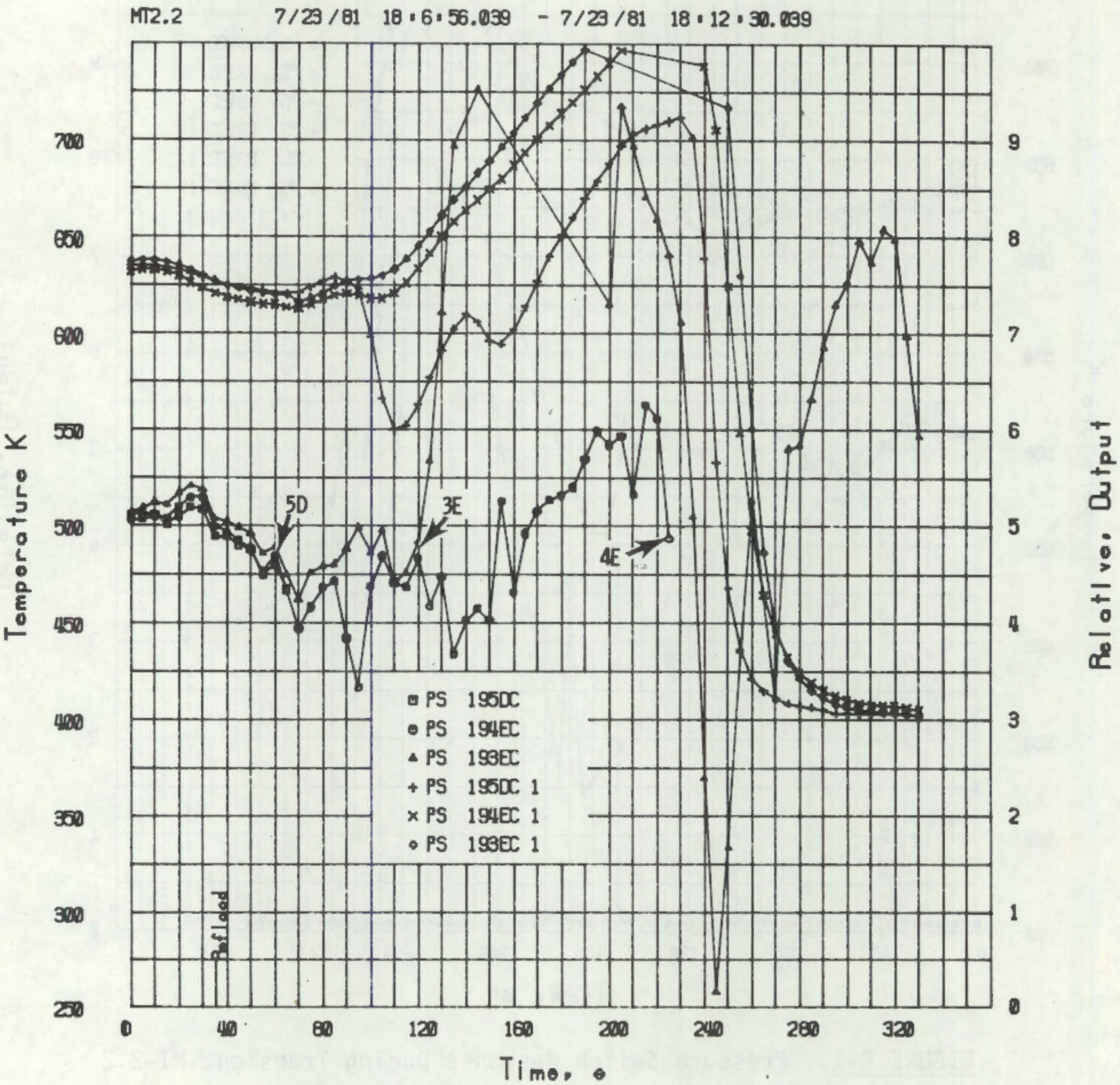

FIGURE G-2. Pressure Switch Response During Transient MT-2.2

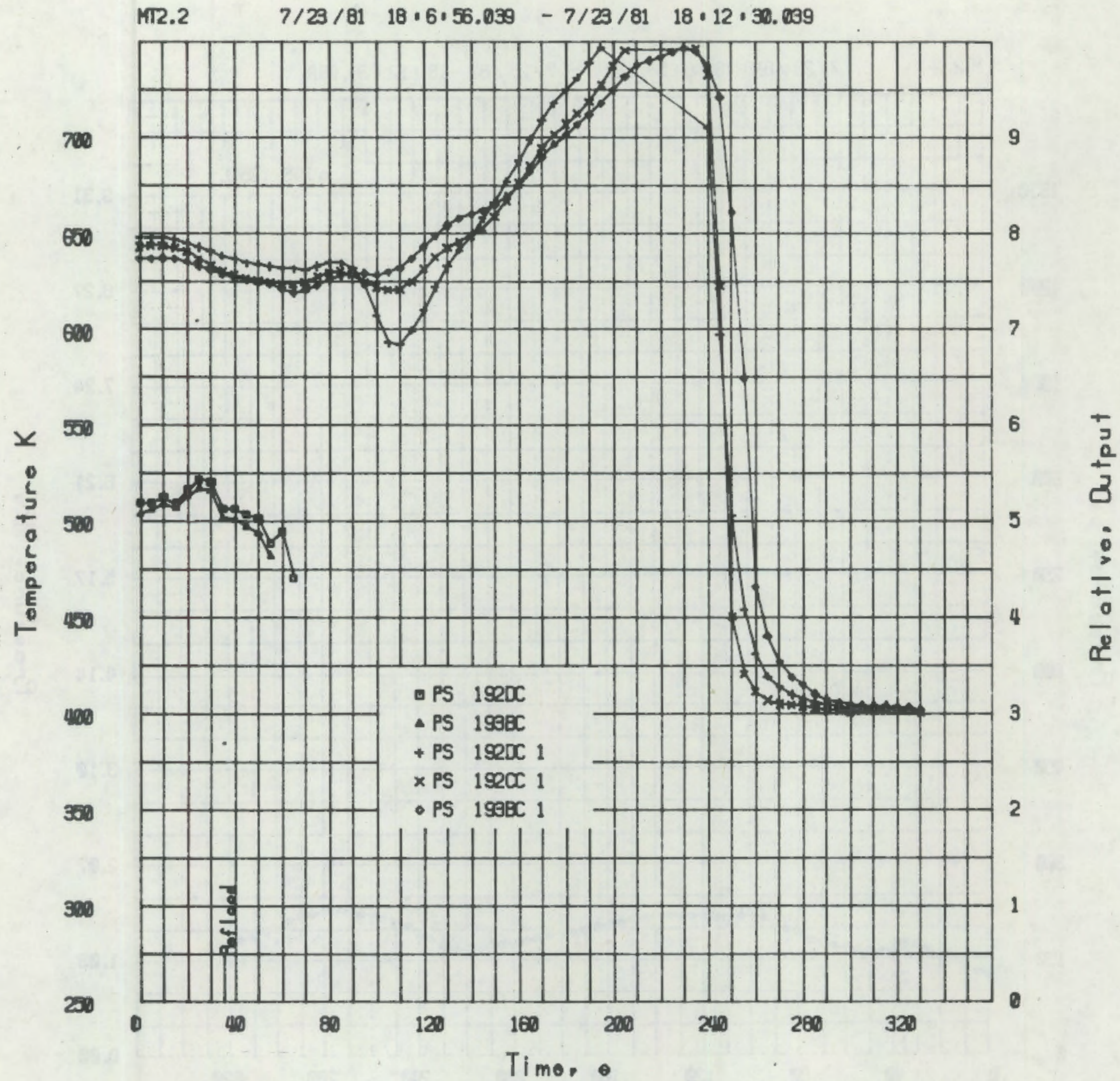

FIGURE G-3. Pressure Switch Response During Transient MT-2.2

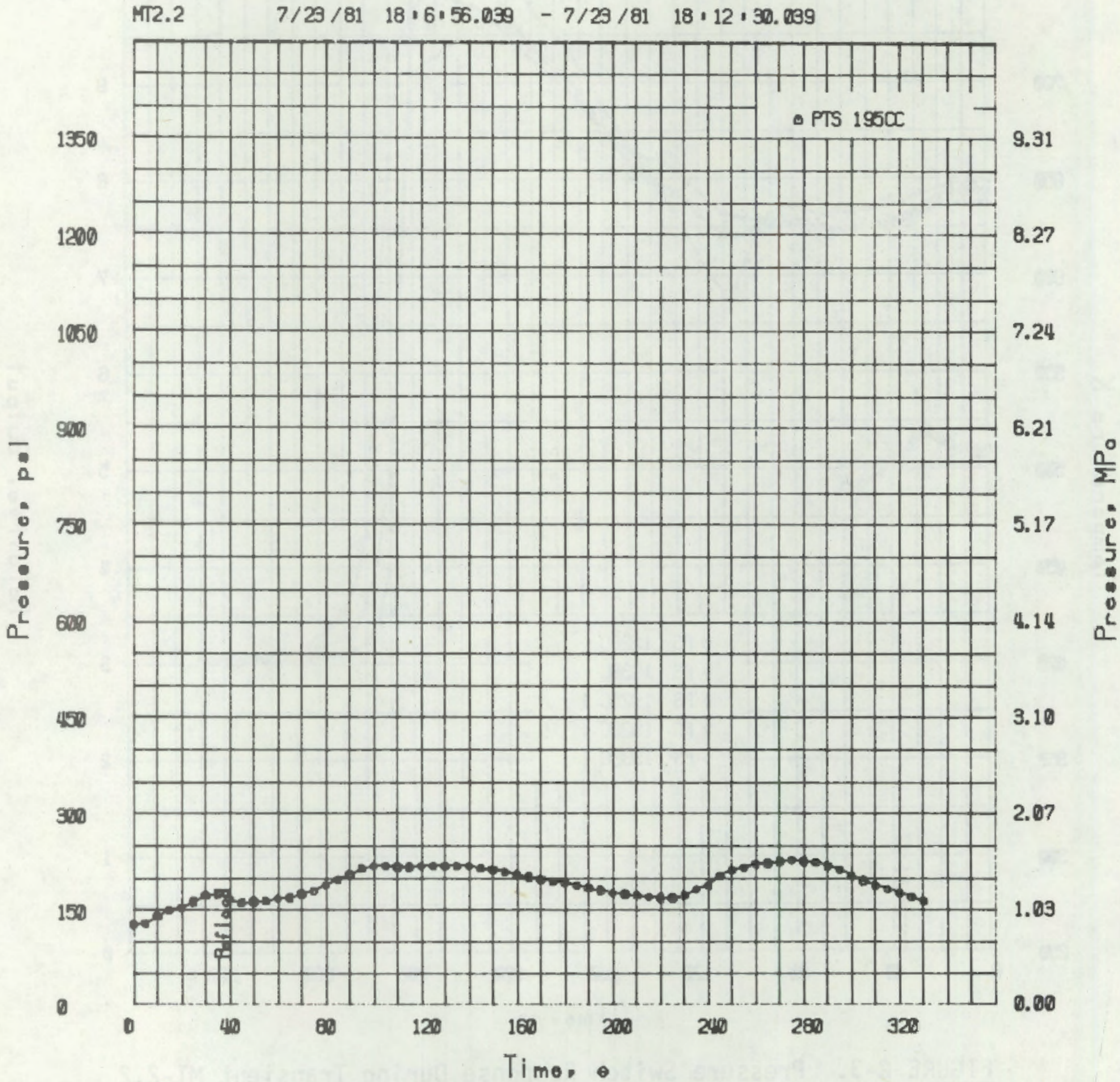

FIGURE G-4. Fuel Rod Pressure Transducer (PTS) Data for Fuel Rod in Position 5C, MT-2.2

APPENDIX H

MECHANICAL DEFORMATION DATA

MT-2 Fuel Rod Bundle

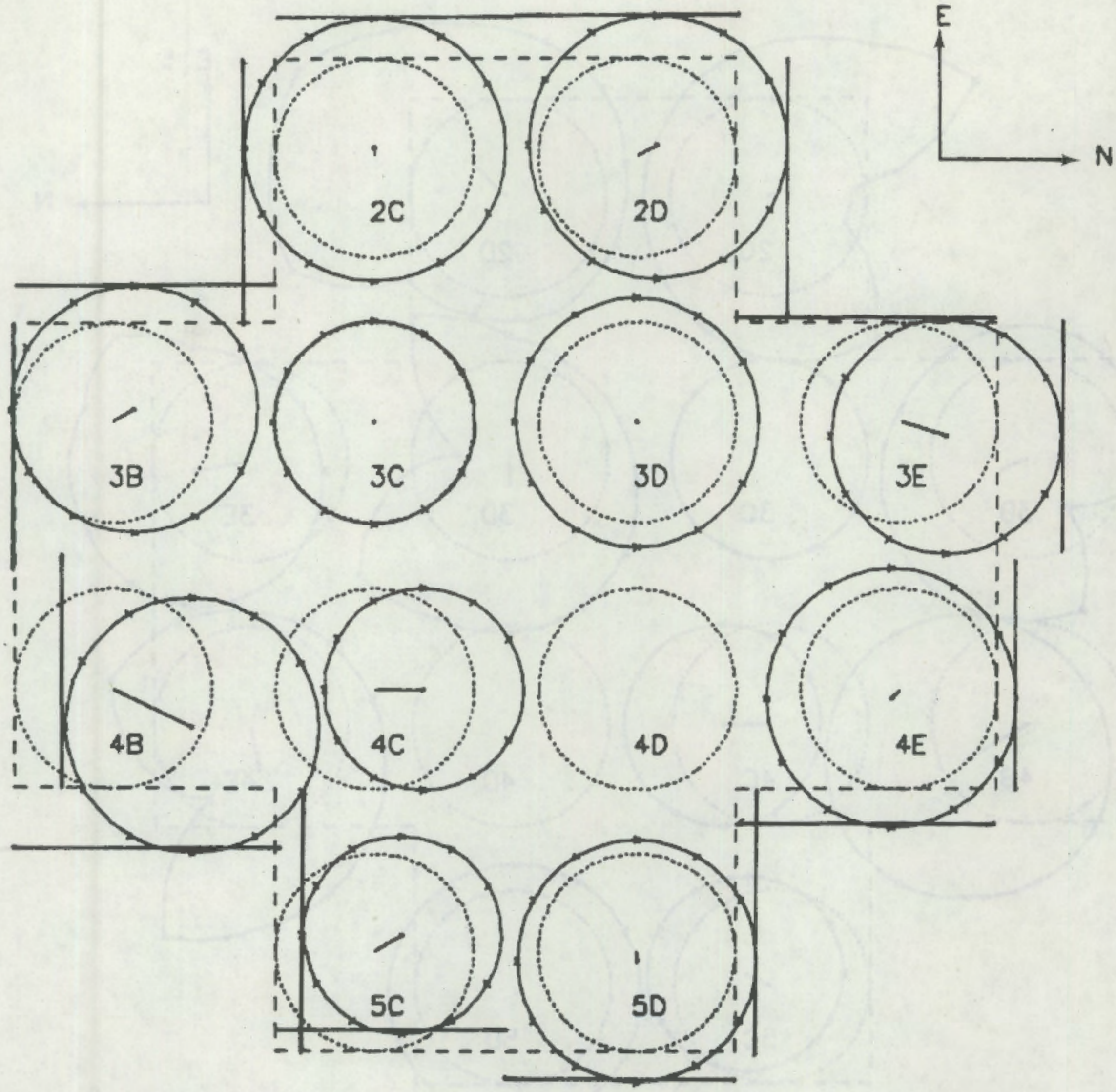

FIGURE H-1. Fuel Cladding Deformation at Axial Elevation Z = 2.032 m (80.0 in)

MT-2 Fuel Rod Bundle

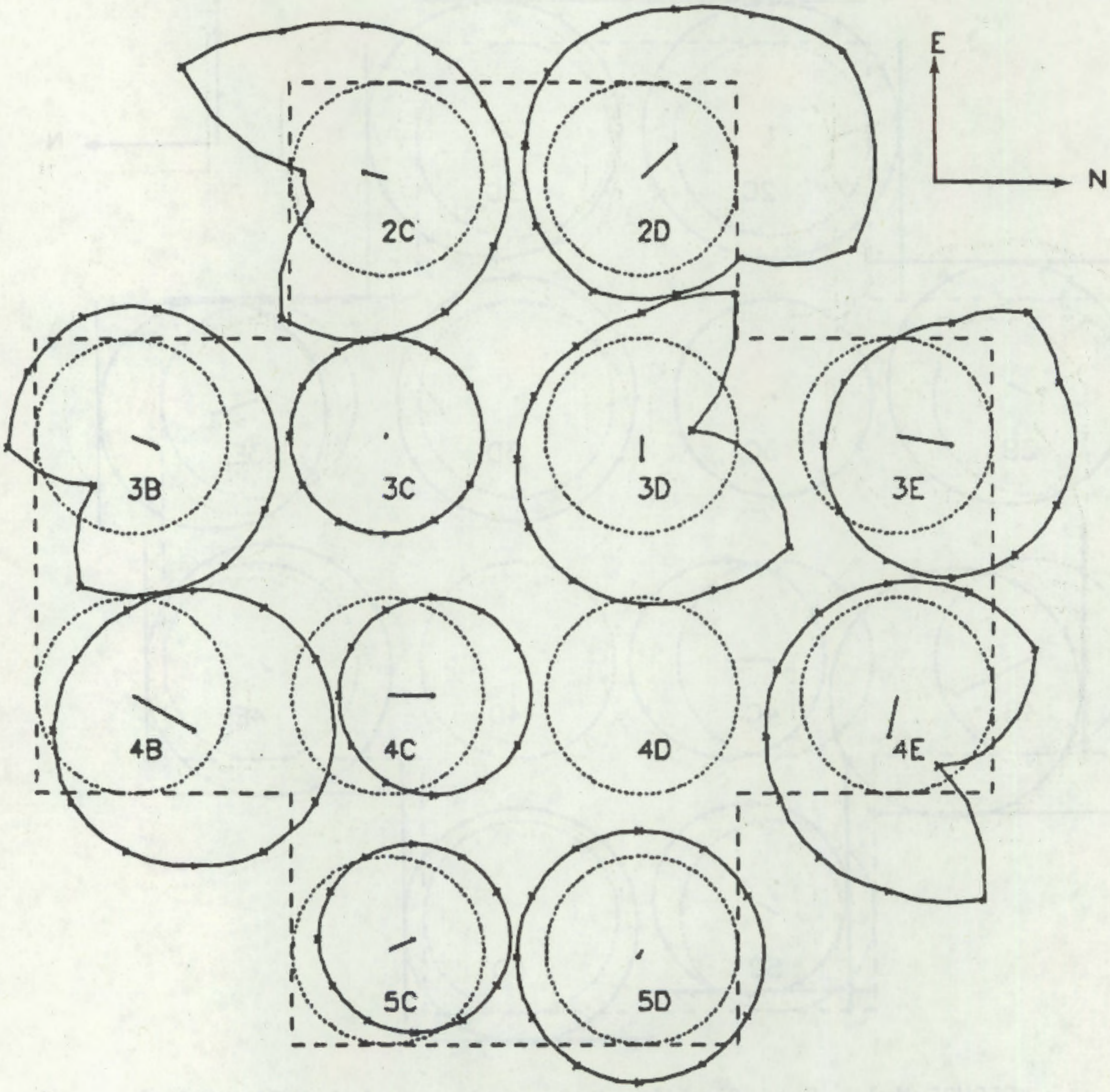

FIGURE H-2. Fuel Cladding Deformation at Axial Elevation
Z = 2.057 m (81.0 in)

MT-2 Fuel Rod Bundle

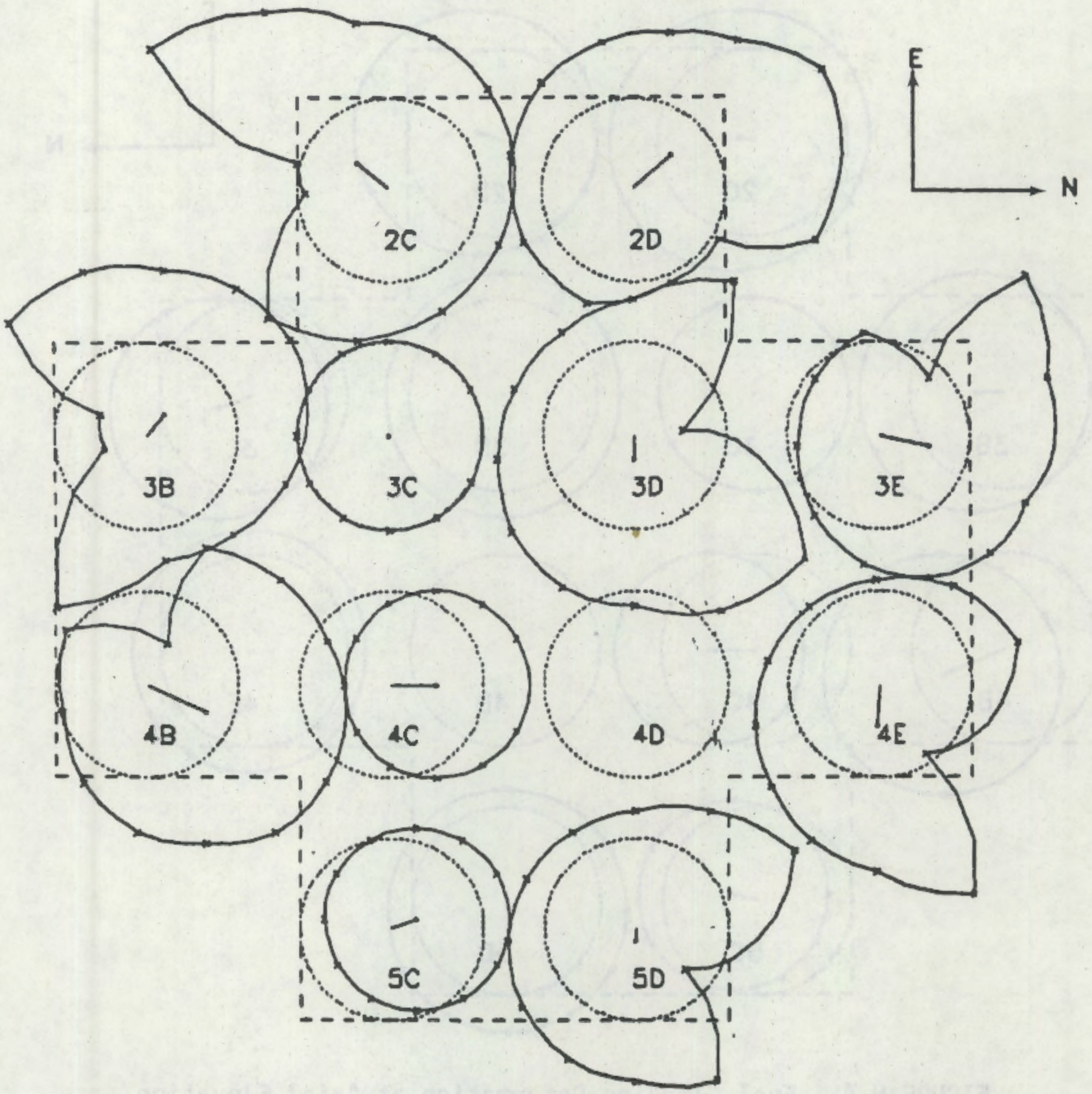

FIGURE H-3. Fuel Cladding Deformation at Axial Elevation
Z = 2.070 m (81.5 in)

MT-2 Fuel Rod Bundle

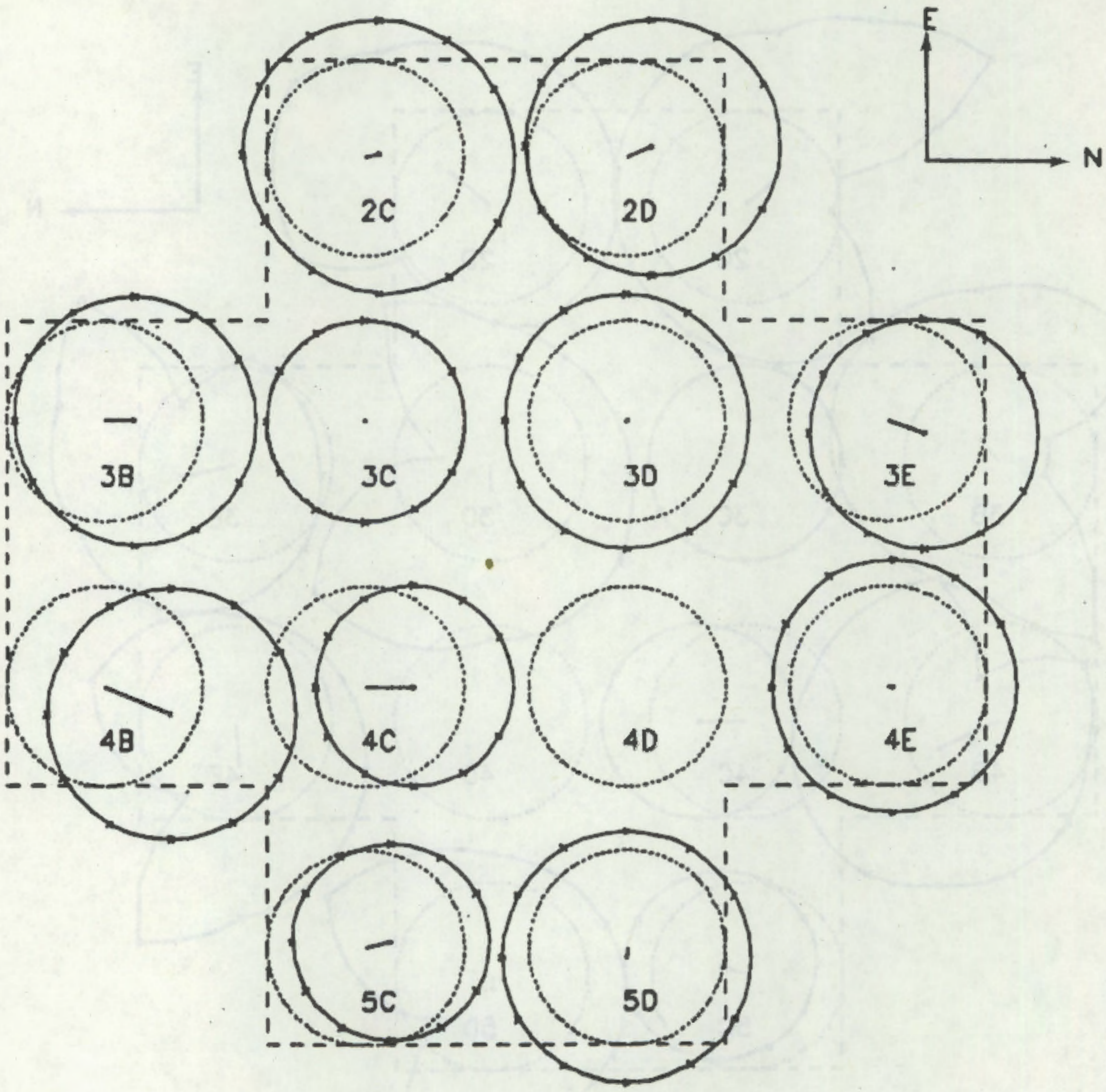

FIGURE H-4. Fuel Cladding Deformation at Axial Elevation Z = 2.083 m (82.5 in)

MT-2 Fuel Rod Bundle

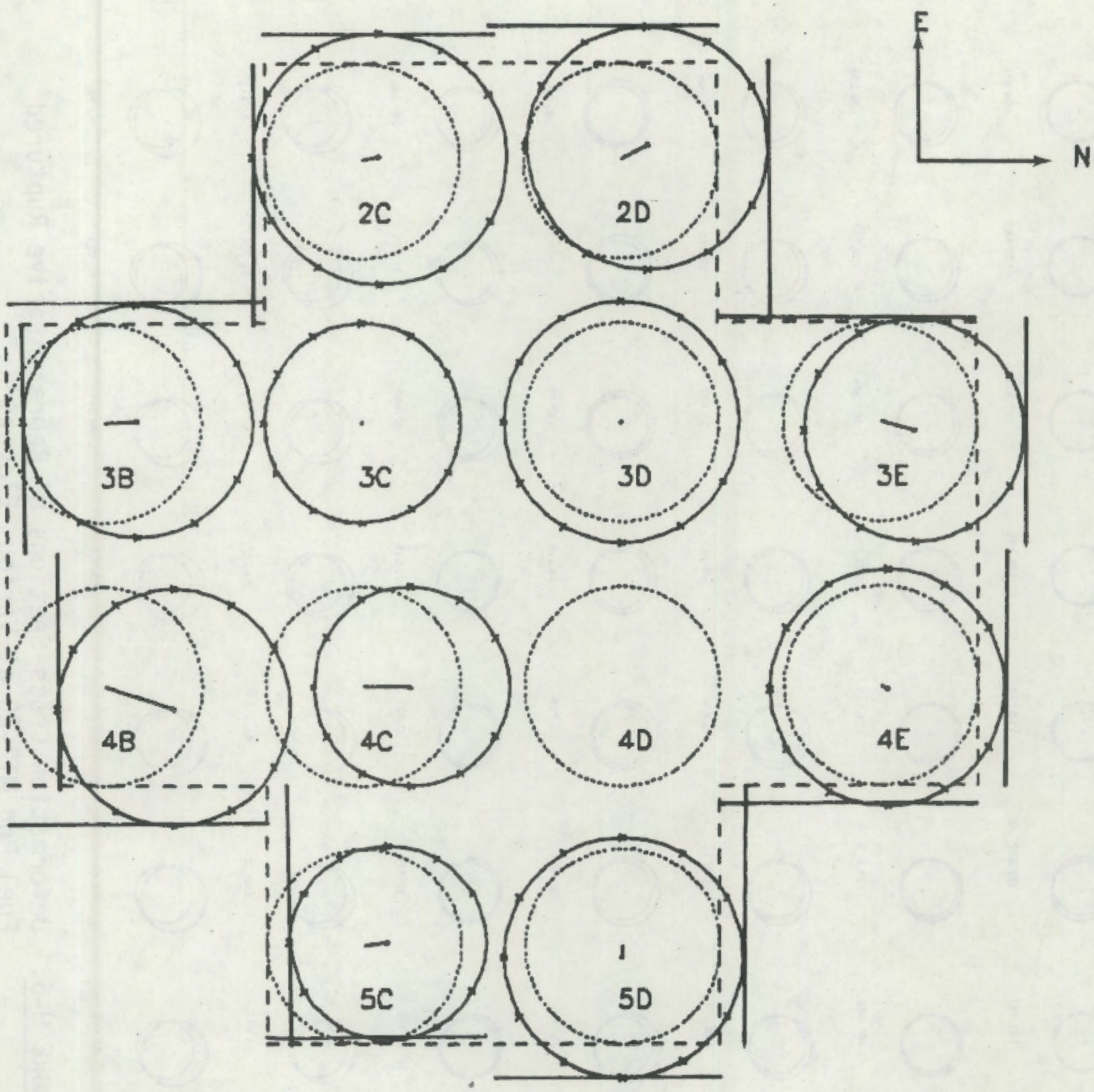

FIGURE H-5. Fuel Cladding Deformation at Axial Elevation Z = 2.108 m (83.0 in)

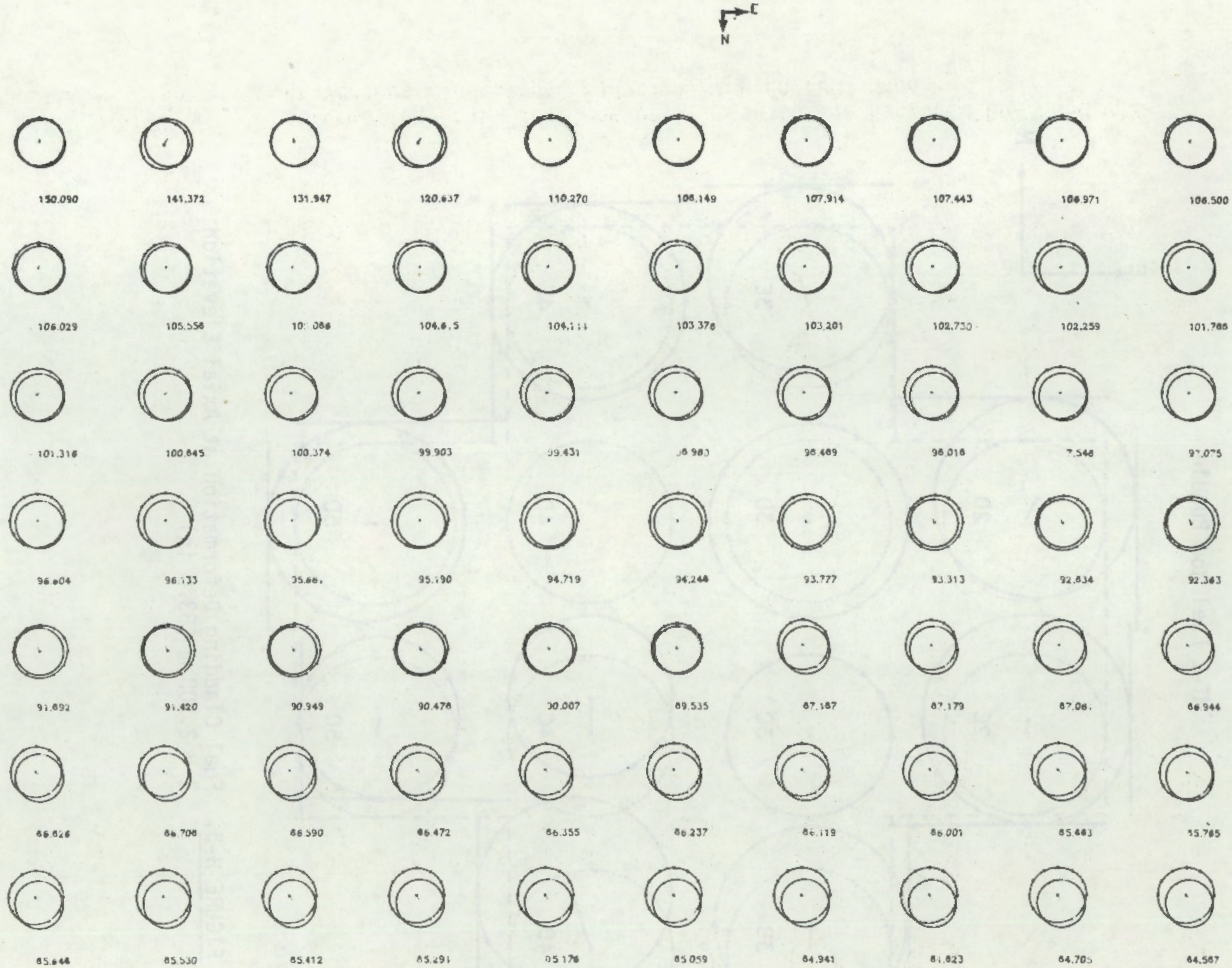

FIGURE H-6. Deformation Cross Sections of Representative Ruptured Fuel Rod MT2-2C at Various Elevations

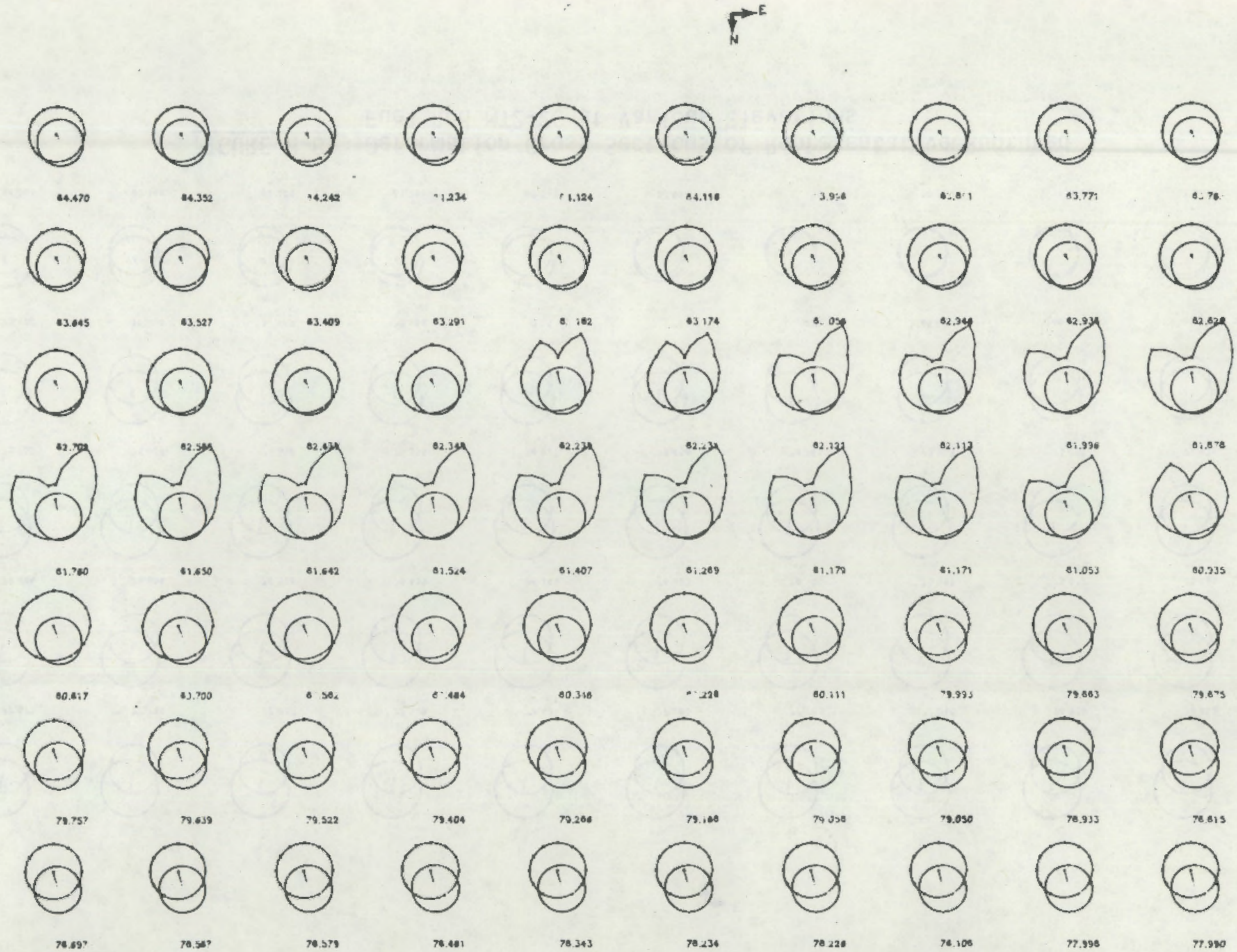

FIGURE H-7. Deformation Cross Sections of Representative Ruptured Fuel Rod MT2-2C at Various Elevations, Fiducial Mark on 180° Side

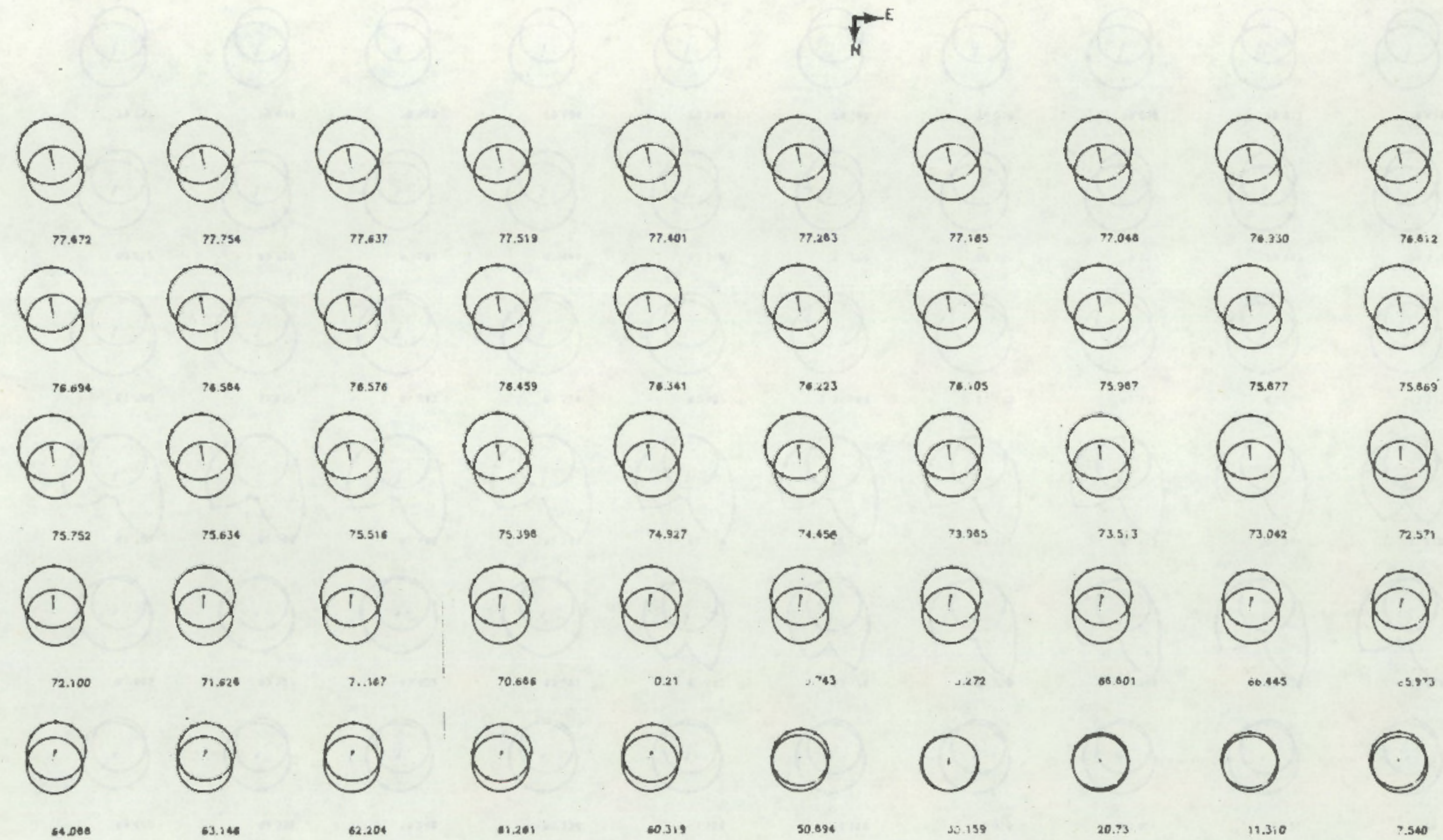

FIGURE H-8. Deformation Cross Sections of Representative Ruptured Fuel Rod MT2-2C at Various Elevations

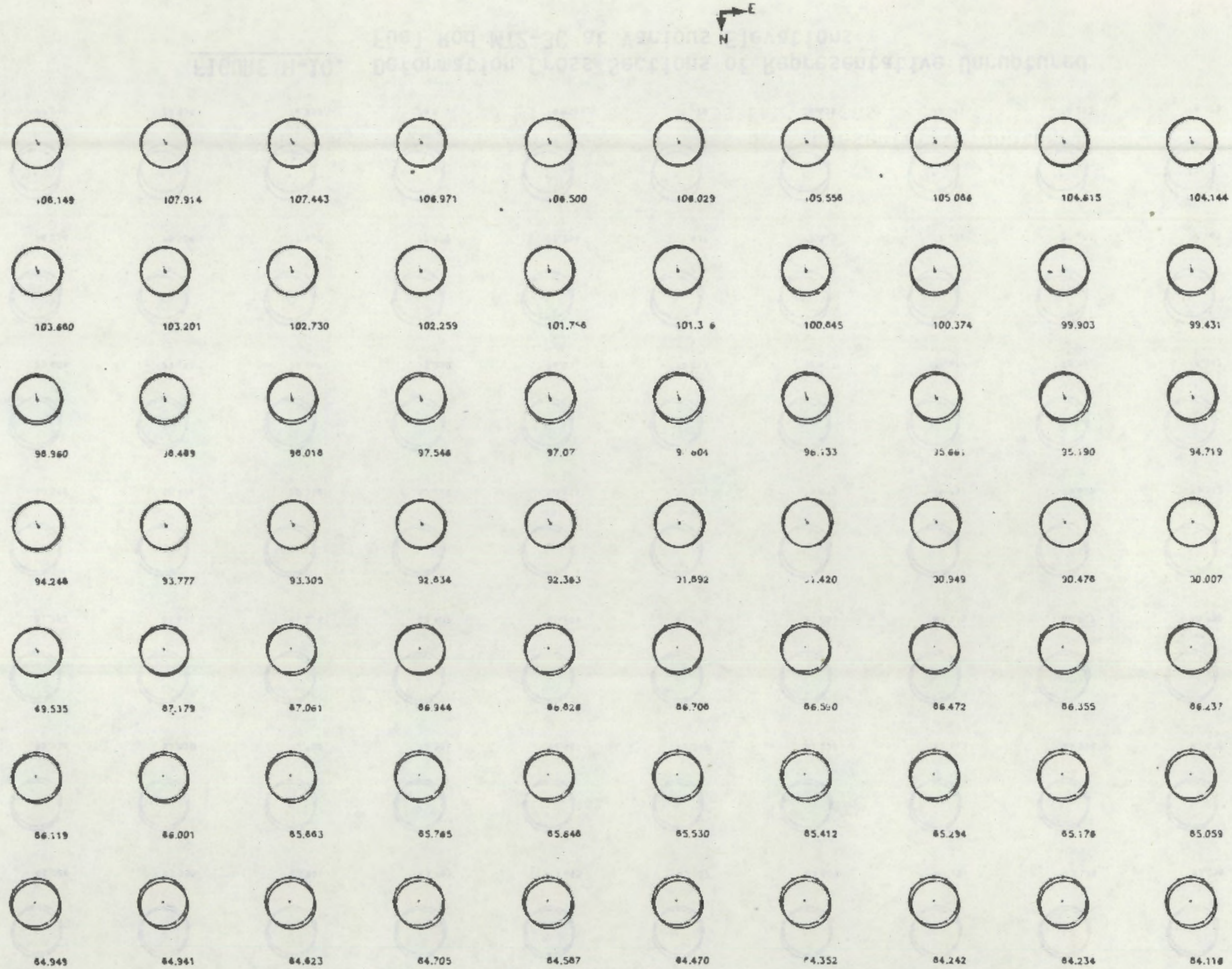

FIGURE H-9. Deformation Cross Sections of Representative Unruptured Fuel Rod MT2-3C at Various Elevations

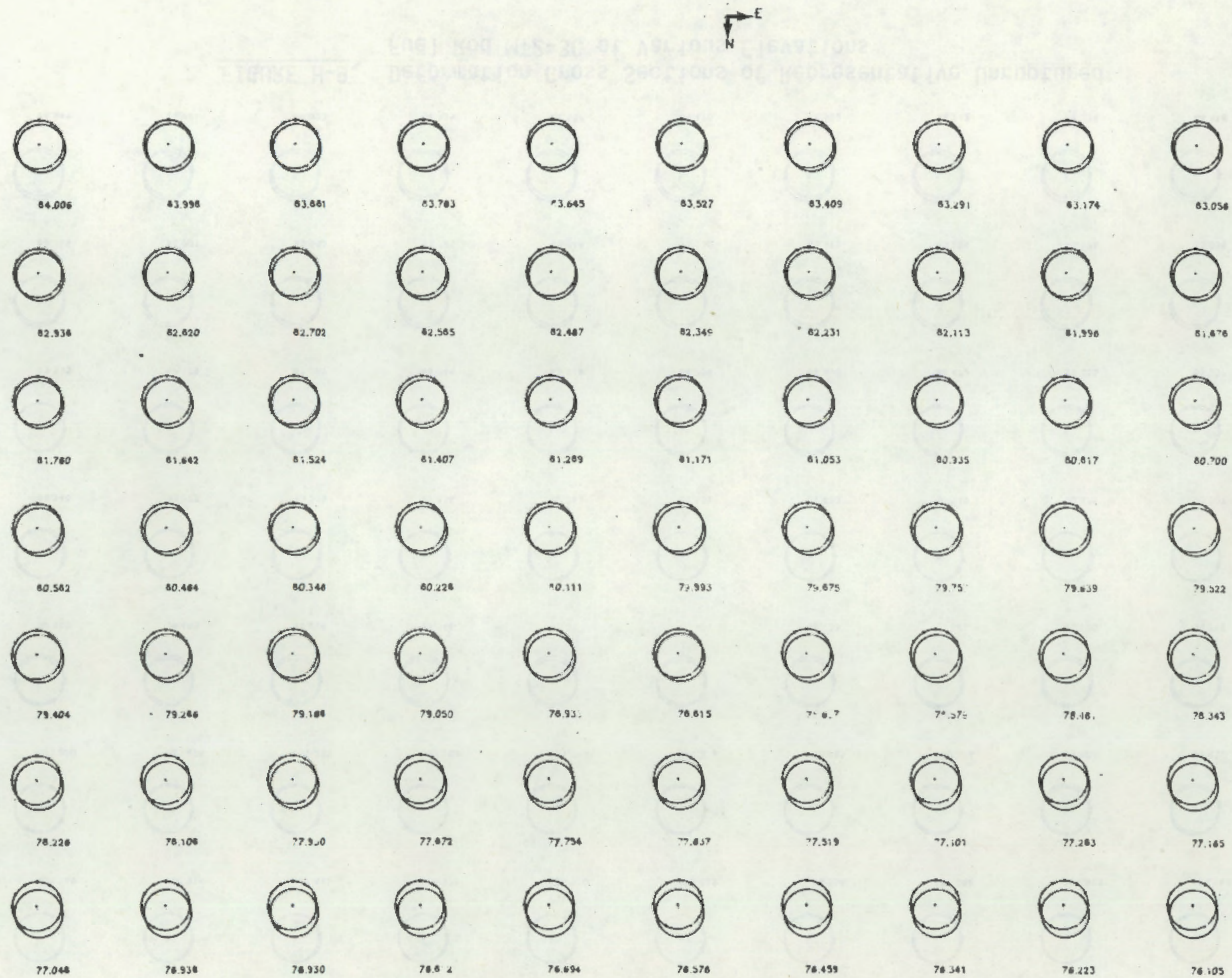

<u>FIGURE H-10</u>. Deformation Cross Sections of Representative Unruptured Fuel Rod MT2-3C at Various Elevations

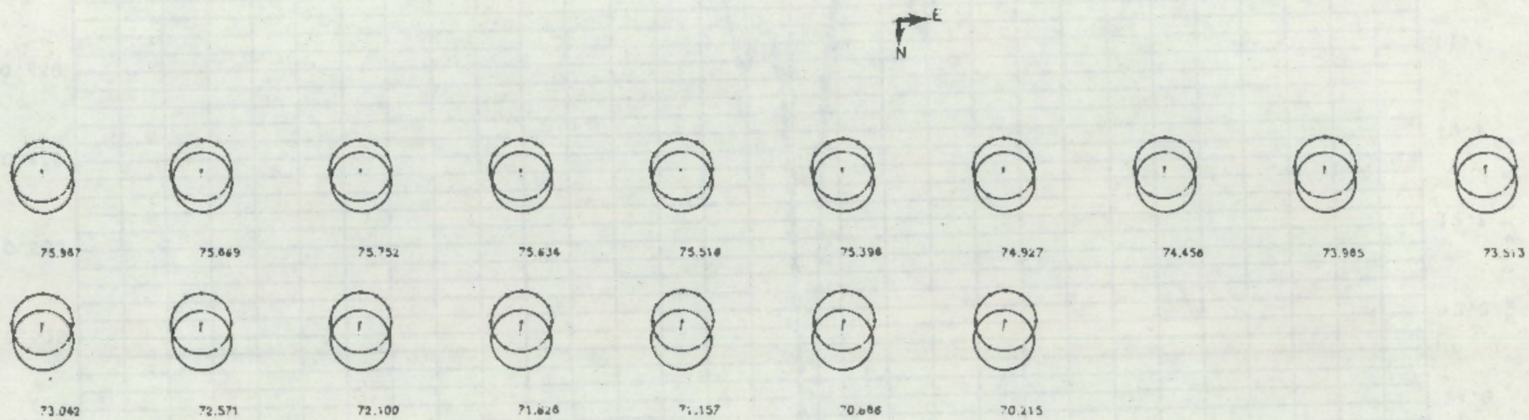

FIGURE H-11. Deformation Cross Sections of Representative Unruptured Fuel Rod MT2-3C at Various Elevations

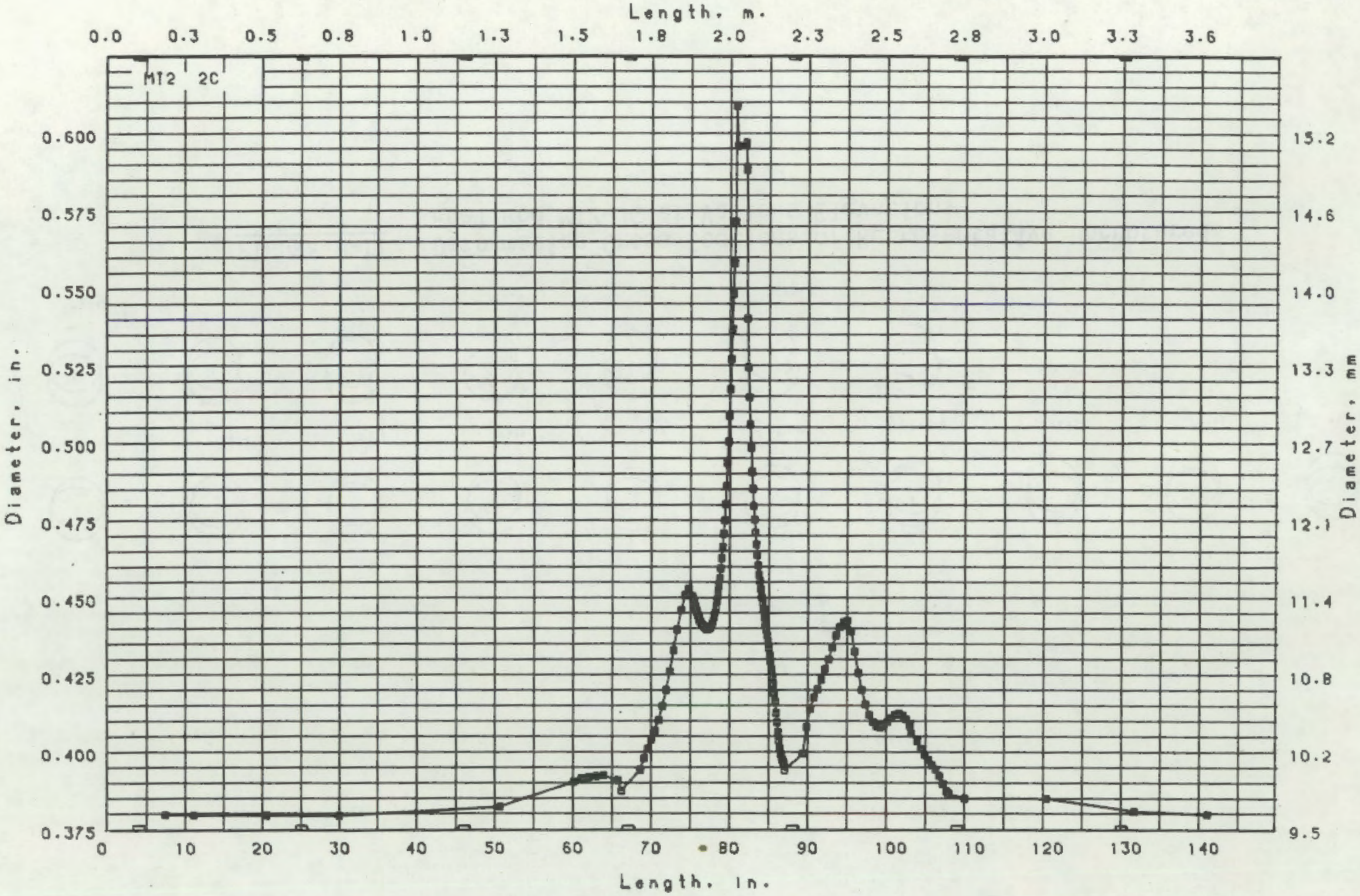

FIGURE H-12. Axial Distribution of Diametral Measurements of Fuel Rod MT2-2C

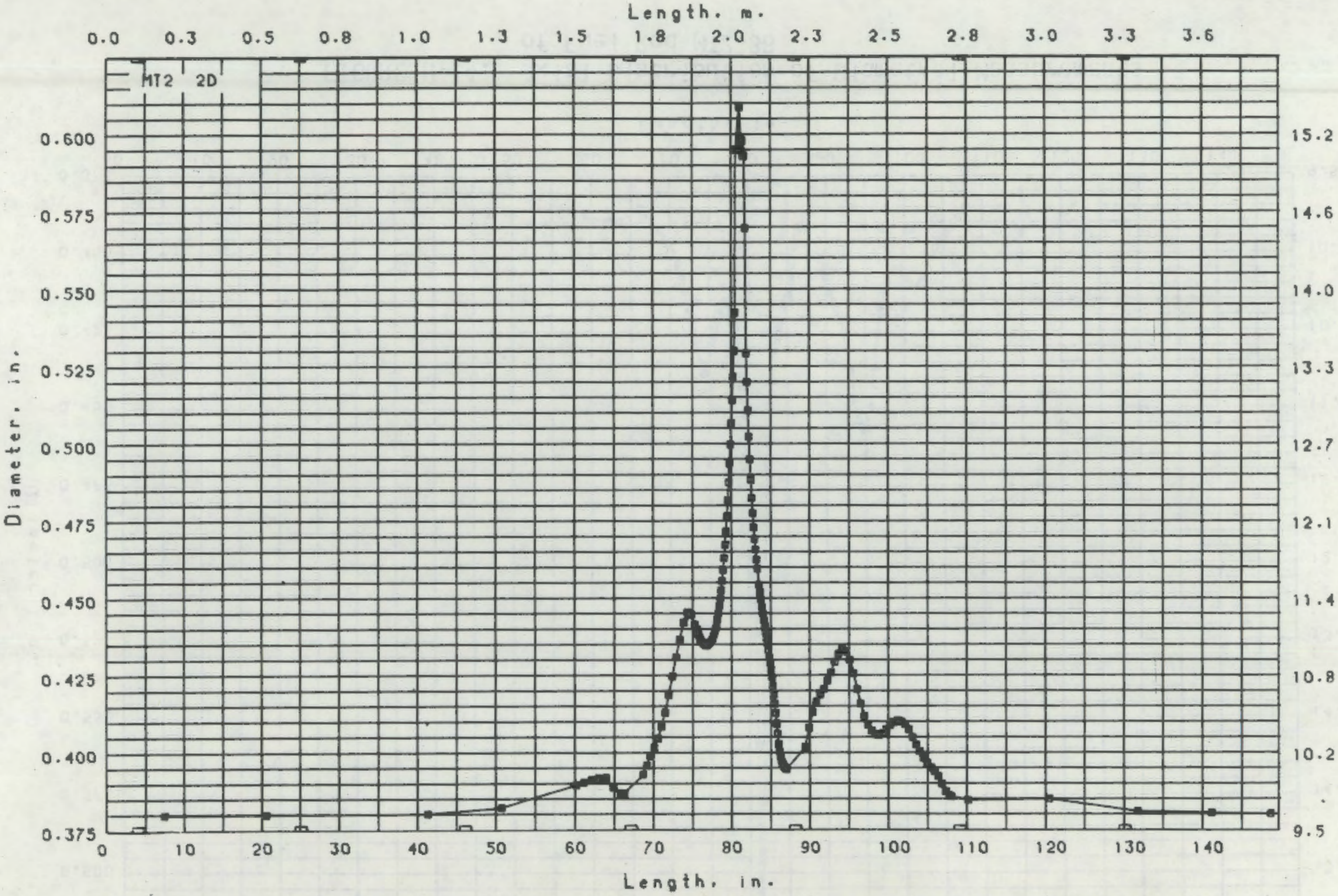

FIGURE H-13. Axial Distribution of Diametral Measurements of Fuel Rod MT2-2D

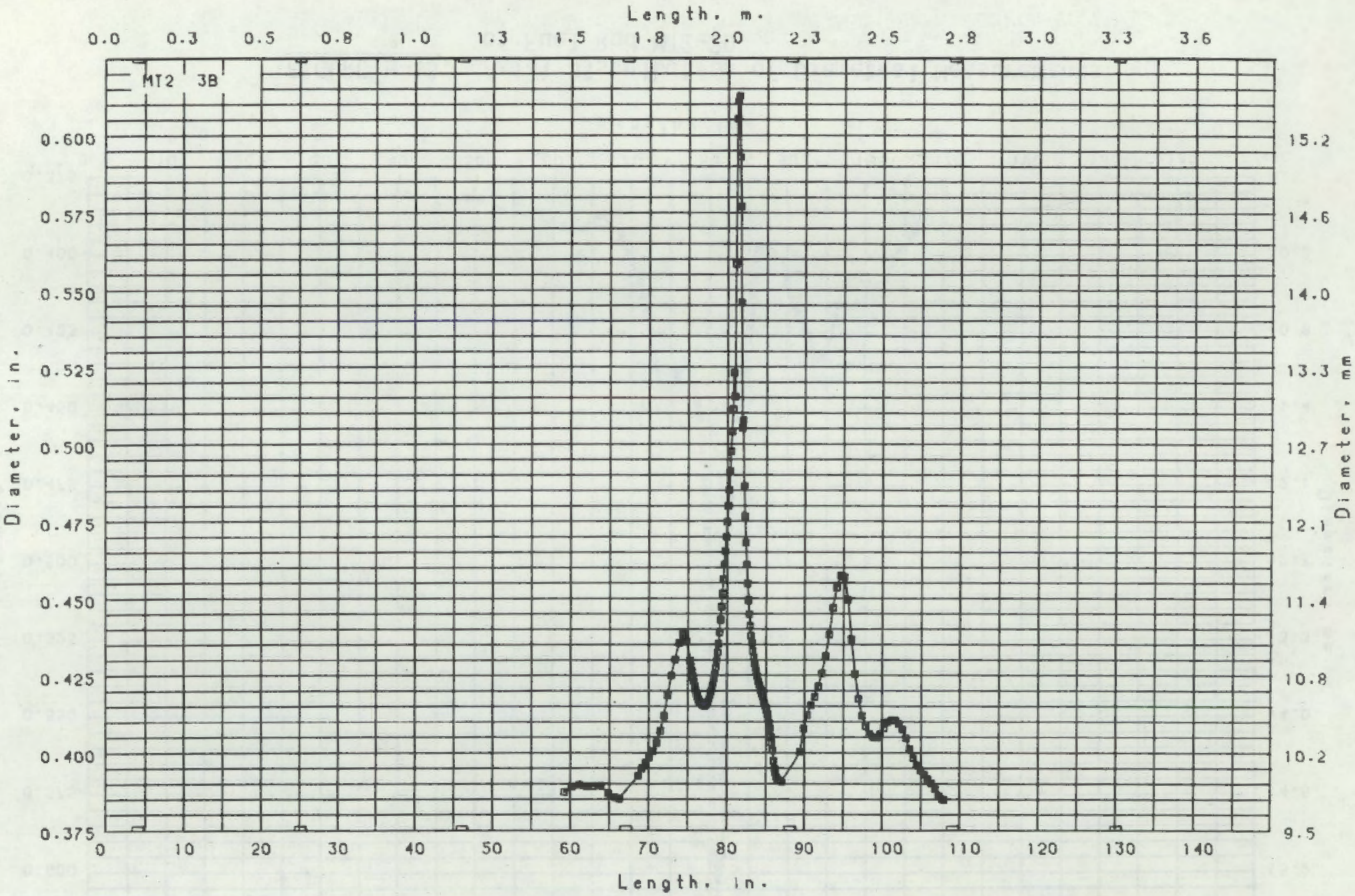

FIGURE H-14. Axial Distribution of Diametral Measurements of Fuel Rod MT2-3B

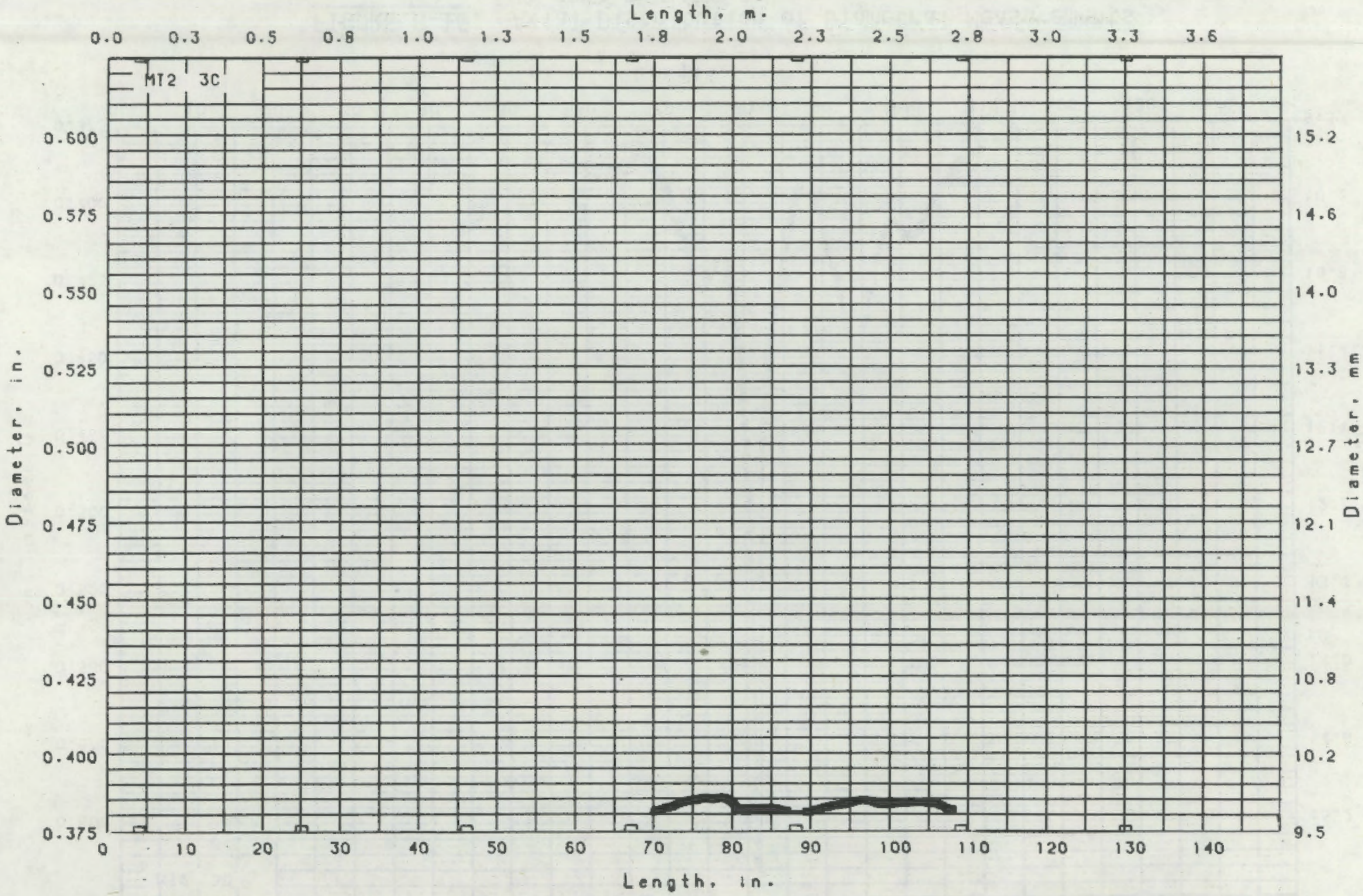

FIGURE H-15. Axial Distribution of Diametral Measurements of Fuel Rod MT2-3C

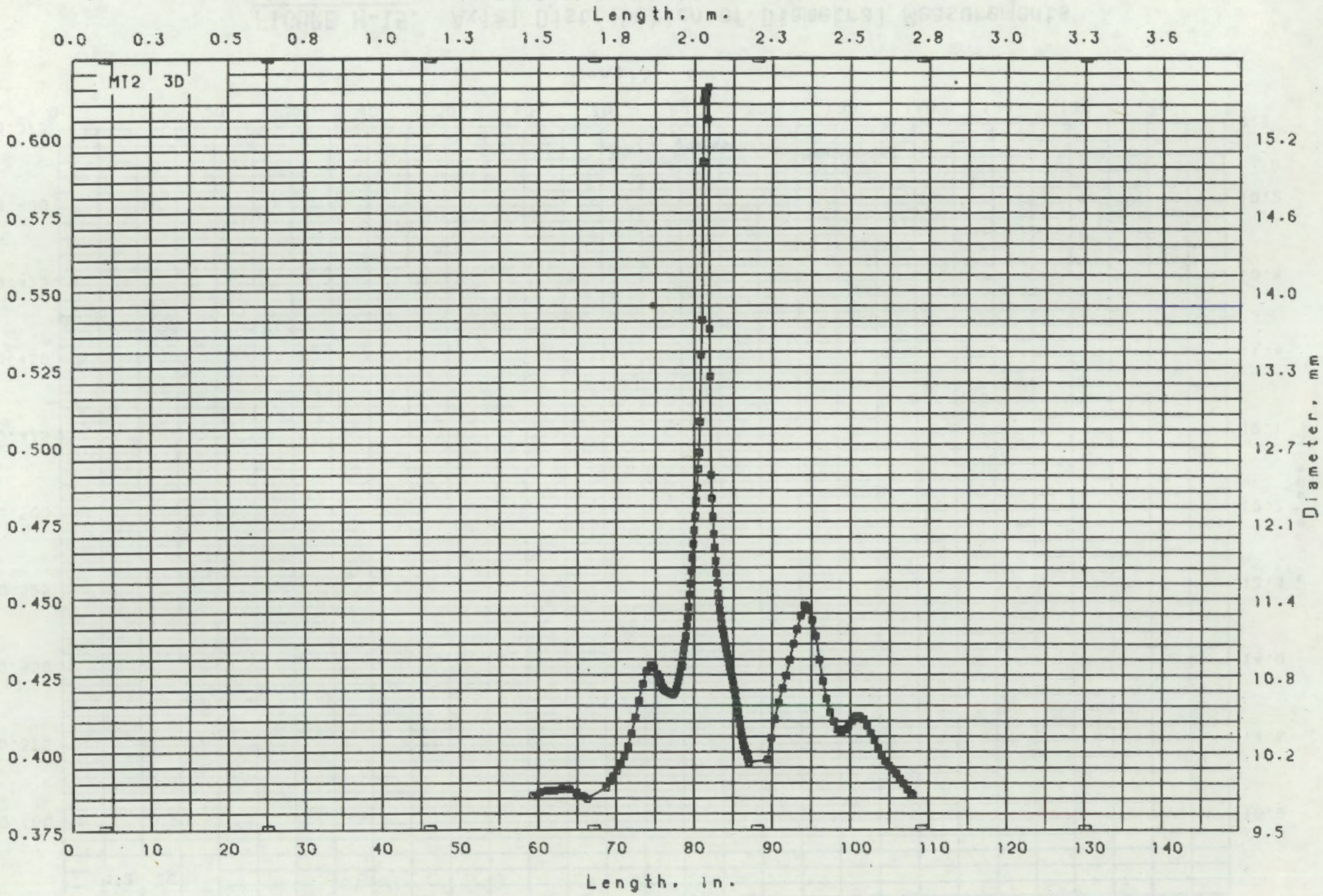

<u>FIGURE H-16</u>. Axial Distribution of Diametral Measurements of Fuel Rod MT2-3D

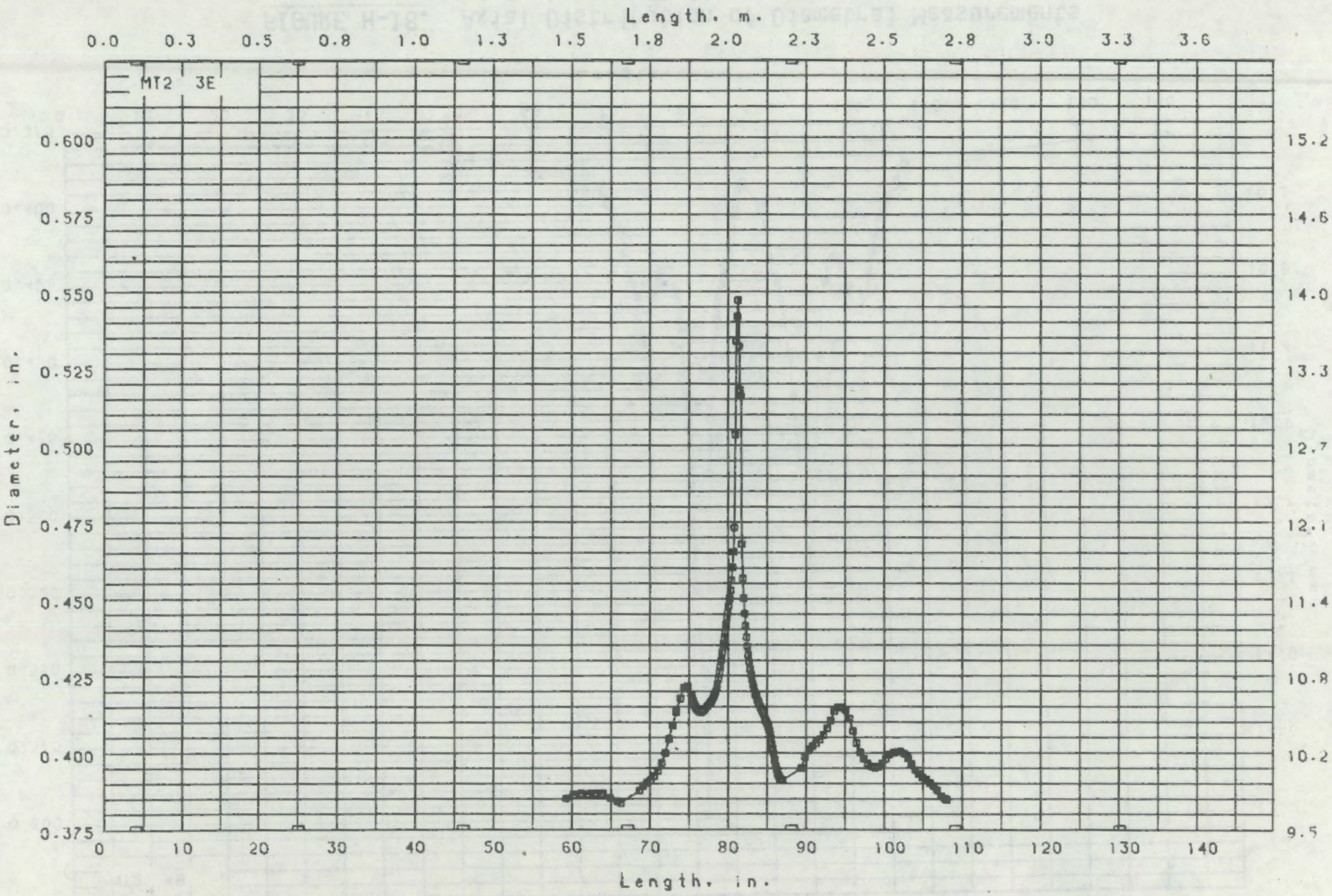

FIGURE H-17. Axial Distribution of Diametral Measurements of Fuel Rod MT2-3E

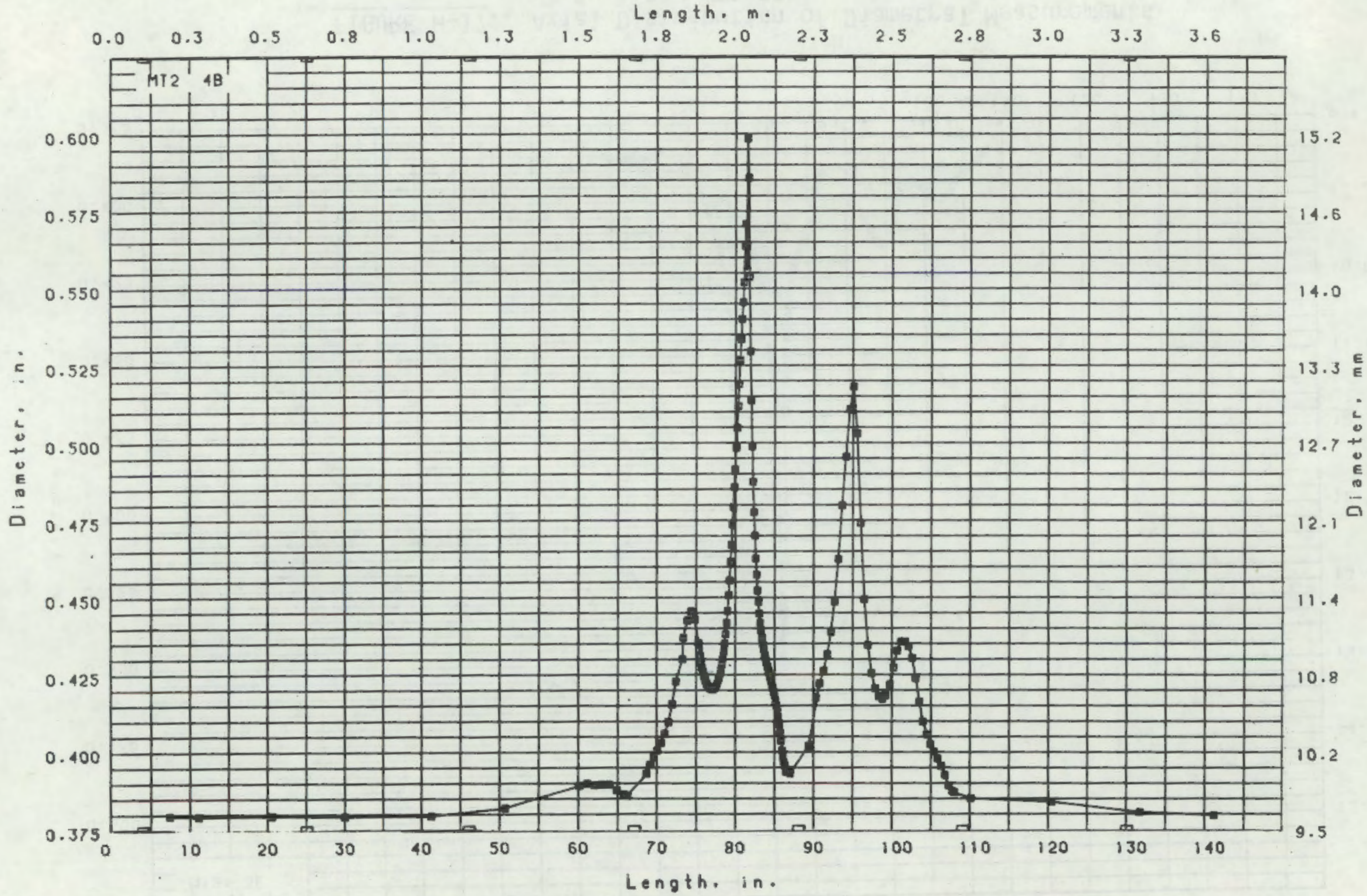

FIGURE H-18. Axial Distribution of Diametral Measurements of Fuel Rod MT2-4B

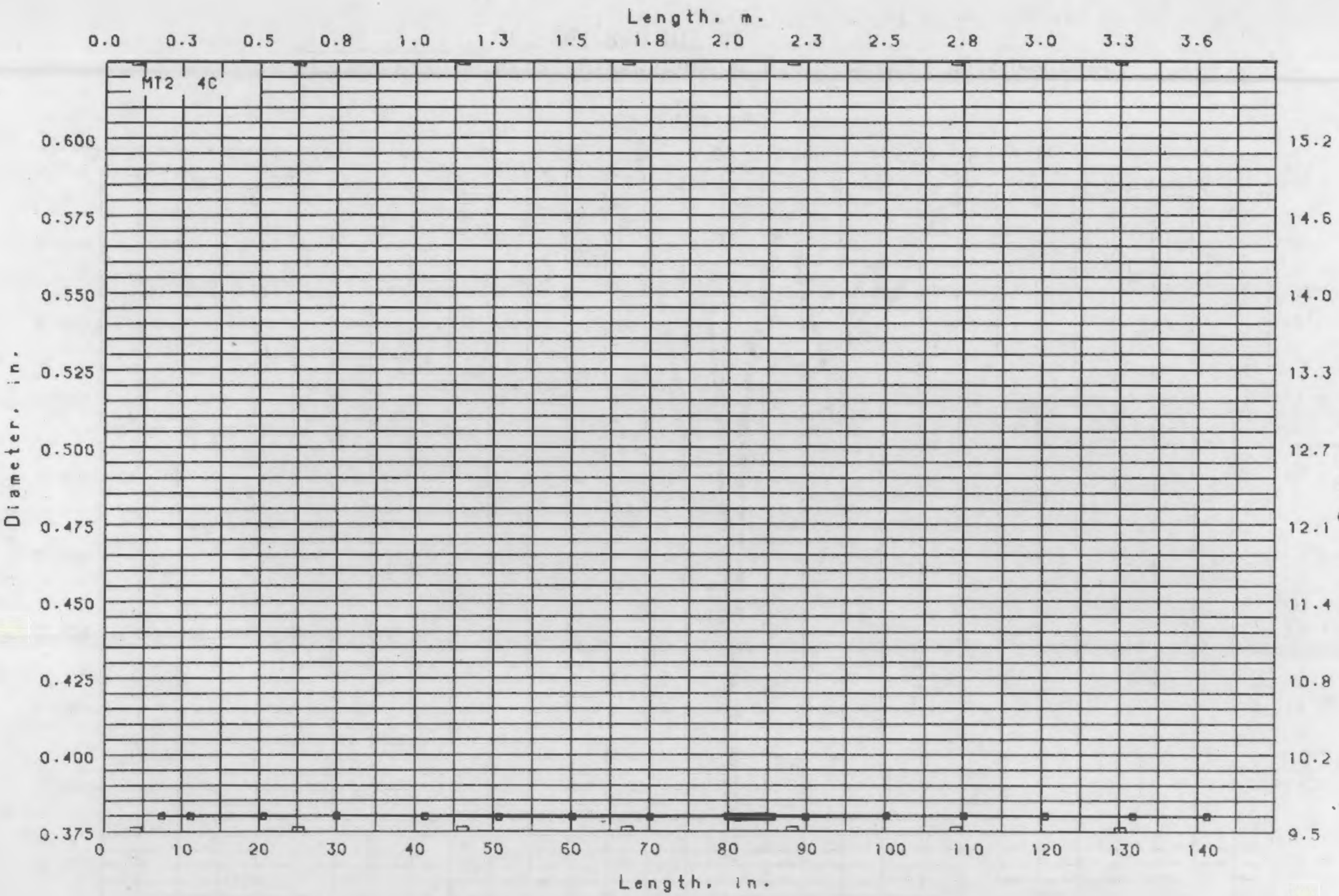

FIGURE H-19. Axial Distribution of Diametral Measurements of Fuel Rod MT2-4C

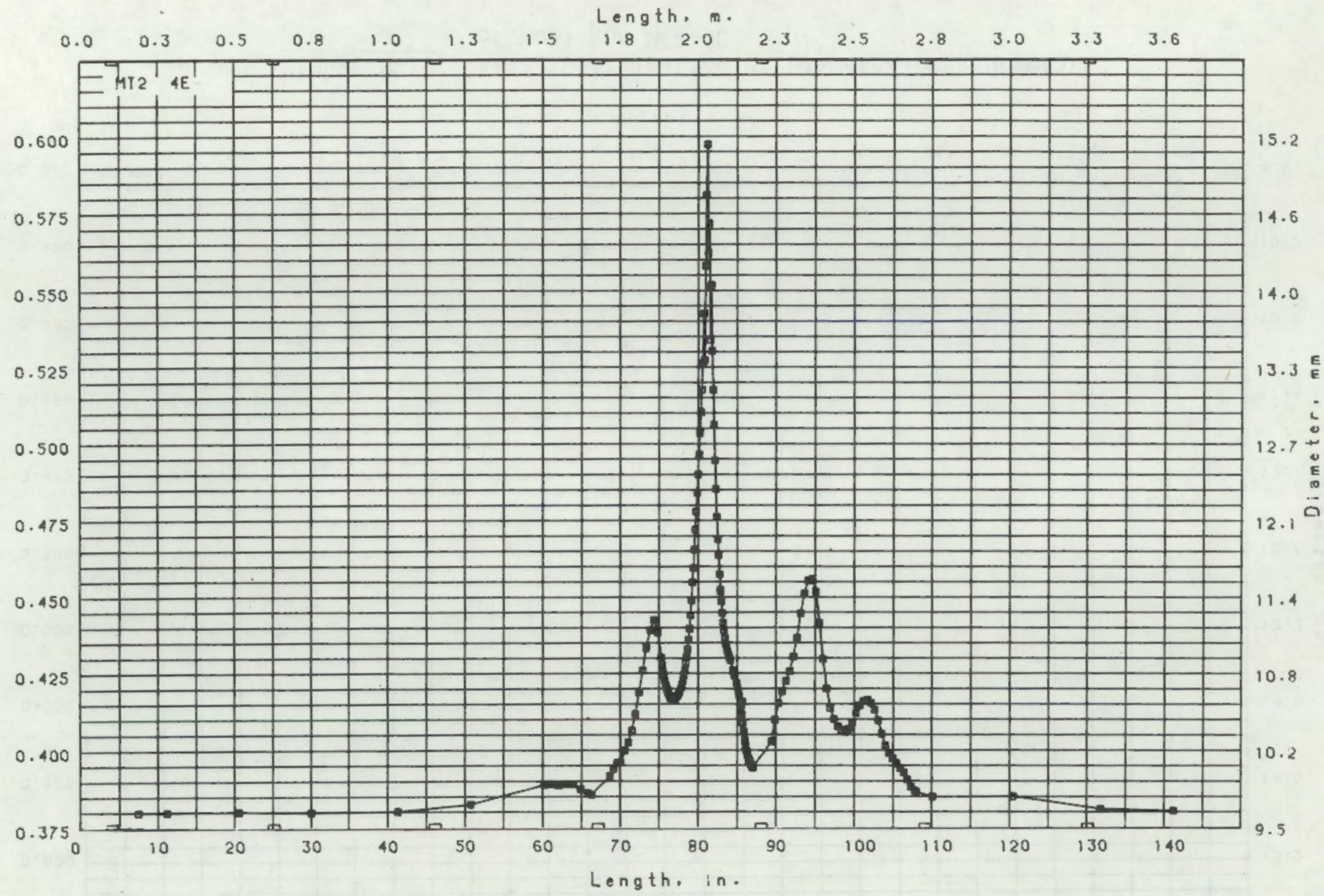

FIGURE H-20. Axial Distribution of Diametral Measurements of Fuel Rod MT2-4E

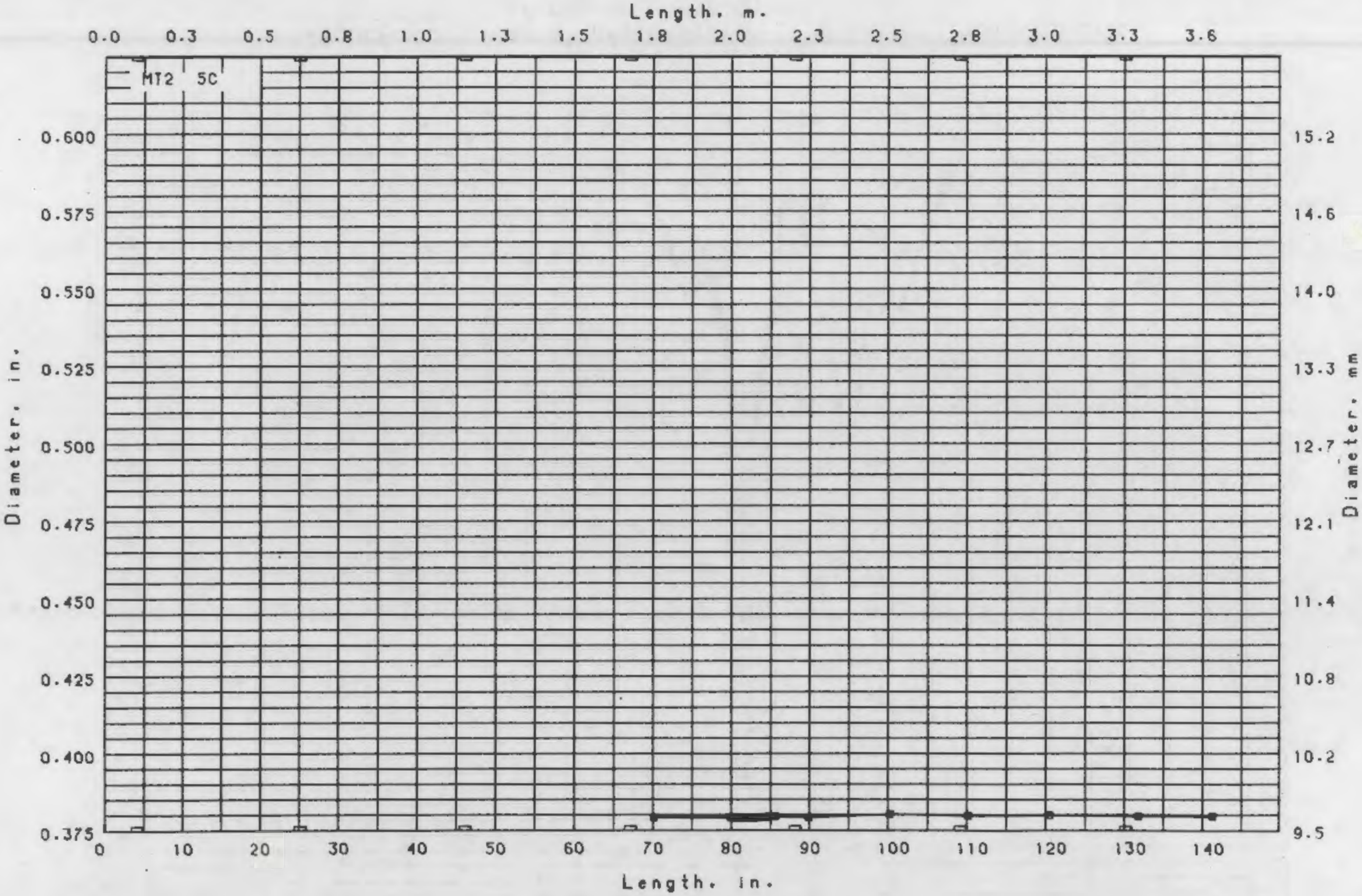

FIGURE H-21. Axial Distribution of Diametral Measurements of Fuel Rod MT2-5C

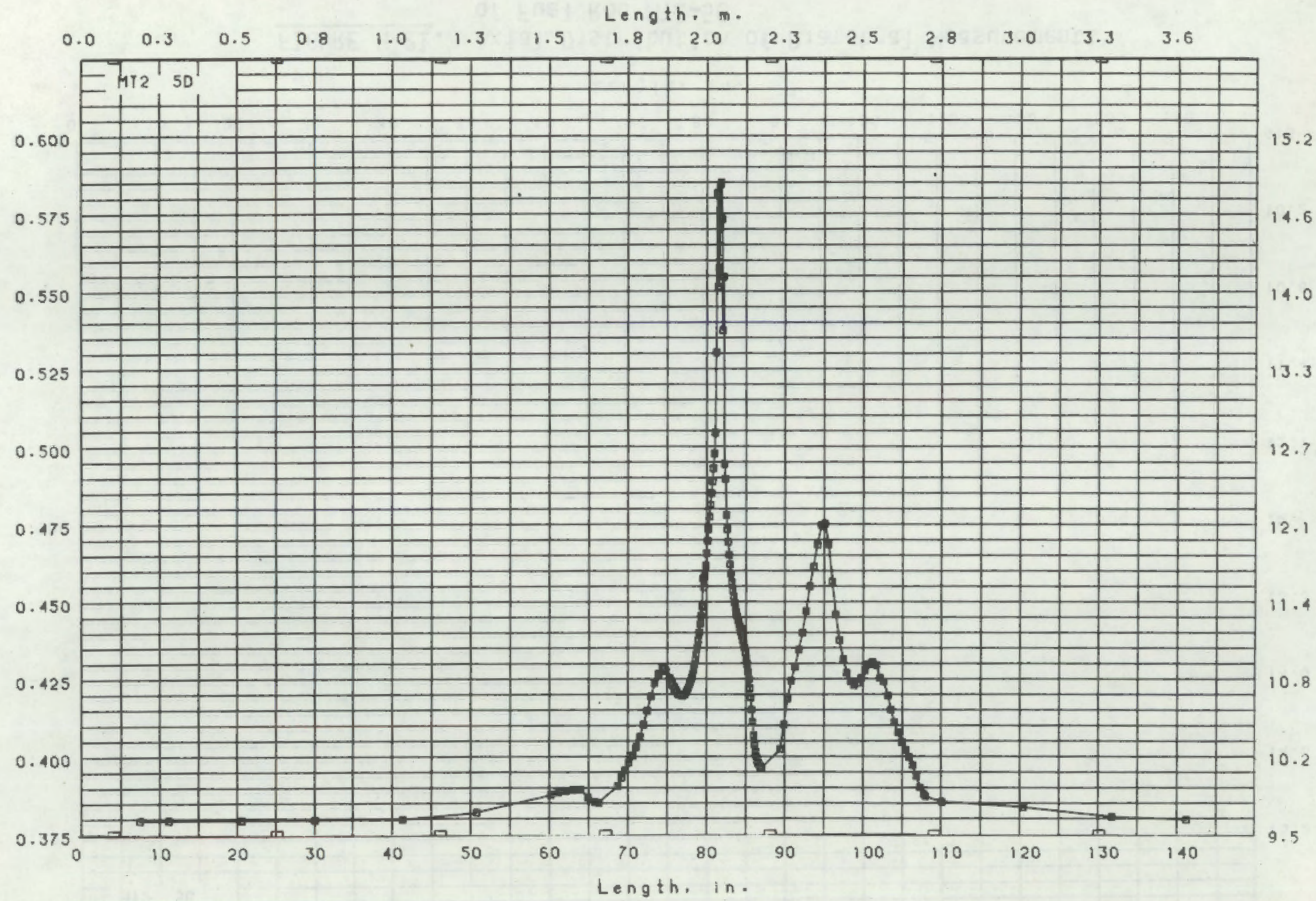

FIGURE H-22. Axial Distribution of Diametral Measurements of Fuel Rod MT2-5D

DISTRIBUTION

No. of Copies

OFFSITE

A. A. Churm
DOE Patent Division
9800 S. Cass Avenue
Argonne, IL 60439

295 U.S. Nuclear Regulatory Commission
Division of Technical Information and Document Control
7920 Norfolk Avenue
Bethesda, MD 20014

2 DOE Technical Information Center

W. Hodges
U.S. Nuclear Regulatory Commission
M/S P-1132
Washington, DC 20555

A. Hon
U.S. Nuclear Regulatory Commission
M/S 1130-SS
Washington, DC 20555

Y. Hsu
U.S. Nuclear Regulatory Commission
M/S 1130-SS
Washington, DC 20555

W. Johnston
U.S. Nuclear Regulatory Commission
M/S P-1114
Washington, DC 20555

N. Lauben
U.S. Nuclear Regulatory Commission
M/S P-1132
Washington, DC 20555

No. of Copies

G. Marino
U.S. Nuclear Regulatory Commission
M/S 1130-SS
Washington, DC 20555

G. McPherson
U.S. Nuclear Regulatory Commission
M/S 1130-SS
Washington, DC 20555

R. Meyer
U.S. Nuclear Regulatory Commission
M/S P-1114
Washington, DC 20555

T. Murley
U.S. Nuclear Regulatory Commission
M/S P-1102
Washington, DC 20555

J. Norberg
U.S. Nuclear Regulatory Commission
M/S NL-5650
Washington, DC 20555

M. Picklesimer
U.S. Nuclear Regulatory Commission
M/S 1130-SS
Washington, DC 20555

L. Phillips
U.S. Nuclear Regulatory Commission
M/S P-1114
Washington, DC 20555

D. Power
U.S. Nuclear Regulatory Commission
M/S P-1114
Washington, DC 20555

No. of Copies		No. of Copies	
	L. Shotkin U.S. Nuclear Regulatory Commission M/S 1130-SS Washington, DC 20555		C. Morgan Babcock and Wilcox Co. P.O. Box 1200 Lynchburg, VA 24505
	L. Tong U.S. Nuclear Regulatory Commission M/S 1130-SS Washington, DC 20555		R. Duncan Combustion Engineering 1000 Prospect Hill Road P.O. Box 500 Windsor, CT 06095
3	R. Van Houten U.S. Nuclear Regulatory Commission M/S 1130-SS Washington, DC 20555		S. Ritterbush Combustion Engineering 1000 Prospect Hill Road P.O. Box 500 Windsor, CT 06095
	Z. Zuber U.S. Nuclear Regulatory Commission M/S 1130-SS Washington, DC 20555	2	L. P. Leach EG&G Idaho, Inc. P.O. Box 1625 Idaho Falls, ID 83401
	P. Boehnert U.S. Nuclear Regulatory Commission Advisory Committee on Reactor Safeguards M/S H-1016 Washington, DC 20555		D. Ogden EG&G Idaho, Inc. P.O. Box 1625 Idaho Falls, ID 83401
	D. Okrent U.S. Nuclear Regulatory Commission Advisory Committee on Reactor Safeguards M/S H-1016 Washington, DC 20555		P. Davis (ITI) Electric Power Research Institute 3412 Hillview Avenue Palo Alto, CA 94022
	P. Shewmon U.S. Nuclear Regulatory Commission Advisory Committee on Reactor Safeguards M/S H-1016 Washington, DC 20555		R. Duffey Electric Power Research Institute 3412 Hillview Avenue Palo Alto, CA 94022
	B. Bingham Babcock and Wilcox Co. P.O. Box 1200 Lynchburg, VA 24505		R. Oehlberg Electric Power Research Institute 3412 Hillview Avenue Palo Alto, CA 94022

No. of Copies

W. Sun
Electric Power Research Institute
3412 Hillview Avenue
Palo Alto, CA 94022

G. Thomas
Electric Power Research Institute
3412 Hillview Avenue
Palo Alto, CA 94022

L. Thompson
Electric Power Research Institute
3412 Hillview Avenue
Palo Alto, CA 94022

S. Armijo
General Electric Company
175 Curtner Avenue
San Jose, CA 95114

L. Noble
General Electric Company
175 Curtner Avenue
San Jose, CA 95114

N. Shirley
General Electric Company
175 Curtner Avenue
San Jose, CA 95114

G. Sozzi
General Electric Company
175 Curtner Avenue
San Jose, CA 95114

R. Williams
General Electric Company
175 Curtner Avenue
San Jose, CA 95114

W. Kirchner
Los Alamos Scientific Laboratory
P.O. Box 1663
Los Alamos, NM 87544

No. of Copies

D. M. Chapin
MPR Associates, Inc.
1140 Connecticut Avenue, NW
Washington, DC 20036

P. Griffith
Massachusetts Institute of Technology
Department of Nuclear Engineering
Cambridge, MA 02139

J. Davis
Nuclear Engineering Department
Potomac Electric Avenue, NW
Washington, DC 20068

2 R. Chapman
Oak Ridge National Laboratory
P.O. Box X
Oak Ridge, TN 37830

F. Mynatt
Oak Ridge National Laboratory
P.O. Box X
Oak Ridge, TN 37830

D. Burman
Westinghouse Electric Corporation
P.O. Box 355
Pittsburgh, PA 15230

L. Hochreiter
Westinghouse Electric Corporation
P.O. Box 355
Pittsburgh, PA 15230

R. Rosal
Westinghouse Electric Corporation
P.O. Box 355
Pittsburgh, PA 15230

FOREIGN

D. J. Axford
Chalk River Nuclear Laboratories
Atomic Energy of Canada, Ltd.
Chalk River, Ontario, Canada
KOJ 1JD

No. of Copies		No. of Copies	
6	C. A. Herriot Chalk River Nuclear Laboratories Atomic Energy of Canada, Ltd. Chalk River, Ontario, Canada KOJ 1J0		S. Finzi JRC-ISPRA, EURATOM CCR ESSOR Division 21020 Cento Euratom Di Ispra (Varese) Italy
	D. T. Nishimura Chalk River Nuclear Laboratories Atomic Energy of Canada, Ltd. Chalk River, Ontario, Canada KOJ 1J0		R. Klersy JRC-ISPRA, EURATOM CCR ESSOR Division 21020 Cento Euratom Di Ispra (Varese) Italy
	I. D. Ross Chalk River Nuclear Laboratories Atomic Energy of Canada, Ltd. Chalk River, Ontario, Canada KOJ 1J0		J. Randles JRC-ISPRA, EURATOM CCR ESSOR Division 21020 Cento Euratom Di Ispra (Varese) Italy
	A. Smith Chalk River Nuclear Laboratories Atomic Energy of Canada, Ltd. Chalk River, Ontario, Canada KOJ 1J0		J. Upton JRC-ISPRA, EURATOM CCR ESSOR Division 21020 Cento Euratom Di Ispra (Varese) Italy
2	T. Healey Central Electricity Generating Board Berkeley Nuclear Laboratories Berkeley, Gloucestershire GL13 9PB England		F. Erbacher Kernforschungzentrum Karlsruhe Weberstrasse 5 75 Karlsruhe 1 Federal Republic of Germany
4	M. Ishikawa, Chief Reactivity Accident Laboratory Japan Atomic Energy Research Institute Tokai Research Establishment Tokai-Mura, Naka-Gun Ibaraki-Ken Japan		A. Fiege Kernforschungzentrum Karlsruhe Weberstrasse 5 75 Karlsruhe 1 Federal Republic of Germany
	T. Doyle JRC-ISPRA, EURATOM CCR ESSOR Division 21020 Cento Euratom Di Ispra (Varese) Italy		

No. of Copies

2 H.·Rininslandd
Kernforschungzentrum Karlsruhe
Weberstrasse 5
75 Karlsruhe 1
Federal Republic of Germany

5 J. Gittus
Springfields Nuclear Power Development Laboratory
United Kingdom Atomic Energy Authority
Springfields, Salwick
Preston PR 4 ORR
England

C. A. Mann
Springfields Nuclear Power Development Laboratory
United Kingdom Atomic Energy Authority
Springfields, Salwick
Preston PR 4 ORR
England

ONSITE

4 Exxon Nuclear Inc.

T. Doyle
W. Kayser
J. Morgan
W. Nechodom

No. of Copies

50 Pacific Northwest Laboratory

W. J. Bailey
J. O. Barner
W. D. Bennett
L. W. Cannon
E. L. Courtright
M. D. Freshley
R. L. Goodman
C. R. Hann
G. M. Hesson (3)
L. L. King
R. K. Marshall
P. N. McDuffie (3)
C. L. Mohr (5)
C. Nealley
F. E. Panisko
L. J. Parchen (5)
J. P. Pilger
W. N. Rausch
G. E. Russcher (5)
B. J. Webb
N. J. Wildung
C. L. Wilson (5)
M. D. Wismer
Publishing Coordination (2)
Technical Publication (5)

NRC FORM 335 (7-77) U.S. NUCLEAR REGULATORY COMMISSION **BIBLIOGRAPHIC DATA SHEET**	1. REPORT NUMBER *(Assigned by DDC)* NUREG/CR-2509 PNL-4155	
4. TITLE AND SUBTITLE *(Add Volume No., if appropriate)* Materials Test-2 LOCA Simulation in the NRU Reactor	2. *(Leave blank)*	
	3. RECIPIENT'S ACCESSION NO.	
7. AUTHOR(S) J.O. Barner, G.M. Hesson, L.L. King, R.K. Marshall, L.J. Parchen, J.P. Pilger, W.N. Rausch, G.E. Russcher, B.J. Webb, N.J. Wildung, C.L. Wilson, M.D. Wismer, C.L. Mohr	5. DATE REPORT COMPLETED MONTH January	YEAR 1982
9. PERFORMING ORGANIZATION NAME AND MAILING ADDRESS *(Include Zip Code)* Pacific Northwest Laboratory Richland, WA 99352	DATE REPORT ISSUED MONTH March	YEAR 1982
	6. *(Leave blank)*	
	8. *(Leave blank)*	
12. SPONSORING ORGANIZATION NAME AND MAILING ADDRESS *(Include Zip Code)* Division of Accident Technology Office of Nuclear Regulatory Research U.S. Nuclear Regulatory Commission Washington, DC 20555	10. PROJECT/TASK/WORK UNIT NO.	
	11. CONTRACT NO. FIN B2277	
13. TYPE OF REPORT	PERIOD COVERED *(Inclusive dates)*	
15. SUPPLEMENTARY NOTES	14. *(Leave blank)*	

16. ABSTRACT *(200 words or less)*

A simulated loss-of-coolant accident was performed with a full-length test bundle of pressurized water reactor fuel rods. This third experiment of the program produced fuel cladding temperatures exceeding 1033 K (1400°F) for 155 s and resulted in eight ruptured fuel rods. Experiment data and initial results are presented in the form of photographs and graphical summaries.

17. KEY WORDS AND DOCUMENT ANALYSIS

17a. DESCRIPTORS

17b. IDENTIFIERS/OPEN-ENDED TERMS

18. AVAILABILITY STATEMENT	19. SECURITY CLASS *(This report)*	21. NO. OF PAGES
Unlimited	Unclassified	
	20. SECURITY CLASS *(This page)*	22. PRICE
	Unclassified	S

NRC FORM 335 (7-77)

U.S GOVERNMENT PRINTING OFFICE 361-297/2036